Preliminary Report of the Hakuho Maru Cruise KH 92-3

July 17~August 10, 1992

Geophysical and Geological Investigation
of
Western Kuril Trench and Eastern Nankai Trough

[ODP and KAIKO-TOKAI Site Survey]

Ocean Research Institute
University of Tokyo
1993

Preliminary Report of the Hakuho Maru Cruise KH 92-3

July 17~August 10, 1992

Geophysical and Geological Investigation
of
Western Kuril Trench and Eastern Nankai Trough

[ODP and KAIKO-TOKAI Site Survey]

by
The Scientific Members of the Expedition
Edited by
Kazuo KOBAYASHI

(4.5 km) were taken in a direction roughly perpendicular to the trench axis. Better than 100% coverage of swath bathymetry was obtained for the axial zone deeper than 5,000 m. One long track was selected for comprehensive survey including multi-channel (24 channel) seismic reflection profiling with ship's speed of approximately 5 knots. Very clear results of 3.5 kHz subbottom profiler were obtained along this track. The other tracks were surveyed by a cruising speed of the Hakuho Maru, 16 knots in average and 18.5 knots in maximum. Sea Beam data were very good even with such high speeds except for under very rough sea condition. Fortunately the sea was generally calm and very few hours of thick fog were encountered in this region. Acoustic signals of Sea Beam were measured and analysed to access the bottom scattering characteristics.

As described in this report the topography of the oceanward slope of the Kuril Trench shows a distinct contrast to that of the Japan Trench. It is because the Kuril Trench trends in a direction nearly parallel to the magnetic lineations (spreading ridge) of the Pacific basin, whereas the Japan Trench is near to that perpendicular to them. Very unique topographic features of nearly 100 million years old ocean floor were revealed in the trench slope in which the oceanic plate is bent to be subducted beneath the arc. Surface extensional force caused by downward bending of the lithosphere is responsible for a great number of escarpments possibly due to normal faulting. Some of the scarps seem to provide evidence of non-transform offsets of the past ridge which has long dissappeared under the trench. The shipboard GPS (global positioning system) worked well in the Kuril Trench region at which Loran C is insufficient to provide precise navigation. Swath bathymetric data between two adjacent tracks are quite consistent to each other without any correction of positions.

Magnetic total force and three-components were measured throughout the whole cruise. Two types of three-components magnetometers the sensors of which were installed on the upper deck of the ship provided excellent consistent results as described in Chapters 12 and 13 of this report. Nevigation data needed for these instruments were fed through the local area network (LAN) of the ship via fibre-optical cables. Precise gravity was measured throughout the cruise. Measured values were fixed to the land measurement at the ports of Harumi, Tokyo and Kushiro, Hokkaido.

Bottom features of the landward slope of the Kuril Trench and the crestal area of Erimo Seamount were visually observed by DESMOS in Leg. 2. At the Erimo Seamount the previous KAIKO site with Ocean Bottom Tiltmeter and Seismometers was visually searched without success. One beam trawl and a few dredge hauls collected useful samples of benthic animals and rocks from the Kuril Trench slope and crests of Erimo and Bosei (Mizunagidori) Seamounts.

We would like to acknowledge officers and crew of the R. V. Hakuho Maru for their skillful shipboard operations and collaboration to our research work.

March 1992

Kazuo KOBAYASHI
Chief Scientist of the Cruise

CONTENTS

Preface
1. Scientists aboard the R. V. Hakuho Maru Cruise KH 92-3 1
2. Index Map of Cruise KH 92-3 Leg 1
— Nankai Trough Upper Slope and ODP 808 Site 2
3. Index Maps of Cruise KH 92-3 (Leg 1 + Leg 2)
— Survey Tracks for Joban Seamount Chain 3
— Survey Tracks for Kuril Trench, Western Part 4
4. Outline of Nankai Trough Upper Slope surveyed by Cruise KH 92-3 Leg 1 5
5. Topography of the Western Part of the Kuril Trench off Hokkaido based on the Sea Beam Map and 3.5 kHz Profiles 10
6. Bathymetric Mapping of Nine Seamounts near the Kuril and Japan Trenches 26
7. Topography of the Joban Seamount Chain 41
8. Conical Knolls in the Northwestern Pacific Ocean and Adjacent Seas 44
9. Magnetic Anomalies near the Kuril Trench 53
10. Geomagnetic Survey of Seamounts near the Kuril and Japan Trenches 56
11. Magnetic Anomalies over the Joban Seamount Chain 64
12. Measurement of Geomagnetic Three-component Anomalies in the Southwesternmost Part of the Kuril Trench 68
13. Geomagnetic Measurements over the Kuril Trench by use of an Integrated Data Logger System of Portable GPS/Fluxgate Magnetometer/Proton Magnetometer/Tiltmeter linked with the Onboard LAN Data Network 77
14. Gravity 83
15. MCS/OBS Survey by the R.V. Hakuho Maru KH 92-3 Cruise Leg 1 84
16. Multi-Channel Seismic Reflection Survey across the Kuril Trench 87
17. Bottom Observations by the Deep Sea Multi-Monitoring System 94
18. Dredge Hauls
    18. 1. Dredge Logs 100
    18. 2. Description of dredged samples from the Erimo and Mizunagidori seamounts during the second leg (Kushiro to Tokyo) of KH 92-3 cruise 102
19. Collection of Megabenthos and Macrobenthos with a Beam Trawl 117
20. Test of a Personal GPS Receiver for Navigation 119
21. Collection of Acoustic Backscattering Wave Level Data from the Sea Bottom in Sea Beam Survey in the Kuril Trench 121
22. SSBL Navigation in KH 92-3 Cruise Leg 2 127
23. Station and Work Log of the R. V. Hakuho Maru Cruise KH 92-3 128

Foldouts on the Back Cover—
1. Bathymetric Maps of the Western Kuril Trench
— Eastern Part & Western Part (2 sheets)
2. 3.5 kHz Profile along Line #32 measured during the Multichannel Seismic Profiling across the Kuril Trench off east Hokkaido (Fig. 5-5).
3. Onboard Near Trace Monitor Record across the Nankai Trough and Zenisu Ridge (KAIKO-TOKAI area) (Fig. 15-2).
4. Stacked Section of the 24-channel Seismic Profiling Data across the Western Kuril Trench south off Nemuro City (Fig. 16-3).

1. SCIENTISTS ABOARD THE R. V. HAKUHO MARU CRUISE KH 92-3

Port of Call: July 25 to July 29 at Kushiro, Hokkaido

KOBAYASHI, Kazuo [Chief Scientist]	Ocean Research Institute, University of Tokyo
ARIIE, Yoshiro**	Ocean Research Institute, University of Tokyo
FUJIMOTO, Hiromi*	Ocean Research Institute, University of Tokyo
FURUTA, Toshio**	Oki Electric Industry Co., Ltd.
HANAMURA, Yasuaki**	Dept. of Earth & Planetary Sci., Kyushu University
ISEZAKI, Nobuhiro**	Department of Earth Sciences, Chiba University
ISHII, Teruaki**	Ocean Research Institute, University of Tokyo
KASAHARA, Junzo**	Earthquake Research Institute, University of Tokyo
KIM, Dong Sung	Ocean Research Institute, University of Tokyo
KINOSHITA, Hajimu**	Earthquake Research Institute, University of Tokyo
KITAHARA, Asako**	Department of Earth Sciences, Chiba University
KOIZUMI, Kin-ichiro**	Ocean Research Institute, University of Tokyo
KONO, Yoshiteru**	Dept. of Earth Sciences, Kanazawa University
KORENAGA, Jun	Ocean Research Institute, University of Tokyo
KUDO, Takeshi**	Dept. of Earth Sciences, Kanazawa University
MASALU, Desiderius C. P.	Ocean Research Institute, University of Tokyo
MATSUMOTO, Koji**	Ocean Research Institute, University of Tokyo
MOE, Kyaw Thu	Ocean Research Institute, University of Tokyo
MOCHIZUKI, Kimihiro**	Earthquake Research Institute, University of Tokyo
NAKANISHI, Masao**	Ocean Research Institute, University of Tokyo
NAKASA, Yukari**	Earthquake Research Institute, University of Tokyo
OGAWA, Yujiro**	Institute of Geoscience, University of Tsukuba
OGURA, Kazuya**	University of Telecommunication
OHTA, Suguru	Ocean Research Institute, University of Tokyo
SAYANAGI, Keizo	Ocean Research Institute, University of Tokyo
SHINOHARA, Masanao*	Ocean Research Institute, University of Tokyo
SUYEHIRO, Kiyoshi **	Ocean Research Institute, University of Tokyo
TAKAHASHI, Narumi*	Department of Earth Sciences, Chiba University
TAKEUCHI, Tomoyoshi**	University of Telecommunication
TAMAKI, Kensaku**	Ocean Research Institute, University of Tokyo
TANAKA, Toshiyuki**	Dept. of Earth Sciences, Kanazawa University
TOKUYAMA, Hidekazu*	Ocean Research Institute, University of Tokyo
WATANABE, Masaharu	Ocean Research Institute, University of Tokyo
YAMAMOTO, Fujio*	Ocean Research Institute, University of Tokyo

No Mark: From Tokyo (JuLy 17) to August 10 (Tokyo)
* : From July 17 (Tokyo) to July 27 (Kushiro)
**: From July 27 (Kushiro) to August 10 (Tokyo)

2. Index Map of Cruise KH 92-3 Leg 1
–Nankai Trough Upper Slope and ODP 808 Site

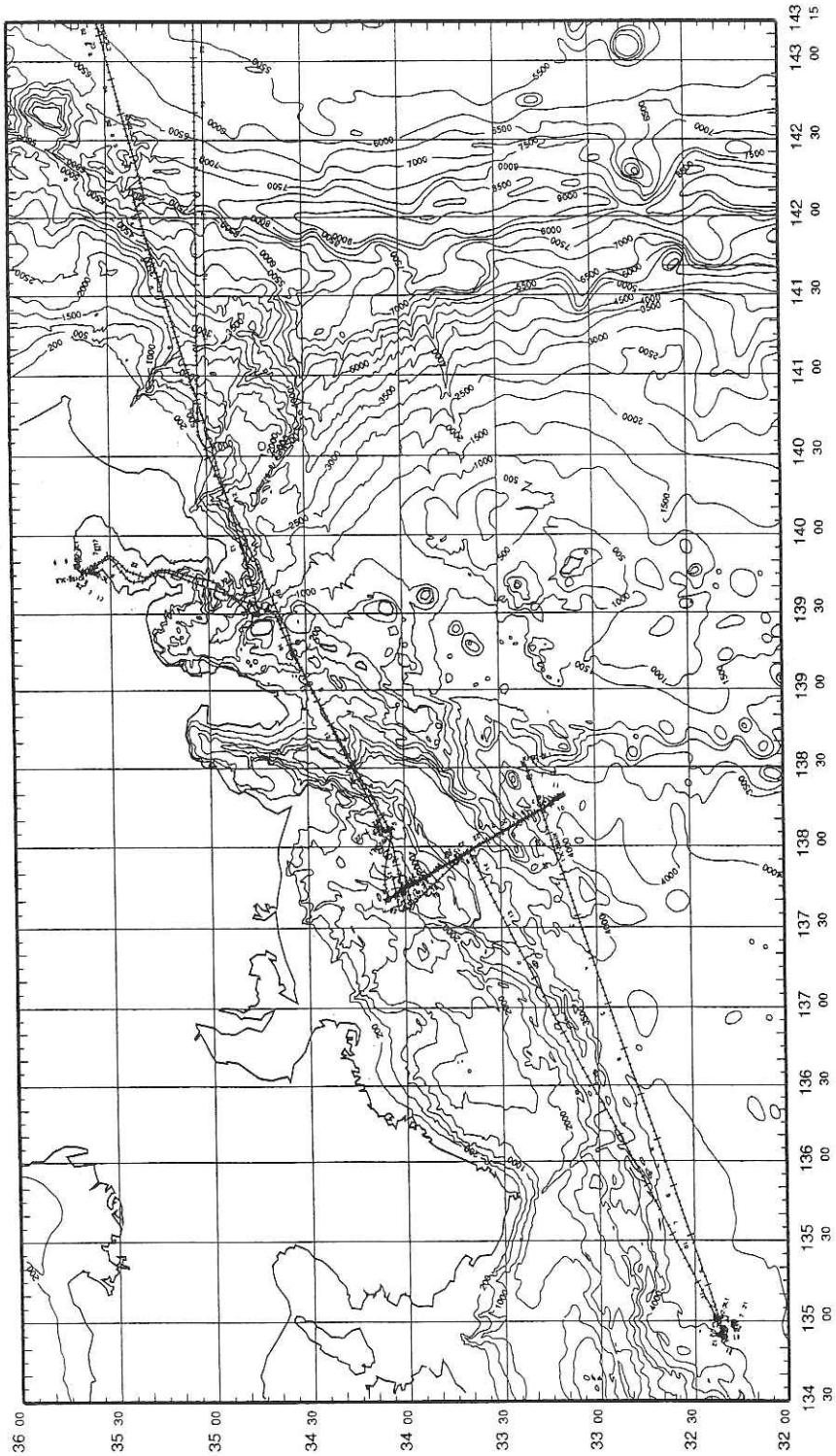

3. Index Maps of Cruise KH 92-3 (Leg 1 + Leg 2) – Survey Tracks for Joban Seamount Chain

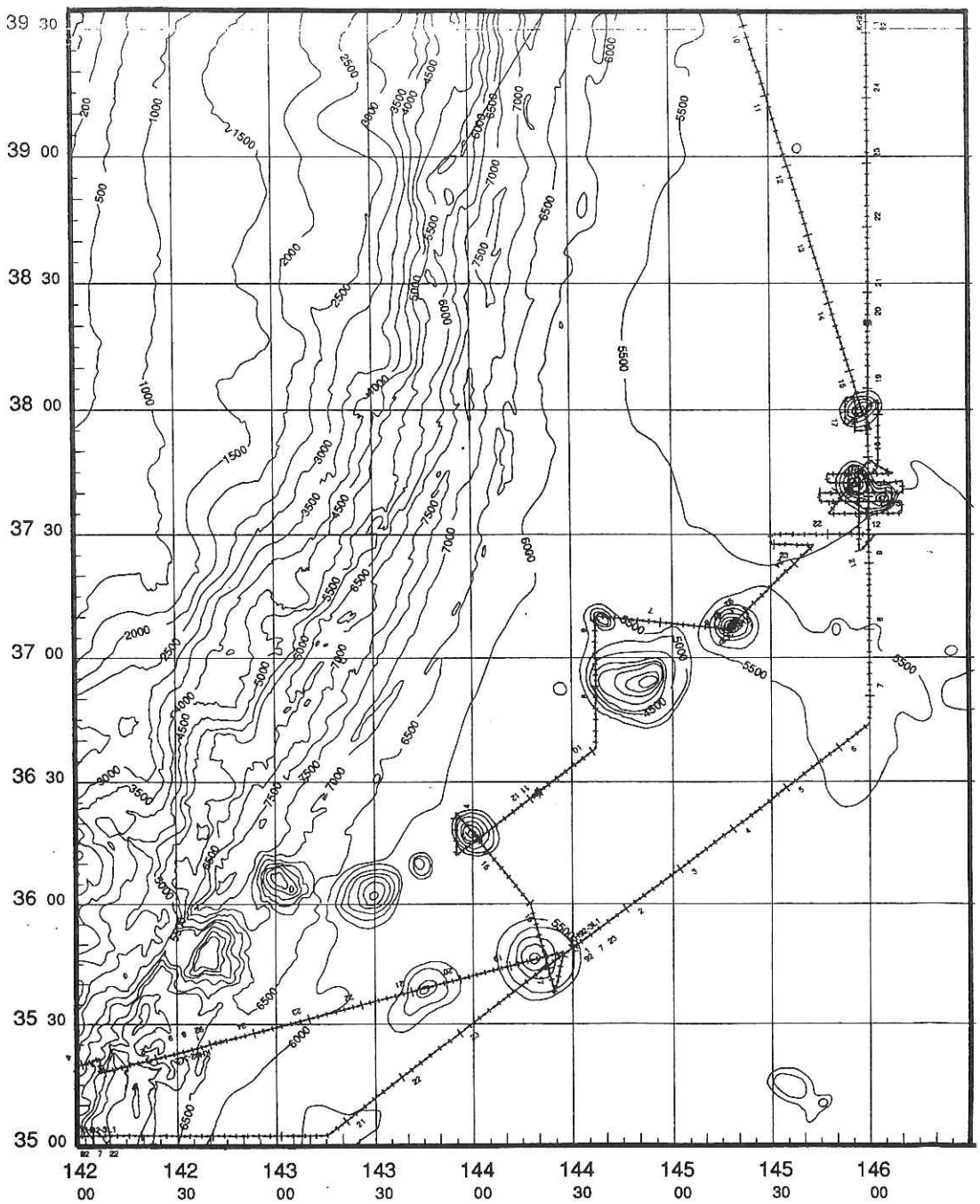

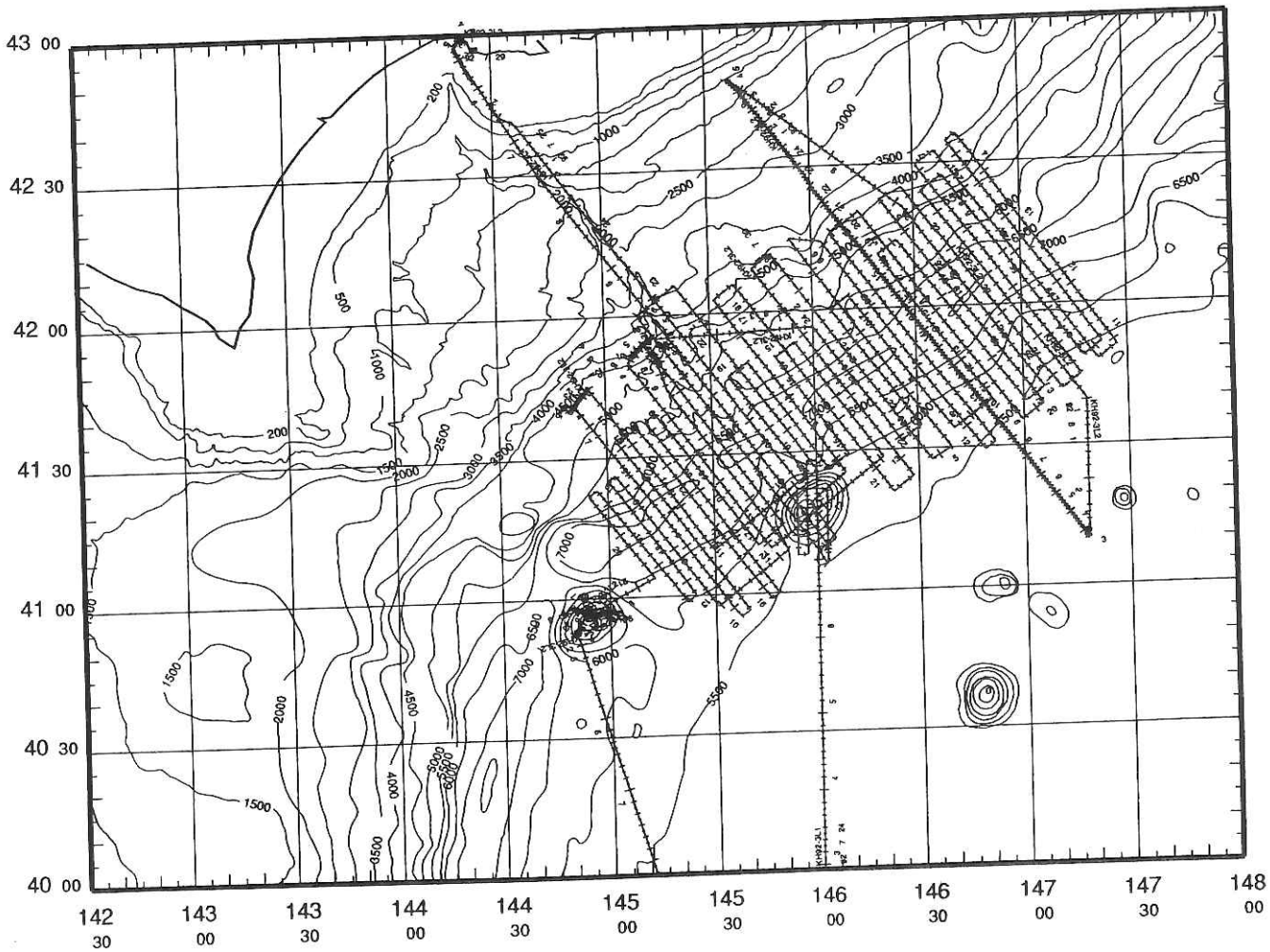

– Survey Tracks for Kuril Trench, Western Part

4. Outline of Nankai Trough Upper Slope surveyed by Cruise KH 92-3 Leg 1

K. Kobayashi, H. Fujimoto and J. Korenaga

The upper slope of the eastern portion of Nankai Trough was surveyed by multi-channel seismic profiler and deep-sea television system (DESMOS) installed on R. V. Hakuho Maru. A detailed seabeam map (Figs. 4-1; 4-2) was available by courtesy of Hydrographic Department, Maritime Safety Agency of Japan. In this cruise only small areas surrounding the target sites were investigated by our Sea Beam to confirm positions and to delineate detailed topographic features (Fig. 4-3). Since Hydrograhic Dept. charts use Tokyo Datum for geographic cordinates, whereas all of our descriptions and maps are based upon the WGS-75, minor difference of the positions between the two was inevitably recognized. The following descriptions in this reports are hereafter all according to our results using the former charts as a general frame-guide.

Most remarkable in the topographic features recognized in the charts and surveyed results is existence of steep escarpments trending in a direction roughly parallel to the axis of the eastern Nankai Trough and Suruga Trough. They appear to have been formed by horizontal compression accumulated in the crust deeper in the accretionary prism. Offset of the scarps is seen at about 34°00'N; 138°00'E. Topography indicating land slides are recognized at several locations.

In the operation of R. V. *Yokosuka* (directed by K. Kobayashi) with a research submersible *Shinkai 6500* taking place in May, 1992 immediately before the present cruise two dives (#116 and 117) by two French scientists, J.-P. Cadet and M. Fournier observed one of the scarps situated around 33°54.2'N; 137°45.6'E with water depths ranging from 2,500 to 2,000 m (Fournier and Cadet, 1992). The scarp trends N60°E and extends longer than 30 km. Strata identified dips a few degrees both at the bottom and at the top of the talus, increasing regularly to reach 40° at mid-slope. At mid-slope several cliffs with fallen blocks at the bottom and with erosional gully were seen, suggesting active tectonics. Only vestimentiferan tube worms and galatheids were found at a depth of 2,260 m, although no clam communities indicating fluid seepage were discovered by the submersible.

The investigation by DESMOS in the present cruise, Leg 1 aimed at examining other scarps and searching for clam communities. As described in Chapter 17 of this report, we found small clusters of clams with many dead shells, indicating nearby occurrence of a living community. In addition the floor in accretionar wedge around the ODP site 808 was also surveyed (Fig. 4-4) and observed by DESMOS operation no. 2 for the purpose of locating and observing present status of the acoustic transmitter deployed beside the drilled hole for the downhole temperature measurement, although we were unable to find it.

References

Fournier, M. and J.-P. Cadet, Inner eastern Nankai accretionary wedge, *Paper presented at the 9th Shinkai Symp., Dec. 1-2,'92*, JAMSTEC, 108-111, 1992.

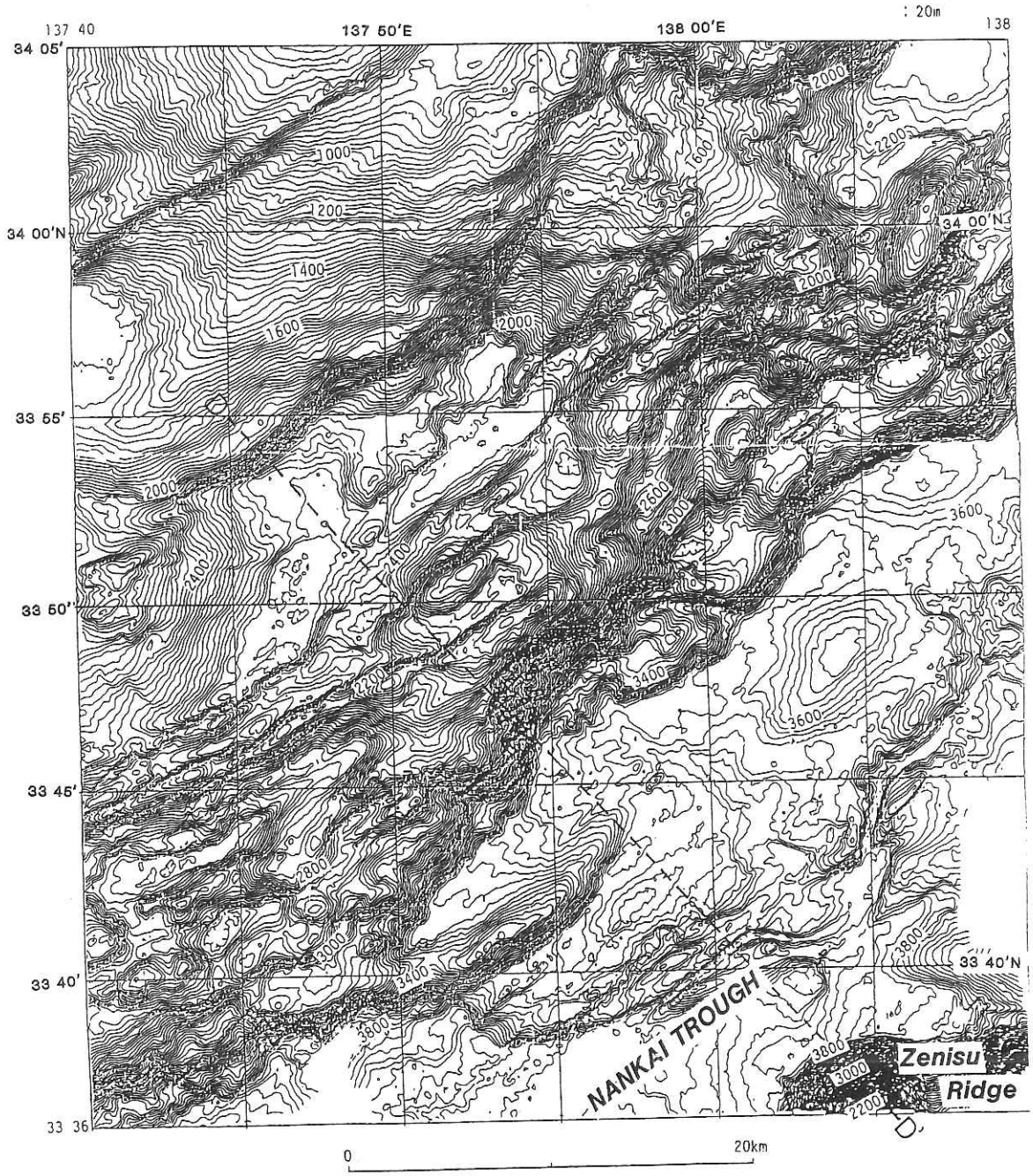

Fig. 4-1. Seabeam map of the eastern Nankai Trough upper slope region made available to the present cruise by courtesy of Hydrographic Department, Maritime Safety Agency of Japan. A line indicated by D–D' denotes a part of the lines for multi-chnnel seismic profiling in this cruise.

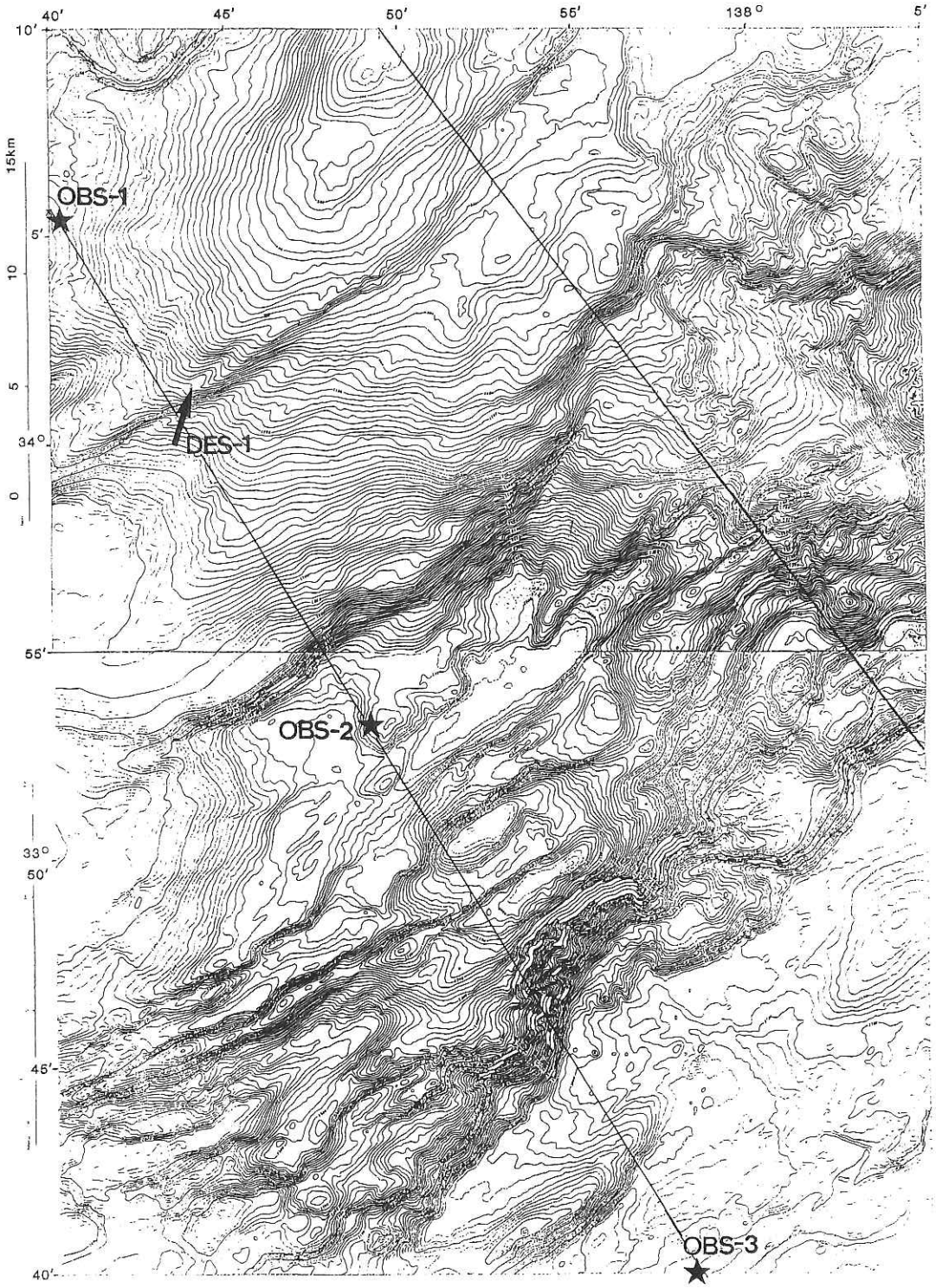

Fig. 4-2. Seabeam chart combined from a set of three maps for topography off Enshu-nada with contour interval of 20 m published by Hydrographic Department, MSA of Japan (1992).

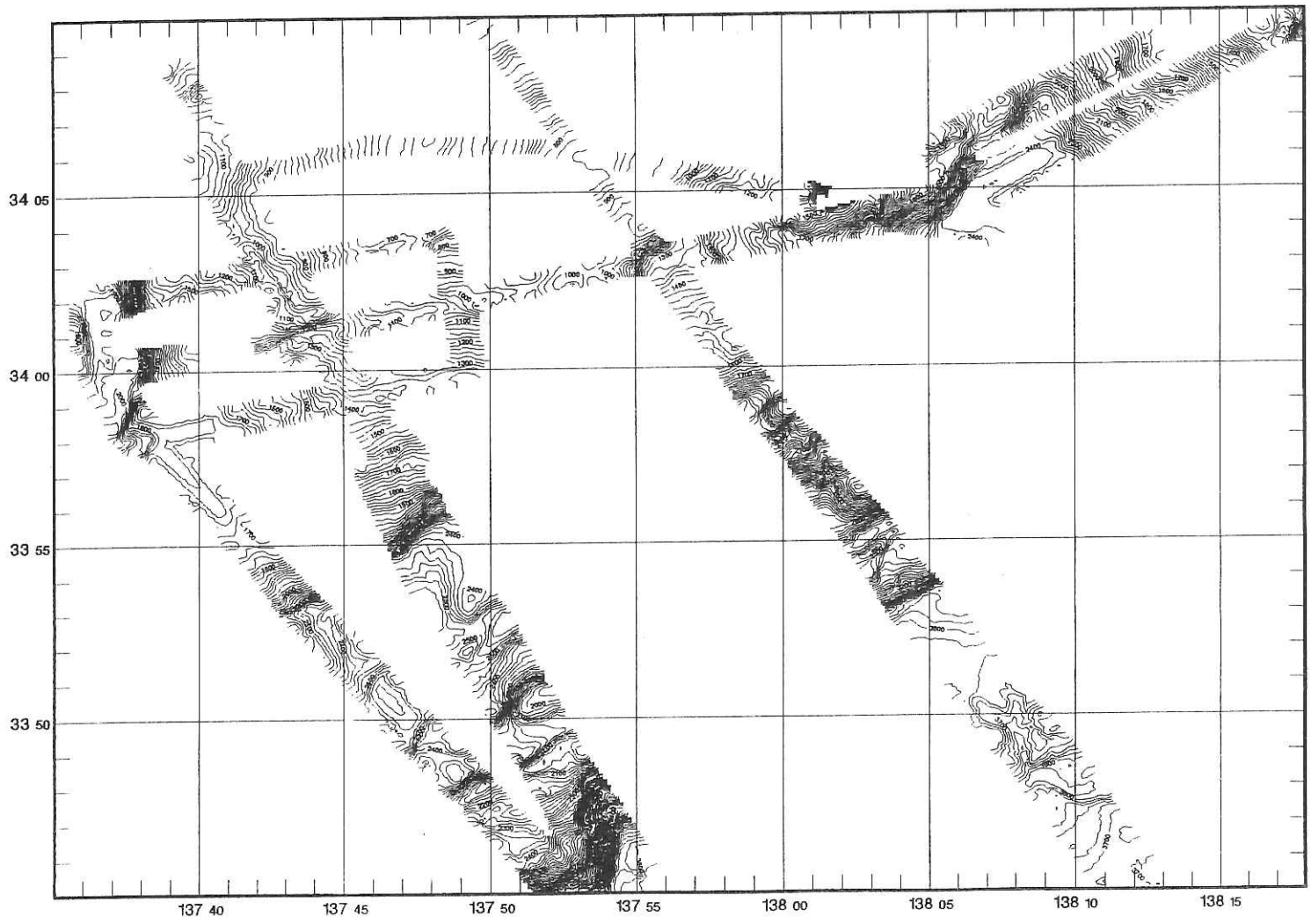

Fig. 4-3. Bathymetric plots from Seabeam for DESMOS and OBS sites during Leg 1 of this cruise.

KH92-3 Leg 1: DESMOS site 2

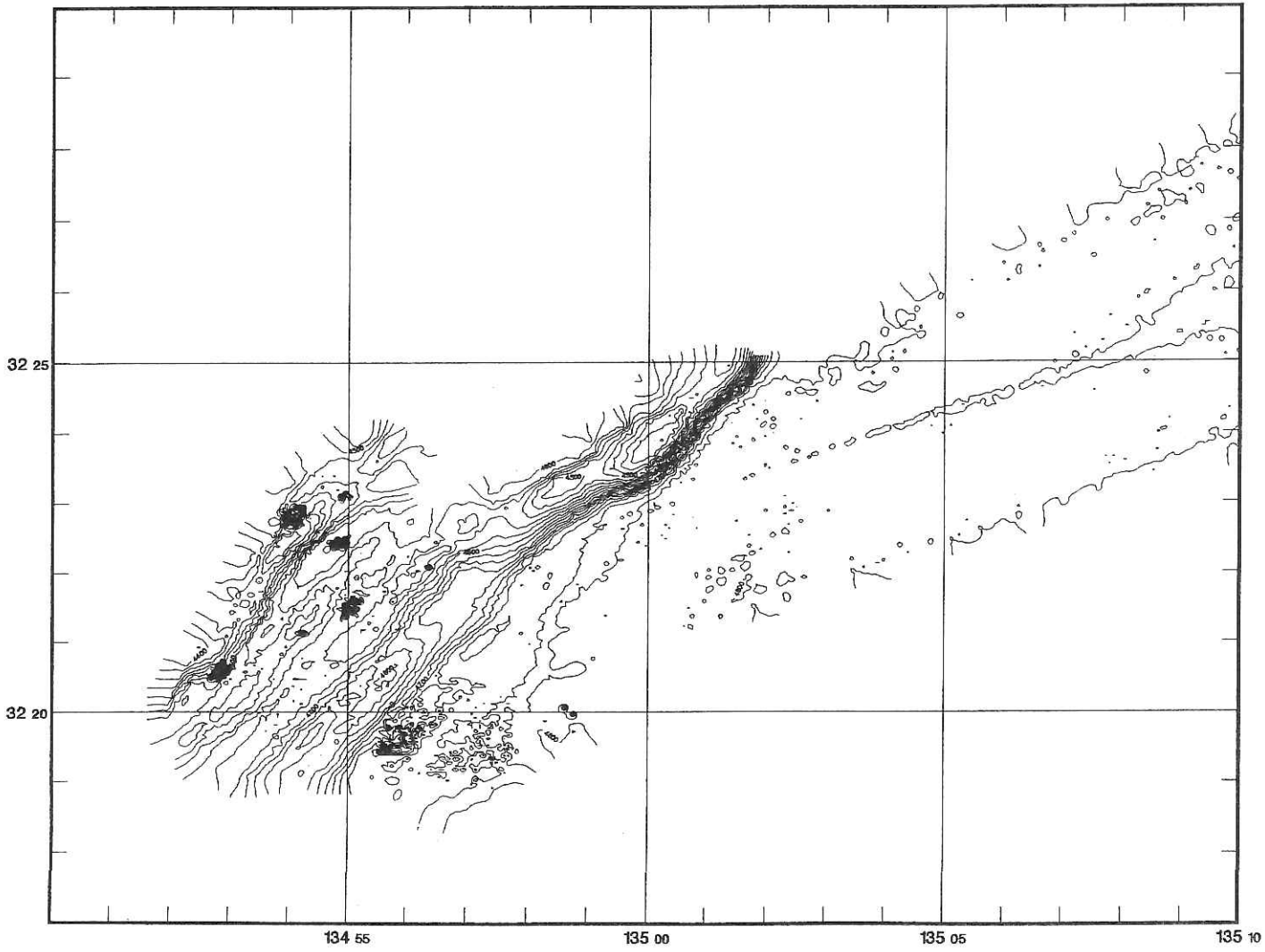

Fig. 4-4. Bathymetric plots from Seabeam for DESMOS at ODP site 808 during Leg 1 of this cruise.

5. Topography of the Western Part of the Kuril Trench off Hokkaido based on the Sea Beam Map and 3.5 kHz Profiles

Y. Ogawa, K. Kobayashi, K. Tamaki, Moe Kyaw Thu and Y. Hanamura

Introduction

During Leg 2 of KH 92-3 cruise of Hakuho Maru, we surveyed the westernmost part of the Kuril (Chishima) Trench area south off eastern Hokkaido (Fig. 5-1) using the Sea Beam (multi-narrow beam echo sounder) and a 3.5 kHz subbottom profiler. The same area (around Takyou-Daiichi Seamount and Kushiro Canyon) was partially surveyed in the later period of Leg 1 of the same cruise. In the present report we will summarize general characteristics of the topography based upon combined data with special attention to topographic lineaments and their tectonic significance. The mapped area is surrounded by four points; 40°50'N, 144°50'E; 40°50'N, 147°30'E; 42°40'N, 147°30'E and 42°40'N, 144°50'E (Figs. 5-2 and 5-3). The ship's tracks are mostly in a direction to NW or SE, normal to the general trend of the Kuril trench (N60°E). They are mostly spaced with 2.5 nautical miles (4.5 km) which provide full coverage of swath bathymetry for the axial zone of the trench. The tracks are conventionally numberd from 1 to 44 from SW to NE (Fig. 5-2).

Topography

Fig. 5-3 represents topographic map of the whole area with contour interval of 20 m. Two charts covering the same area with a scale of 300,000 and contour interval of 10 m are attached in the back pocket of this report as foldouts. The survey area is divided into three parts; the trench oceanward (outer) slope on the Pacific plate, the trench axis and the trench landward (inner) slope situated on the North America plate. The relative convergence rate between the subducted Pacific plate and the landward North America plate in this region is 8.57 cm/yr in a direction of 297.9° (about N62°W) according to the model Neuvel One (DeMets *et al.*, 1990) (indicated by a big arrow in Fig. 5-4). General topographic cross-section is best observed in the 3.5 kHz profile on line #32 taken during the multi-channel seismic survey when the ship speed was at about 5 knots (Fig. 5-5 as a foldout).

Fig. 5-6 summarizes the topographic lineaments in the landward slope in A, and those in the oceanward slope in B. The data were taken from the Sea Beam map (foldout-1), whose contour interval is 20 m. In this diagram, NO means the direction of the relative plate convergence after the Neuvel One, T is trend of the trench axis, M is mode (the maximum peak) of the lineaments. ML in B is the magnetic lineations on the Pacific plate in this area after Nakanishi *et al.* (1989 and also Chapter 8 of this report).

Oceanward slope

The trench oceanward slope is about 5,100 m deep in its shallowest part on the outer swell, in which several seamounts are known around the surveyed area

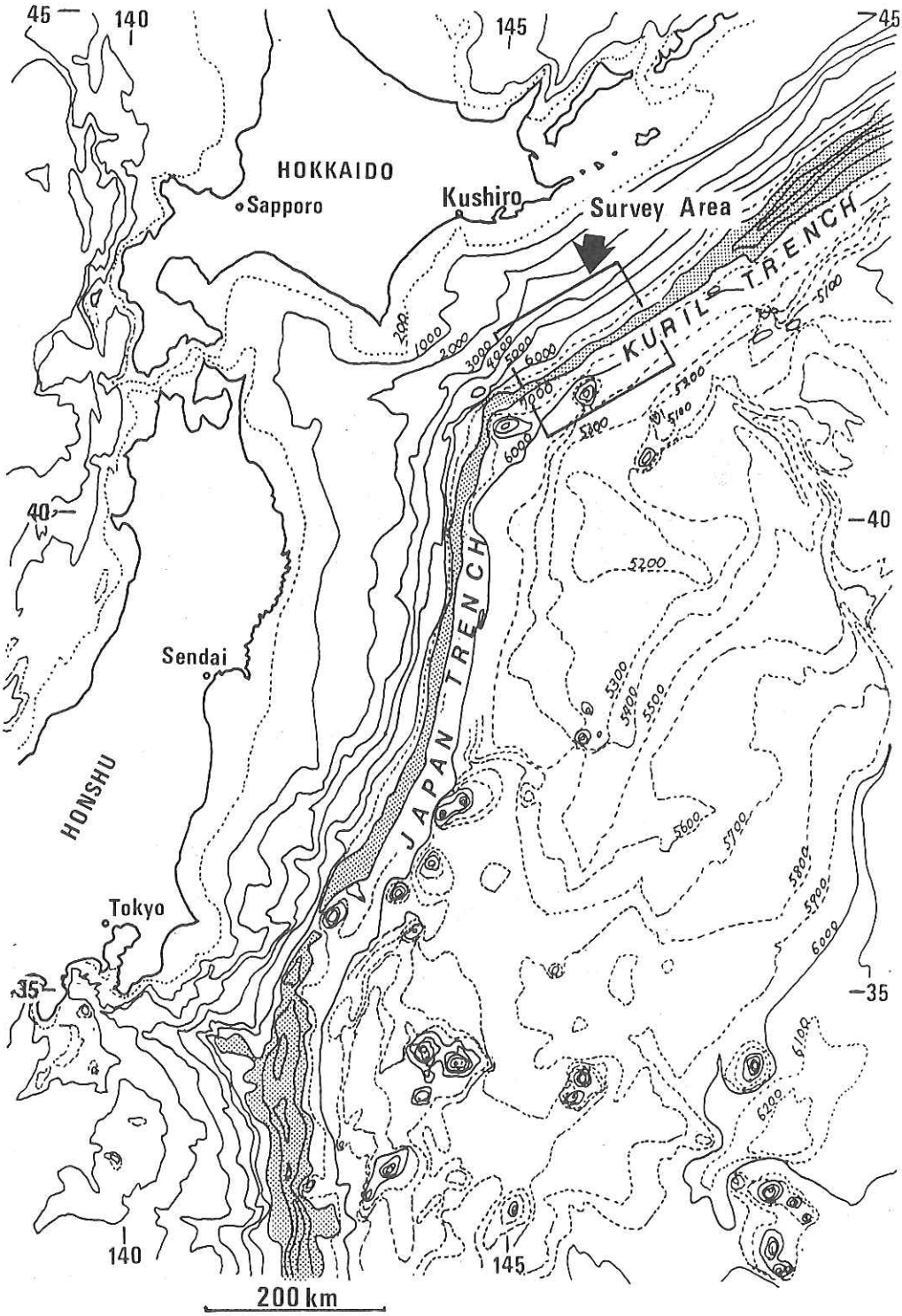

Fig. 5-1. Index map of the survey area from Mammerickx *et al.* (1976).

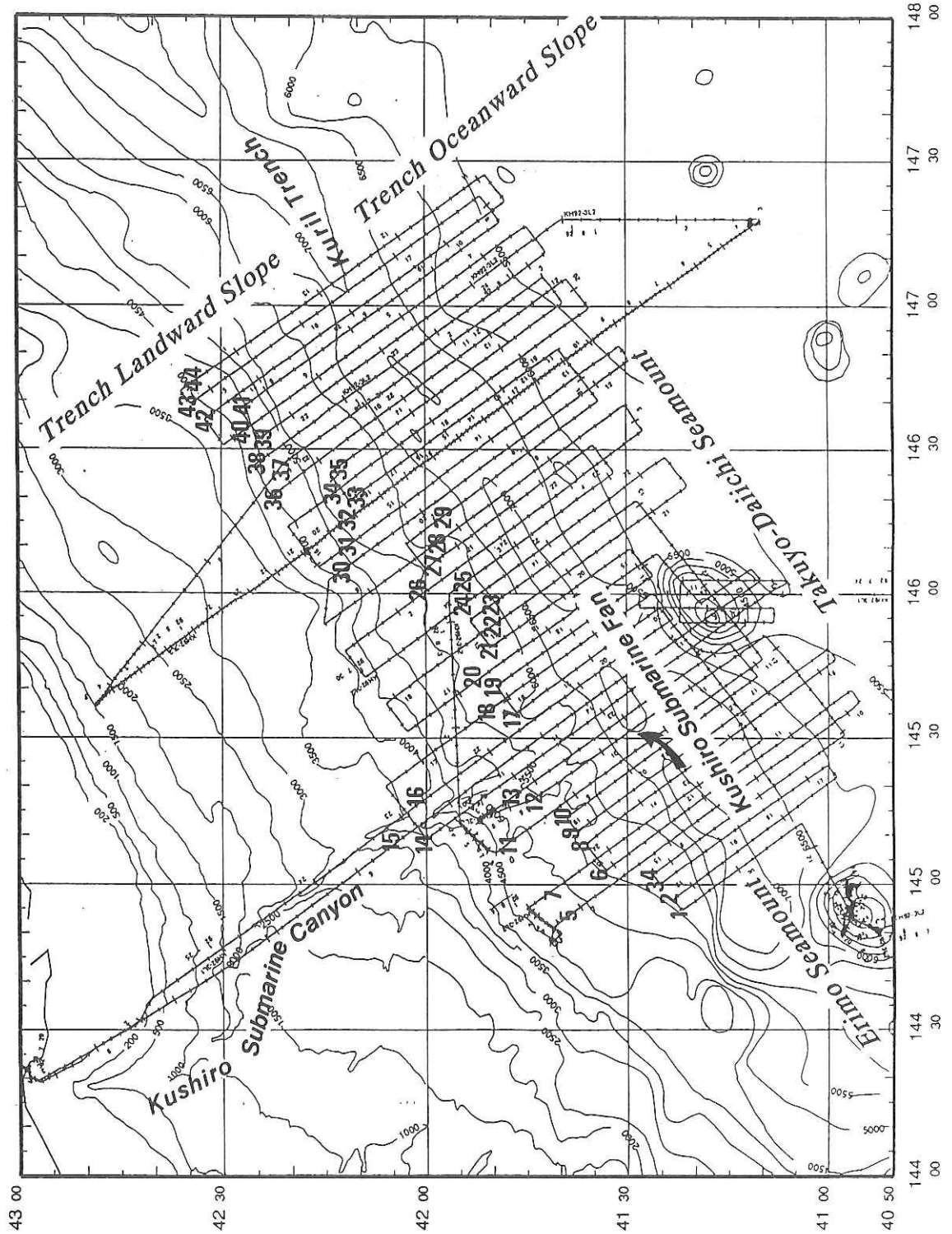

Fig. 5-2. Ship's tracks in the survey area.

(Fig. 5-1). The oceanward slope is about 70 km wide. Its dip is less than 1 degree on the upper slope, and it rapidly increases to 5 degrees through 3 degrees in the middle and lower slopes (Figs. 5-3, 5-4). A large seamount, Takuyo-Daiichi Seamount, 40 km long to NE, and a few small knolls are situated on the slope. One small knoll with diameter of 5 km, named the Mashu Knoll in this report, is situated 55 km NE of the Takuyo-Daiichi Seamount, whereas one very small knoll, 3 km in diameter, called the Kamuishu Knoll in this report, is located just on the trench side in 142°52'E. These knolls appear to be aligned in one direction of NE, suggesting some tectonic significance such as the trace of a hot spot or a tectonic fissure activated at a certain geological period (also see Chapter 8 of this report).

The most characteristic topographic feature of the oceanward slope is the distinct lineaments trending N65° to 70°E (Fig. 5-5. B). This is definitely controlled by the horst and graben structures, or sometimes better called ridge and trough structures. These structures best follow the magnetic lineaments of the same direction (ML in Fig. 5-3. B). The magnetic anomalies around the Kuril trench off Hokkaido correspond to the isochrons M6 to 9, correlatable to Hauterivian to Barremian of Early Cretaceous around 120 MaBP.

According to the 3.5 KHz profile in the middle of the survey area (Fig. 5-3), small normal faults begin to be observed around 5,400 m in depth in the upper slope (A and B in Fig. 5-5), suddenly largely dislocated around the depth of 5,900 m (C in Fig. 5-5). The largest dislocation can been seen in the lower slope with 500 m, then the horst and graben structures become distinct. The horst and graben structure is composed of fairly sharp ridges and troughs, asymmetrically arranged by normal faults dominantly dipping trenchward. The distance between the horst and graben varies from 1 or 2 km to 5 or 6 km. Measuring from the oceanward to the trenchward, the distance from the graben to the horst is far shorter than the distance from the horst to the graben, corresponding to the dominance of the above mentioned trenchward dipping normal faults (C in Fig. 5-5). The horsts and grabens are generally 20 to 50 km long.

The seamount and knolls, particularly the Takuyo-Daiichi Seamount, are not drastically dislocated by these normal faults unlike the Erimo or Daiichi-Kashima Seamounts faulted down toward the trench axis. The moat of each seamount is dislocated by faults, but offsets are not so remarkable in the seamount bodies themselves. However, it is recognized in bathymetric map (Fig. 5-3) that shape of the Takuyo-Daiichi Seamount is elongated in a direction to the lineaments. Whether it is the primary topographic feature formed at the time of eruption or the secondary structure caused by faulting at the trench region will be an interesting task to be solved.

Sediments in the ocean floor in the upper slope are transparent in 3.5 KHz profiles, and seem to be pelagic with some ash layers. In the trough part of the horst and graben structures no other significant sedimentes are seen except for

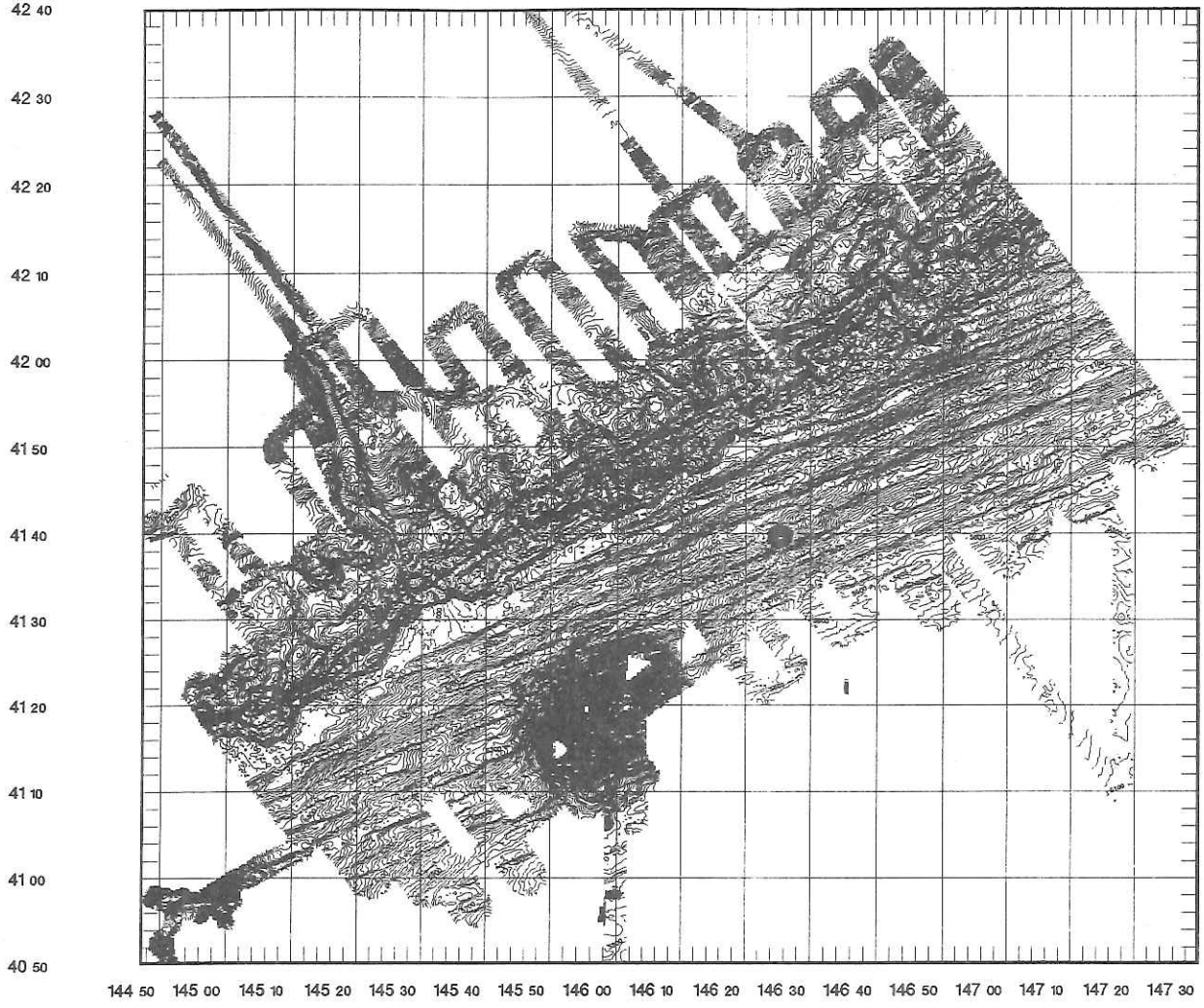

Fig. 5-3. Sea Beam map of the western Kuril Trench south off Hokkaido with contour interval of 20 m. Two charts of bathymetry for the same area are attached as the foldout 1 on the backcover.

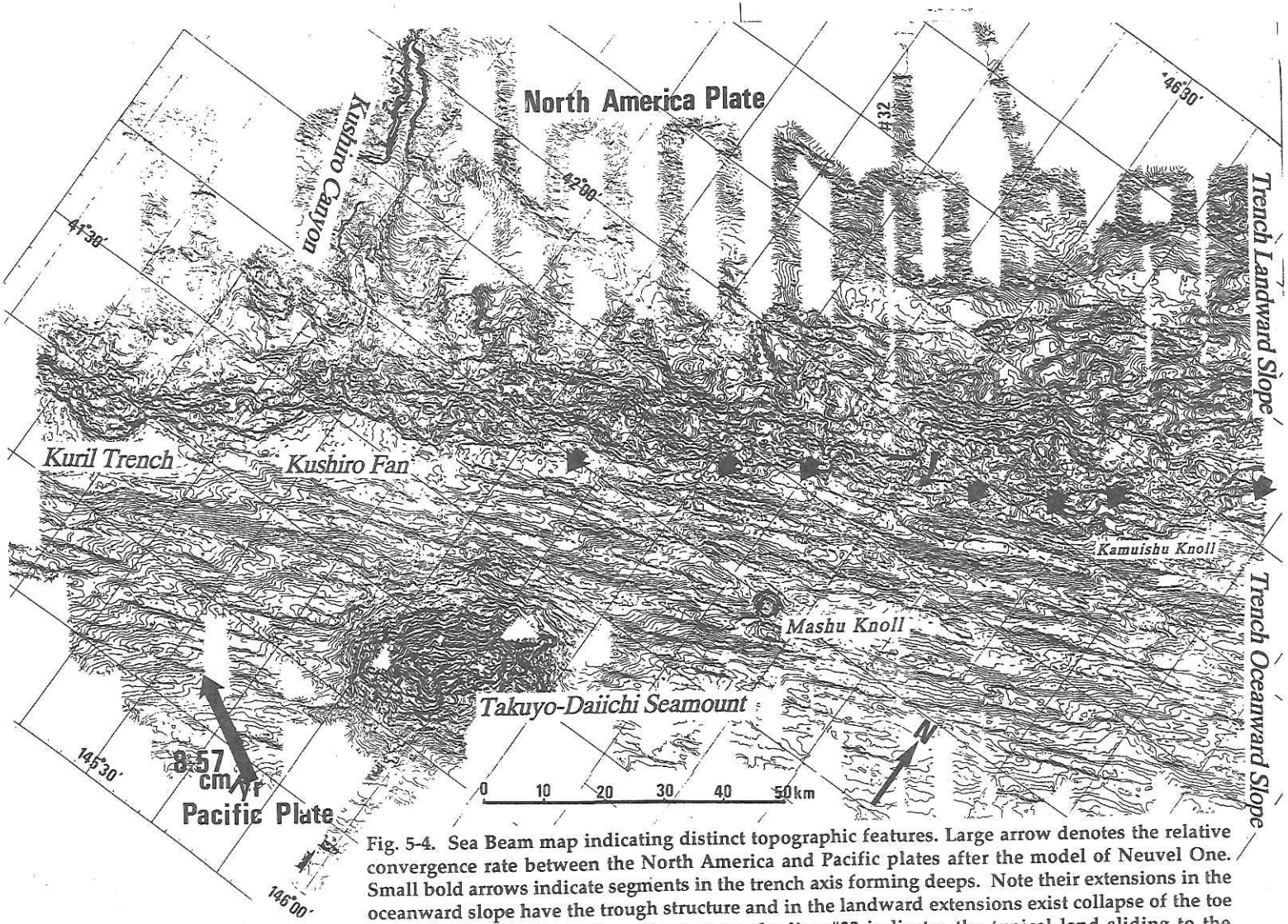

Fig. 5-4. Sea Beam map indicating distinct topographic features. Large arrow denotes the relative convergence rate between the North America and Pacific plates after the model of Neuvel One. Small bold arrows indicate segments in the trench axis forming deeps. Note their extensions in the oceanward slope have the trough structure and in the landward extensions exist collapse of the toe of the landward slope. Curved arrow on the line #32 indicates the typical land sliding to the trench.

some benches near the foot of the trench in the lower trench oceanward slope, where a flat reflective surface is seen in the profiles, suggesting to be ponded by terrigenous sediments as in the profiles #11 to 13 of Fig. 5-7 as mentioned later.

Trench Axis

The axis of the Kuril trench trends N60°E with its depths ranging from 7,000 to 7,200 m. The trench floor is segmented into several individual zones of about 30 to 50 km in length, and about 4 to 5 km in width. These trench segments are aligned in *en echelon* fashion, trending about N72°E (TS in Fig. 5-6. A). This trend is about 12° clockwisely oblique to the general trend of the trench axis. The former is quite parallel to the trend of the horst and graben structure in the oceanward slope (Fig. 5-4). General morphology of the trench axis indicates that the axial zone is still much affected by the structure of the oceanward slope.

As the grabens are rarely buried by terrigenous sediments, the original topography of the oceanward slope commonly remains in the axial zone, and the toe of the trench landward slope is apt to be collapsed into the graben in the axis. It is clearly shown in the Sea Beam map (Fig. 5-3), in which bold arrows indicate the graben in the trench axial zone. This configuration is best represented in the profile of 3.5 KHz (#32) taken during the multichannel seismic survey (D in Fig. 5-5, also indicated by a curved arrow in Fig. 5-4). Large-scale collapses of the toe of the landward slope into the trench axis form a number of knolls caused by slumping. Similar topography is seen in the frontal area of the landward slope in the Sea Beam map (Fig. 5-3) and also recognized in the Multi-channel seismic profile reported in Chapter 16 of this report. Similar morphology has been reported with the Japan Trench area off Miyako by KH 90-1 cruise (Kobayashi, 1991).

Several representative profiles of the trench floors are compared from SW to NE in Fig. 5-7. All of the trench floors are surrounded with steep scarps on both ocean and landward slopes, which have dips of 10° to 15°. Some benches on foot of the oceanward slope are ponded by thin flat sediments, most of which are rather reflective, suggesting their terrigenous origin. In contrast the sediment in the trench floor is much thicker, although not so thick as to completely bury the horst and graben structure in the oceanward slope. Judging from the reflection and transparency in the profiles, it does not seem to be highly coarse. It is relatively fine to be mud or clay with some ash layers, except for the case around the Kushiro Trench Fan, as mentioned later, where coarse and thick sediments bury the grabens in the trench axis (Figs. 5-8 and 5-9). A small ridge which is the extension of the horst is now being buried by the trench fan sediments (Fig. 5-7, line # 15).

Actually, by examining the profiles across the trench carefully, the surface of the axial floor is inclined landward with a very shallow dip. This is due to the landward tilting of the trench axis during sedimentation by means of downgoing slab of the Pacific plate. In the trench sediments, small-scale dislocation or

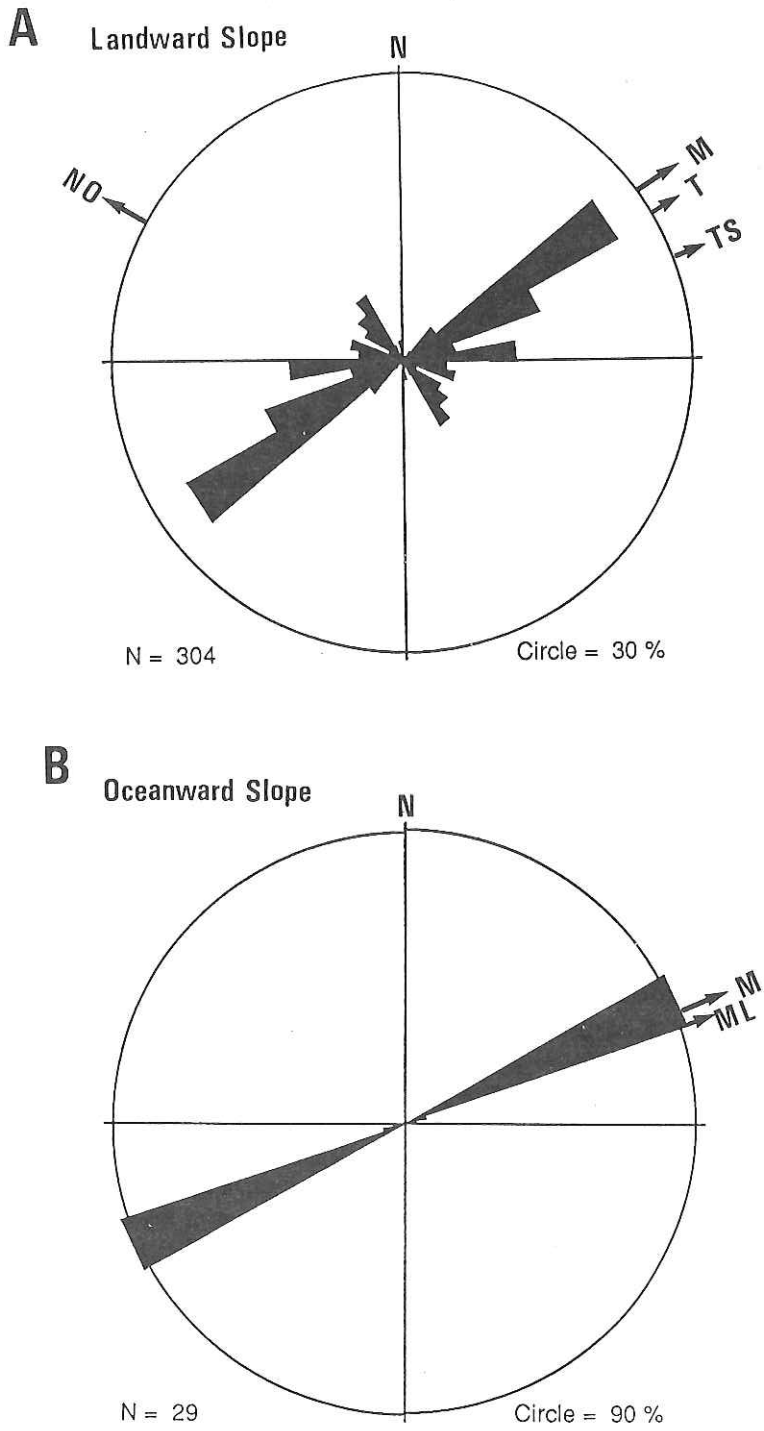

Fig. 5-6. Rose diagrams of lineaments in the landward slope (A) and those in the oceanward slope (B). NO; Plate relative convergence after the model of Neuvel One, M; mode of the lineaments, T; General trend of the trench axis, TS; Representative trench segment direction, ML; Magnetic lineament after Nakanishi *et al.* (1989).

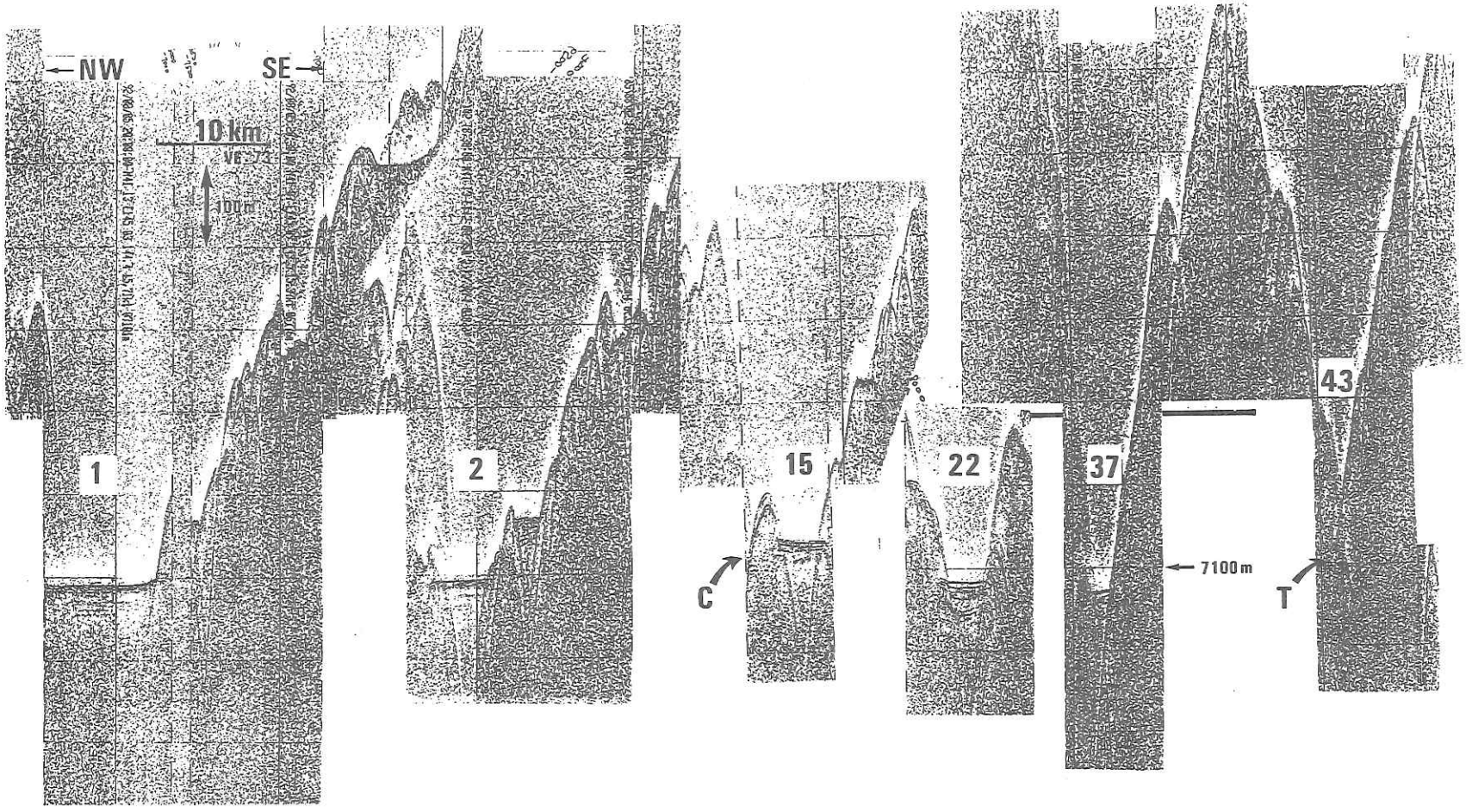

Fig. 5-7. 3.5 KHz profiles of the trench area. In all profiles left is NW. Numbers are assigned to the lines of 3.5 KHz profiles from Fig. 5-2. Curved arrow with C in #15 is the channel from the northeastern corner of the NE Kushiro Fan, and that with T in #43 is the deepest part of the trench. Vertical exaggeration is 73.

warping is recognized, probably due to the deformation. In the case of the examples along lines # 15 and 22, the dislocation appears very likely to originate from the still active normal faulting, probably responsible for generation of the horst and graben structure. No evidence for thrusting and folding characteristic with formation of an accretionary prism has been found in these sections.

In contrast to general features of the flat trench floor, some exceptions are seen at which no sediments cover is identified. For example, the deepest part in the profiles # 32 and 43 is neither flat nor ponded but very rough. In case of # 32, it is even dipping landward, still keeping the characterestis of the oceanward slope. Here exists still the trench oceanward realm, but the oceanward slope is directly subducted without any sedimentation.

Kushiro Fan and Kushiro Canyon

In addition to the ordinary cases of the trench floor mentioned above, Figs. 5-8 and 5-9 show different nature of the trench floor in the mouth of the Kushiro Canyon, where a remarkable trench fan is formed. The fan, called the Kushiro Fan in this report, represents a typical fan shape, about 10 km in radius with thick clastic sediments (Fig. 5-8). These sections show distinct features of relatively steep oceanward dipping floor with some channels and upward concave undulation in contrast to usual flat trench floors . This undulation may be due to thrusting and folding by horizontal compression. Sediment reflectors are stronger than the other examples in Fig. 5-7, suggesting coarser clastic sediments in this fan area. The terrigenous clastics, probably not too coarse but of silt to fine sand sizes, are derived from the Kushiro Canyon to the trench fan, while no such sediments are transported to the usual segmented trench floors.

The tributary channels of the fan are recognizable in its west and east, but they are not connected to the Kushiro Canyon as mentioned later in this report. This means that the fan is no active at present, as in the case of the Mogi Fan in the Boso triple junction area (Soh *et al.*, 1988).

The Kushiro Canyon can be traced in Fig. 5-8 as denoted by bold arrows. It meanders in the lower slope. However, if we see it carefully, this canyon has no mouth to the trench. Instead the present canyon is connected to the trench floor, through a narrow channel in the innermost part of the trench floor (shown by a curved arrow in Fig. 5-8 and by a curved arrow C in # 15, Fig. 5-7) in the eastern side of the main Kushiro Canyon. It is denoted by narrow arrows in Fig. 5-8. This can be traced upward to the slope, and then merely merges to the main canyon. The present channel of the Kushiro Canyon erodes the small canyon, implying that the past small canyon shown by the narrow arrows had been the main canyon before the present Kushiro Canyon became the main thalweg.

The mouth of the present Kushiro Canyon is bent in S-shape, and its estuary is choked by a small ridge in the toe of the landward slope (Fig. 5-8). The fan has no conduit for clastics, suggesting that the fan is not active at present. This is partly

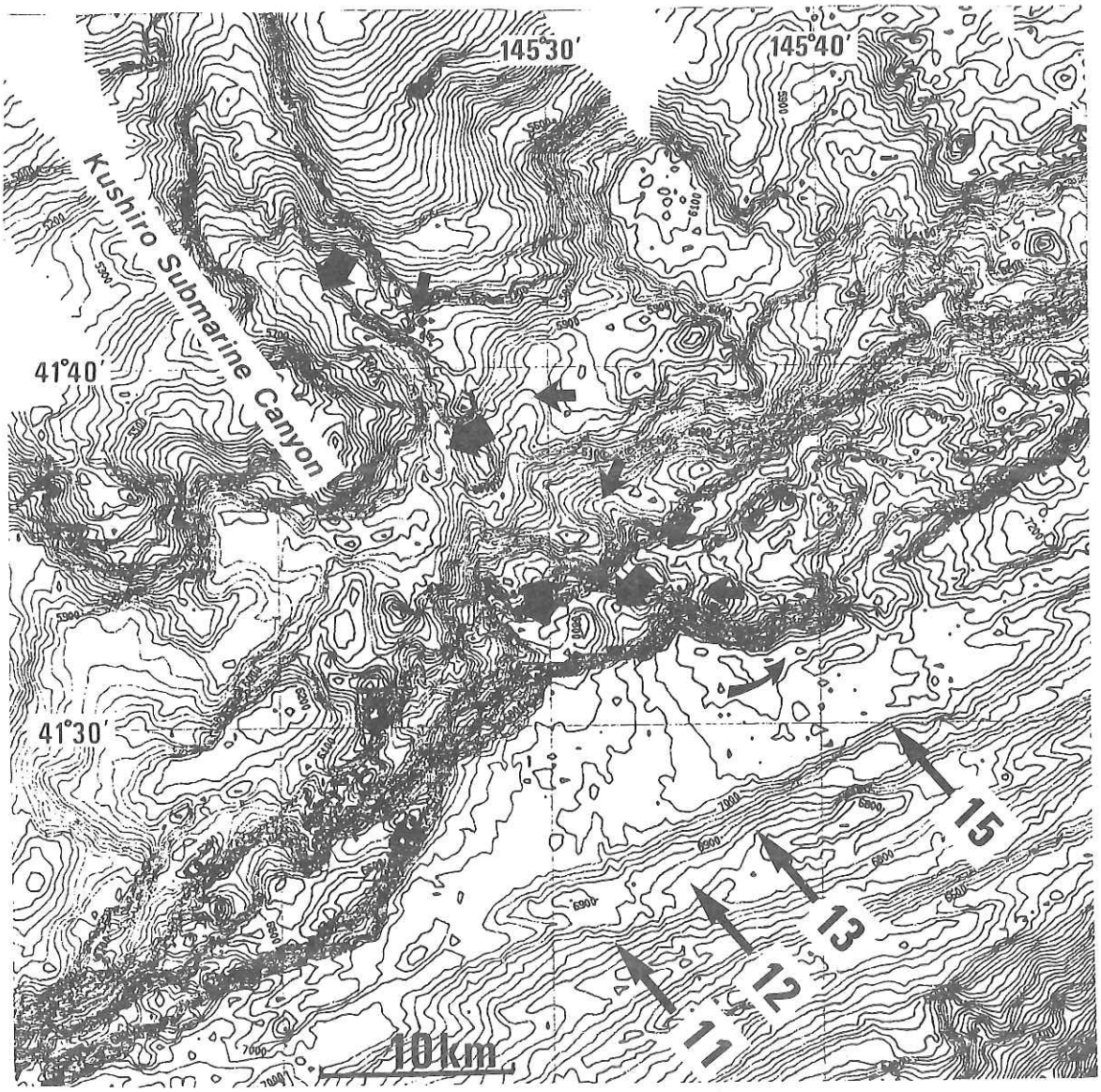

Fig. 5-8. Sea Beam map around the Kushiro Fan. Numbers are to the lines of 3.5 KHz profiles in Figs. 5-6 and 5-8. Bold arrows trace the main Kushiro Canyon, and small arrows trace the small canyon. Curved arrow in the trench area is the channel from the small canyon.

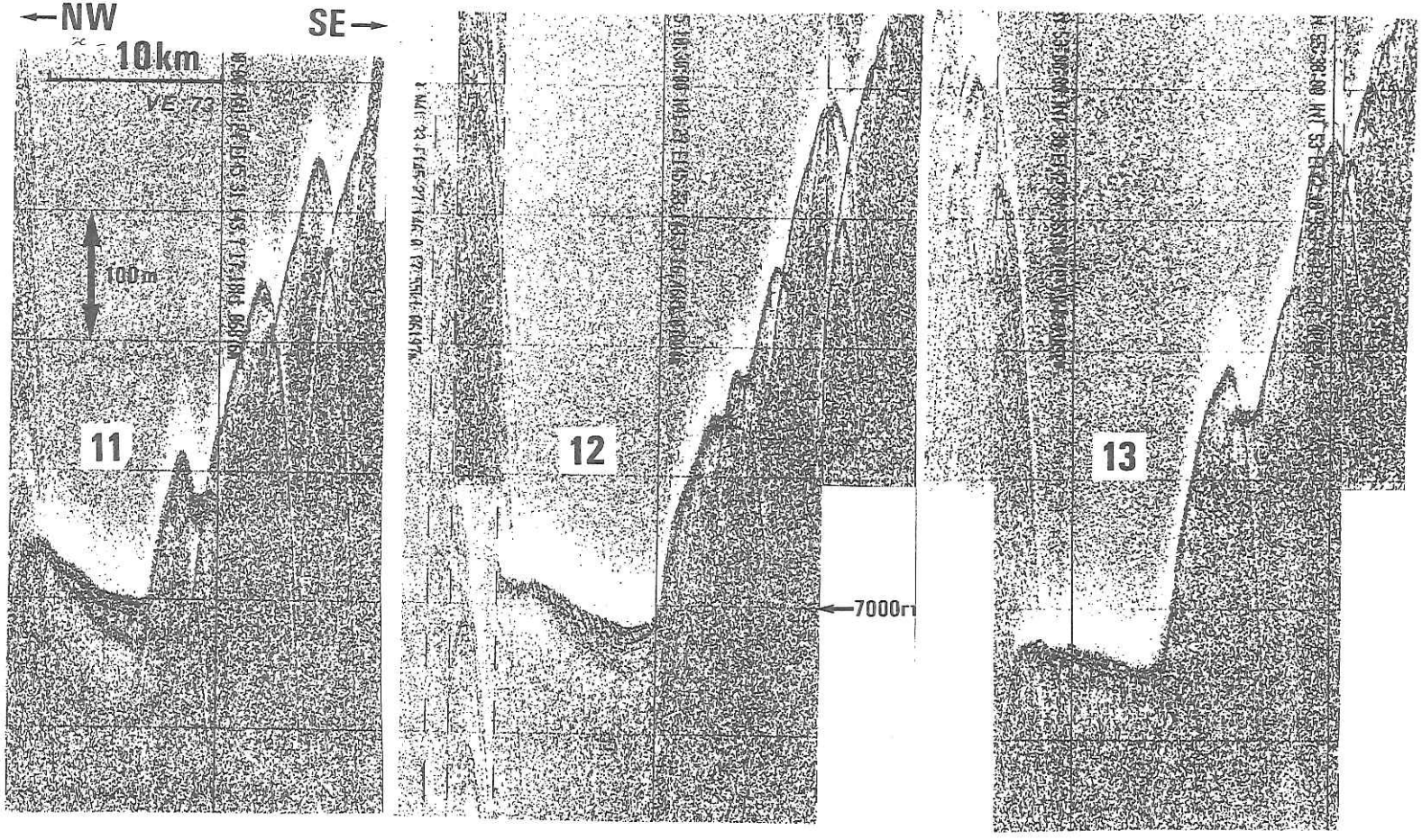

Fig. 5-9. 3.5 KHz profiles of the Kushiro Fan area. In all profiles the left is NW. Vertical exaggeration is 73.

due to the dam-up effect probably caused by accretionary process of the fan deposits, and partly owing to the strike-slip dislocation between the trench and landward slope; between the Pacific and North America plates. This problem should be more critically considered in future.

The Kushiro Canyon is one of the largest submarine canyon around the Japanese Islands. It was very extensively mapped during the present cruise. The lower part is described above. The trap or competition of the channels is considered as mentioned above. The direction of the canyon is approxmately at right angle to the trench, so that the origin of the canyon might be gravitational. Around the canyon many submarine slidings parallel to the canyon direction are seen. The trenchward cancave topography or indentation in the lower slope is very common as mentioned next. Therefore, the origin is corelatable to this gravitational collapse of the trench lower slope.

In a large bathymetric map (Mammetrichx *et al.*, 1976) as well as the precise magnetic anomaly chart of the Northwestern Pacific (Nakanishi *et al.*, 1989), there is no fracture zone recognized to be subducted under the Kushiro Canyon at present. An elongated topography called the Nakwe Channel which joins the Nosappu Fracture Zone at its northern end cuts the Kuril Trench at a site further east. Therefore, the Kushiro Canyon is not directly correlatable to ongoing subduction of any oceanward offset. It may be plausible that an ancient topographic anomaly such as a seamount chain initiated the structure on the landward slope which has been inherited in the present features.

Landward slope

The trench landward slope is about 150 km wide upto 1,500 m in depth, where a very gentle slope bigins further landward. The landward slope is divided into three; the lower, middle and upper, each has each characteristic features. The lineaments on the landward slope are summarized in the rose diagram in Fig. 5-6-A.

The lower slope; about 30 km wide, from 7,200 to 5,500 m deep, has the average dip of about 15°, but locally much steeper. This slope is characterized by many ridges or domes and troughs or depressions, shown by overlapped parabolic reflectors in the 3.5 KHz profiles (Fig. 5-5), due to many irregular hummocky topography in the Sea Beam map (Fig. 5-3). Similar topography is also recognized in the northern Japan Trench as reported by Kobayashi (1991).

Most dominant steep slopes in the toe of the slope trend about N68°E, roughly parallel to the trench direction (T and M in Fig. 5-6. A, respectively). Another dominant trend is east-west. In the upper part of the lower slope, some steep slopes trend not exactly parallel to the trench direction but slightly oblique to the trend of N55°E. We do not know the reason for the diversity of the trench parallel or sub-parallel lineaments. However, those in the lower part are not exactly straight but convex trenchward, particularly in the toe area of the lower

slope. This might reflect low angle oceanward verging thrust faults, forming a listric fashion. Such listric thrusts are common in the toe area of the Nankai accretionary prism off Omaezaki (Iwabuchi *et al.*, 1991; Chamot-Rooke *et al.*, 1992).

On the other hand, the strong lineaments with directions subparallel to the trench axis exist in the upper part of the lower gentle slope and are not convex to the trench side but rather straight or even concave to the trenchward. The straight lineaments seem be caused by high angle thrusts, and the trenchward concave topography must be due to submarine sliding as described later.

As seen in the SeaBeam map, the former dislocates the latter. The trenchward concave structure is also seen in the toe part of the lower slope as a gravity collapse to the graben structure in the trench as already mentioned previously. The indatation is commoly observed as well as trenchward convex curve, suggesting both thrusting and gravity sliding (or normal faulting) coexist in this toe area. These two are also recognized in the Nankai accretionary prism off Omaezaki in its upper part of the lower trench slope.

One more different direction of the lineament is quite distinct in the lower slope. That trends N40° to 50°W (Fig. 5-6. A). This is particularly remarkable in the upper part of the lower slope. In this area there are many small scale (several km in length or width) ridges and troughs, or basins and domes. Some of them trend NE, but many trend NW. Ridges and troughs appear alternatedly. The NW lineaments are not seen in the trench oceanward slopes. However, in the toe area of the trench landward slope, there are several small topography which is bounded by NW direction slopes. This is a trenchward concave topography showing basin or depression which was made by slumping to the trough entering from the oceanward slope. This suggests that the landward slope is collaped gravitationary to the trough at the trench floor which is affected by the topography of the oceanward slope as mentioned previously.

In this case the NW trend is more or less at right angle to the trench direction, suggesting the gravity driven topography. Looking at the Sea Beam map, it is reasonable to say the rectangle basin of this trend might be of submarine slumping origin. Such basins of the NW direction in the lower slope are cut by steep cliffs which parallel the trench. Those steep cliffs might be thrusts. These suggest that in this area gravitationally driven sliding and slumping occurs simultaneously with trench sub-parallel thrusting.

The middle slope is about 50 km wide, from about 5,700 to 3,000 m deep. the slope is about 10 degrees dip, having several steps. Some gentle slopes are recognized in the Sea Beam map, but some steep slopes or cliffs are also seen (Figs. 5-3 and 5-4).

A distinct basin trends N55°E bewteen the lower slopes and middle slope. It

extends for more than 80 km in the depth of around 5,700 to 5,400 m. The surface and the sediments inside of the basin dip not trenchward (E in Fig. 5-4) unlike to the other basin floors but dips landward (F in Fig. 5-4). This may be due to the strong upheaval of the ridges between the lower and middle slope just trenchward of the basin.

The upper slope is more than 80 km wide, from about 3,500 to 1,500 m deep, and has very gentle slope of 3 to degrees. This area was only mapped locally, but distinc features are seen in the profile (Fig. 5-4). 10 km wide basin, whose surface is very gently dipping trenchward, is at the lowerst part of the slope (G in Fig. 5-4). This basin may correspond to a kind of a forearc basin. More precise mapping is needed. Gravity sliding is commonly recognized in the upper slope like around H in Fig. 5-4. Some thin clastics are deposited on the slope.

Discussion and Summary

In this way the topography of both trench oceanward and landward slopes and trench itself of the westernmost part of the Kuril Trench were well studied by Sea Beam map and 3.5 KHz profiles. The characteristic features are known for the first time. The Kushiro Canyon and Kushiro Trench Fan are also well analyzed. The diagnostic features are but very similar to those in the northern part of the Japan trench off Miyako, where it was studied by the same methods, except for several different points summarized below.

In the northern Japan Trench several lineaments are seen in the oceanward slope, but in the Kuril trench slope there is only one distinct lineament parallel to the mangetic anomaly. This is very remarkable difference between the two areas. Probably the complicated fashion in the Japan Trench slope is due to the effect of the merging of the Pacific plate to the former triple junction at around the Erimo Seamount. This effect does not occur in the Kuril Trench slope, although this problem will be critically treated elsewhere (Kobayashi *et al.*, 1992).

In the Japan Trench area there is neither significant channel nor canyon, transporting clastics from the land, while the western Kuril Trench has a big canyon. This is diferent for the sedidmentation style around the trench fan. This trench fan, the Kushiro Fan, is similar in fashion to the Mogi Fan in the northen Izu-Ogasawara (Bonin) trench just on the Boso triple junction. The development of such trench fan must be also studied precisely later.

Other characteristics, the thrust faulting and gravity sliding in the trench landward slope, particularly in the toe area, are very similar, something to the Japan Trench area, and something to the Nakai Trough area. Large development of trenchward convex lineament, probably by listric thrust faults are the remarkalbe features both in the Kuril and Nankai. However, the trenchward concave topography due to gravity sliding is the common featuresboth in the Kuril and Japan Trenches. This is also recognized in the Nankai area.

The gravity sliding near the toe of the lower landward slope is one of the diagnostic features in the survey area. As mentioned in the text, the sliding is critically controlled by the collapse of the landward slope into the trough which enters from the oceanward sloped originated from the normal faulting. This is responsible for sediment subduction or tectonic erosion also shown in the northern Japan trench landward slope (Kobayashi, 1991). The problem on what is the most crucial condition determining accretion, subduction or erosion of the trench sediments may possibly be solved by this idea, as already proposed by Hilde (1983).

References

Chamot-Rooke, N. and 17 others, Tectonic context of fluid venting at the toe of the eastern Nankai accretionary prism: Evidence for a shallow detachment fault. *Earth Planet. Sci. Lett .*, **109** , 319-332, 1992.

DeMets, G. R. G., D. F. A. Gordon and S. Stein, Current plate motion, *Geophys. J. Intn.*, **101**, 425-478.

Hilde, T. W. C., Sediment subduction versus accretion around the Pacific. *Tectonophysics* , **99** , 381-397, 1983.

Iwabuchi, Y., N. Sasahara, N., S. Yoshioka, T. Kondo, and F. Hamamoto, Submarine tectonic relief off Enshunada. *Jour. Geol. Soc. Japan* , **97** , 621-629, 1991.

Kobayashi, K. (ed.), *Preliminary Report of the Hakuho Maru cruise KH 90-1* . Ocean Research Institute, University of Tokyo, 1991.

Kobayashi, K. , K. Tamaki, Y. Ogawa and Shipboard Scientific Staff of KH 92-3, Normal faults of oceanward slope of Kuril Trench, *Abstr. Seism. Soc. Japan,* Oct., 1992.

Mammerickx, J., R. L. Fisher, F. J. Emmel, and S. M. Smith, *Bathymetry of the East and Southeast Asian Seas* . Lammont-Doherty Geol. Observatory, 1976.

Nakanishi, M., K. Tamaki, and K. Kobayashi, Mesozoic magnetic anomaly lineations and seafloor spreading history of the northwestern Pacific. *Jour. Geophys. Res .*, **94** , 15437-15462, 1989.

Soh, W., A. Taira, and H. Tokuyama, A trench fan in the Izu-Ogasawara Trench off Boso trench triple junction, Japan. *Marine Geol .*, **82** , 235-249, 1988.

6. Bathymetric Mapping of Nine Seamounts near the Kuril and Japan Trenches

D. C. P. Masalu, K. Sayanagi, J. Korenaga, M. Nakanishi, K. Tamaki , Y. Ogawa and K. Kobayashi

Introduction

We mapped the bathymetry of nine seamounts near the Japan and Kuril trenches during the cruise KH 92-3 using the SeaBeam system installed in the R. V. Hakuho-Maru of the Ocean Research Institute, University of Tokyo (Fujimoto *et al.*, 1990). These seamounts are; Soma Seamount, Ryofu, Takuyo-Daiichi, Mizunagidori (Bosei), Futaba, Hitachi, Daiyon-Kashima, Daigo-Kashima, Dairoku-Kashima and Dainana-Kashima Seamounts (Fig. 6-1).

The Soma Seamount is situated at the northeastern end of the Joban Seamount Chain (Masalu *et al.*, 1991) next to Mizunagidori Seamount. Hitachi and Daiyon-Kashima Seamounts lie in the Joban Seamount Chain. Futaba Seamount on the northwest of Iwaki Seamount lies nearby but slightly off the Joban Seamount Chain. Daigo-Kashima Seamount is located about 74 km southeast of Daiyon-Kashima Seamount. Dairoku- and Dainana-Kashima Seamounts are aligned southwest of Daiyon-Kashima but their trend appears to be subparallel to the Joban Seamount Chain.

Takuyo-Daiichi Seamount is situated on the oceanward side edge of the Kuril Trench. Erimo Seamount surveyed by the French-Japanese *KAIKO* Project in 1985 (Cadet *et al.*, 1987) is located at the junction of the Japan and Kuril Trenches.

In Leg 1 of cruise KH 90-1 in 1990 the Mizunagidori and Hitachi Seamounts were surveyed intensively, whereas Futaba and Daiyon-Kashima Seamounts were surveyed only along one and two tracks, respectively. Survey in the present cruise was attempted to complement the previous one.

Outline of the Survey

We show in Fig. 6-1 the ship's tracks during bathymetric survey of the seamounts herein described. The Soma, Ryofu and Takuyo-Daiichi Seamounts were most intensively surveyed (Figs. 6-2~6-4). Takuyo-Daiichi Seamount was surveyed in both the end of leg 1 and the beginning of leg 2. The Soma and Ryofu Seamounts were surveyed at the end of both legs 1 and 2 on the way to and from the Kuril Trench. Daiyon-, Daigo-, Dairoku- and Dainana-Kashima Seamounts were surveyed at the end of leg 2 on the way home from the Kuril Trench (Figs. 6-5 & 6-6). Mizunagidori, Hitachi and Futaba Seamounts (Figs. 6-7~ 6-9) were each surveyed only along one track on the way from the Kuril Trench at the end of leg 2. Erimo Seamount (Fig. 6-10) were surveyed to locate precise sites for DESMOS observation and dredge hauls.

Brief Description of Seamounts Surveyed

We summarize in Table 6-1 the principal morphological characteristics of the seamounts surveyed in the present cruise and briefly describe the results below.

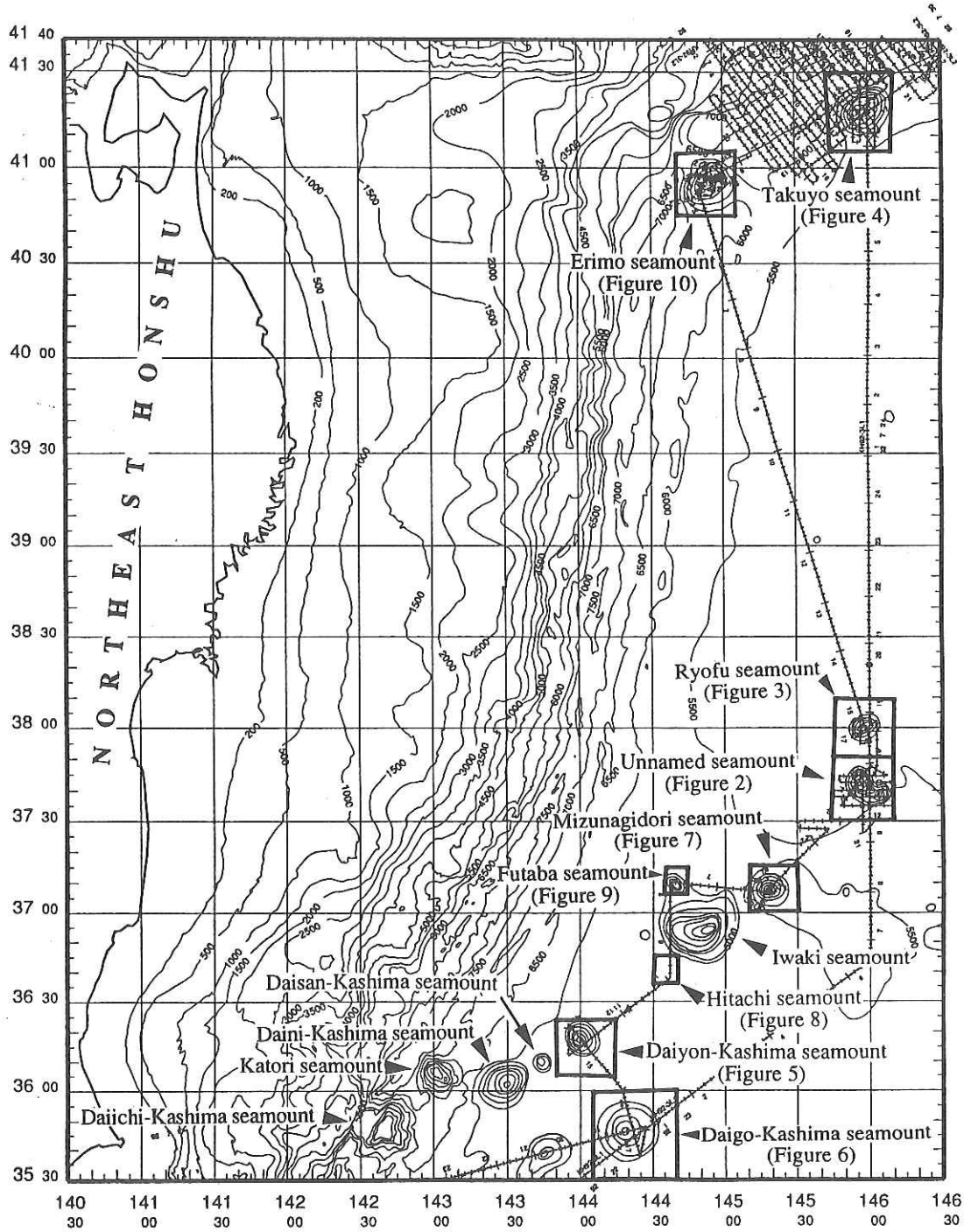

Fig. 6-1. Index map for seamounts surveyed and detailed figures (boxes) shown in this article. The map shows ship's tracks during the survey on seamounts.

Soma Seamount (Provisional name)

This seamount (Fig. 6-2) is situated far northeast of in the Joban Seamount Chain next to Mizunagidori Seamount. It has a crestal depth of 2,180 m rising by about 3,200 m above the abyssal plain. The eastern and southern flanks are 5,500 m deep. The northern flank is 5,300 m and the western flank is 5,400 m deep. Flank depths indicate that the ocean floor upon which this seamount resides as well as the seamount itself are inclined north of northeastward. Its shape is nearly round with a crestal ridge oriented along the NE direction. The topmost contour of the crestal ridge is flat. Several ridges on the slope of this seamount run in the west, southwest, south and northeast directions. A provisional name "*Soma*" is proposed here for this seamount after name of a Pacific coast city in the north of Joban District, northeastern Honshu, Japan and will be used hereafter in this report.

Ryofu Seamount

Ryofu Seamount (Fig. 6-3) is located due north of Soma Seamount. This seamount is conical in shape with a crestal depth of about 2,900 m and rises by about 2,350 m from the 5,250 m deep abyssal plain. Its crest is composed of a small ridge oriented in the NE direction. Its flank is about 5,250 m deep on all sides. This indicates that the ocean floor upon which Ryofu Seamount resides is almost horizontal, *i.e.* neither the ocean floor nor the seamount are inclined. Three ridges run down on the slope of Ryofu Seamount. One runs along the northwest direction, another along the southwest and the other along north of northeast direction.

Takuyo-Daiichi Seamount

Takuyo-Daiichi Seamount (Fig. 6-4) is located on the oceanward edge of the Kuril Trench. This seamount has an oblate-like shape oriented along the northeast direction. It has a crestal depth of about 2,500 m that rises by about 3,300 m above the ocean floor. Its flank on the northeastern side counter clockwise down to the western side is about 5,850 m deep, and about 5,550 m deep on the south. As expected, flank depths of this seamount indicate that the ocean floor upon which the seamount resides as well as the seamount itself are inclined northwestward. Three ridges on the northern part of this seamount run along north, northeast and east directions. On the southern part of this seamount one ridge runs along the southeastern direction and another ridge along southwestern direction.

Daiyon-Kashima Seamount

Daiyon-Kashima Seamount (Fig. 6-5) is aligned in the Joban Seamount Chain. This seamount is conical in shape with a crestal depth of about 2,900 m that rise by about 2,700 m above the ocean floor. The flank of this seamount is about 5,650 m on the northeastern and about 5,600 m on the southeastern sides.

Daigo-Kashima Seamount

Daigo-Kashima Seamount (Fig. 6-6) is located about 74 km on the southeast of Daiyon-Kashima Seamount. This seamount is conical in shape with a flat top at a depth of about 1,500 m. We herenow classify this seamount as a guyot. The flank of this seamount is about 5,700 m on the northern and western sides. Two

ridges on the slope of Daigo-Kashima Seamount run along the eastern and southeastern directions. Dairoku- and Dainana-Kashima Seamounts were surveyed on the end of Leg 2, the results of which are shown in the next chapter.

Futaba Seamount

Futaba Seamount (Fig. 6-7) is located northwest of Iwaki Seamount. The crestal depth of this seamount is about 3,400 m and rises by about 2,000 m above the surruonding abyssal plain that is about 5,400 m deep. The flank of Futaba seamount is about 5,400 m deep on the southwestern side and about 5,500 m on the eastern side. One ridge on the slope of this seamount runs along south of northeast direction and another ridge runs along southwest direction.

Hitachi, Mizunagidori and Erimo Seamounts

Hitachi Seamount (Fig. 6-8) lies on the Joban Seamount Chain about 10 km southwest of the flank of Iwaki Seamount. Mizunagidori Seamount (Fig. 6-9) lies on the Joban Seamount Chain next to Iwaki Seamount on the northeast. Erimo Seamount (Fig. 6-10) is located at the junction of the Japan and Kuril trenches. Hitachi Seamount was only surveyed along one track on its eastern flank and Mizunagidori Seamount was surveyed simultaneously during dredge hauls, while bathymetric data of Erimo Seamount were used to facilitate other works.

We hope that bathymetric data collected from these seamounts during this cruise used together with other geophysical data such as magnetic data (Masalu *et al.*, this report) also collected in the same cruise, will provide us valuable information on the tectonics of the Pacific plate and origin of the Joban Seamount Chain. Combined use of data obtained in the present cruise and those from leg 1 of cruise KH 90-1 and *KAIKO* Project which will be described in the next chapter of this report may broaden our scope of knowledge on these abundant northwestern Pacific seamounts.

References

Cadet, J.-P., K. Kobayashi, J. Aubouin, J. Boulegue, C. Deplus, J. Dubois, R. von Huene, L. Jolivet, T. Kanazawa, J. Kasahara, K. Koizumi, S. Lallemand, Y. Nakamura, G. Pautot, K. Suyehiro, S. Tani, H. Tokuyama and T. Yamazaki, The Japan Trench and its juncture with the Kuril Trench: cruise results of the Kaiko project, Leg 3, *Earth and Planetary Science Letters*, **83**, 267-284, 1987.

Fujimoto, H., T. Furuta, A. Oshida, M. Nakanishi and K. Kobayashi, Bathymetric Mapping using the SeaBeam system, in J. Segawa (ed.), *Preliminary Report of the Hakuho-Maru Cruise KH89-1*, Ocean Research Institute, University of Tokyo, 30-40, 1990.

Masalu, D. C. P., A. Oshida, M. Nakanishi, K. Tamaki, K. Kobayashi and Y. Ogawa, Bathymetric mapping of the Joban seamount chain, in *K. Kobayashi* (ed.), *Preliminary Report of the Hakuho-Maru Cruise KH90-1*, Ocean Research Institute, University of Tokyo, 30-37, 1991.

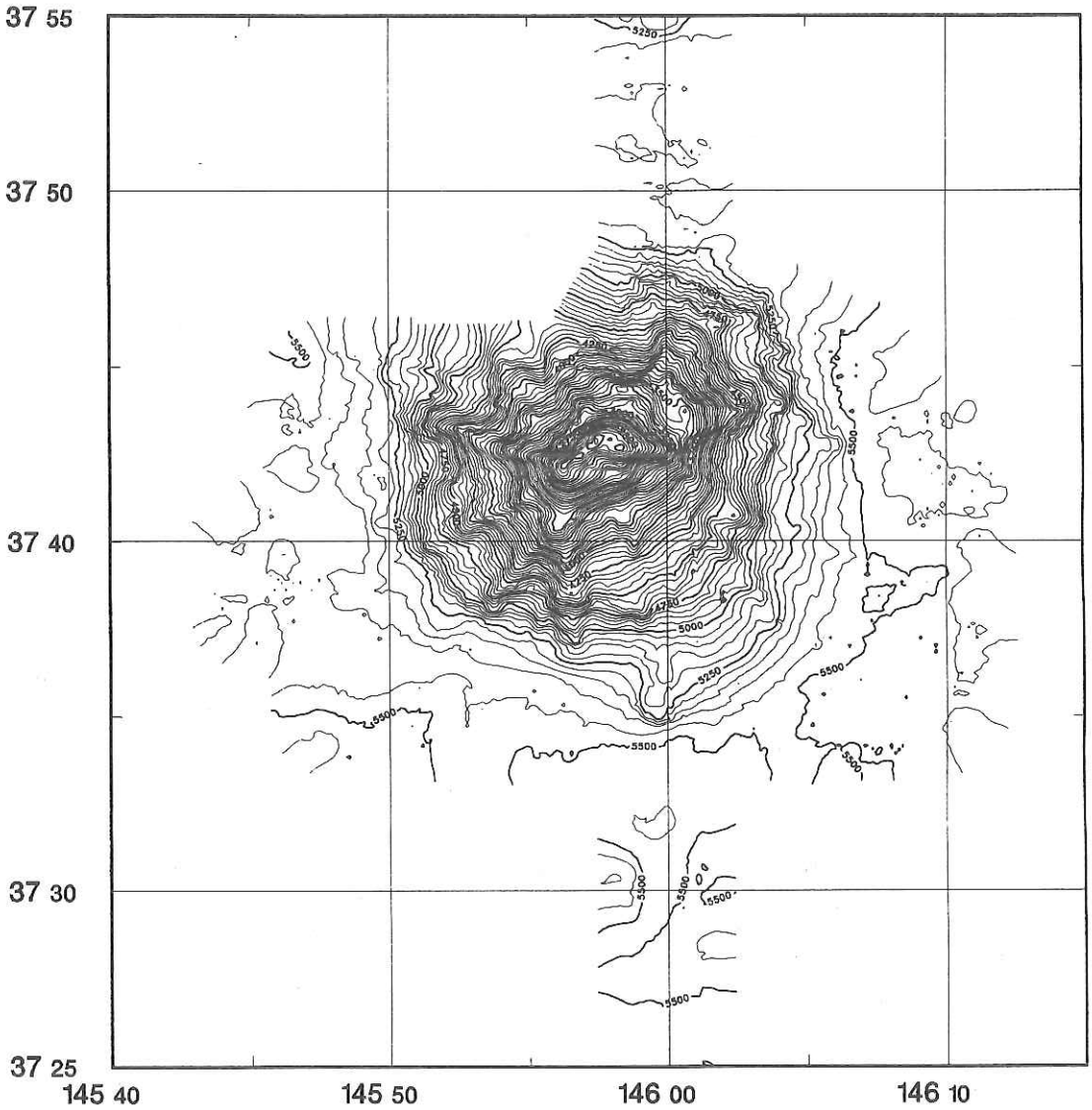

Fig. 6-2. Bathymetric map of Soma Seamount based on data obtained by this cruise. Contour interval 50 m.

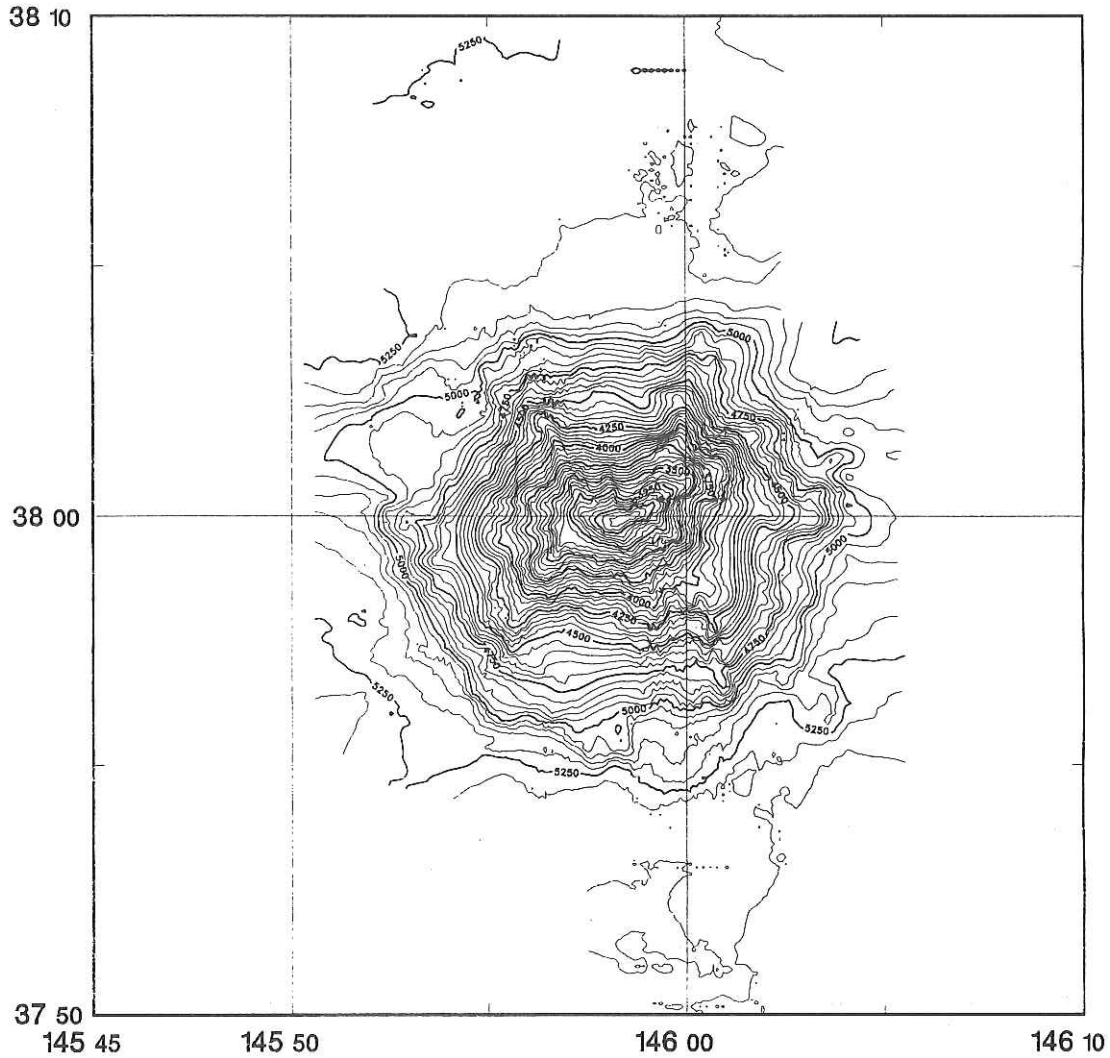

Fig. 6-3. Bathymetric map of Ryofu Seamount. Other details as in Fig. 6-2.

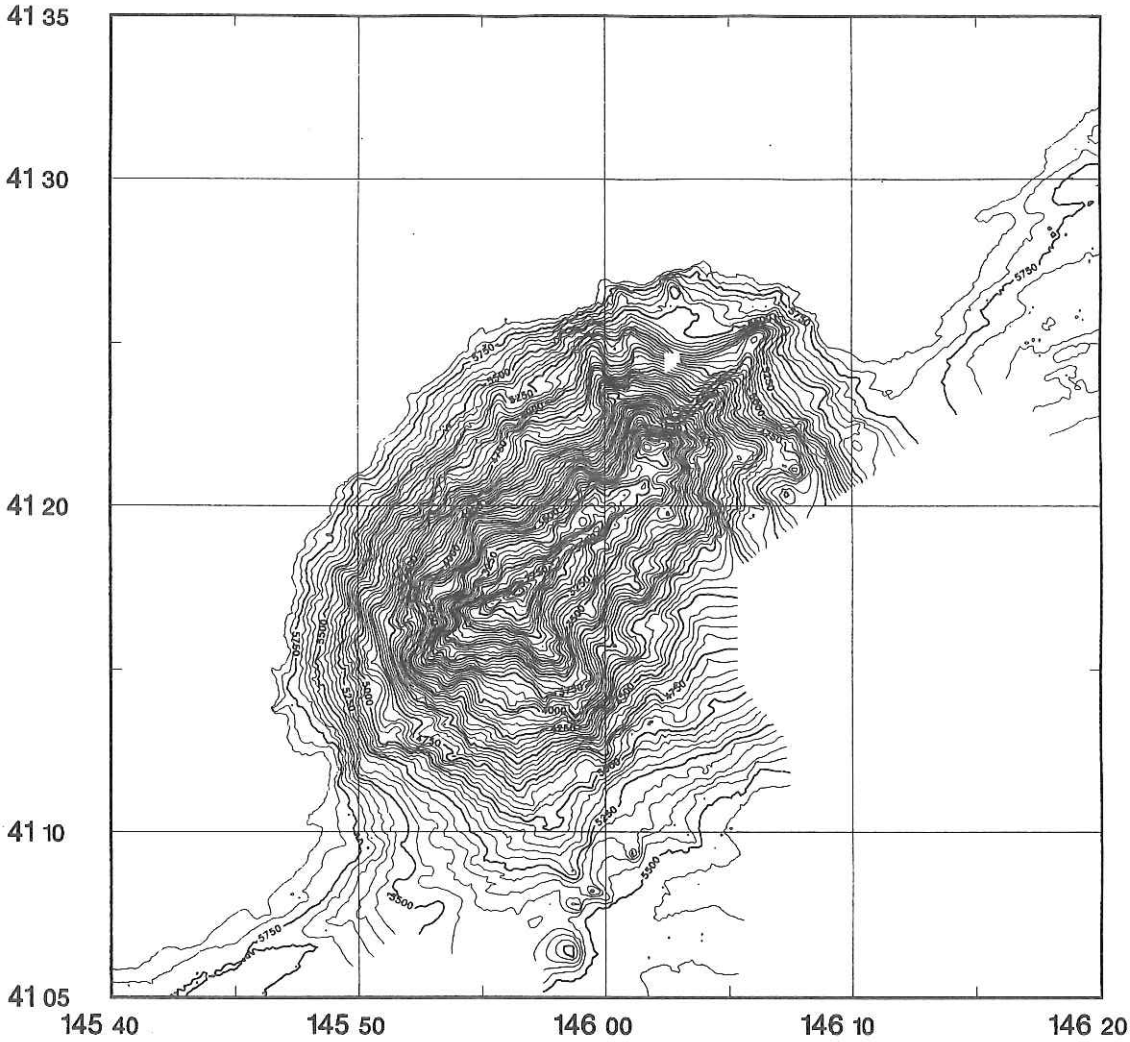

Fig. 6-4. Bathymetric map of Takuyo-Daiichi Seamount. Other details as in Fig. 6-2.

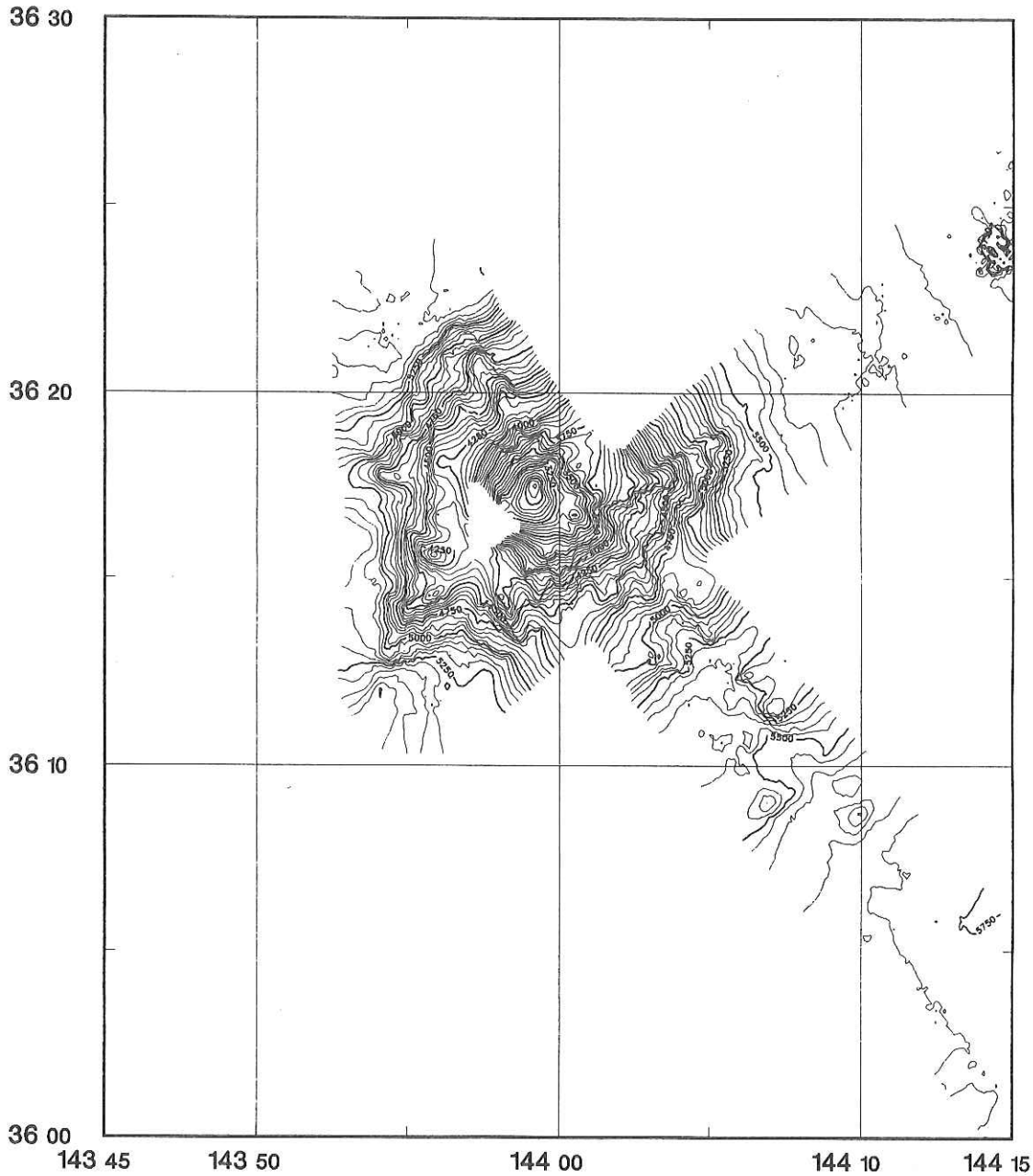

Fig. 6-5. Bathymetric map of Daiyon-Kashima Seamount. Other details as in Fig. 6-2.

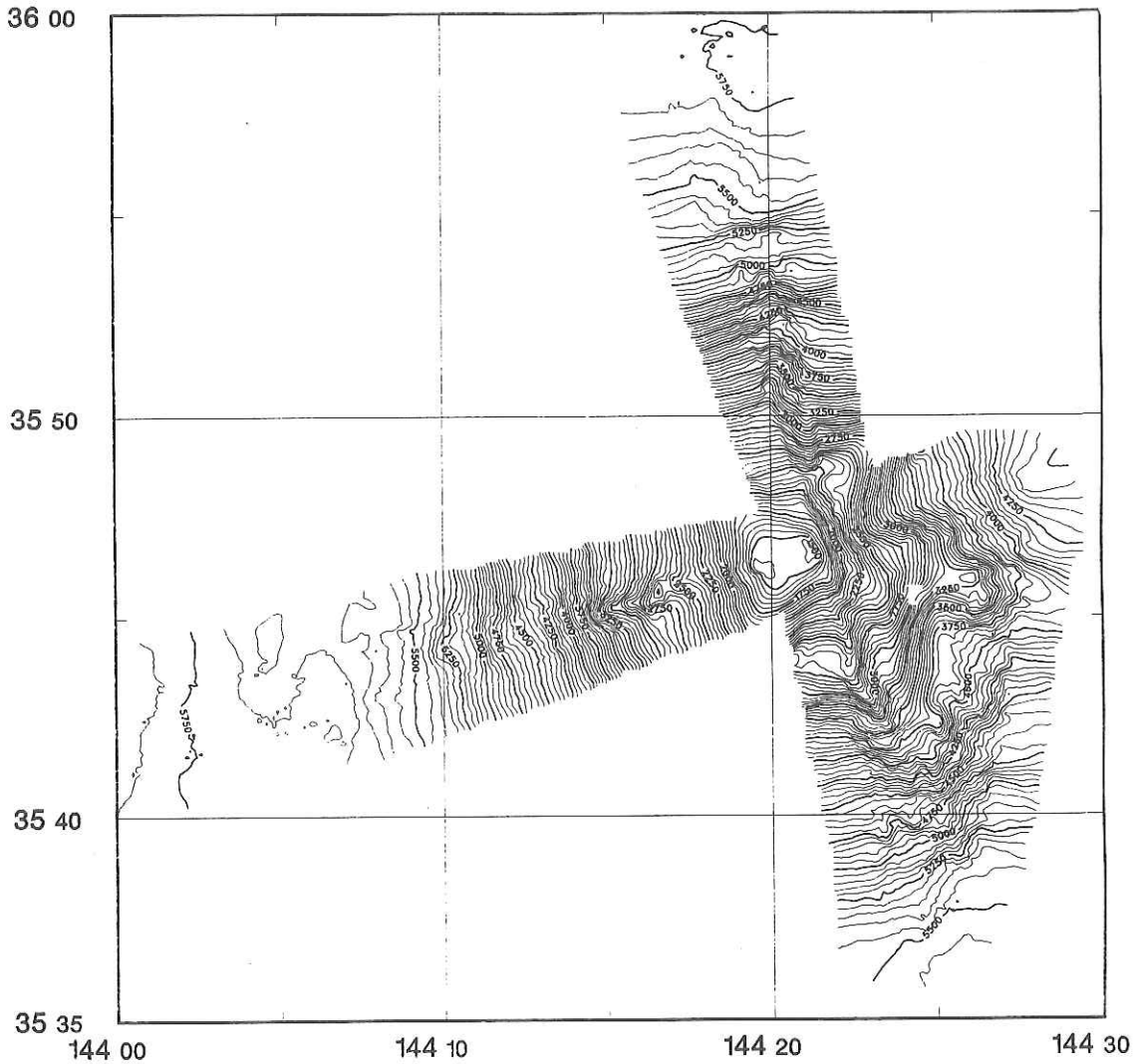

Fig. 6-6. Bathymetric map of Daigo-Kashima Seamount. Other details as in Fig. 6-2.

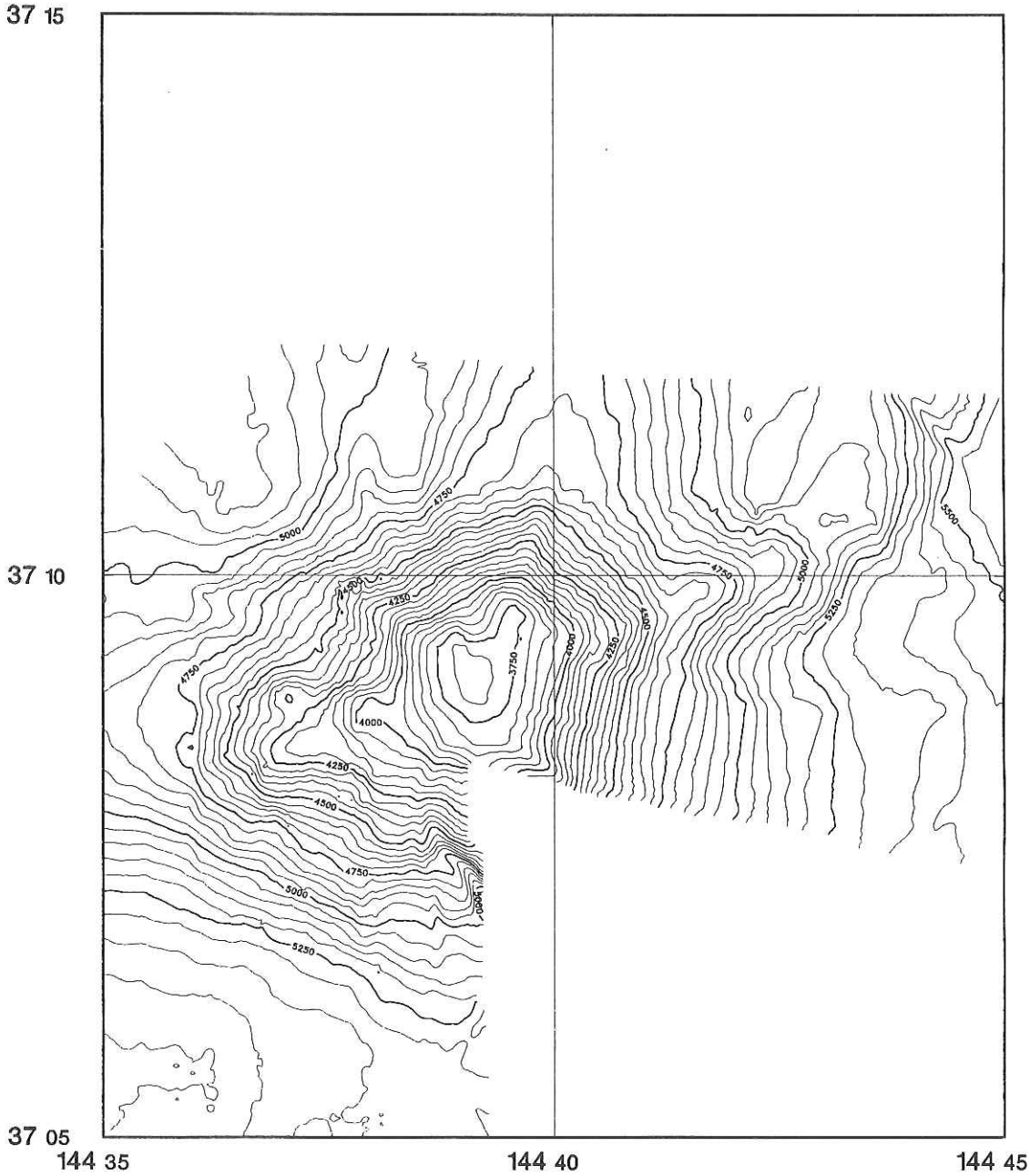

Fig. 6-7. Bathymetric map of Futaba seamount. Other details as in Fig. 6-2.

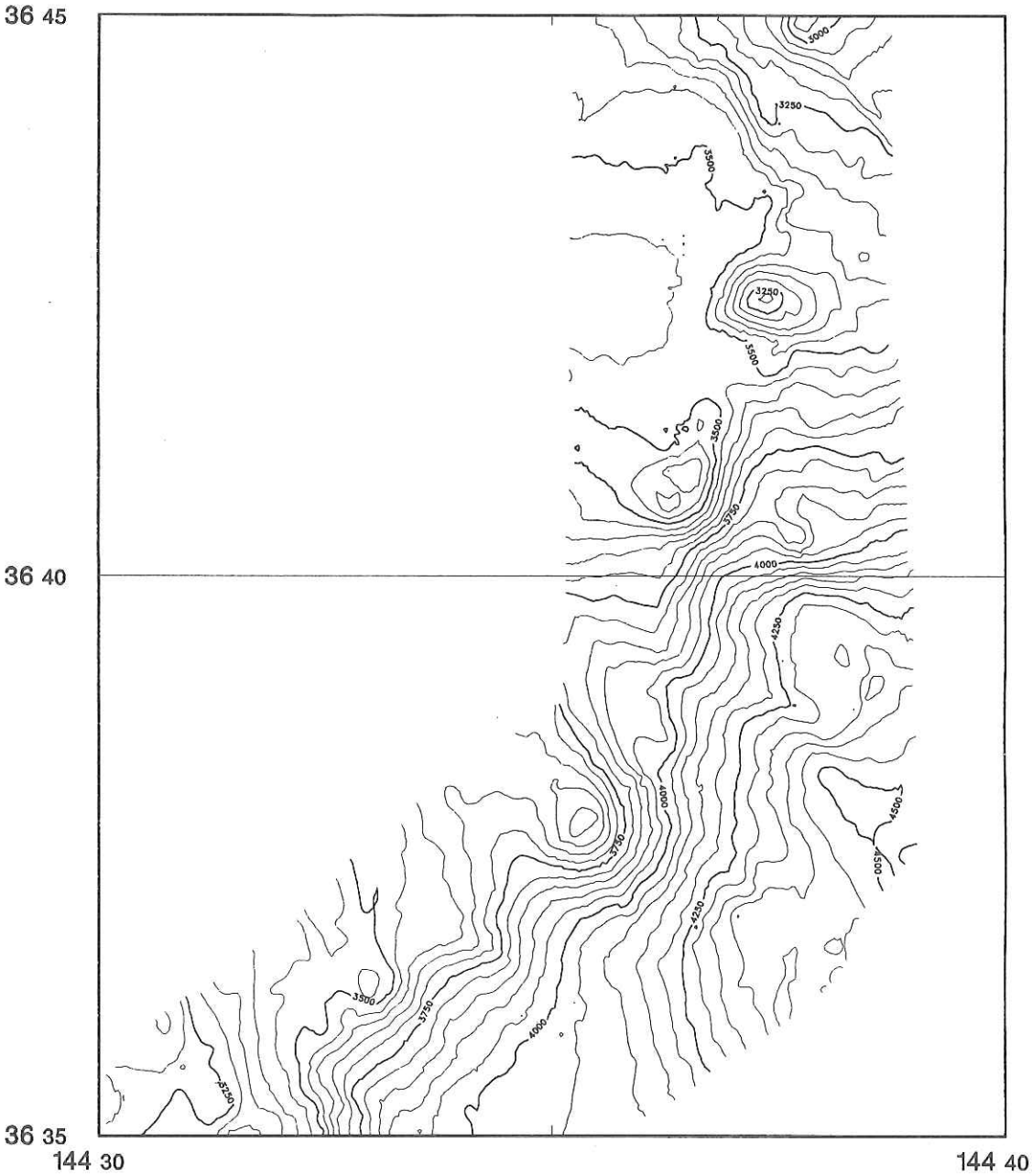

Fig. 6-8. Bathymetric map of Hitachi seamount. Other details as in Fig. 6-2.

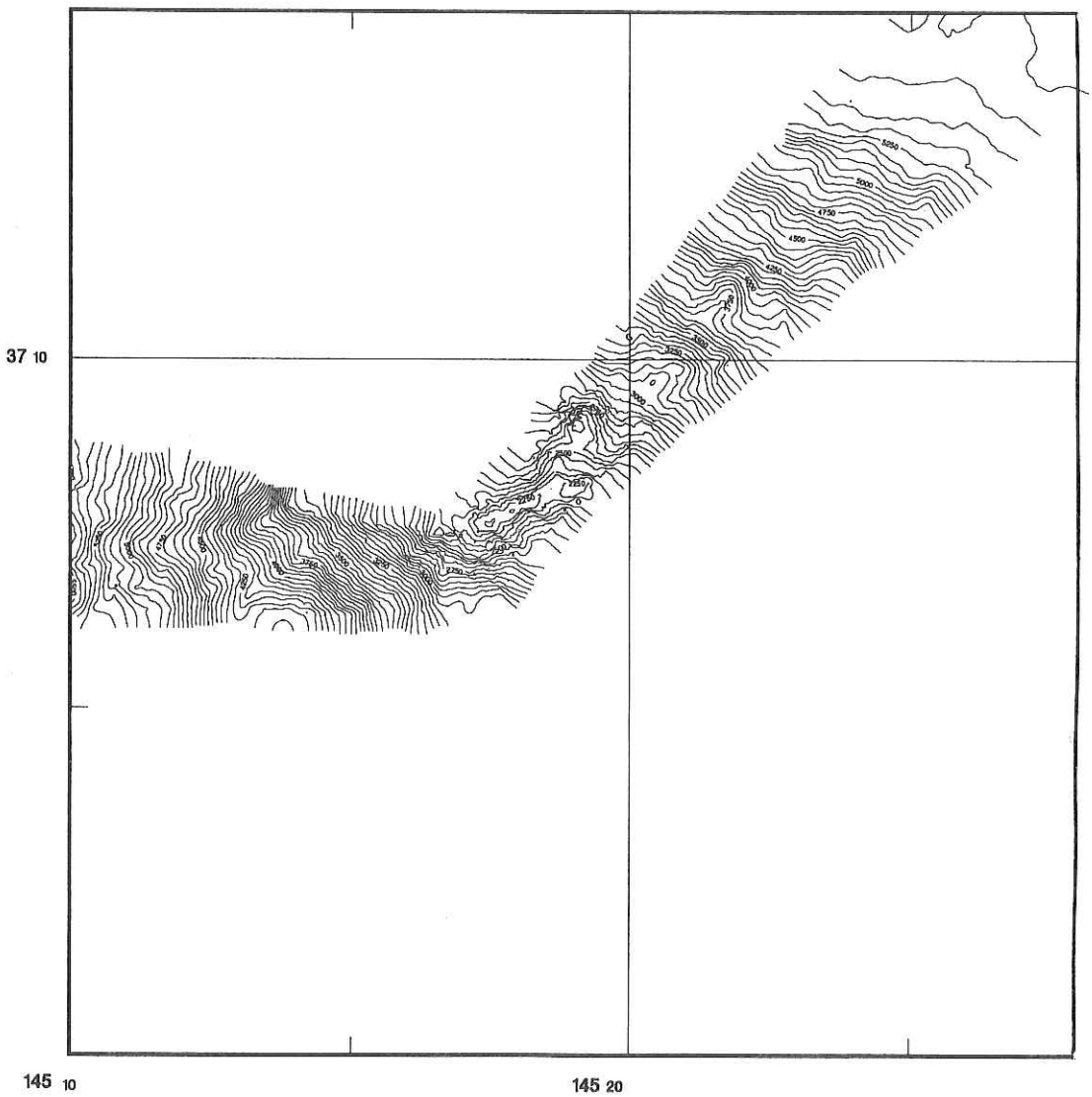

Fig. 6-9. Bathymetric map of Mizunagidori Seamount. Other details as in Fig. 6-2.

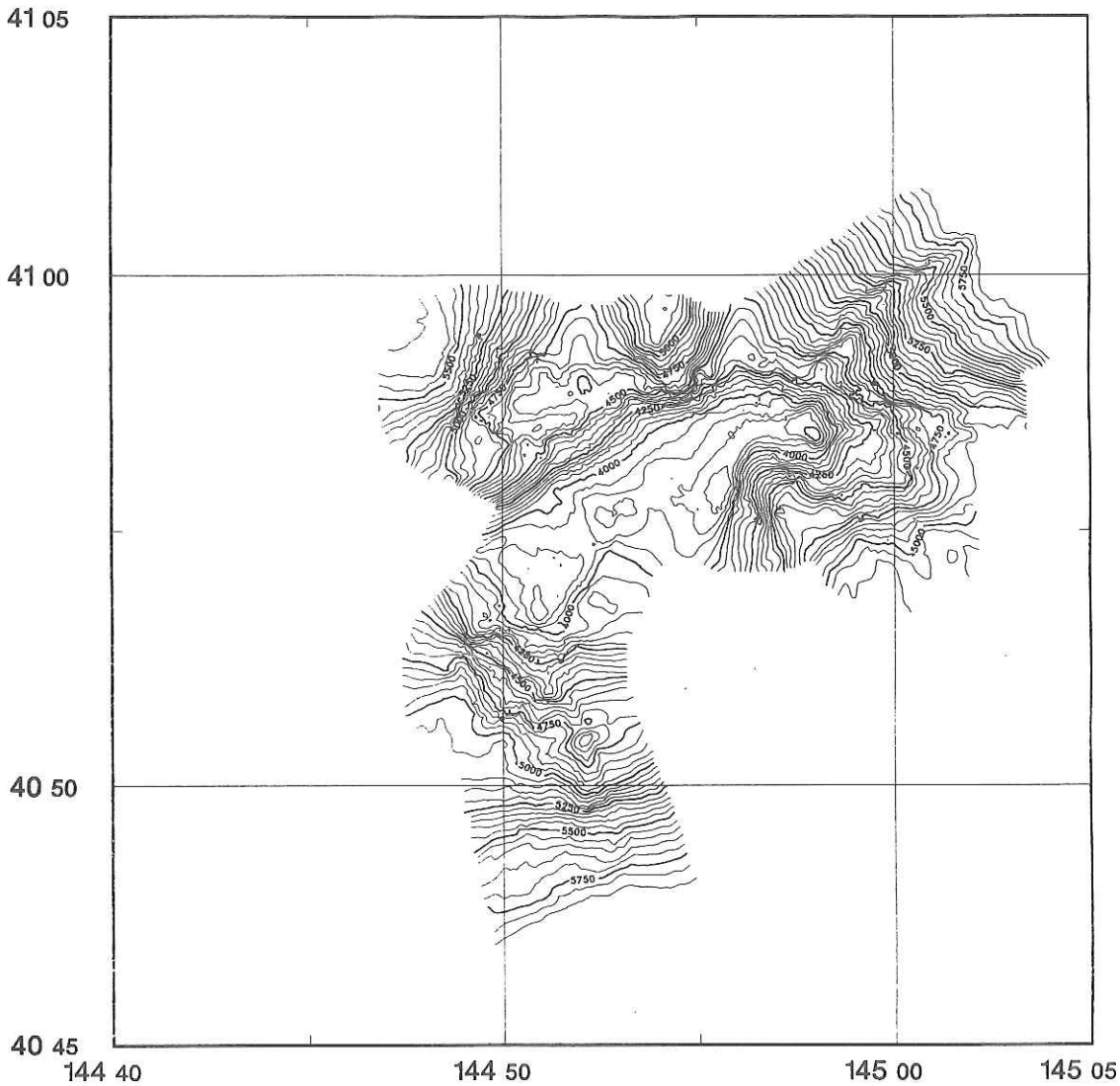

Fig. 6-10. Bathymetric map of Erimo seamount. Other details as in Fig. 6-2.

Table 6-1-1. Seamounts and knolls in the Joban Seamount Chain and Adjacent Area.

Seamount or Knoll	Location of Crest	Crestal Depth(m)	Flank Depth(m)	Height (m)	Diame-ter (km)	Vol. (km^3)	Remarks
Ryofu Seamount	37°59.9'N 145°58.5'E	2,880	5,360	2,400	18	215	Conical
Soma Seamount (New Name)	37°42.9'N 145°57.5'E	2,180	5,400~ 5,500	3,200	24	555	Twin peaks trending NE
Mizunagi-dori(Bosei) Seamount	37°08.8'N 145°17.5'E	~2,000	5,400~ 5,800	~3,800	33	1,069	Ref. 2 Large Parasitic cone west
Futaba Seamount	37°08.8'N 144°39.0'E	3,400	~5,400	~2,000	14	110	Found in KH 90-1
Iwaki Seamount	36°53.0'N 144°46.0'E	1,700	~5,400	3,700	60	2,282	Position corrected
Hitachi Seamount	36°39.5'N	2,360	5,660	3,300	18	488	Guyot Found in KH 90-1
Daiichi-Kashima Seamount	35°49.0'N 142°40.0'E	3,550	6,200	2,650	50	1,800	Guyot Faulted by ~1,500 m
Daini-Kashima Seamount	36°03.0'N 143°39.0'E	2,800	5,800	3,000	30	626	Conical
Daisan-Kashima Seamount	36°11.0'N 143°59.0'E	3,100	5,800	2,700	11	315	Conical Starfish
Daiyon -Kashima Seamount	36°17.6'N 143°59.0'E	2,900	5,500	2,600	24	341	Topography corrected Parast. cone
Katori Seamount	36°05.0'N 143°21.0'E	4,110	6,200	2,100	31	528	Small flat-top
Daigo-Kashima Seamount	35°48.0'N 144°21.0'E	1,425	5,600	3,200 ~4,200	40	1,144	reefal top lagoon Guyot
Dairoku-Kashima Seamount	35°38.0'N 143°45.0'E	3,000	5,800	2,800	35	900	irregular EW elonga-ted
Dainana-Kashima Seamount	35°31.5'N 143°17.0'E	5,200	6,000	800 ~1,000	5.8	7	small, irre-gular New Name
Yoyoi Knoll [New Name]	37°30.2'N 145°57.0'E	4,840	5,540	~700	7.5	10	Conical sharp crest w/Moat
Harumi Knoll [New Names]	37°29.0'N 145°41.0'E	4,750	5,500	~830	7.5	12	Conical sharp crest w/Moat

Table 6-1-2. Seamounts and knolls in the Kuril Trench area.

Seamount or Knoll	Location of Crest	Crestal Depth(m)	Flank Depth(m)	Height (m)	Diameter (km)	Vol. (km^3)	Remarks
Erimo Seamount	40°57.0'N 144°58.0'E	3,720	4,650	930	32	250	NE elong. twin peaks
Takuyo-Daiichi Seamount	41°17.5'N 145°56.5'E	2,500	5,400	2,900	30	894	N60°E elongated
Chitose Knoll [New Name]	41°27.0'N 145°54.5'E	5,900	6,500	280 ~540	2.6	0.9	parasitic to Takuyo-I
Mashu Knoll [New Name]	42°39.5'N 146°25.5'E	5,700	6,540	500 ~820	3.9	2.0	Conical
Kamuish Knoll [New Name]	42°02.7'N 146°52.0'E	6,700	6,980	280 ~440	2.6	0.5	Conical

Table 6-1-3. Knoll in the northern Japan Trench area.

Seamount or Knoll	Location of Crest	Crestal Depth(m)	Flank Depth(m)	Height (m)	Diameter (km)	Vol. (km^3)	Remarks & Ref.
Sanriku-Miyako Knoll (Bertheau Seamount)	39°43.5'N 144°43.0'E	5,715	6,100	415	3.0	n. d.	Found by Jean Charcot KAIKO fault-disected Conical

7. Topography of the Joban Seamount Chain

D. C. P. Masalu, K. Sayanagi, J. Korenaga, M. Nakanishi, K. Tamaki and K. Kobayashi

Introduction

In the cruise KH 90-1 we surveyed seven seamounts; Mizunagidori (Bosei), Iwaki, Hitachi, Futaba, Daiyon-Kashima, Daisan-Kashima and Daini-Kashima Seamounts in the Joban Seamount Chain (Masalu *et al.*, 1991a; Ogawa *et al.*, 1991). Cruise KH 90-1 marked the first extensive geophysical survey on the Joban Seamount using the SeaBeam system. Indeed, Leg 1 of cruise KH 90-1 yielded tremendously good results that include the discovery of a relatively small guyot seamount that we named 'Hitachi', discovery of Futaba Seamount, classification of Iwaki Seamount as a guyot and precise location and shape of these seamounts, although Futaba and Daiyon-Kashima Seamounts were not surveyed in detail during that time.

In the cruise KH 92-3 which involved comprehensive geophysical surveys on several seamounts near the Japan and Kuril Trenches, we surveyed in detail two northeasternmost seamounts in the Joban Seamount Chain; Ryofu and Soma Seamounts. We also surveyed less intensively, the two seamounts; Futaba and Daiyon-Kashima Seamounts to increase their geophysical survey coverage. Apart from surveying seamounts on the Joban Seamount Chain, we also surveyed Daigo-Kashima Seamount located on the southeast of Daiyon-Kashima Seamount. Daigo-Kashima Seamount is clearly isolated from (not part of) the Joban Seamount Chain. It appears to be aligned with two others for which we propose names, Dairoku- and Dainana-Kashima Seamounts. In this chapter we present the result of bathymetric mapping of the Joban Seamount Chain based on the combined data obtained in these two cruises KH 90-1 and KH 92-3.

Preliminary Results

We show in Fig. 7-1 the bathymetric map of the Joban Seamount Chain and nearby seamounts based solely on bathymetric data we collected from this area during cruises KH 90-1 and KH 92-3. Bathymetric results obtained from these two cruises KH 90-1 and KH 92-3 provide us precise location and shapes of the seamounts. Detailed morphological description of each seamount is given by Masalu *et al.*, (1991a) and Masalu *et al.*, (preceeding chapter in this issue). The results in Fig. 7-1 most clearly demonstrate existence of a chain of seamounts; the Joban Seamount Chain composed of Daini-Kashima, Daisan-Kashima, Daiyon-Kashima, Hitachi, Iwaki, Mizunagidori and Soma Seamounts aligned in a straight line that probably is consistent with the location of Daiichi-Kashima Seamount on its southwestern end (Ogawa *et al.*, 1991).

Futaba and Ryofu Seamounts lie slightly out of this line. These two seamounts appear to lie in another line nearly parallel to the Joban Seamount Chain that probably also includes Katori Seamount as its southwestern end. Crest of a seamount (Dairoku-Kashima) southwest of Daigo-Kashima was identified. Existence of a seamount undescribed in any bathymetric chart was also

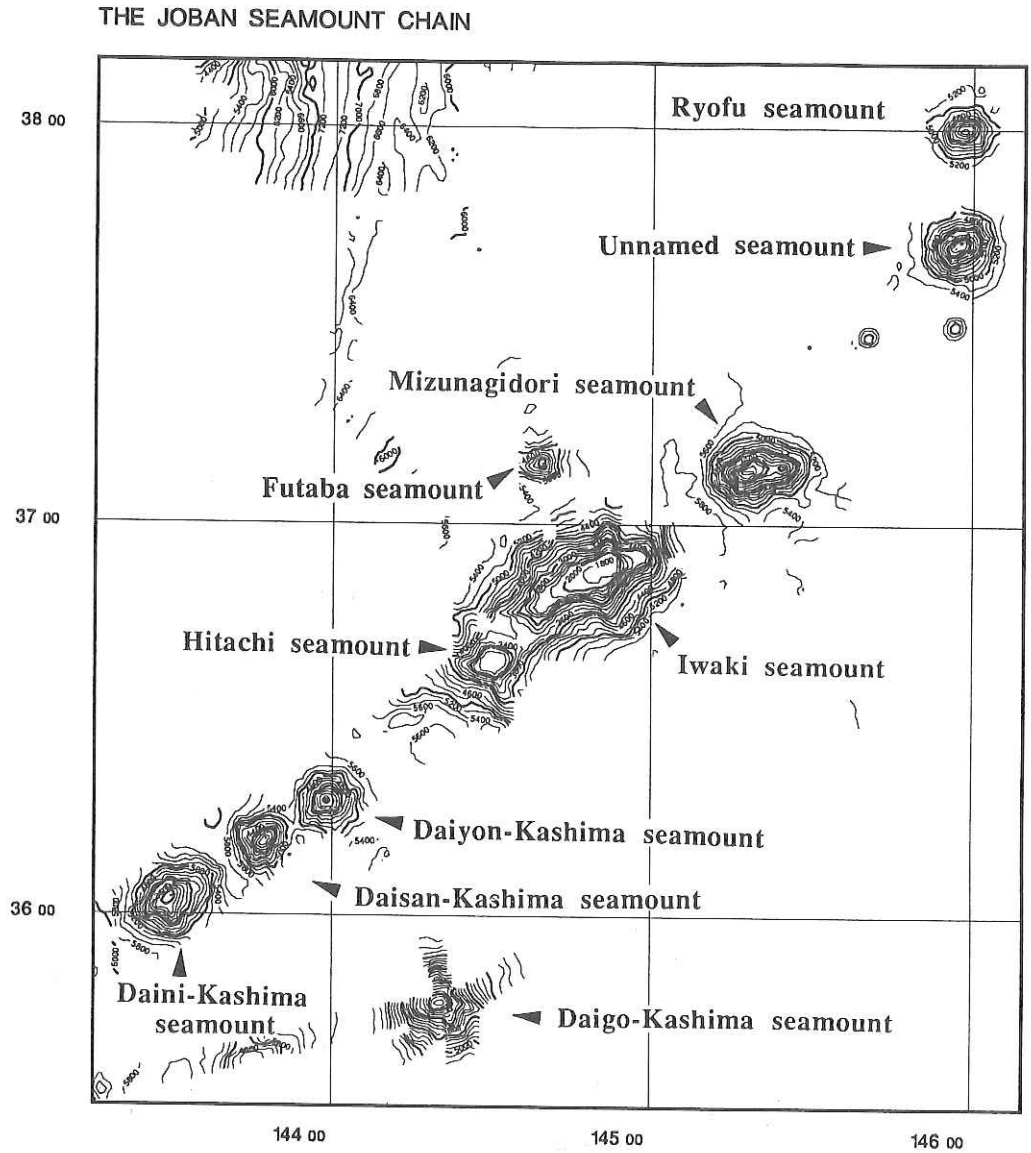

Fig. 7-1. Bathymetric map of the Joban Seamount Chain and nearby seamounts based on the combined data collected during cruises KH 90-1 and KH 92-3. Contour interval is 200 m.

found at a site WSW of Dairoku-Kashima, which appears to be on a line with Daigo- and Dairoku-Kashima Seamounts subparallel to the Joban Chain.

The Joban Seamount Chain trends along N53°E oblique to magnetic lineations on the surrounding ocean floor (Masalu *et al.*, 1991a; 1991b) and extends over a distance of about 394 km from Daiichi-Kashima to Soma Seamounts. Its origin is still unknown. The trend of this seamount chain is inconsistent with any known Mesozic and later trends of hotspot trajectories. Furthermore, magnetic inversion analysis of seamounts forming the Joban Seamount Chain (Masalu *et al.*, 1991b) suggests that this seamount chain was not formed by the passage of the Pacific plate over a single stationary hotspot. Its obliqueness to the magnetic lineations excludes possibility of seamount generation at a stage of seafloor spreading. Two alternative hypotheses may be postulated; that of formation of these seamounts on a congregation of hotspots and that of formation by volcanic pulse or events in the earth's history, as has been proposed to explain the origin of the abundant western Pacific seamounts (Sager, 1992).

We hope that with the present complete coverage of geophysical survey on the Joban Seamount Chain, further analyses and study may eventually give us answer to the question of the origin of these seamount chains.

References

Masalu, D. C. P., A. Oshida, M. Nakanishi, K. Tamaki, K. Kobayashi and Y, Ogawa, Bathymetric mapping of the Joban seamount chain, in *Preliminary report of the Hakuho-Maru cruise KH90-1*, ed. K. Kobayashi, Ocean Research Institute, University of Tokyo, 30-37, 1991a.

Masalu, D. C. P., K. Tamaki, and K. Kobayashi, Paleomagnetism of the seamounts forming the Joban seamount chain in the northwestern Pacific, *EOS Transactions*, AGU, Washington, 1991b.

Ogawa, Y., K. Kobayashi and D. C. P. Masalu, Topography and nomenclature of the Joban seamount chain, in *Preliminary report of the Hakuho-Maru cruise KH90-1*, ed. K. Kobayashi, Ocean Research Institute, University of Tokyo, 37-40, 1991a.

Sager, W. W., Seamount age estimates from paleomagnetism and their implications for the history of volcanism on the Pacific plate, in *Geology and Offshore Mineral Resources of the Central Pacific Basin*, eds. B. H. Keating & B. R. Bolton, C-PCEMR, Earth Sci. ser. 14, Springer-Verlag, 21-37, 1992.

8. Conical Knolls in the Northwestern Pacific Ocean and Adjacent Seas

K. Kobayashi

As described in previous chapters of this report (particularly Chapters 5 and 7), three isolated knolls were found in the oceanward slope of the western Kuril Trench (Figs. 8-1, Fig. 5-1 and foldout charts) and in abyssal plain south of Soma Seamount in the north-western Pacific Ocean (Fig. 8-2, see Fig. 7-1 for their location). These topographic highs have quite conical shape with round fringe of 2~5 km in diameter and sharp crest of 200~700 m in height from surrounding bottom. Water depths of their crests range from 4,500 m to 5,500 m dependent upon depths of the surrounding plain. Since we have been accustomed to call them knolls rather than seamounts, if their relative height does not exceed 1,000 m, we will follow this definition.

New names ; Chitose, Mashu and Kamuish for Kuril Trench knolls, while Harumi and Yayoi for Soma seamount region, are proposed tentatively used here for these knolls as listed in Table 6-1-1 and 6-1-2.

One knoll close to the northern Japan Trench axis with the crestal depth as deep as 6,000 m (Fig. 8-3) was discovered in Leg 3 of KAIKO cruise by *Jean Charcot* (KAIKO I Research Group, 1985; 1986; Cadet *et al.*, 1987). This knoll was named as Bertheau Seamount after name of a retiring sailor of *Jean Charcot*, but a new name "Sanriku-Miyako Knoll" was recently proposed following the Japanese standard nomenclature. Boulders of basalt were collected by a Shinkai 6500 dive (Fujioka, 1992), which will provide a good constrain for composition of these knolls. Petrography of the collected samples are in progress.

In the later period of the Hakuho Maru cruise KH 92-1 after the ship sailed out of Cebu, Philippines several knolls were found in the Seabeam monitor record between the Daito Ridge and Kyushu-Pakau Ridge (Fig. 8-4 (a)). As the swath width of the Seabeam installed on the ship is nearly the same as water depth (~ 5,500 m), the whole topography of knolls can be drawn in one belt of swath mapping. Morphology of the knolls are quite similar to those in the Pacific Ocean. The crest of one knoll (knoll *KH92-1-K1*) shows peculiar topography suggesting the old central cone like caldera at the depth of 5,460 m (Fig. 8-4 (b)), whereas the other two knolls have typical sharp crest.

Similar knolls were already reported for the western Pacific east off Ogasawara Trench by Hydrographic Department, Maritime Safety Agency of Japan (Kasuga *et al.*, 1992). Distribution of these knolls appears to be clustered in some particular areas, although their characteristic nature of distribution is still unknown. Some of knolls seem to be aligned on a line. For example two knolls and Takuyo-Daiichi Seamount in the oceanward slope of the western Kuril Trench are on one line together with Bertheau Seamount (Sanriku-Miyako Knoll) on the Japan Trench slope. However, tectonic significance of alignment is unknown. Conical knolls are also seen on the slope of mid-oceanic ridge. It seems likely that knolls were formed slightly after ocean floor spreading in a manner similar to

the eruption of parasitic cones on the slope of large volcanoes.

It will be an important task to solve questions when and how these knolls were formed. What are they correlated to surrounding ocean floor and adjacent seamounts (relation of the Kuril Trench knolls to Takuyo-Daiichi and that of Soma knolls to Joban Seamount Chain) ? Is their petrography different from the MORB and plume basalts ?

In the Izu peninsula of the central Honshu, Japan and in southwestern Sagami Bay a number of small monogenic volcanoes have been found (Hamuro, 1985). Their origin seems to be correlatable to prevalance of extensional force in the crust of that region. Therefore, it is an important problem to answer whether or not the origin of the ocean floor knolls is similar to that of monogenic volcano group in Izu region.

References

Cadet, J.-P., K. Kobayashi, J. Aubouin, J. Boulegu, C. Deplus, J. Dubois, R. von Huene, L. Jolivet, T. Kanazawa, J. Kasahara, K. Koizumi, S. Lallemand, Y. Nakamura, G. Pautot, K. Suyehiro, S. Tani, H. Tokuyama and T. Yamazaki, The Japan Trench and its junction with the Kuril Trench: cruise results of the Kaiko project, Leg 3, *Earth & Planet. Sci. Lett.*, **83**, 267-284, 1987.

Fujioka, K., A. Takeuchi, K. Horiuchi and H. Okano, Topography and tectonics of landward and oceanward slopes of the Japan Trench, *Abstr. 9th Shinkai Symposium*, 1-4,1992.

Hamuro, K., Petrology of the Higashi-Izu monogenic volcano group, *Bull. Earthq. Res. Inst., Univ. of Tokyo*, **60**, 335-400, 1985.

Kasuga, S., Y. Kato, S. Kimura, K. Okino, Present and Former Members of the Continental Shelf Surveys Office, Characteristics of arc-trench systems and back-arc basins in the southern waters of Japan—Outline of the geophysical survey by the Hydrographic Department of Japan— (in Japanese with English Abstr.), *Report of Hydrographic Research*, **28**, 19-54, 1992.

KAIKO I Research Group, *Detailed topography of trenches and troughs around Japan* (Charts with explanations), Univ. of Tokyo Press, 1985.

KAIKO I Research Group, *Topography and structure of trenchesaround Japan—Data atlas of Franco-Japanese KAIKO Project, Phase I*—ORI/IFREMER/CNRS, 305pp. 1986.

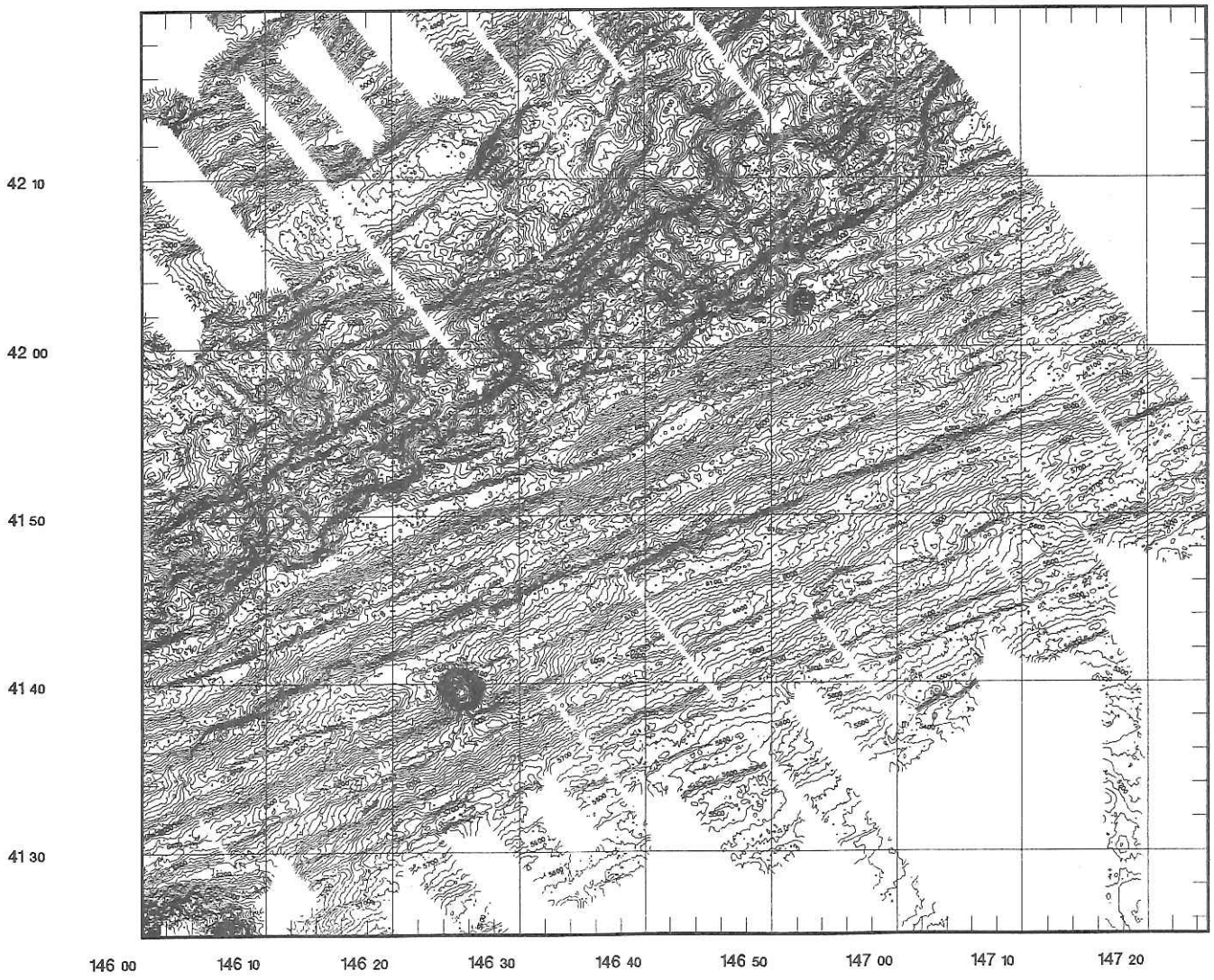

Fig. 8-1. Two knolls in the oceanward slope of the Kuril Trench identified by cruise KH 92-3.

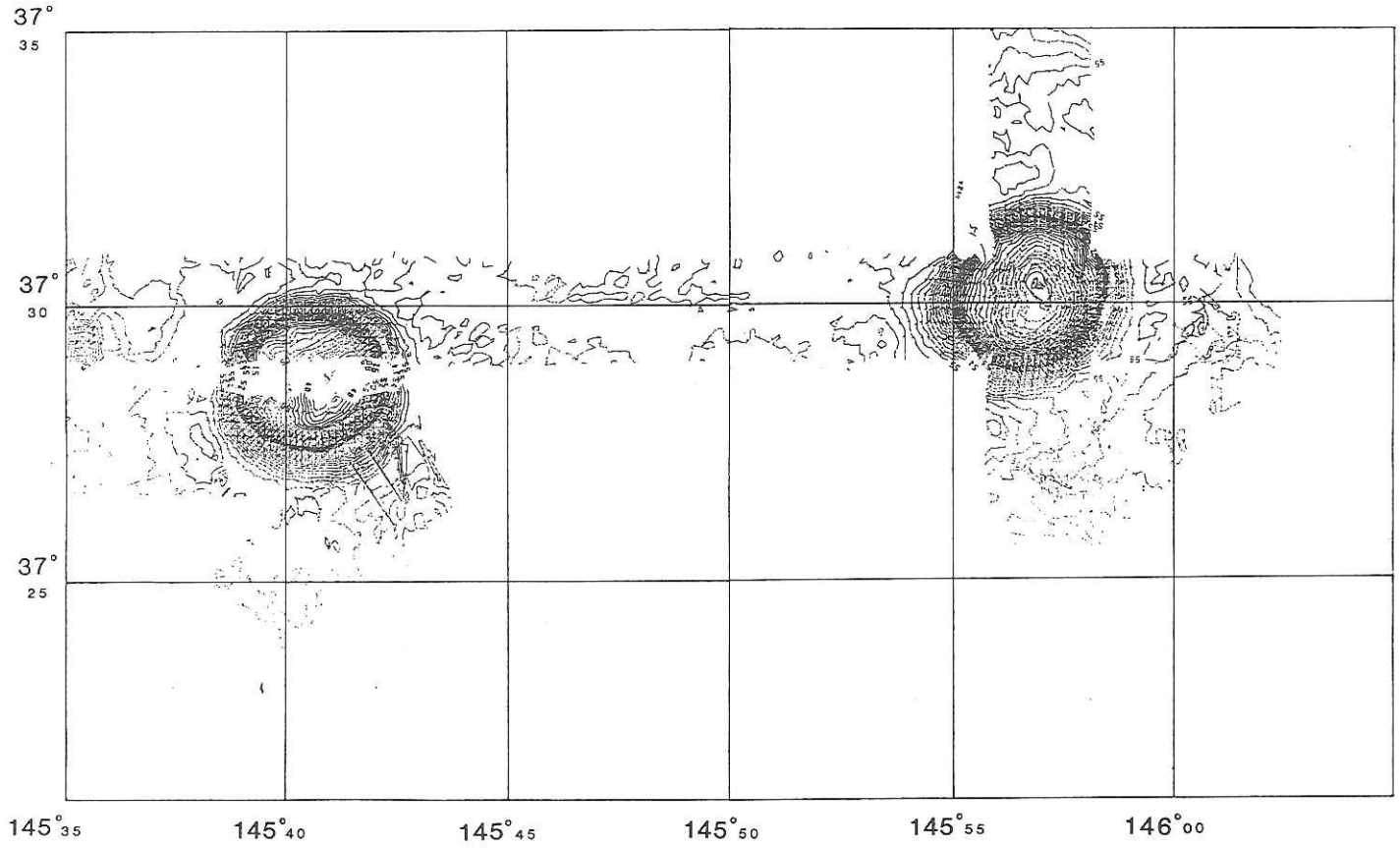

Fig. 8-2. Topography and alignment of two knolls situated south to southwest of Soma Seamount. See Fig. 7-1 for their relationship with the Joban Seamount Chain.

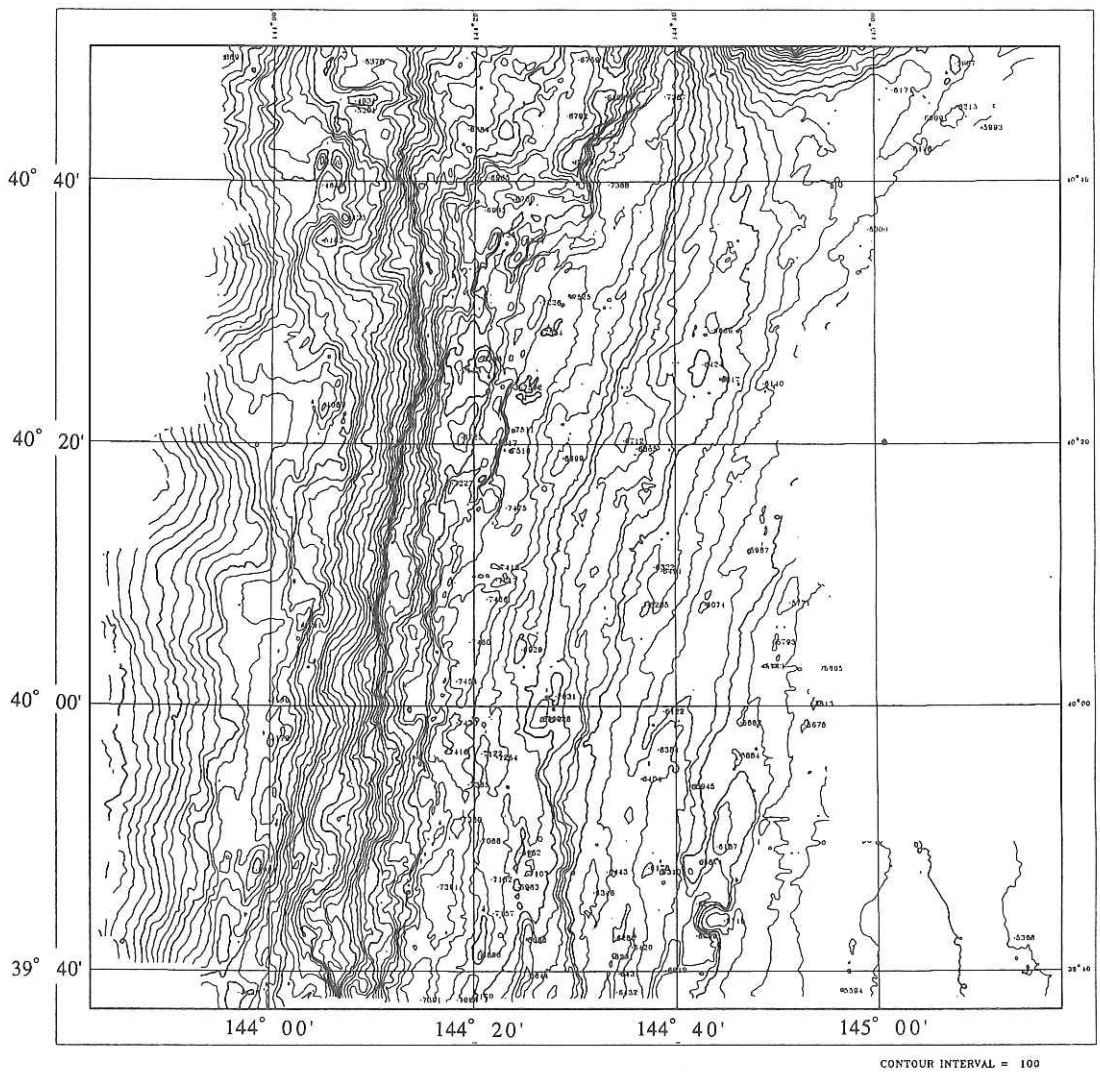

Fig. 8-3. Topography of a knoll in the oceanward margin of the northern Japan Trench (reproduced from KAIKO I Research Group, 1985; 1986; Cadet *et al.*, 1987).

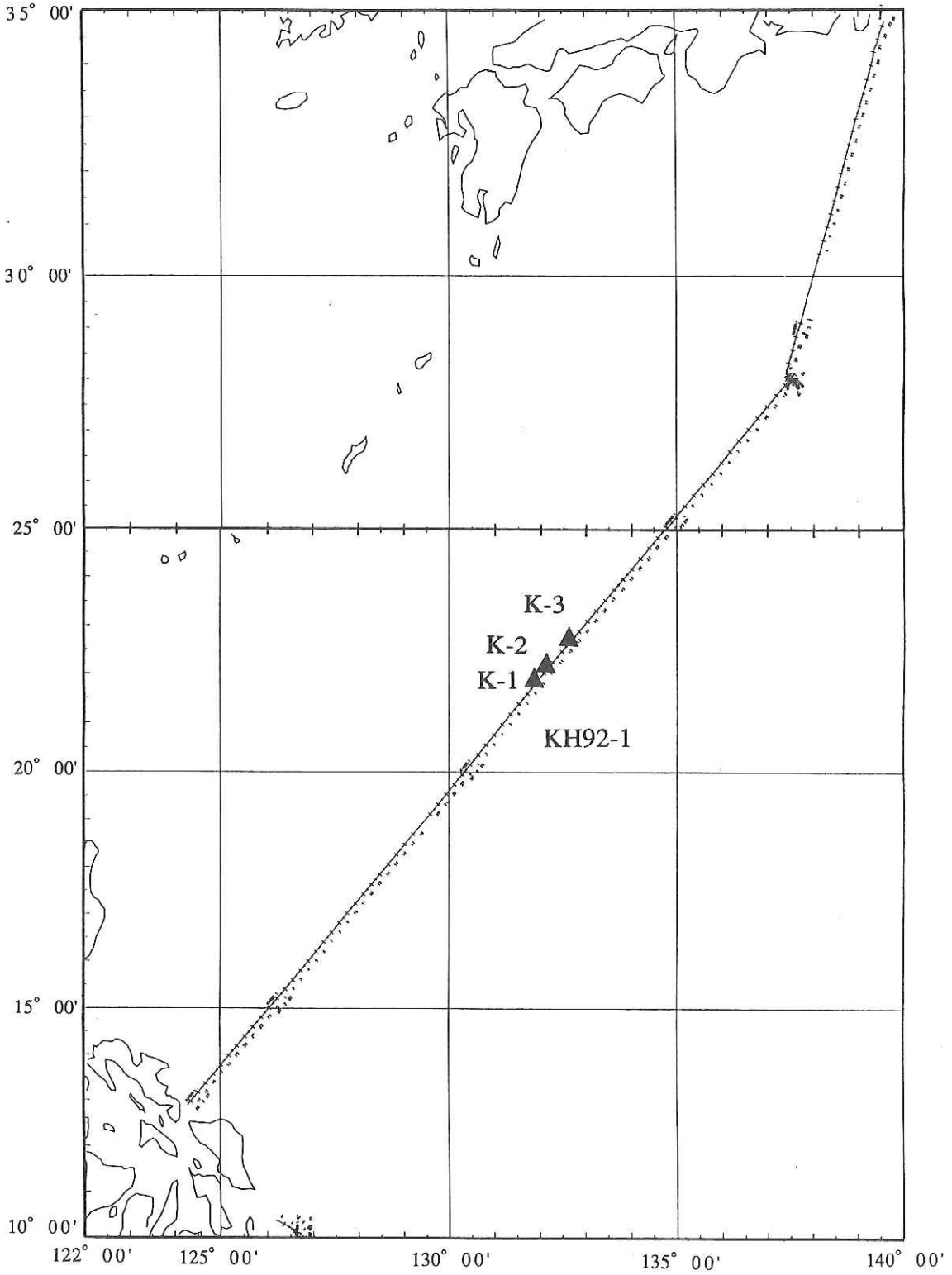

Fig. 8-4 (a). Topography of knolls in the Philippine Sea–Index map

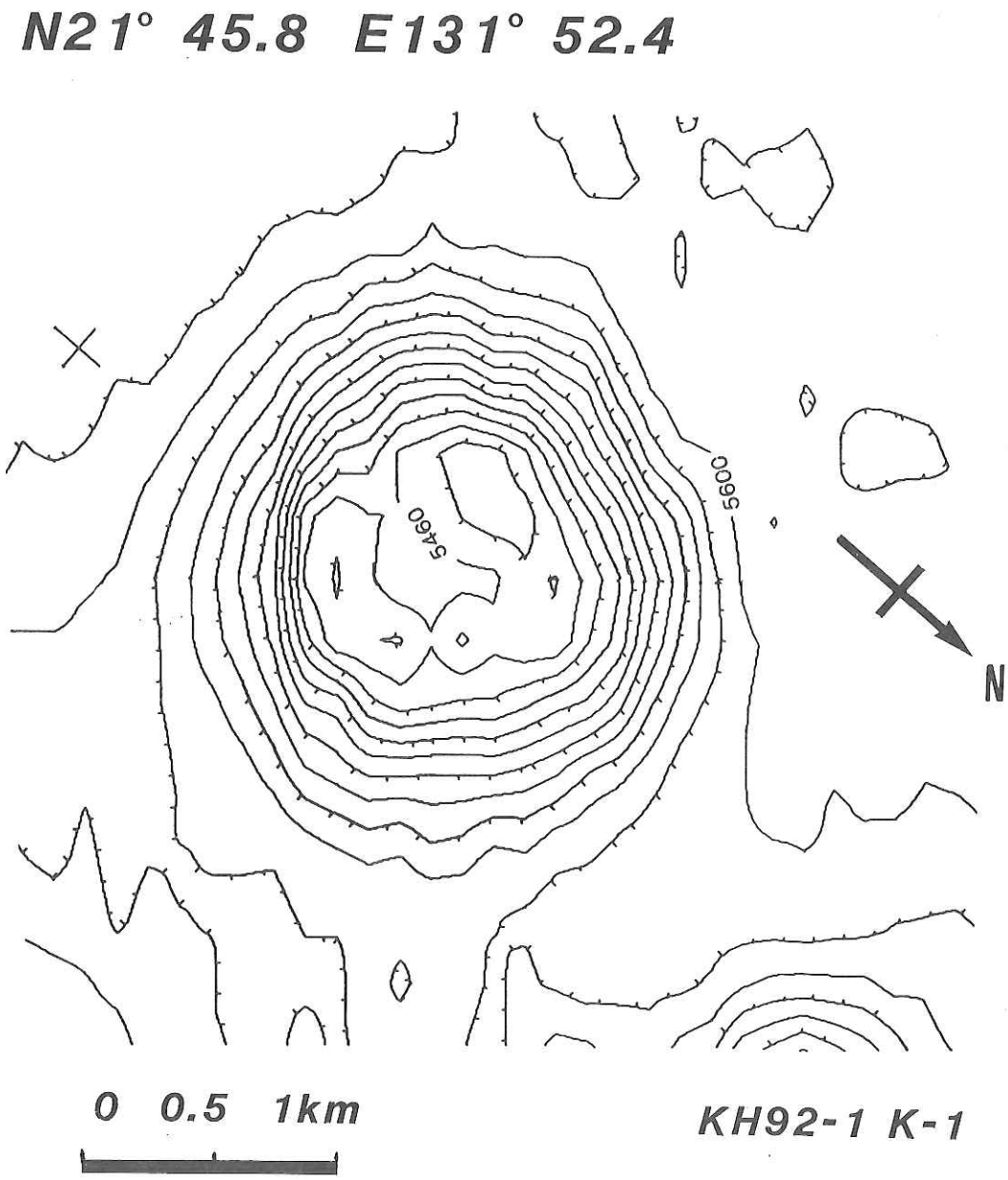

Fig. 8-4 (b). Topography of knolls in the Philippine Sea–Knoll K-1

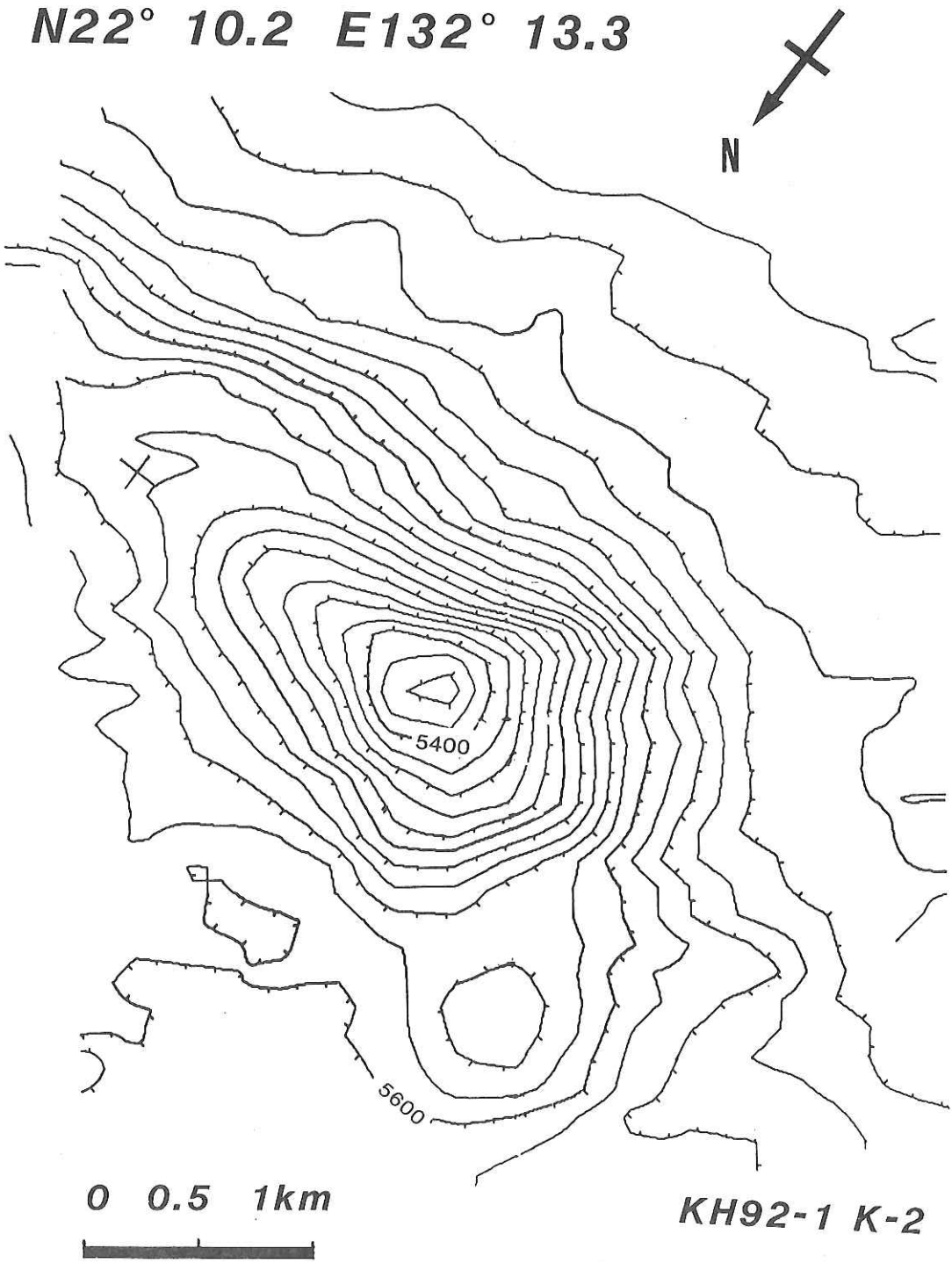

Fig. 8-4 (c). Topography of knolls in the Philippine Sea–Knoll K-2

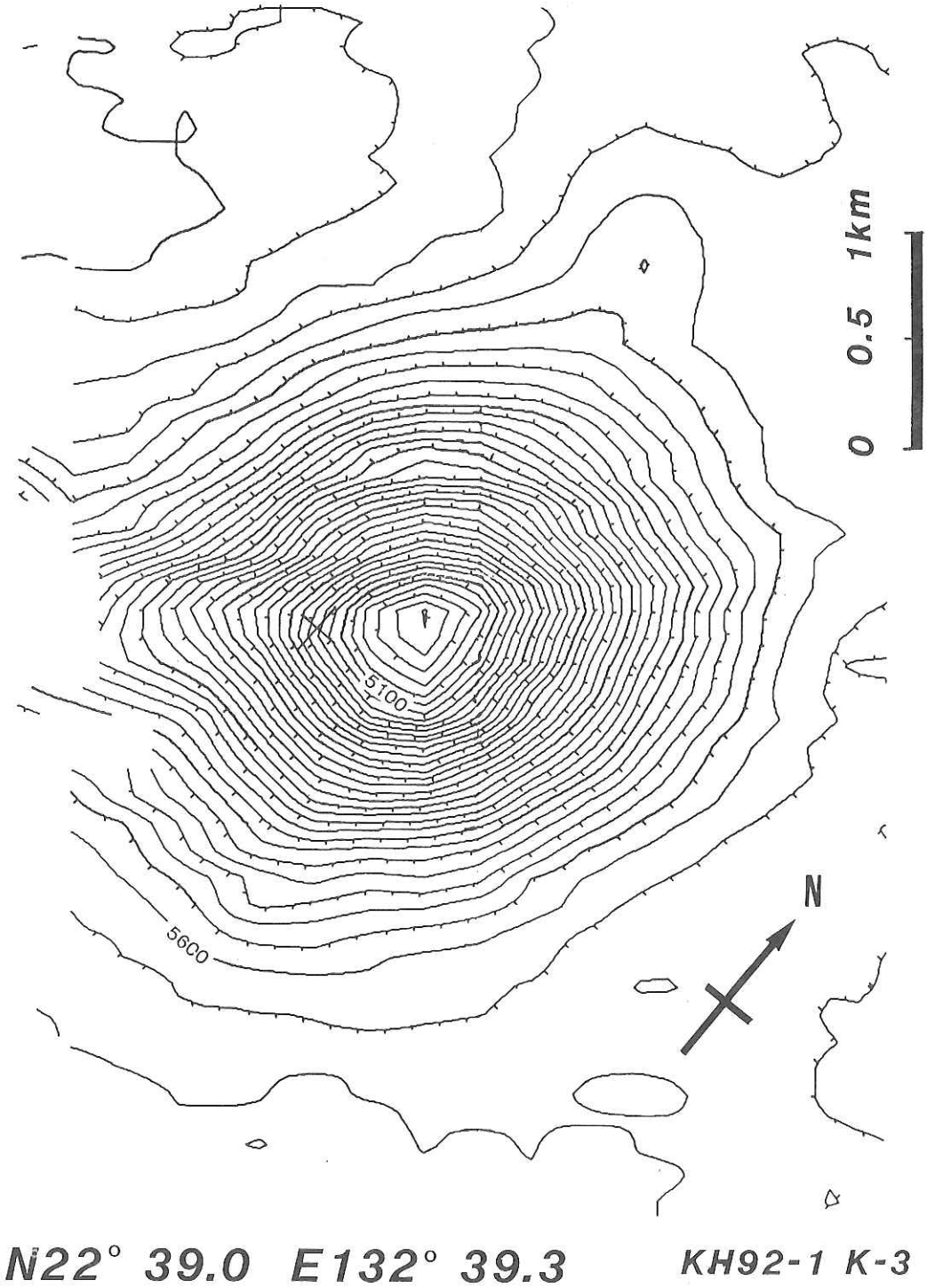

Fig. 8-4 (d). Topography of knolls in the Philippine Sea–Knoll K-3

9. Magnetic Anomalies near the Kuril Trench

M. Nakanishi, K. Sayanagi, D. C. P. Masalu, J. Korenaga, and K. Tamaki

There exist Mesozoic magnetic anomaly lineations near the Kuril Trench (*e.g.*, Nakanishi *et al*, 1989). The strike of the lineations is N70°E. The isochron numbers of lineations are M5, M6 and M7 and their ages are in Early Cretaceous, approximately 126.5~128 Ma. We carried out magnetic measurement with Sea Beam survey to reveal the features of magnetic anomaly lineations near the Kuril Trench in more detail and to clarify influence of a trench on magnetic anomaly lineations.

Magnetic anomalies were calculated with the reference field of IGRF 1985 (IAGA, Division Working Group 1, 1985). The profiles of magnetic anomalies near the Kuril Trench along the ship's tracks are shown in Fig. 9-1. We can identify the Mesozoic magnetic anomaly lineations between chron M5 and M9 from this figure. However, no negative anomaly M4 is identified, probably because it is too deeply subducted. The peak-to-zero amplitude of anomaly M5 decreases from 350 nT to 150 nT westward. That of anomaly M7 decreases from 400 nT to less than 100 nT in the same manner as that of anomaly M5. However, that of anomaly M6 is almost constant, 100~150 nT. Those of lineations older than chron M8 do not decrease westward (see Figure 3 of Nakanishi *et al.*, 1989).

We propose that the decrease of amplitude of anomalies M5 and M7 is due to the subduction of the Pacific Plate at the Kuril Trench. The trend of the Kuril Trench is N65°E, which is not parallel to the strike of lineations from M5 to M7 (N70°E). The distance from the anomaly M5 to the trench axis becomes larger as westward. This imples that the depth of the Pacific Plate below the anomalies becomes greater as westward. Hence, the decrese of amplitude of anomaly M5 corresponds to the subduction of the Pacific Plate. Similarly, the amplitude of anomaly M7 decreases with the subduction of the Pacific Plate.

Distance from anomaly M5 to the Kuril Trench axis increases from 35 to 60 km westward. Magnetic anomaly lineations are identified at a distance as far as 100 km from the trench axis of the Japan Trench (Nakanishi *et al*, 1989). The depth of the Pacific plate at the position is about 20 km (Murauchi and Ludwig, 1980). In contrast the dip-angle of the plate subduction along the Kuril Trench is 20°~25° (Iwasaki *et al.*, 1991). Hence, depth of the Pacific plate at 60 km from the Kuril Trench axis is about 20 km and is nearly the same as that of above-mentioned position in the Japan Trench. The magnetic structure of the Pacific plate seems to be destroyed at depth of 20 km.

No magnetic anomaly lineations are seen at the landward side of the Izu-Ogasawara Trench (Nakanishi *et al*, 1989). This seems to be due to existence of many volcanics preventing identification of any magnetic anomaly lineations.

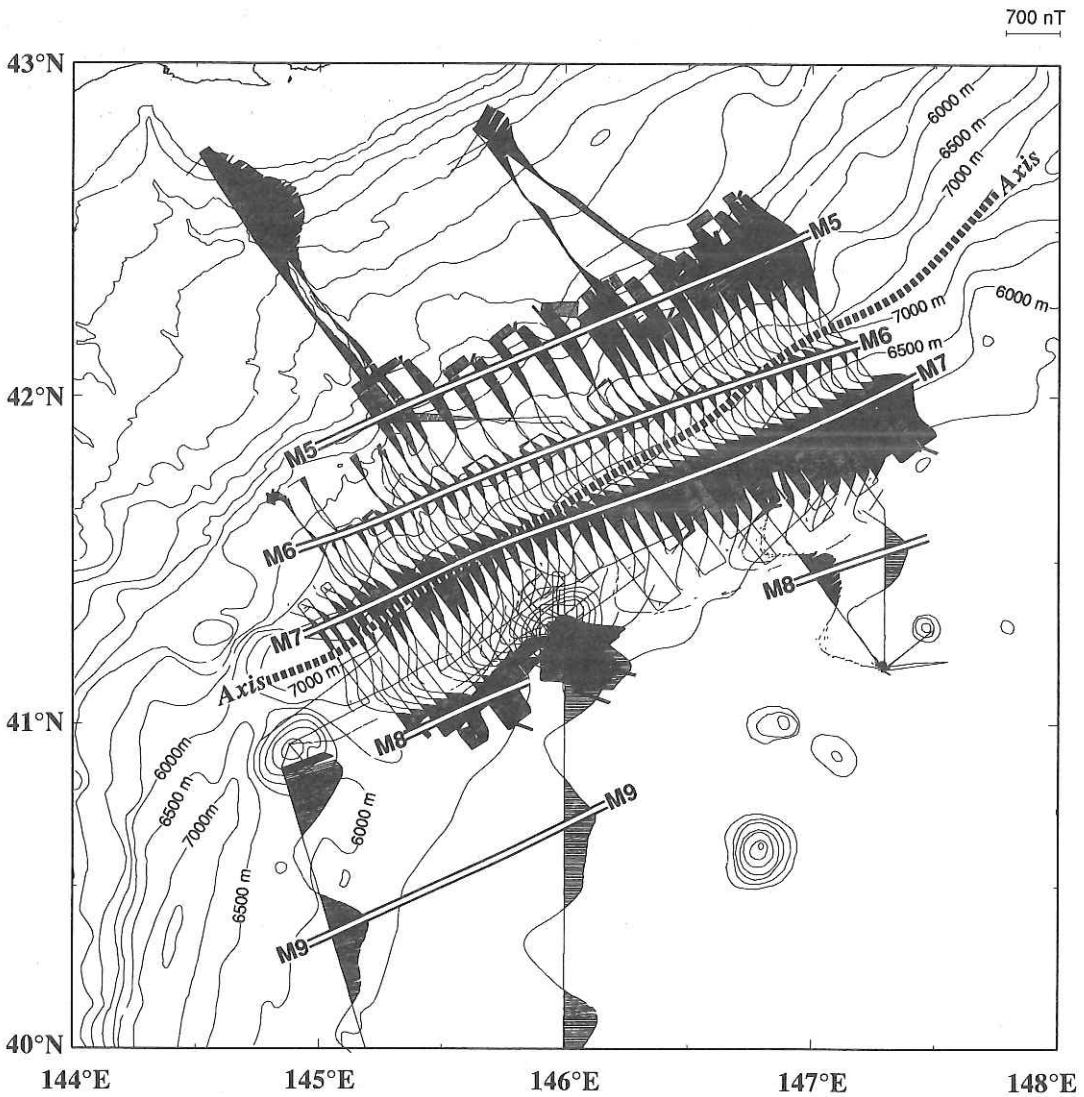

Fig. 9-1. Magnetic anomaly profiles along ships' tracks (reference field: IGRF 1985) near the Kuril Trench. Portions of positive anomalies on the profiles are shades black. The GEBCO (General Bathymetric Chart of the Oceans) bathymetric contours are shown for reference with contour interval is 500 m. The trench axis is shown by a dashed line.

References

IAGA Division I, Working Group 1, Internatinal Geomagnetic Reference Field 1985, *J. Geomag. Geoelectr.*, **37**, 1157-1163, 1985.

Iwasaki, T., N. Hirata, T. Kanazawa, T. Urabe, Y. Motoya, and H. Shimamura, Earthquake distribution in the subduction zone off eastern Hokkaido, Japan, deduced from ocean-bottom seismographic and land observations, *Geophys. J. Int.*, **105**, 693-711, 1991.

Murauchi, S. and W. J. Ludwig, Crustal structure of the Japan Trench: the effect of subducton of ocean crust, *Init. Repts. Deep Sea Drilling Project*, **56/57**, Part 1, 463-469, 1980.

Nakanishi, M., K. Tamaki, and K. Kobayashi, Mesozoic magnetic anomaly lineations and seafloor spreading history of the northwestern Pacific, *J. Geophys. Res.*, **94**, 15437-15462, 1989.

10. Geomagnetic Survey of Seamounts near the Kuril and Japan Trenchs

D. C. P. Masalu, K. Sayanagi, J. Korenaga, M. Nakanishi, K. Tamaki, and K. Kobayashi

Introduction

In the cruise KH 92-3 we conducted detailed systematic geomagnetic total force survey on five seamounts; Takuyo-Daiichi, Ryofu, Soma (provisional name), Daiyon-Kashima and Daigo-Kashima Seamounts (Fig. 10-1). Mizunagi-dori (Bosei), Hitachi and Futaba Seamounts which were investigated in 1990 during Leg 1 of cruise KH 90-1 (Masalu *et al.*, 1991) were surveyed to complement the previous data.

Erimo Seamount that had already been extensively studied by KAIKO investigators (Cadet *et al.*, 1987; Yamazaki, 1988) was surveyed only during transits to and from the working stations. Uyeda and Richards (1966) and Hildebrand and Parker (1987) analyzed the Ryofu Seamount but we revisited it with more precise positioning and bathymetric data. In this article we present the observed magnetic anomalies over the five seamounts that were surveyed in detail (Figs. 10-2 to -6).

Preliminary Results and Interpretation

We computed geomagnetic anomalies over each surveyed seamount from the measured geomagnetic total force with reference to the IGRF 1985 (IAGA WORKING GROUP 1). Magnetic anomalies over Takuyo-Daiichi, Daigo-Kashima, Daiyon-Kashima, Soma and Ryofu Seamounts range between -552.7nT to 715.9 nT, -1288.4nT to 726.3nT, -388.2nT to 335.8nT, -351.1nT to 429.0nT and -624.6 to 116.1nT respectively. In addition to the linear anomalies which are correlatable to seafloor spreading (Figs. 10-2 and -3), magnetic anomalies related to seamount topography are clearly recognized over each seamount.

The pattern of magnetic anomalies over all five seamounts, Soma, Takuyo-Daiichi, Daiyon-Kashima, Ryofu and Daigo-Kashima Seamounts, having a negative seamount magnetic anomaly lobe to the north and a positive seamount magnetic anomaly lobe to the south, suggests that these seamounts may be normally magnetized. However, their exact magnetization structure will only be known after seamount paleomagnetism technicque has been perfomed on their data. The positive lobe of seamount magnetic anomaly of Soma seamount (Fig. 10-2) is partly obscured. This may be due to interference between the seamount magnetic anomaly and magnetic anomaly lineation, or complex magnetization structure of the seamount itself.

We hope that the detailed analysis of the presently acquired seamount magnetic data in combination with seamount magnetic data acquired from the Joban seamount chain during Leg 1 of cruise KH90-1, may provide us more information about the tectonics of the Pacific plate, the origin of the Joban Seamount Chain and, on a larger scale, the origin of the abundunt western Pacific seamounts.

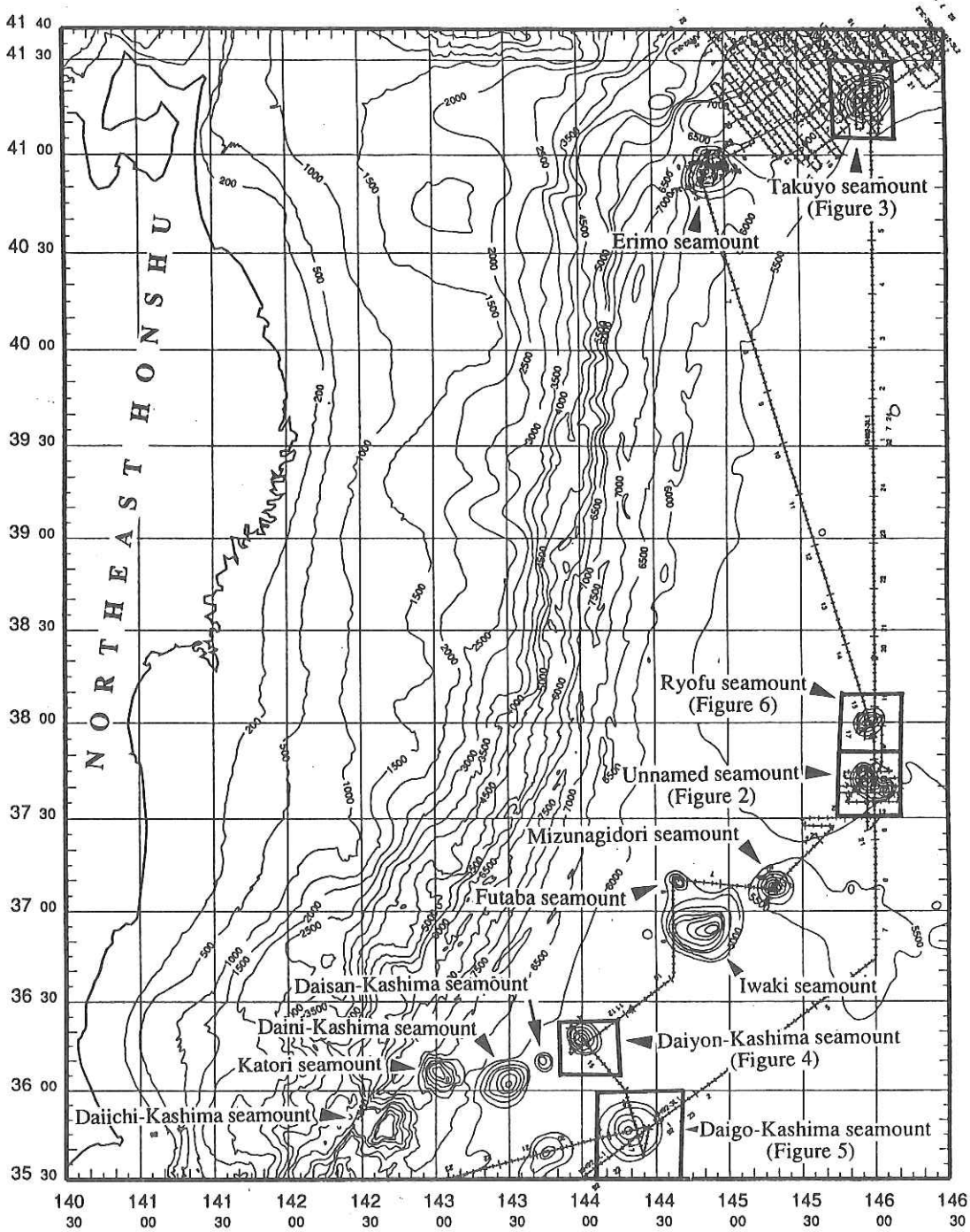

Fig. 10-1. Index map for the seamount surveyed and detail magnetic anomaly figures (boxes) shown in this article. The map shows the ship's tracks during the survey.

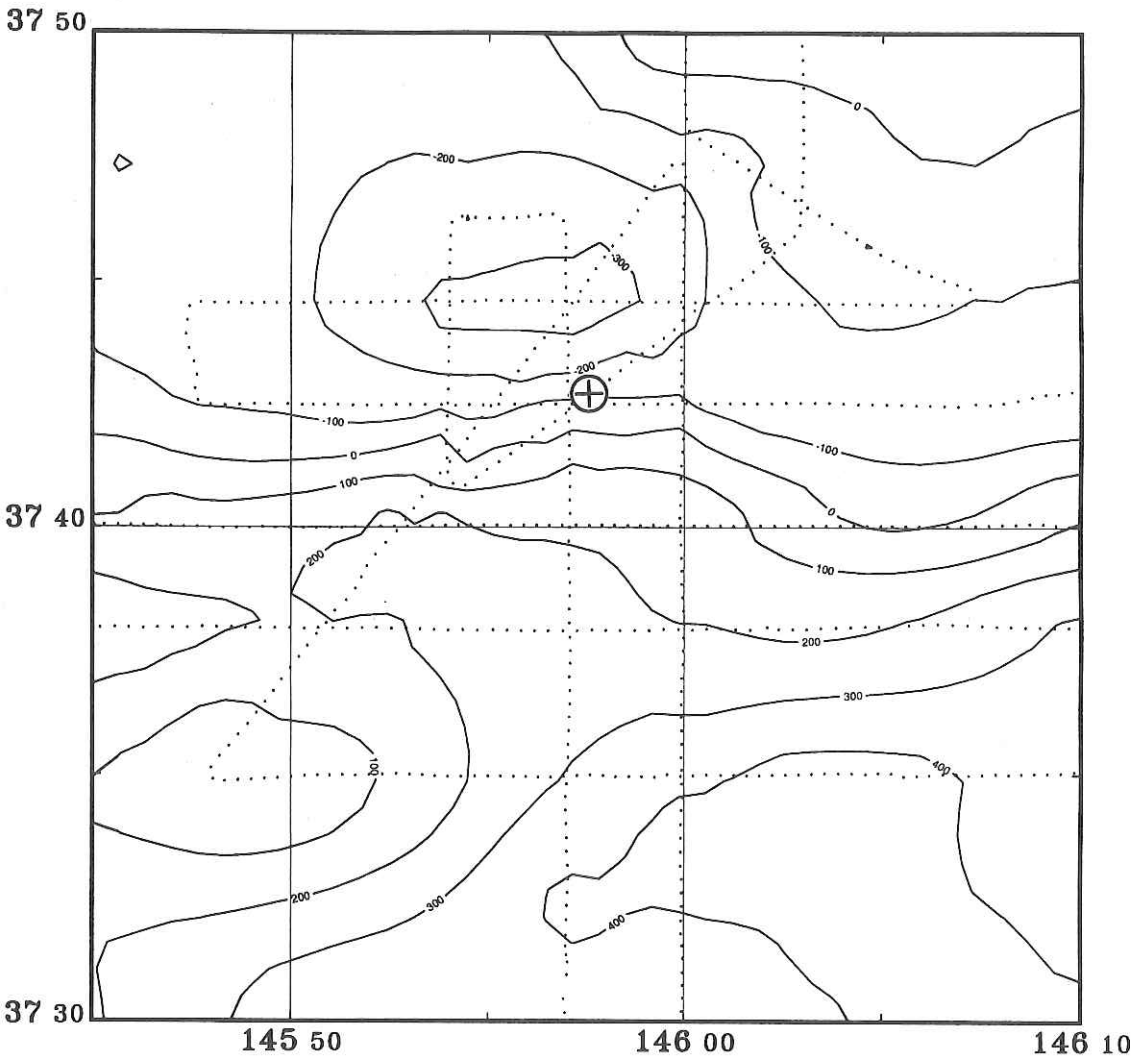

Fig. 10-2. Magnetic anomalies over Soma Seamount. Contour interval is 100nT. Dots are data point locations along ship tracks during the survey in this cruise. Encircled cross is relative position of the peak of the seamount.

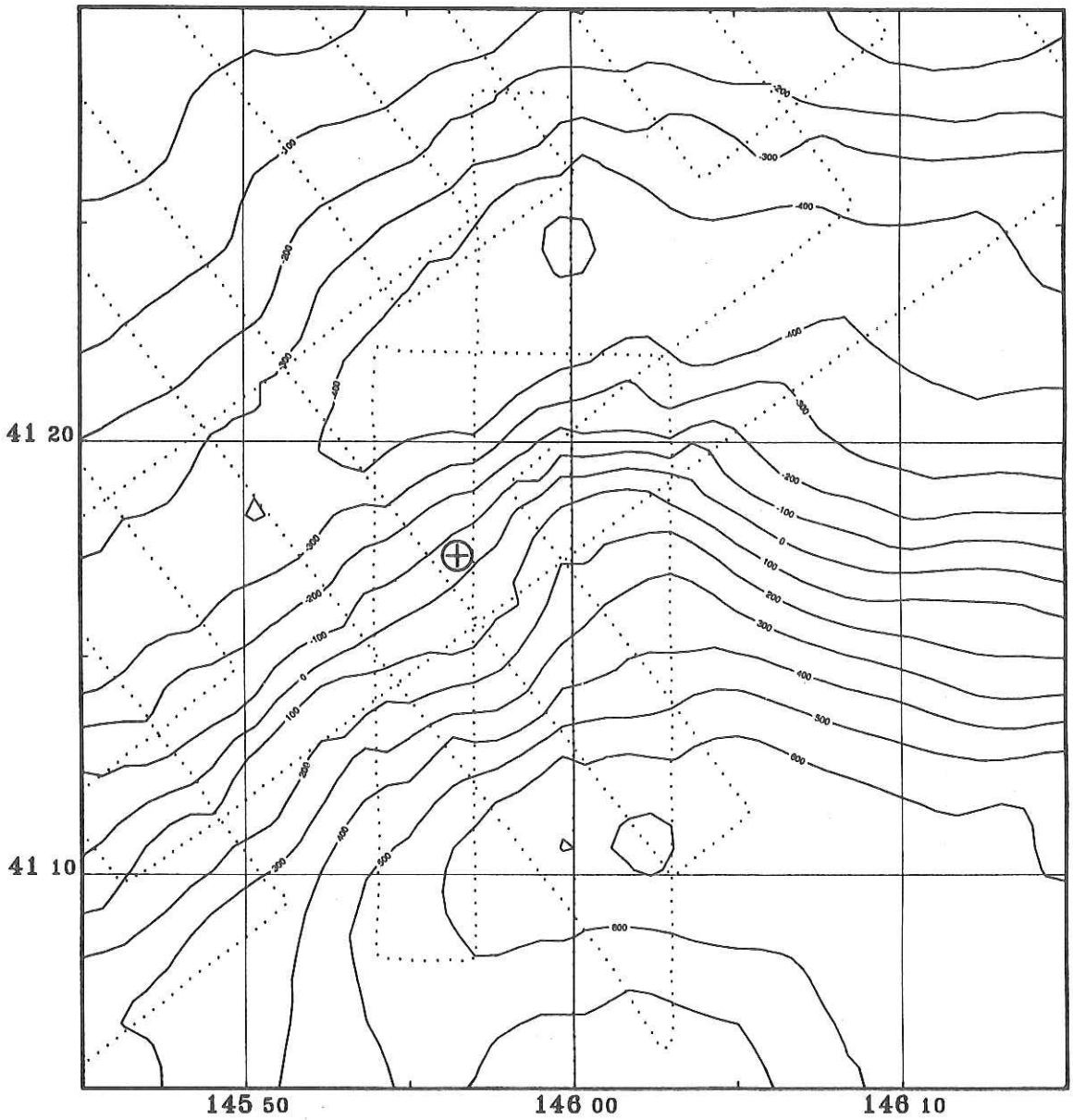

Fig. 10-3. Magnetic anomalies over Takuyo-Daiichi Seamount. Other panels as in Fig. 10-2.

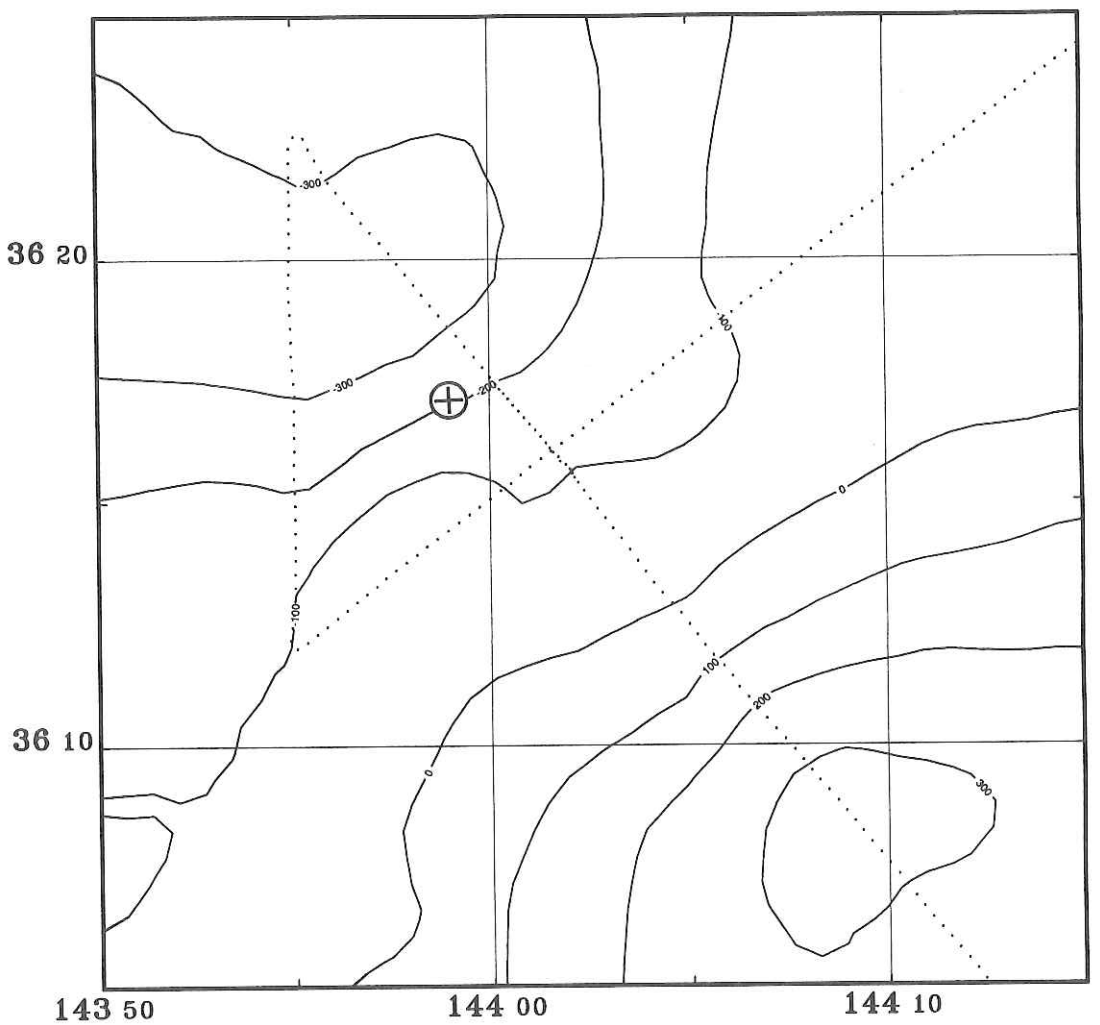

Fig. 10-4. Magnetic anomalies over Daiyon-Kashima Seamount. Other panels as in Fig. 10-2.

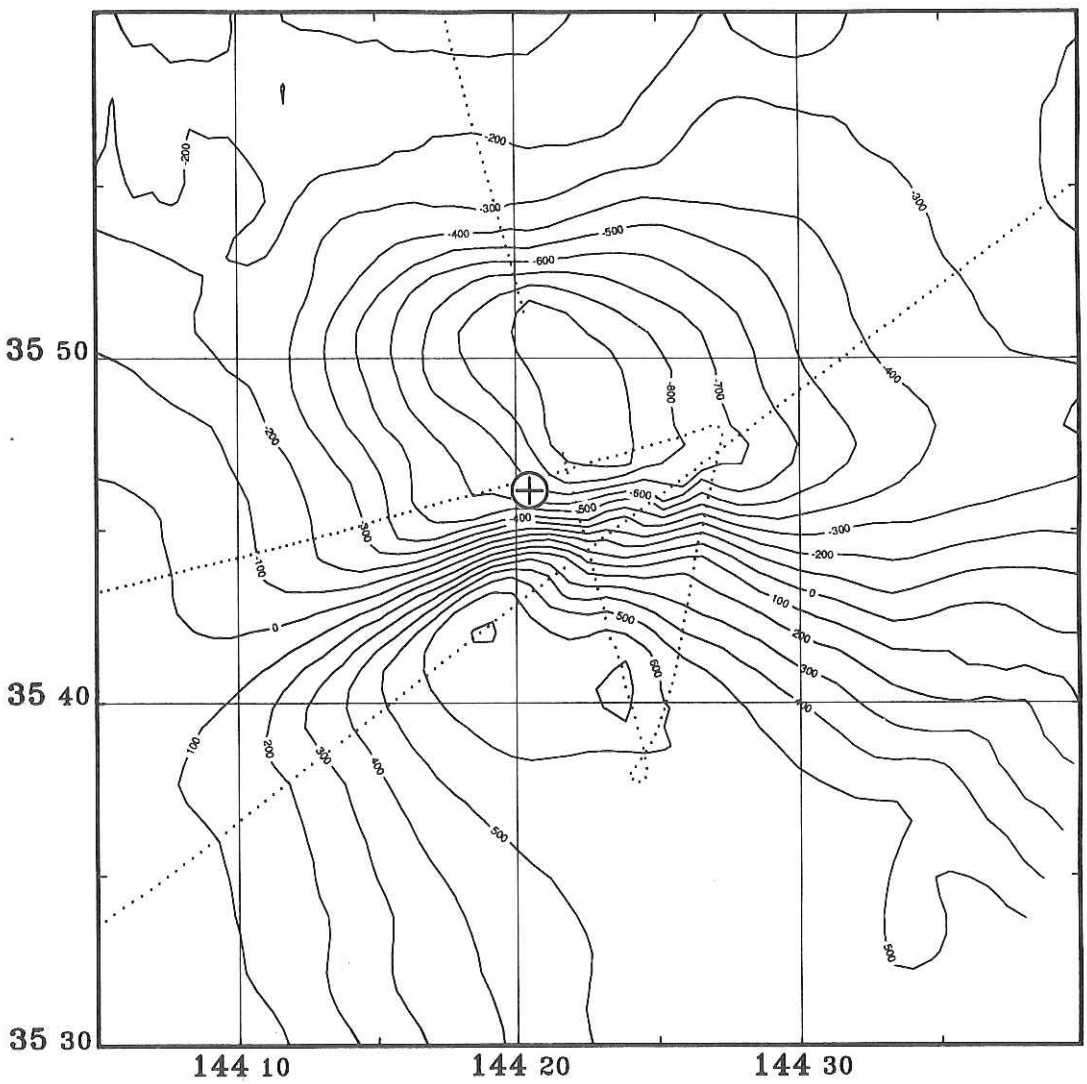

Fig. 10-5. Magnetic anomalies over Daigo-Kashima Seamount. Other panels as in Fig. 10-2.

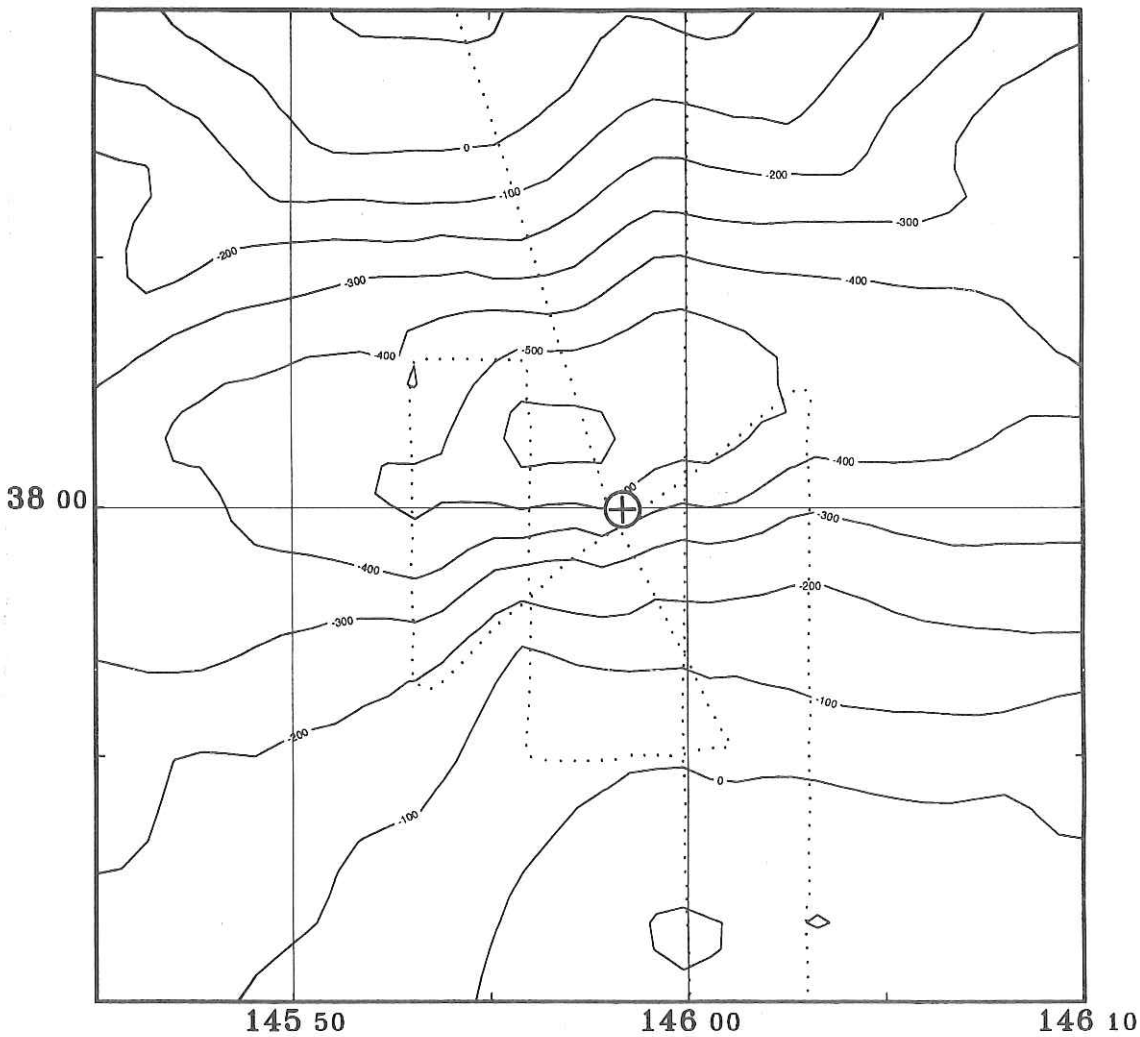

Fig. 10-6. Magnetic anomalies over Ryofu Seamount based upon the present data alone. Other panels as in Fig. 10-2.

REFERENCES

Cadet, Jean-Paul, K. Kobayashi, Aubouin, J., Boulegue, J., Deplus, C., Dubois, J., von Huene, R., Jolivet, L., Kanazawa, T., Kasahara, J., Koizumi, K., Lallemand, S., Nakamura, Y., Pautot, G., Suyehiro, K., Tani, S., Tokuyama, H., and Yamazaki, T., The Japan Trench and its juncture with the Kuril Trench: cruise results of the Kaiko project, Leg 3, *Earth and Planetary Science Letters*, **83**, 267 - 284, 1987.

Hildebrand, J. A. and R. L. Parker, Paleomagnetism of Creatceous Pacific seamounts revisited, *J. Geophys. Res.*, **92**, 12695 - 12712, 1987.

IAGA WORKING GROUP 1, International Geomagnetic Reference Field 1985, *J. Geomag. Geoelectr.*, **37**, 1157 - 1163, 1985.

Masalu, D. C. P., M. Nakanishi, A. Oshida, K. Tamaki and K. Kobayashi, Magnetic anomalies of the Joban seamount chain, in Kobayashi, K.(ed.) *Preliminary Report of the Hakuho Maru Cruise KH90-1*, Ocean Research Institute University of Tokyo, 75 - 78, 1991.

Uyeda, S. and M. L. Richards, Magnetization of four Pacific seamounts near the Japanese Islands, *Bull. Earthquake Res. Inst., Univ. of Tokyo*, **44**, 179 - 213, 1966.

Yamazaki, T., Magnetization of Erimo seamount, *J. Geomag. Geoelectr.*, **40**, 715 - 728, 1988.

11. Magnetic Anomalies over the Joban Seamount Chain

D. C. P. Masalu, K. Sayanagi, J. Korenaga, M. Nakanishi, K. Tamaki, and K. Kobayashi

Introduction

In the present KH 92-3 cruise we conducted detailed systematic geomagnetic total force survey on two seamounts; Ryofu and Soma Seamounts, that lie on the Joban Seamount Chain. We also surveyed to some extent two others; Futaba and Daiyon-Kashima Seamounts, that we could not survey in detail during cruise KH 90-1 (Masalu *et al.*, 1991a & b) due to time restriction. Furthermore, in the KH 92-3 cruise we surveyed magnetics of an isolated nearby seamount ; Daigo-Kashima Seamount, located on the southeast of Daiyon-Kashima Seamount.

We surveyed Futaba and Daiyon-Kashima Seamounts to increase their geophysical and SeaBeam bathymetric survey coverage to enable comprehensive geophysical analyses to be performed on these seamounts. This cruise, therefore, marks the completion of geophysical surveys on all seamounts forming the Joban Seamount Chain. The southwestern end of the Joban Seamount Chain; Daiichi-Kashima anSeamount and adjacent Katori Seamount, have been surveyed by the Kaiko project (Kobayashi *et al.*, 1987) and other investigators (Ueda, 1985), respectively. In this report we present the complete map of magnetic anomalies over the Joban Seamount Chain (Fig. 11-1) base solely on data obtained during cruises KH 90-1 and KH 92-3.

Preliminary Results and Interpretation

We computed magnetic anomalies over the Joban Seamount Chain from the measured total force with reference to the IGRF 1985 (IAGA WORKING GROUP NO 1, 1985). Anomaly values range between -1288.4 nT and 726.3 nT. We plotted these anomalies as it is shown in Fig. 11-1. The detail description of these anomalies over each seamount are given by Masalu *et al.*, (1991b; this issue). The data we collected during this cruise from seamounts on the Joban seamount chain that were surveyed less extensively during cruise KH90-1, however, did not cause any major changes on the shape of anomalies on these seamounts.

Seamount anomaly on Daiyon-Kashima is not clearly recognizable (Fig. 11-1) probably due to being obscured by magnetic lineation. Futaba seamount is surrounded by only positive anomaly contours (Fig. 11-1 & -2). The negative lobe for this seamount is not present. This may be due to interference by the strong field of the nearby Iwaki Seamount, complex magnetization of Futaba Seamount itself or even being obscured by magnetic lineation anomaly. All seamounts on the Joban seamount chain with the exception of Mizunagidori seamount, have a negative lobe of seamount anomaly north of a positive lobe of seamount anomaly. This pattern suggests that these seamounts may be normally magnetized. However actual magnetization structure of these seamounts will be known after a seamount technique has been applied on their data.

We hope that the results of seamount paleomagnetism technique on the complete set of seamount magnetic and bathymetric data from the Joban

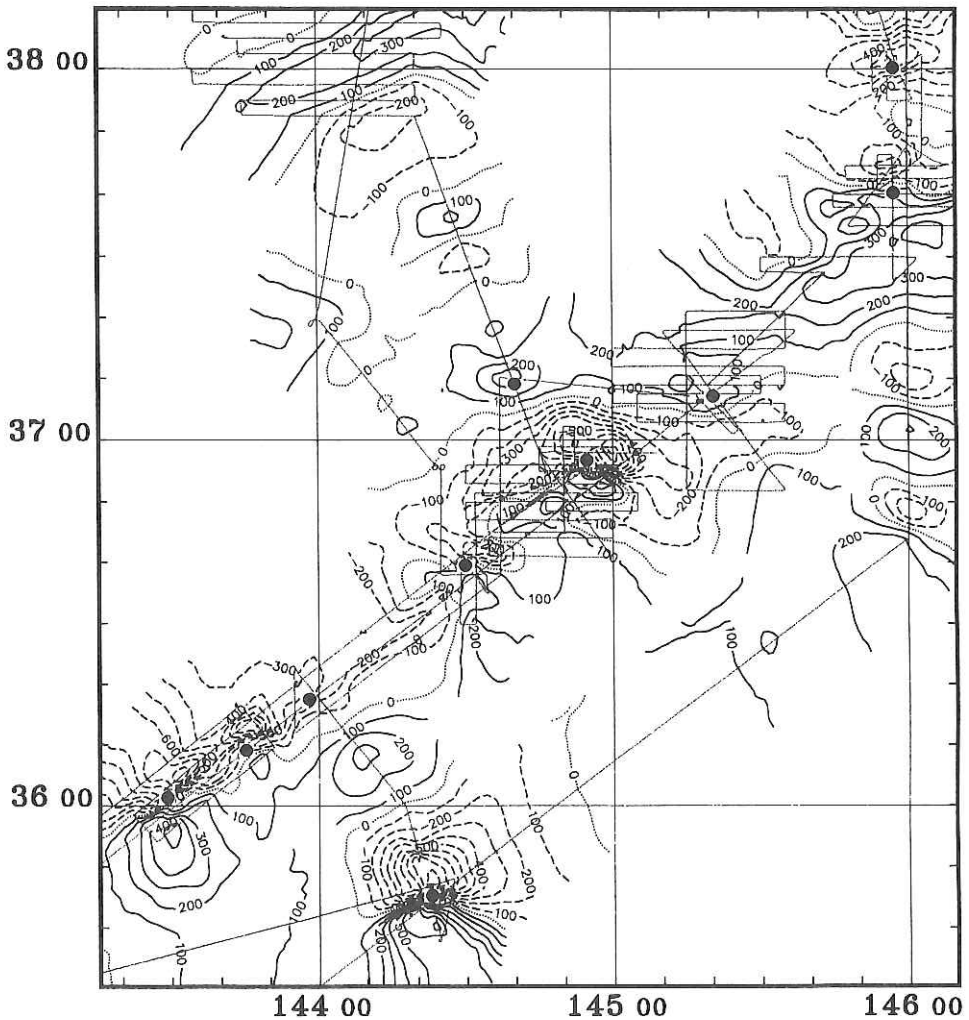

Fig. 11-1. Magnetic anomalies over the Joban seamount chain and nearby seamounts. Negative anomalies are shown by dashed contours. Positive anomalies are shown by solid contours. Zero anomaly is shown by dotted contour. Contour interval is 100 nT. The big solid circles indicate relative position of the peaks of the seamounts (Fig. 7-1 in Masalu *et al.*, this issue). [Small dots along lines indicate data points along the ship tracks.]

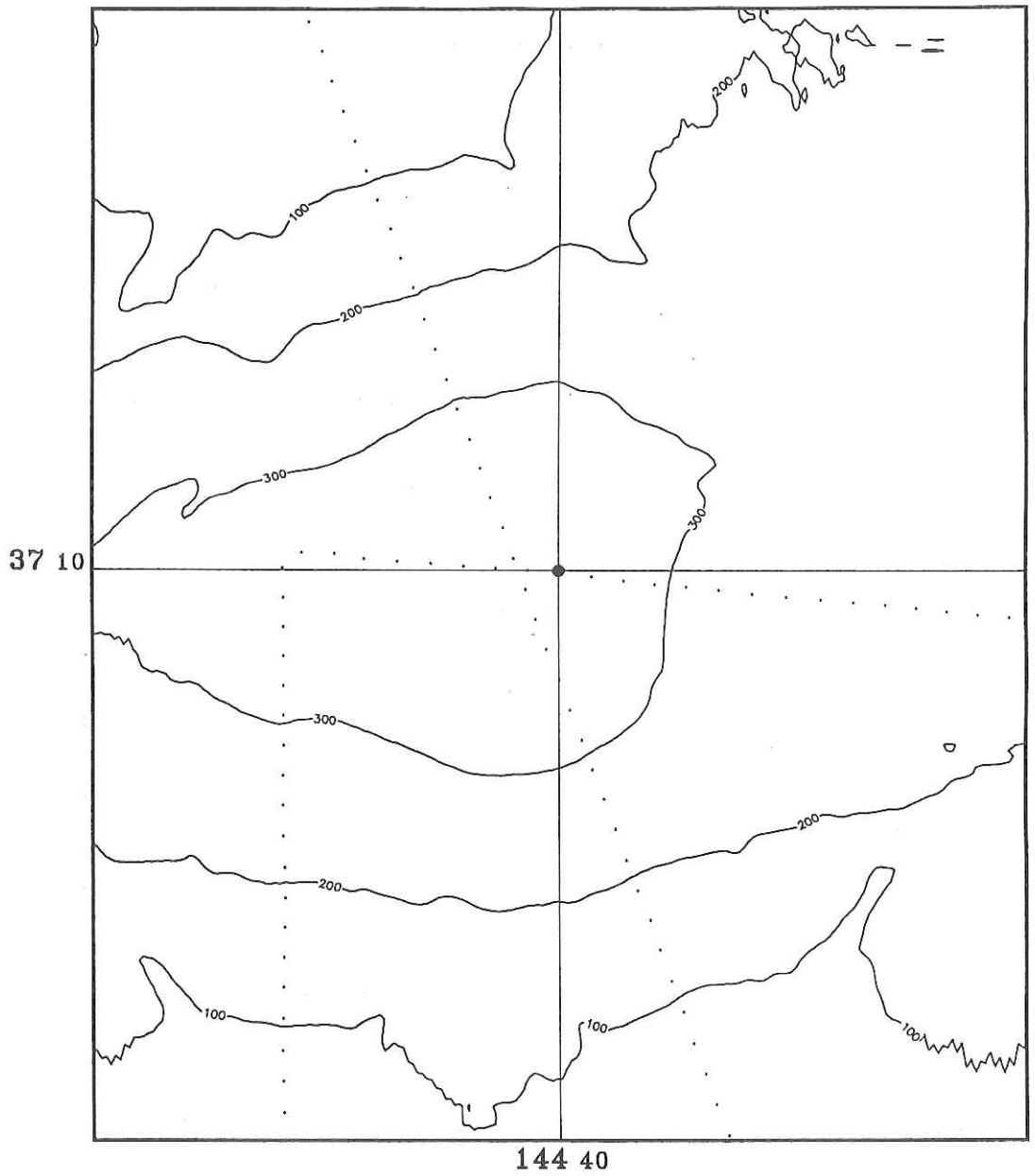

Fig. 11-2. Magnetic anomalies over Futaba seamount chain. Contour interval is 100 nT. Other panels as in Fig. 11-1.

seamount and nearby seamounts that we collected during cruises KH 90-1 and KH 92-3, will give us more information on the origin, geology and geophysics of the Joban seamount chain. They may also be crucial in the tectonics of the Pacific plate.

References

IAGA WORKING GROUP NO 1, International Geomagnetic Reference Field 1985, *J. Geomag. Geoelectr.*, **37**, 1157-1163, 1985.

Kobayashi, K., J. P. Cadet, J. Aubouin, J. Boulegue, J. Dubois, R. von Huene, L. Jolivet, T. Kanazawa, J. Kasahara, K. Koizumi, S. Lallemand, Y. Nakamura, G. Pautot, K. Suyehiro, S. Tani, H. Tokuyama and T. Yamazaki, Normal faulting of the Daiichi-Kashima seamount in the Japan trench revealed by the Kaiko I Cruise, Leg 3, *Earth and Planet. Sci. Lett.*, **83**, 257-266, 1987.

Masalu, D. C. P., A. Oshida, M. Nakanishi, K. Tamaki, K. Kobayashi and Y, Ogawa, Bathymetric mapping of the Joban seamount chain, in *Preliminary report of the Hakuho-Maru cruise KH90-1* (ed. K. Kobayashi), Ocean Research Institute, University of Tokyo, 30-37, 1991a.

Masalu, D. C. P., M. Nakanishi, A. Oshida, K. Tamaki and K. Kobayashi, Magnetic anomalies of the Joban seamount chain, in *Preliminary report of the Hakuho-Maru cruise KH90-1* (ed. K. Kobayashi), Ocean Research Institute, University of Tokyo, 75-78, 1991b.

Ueda, Y., Geophysical study on seamounts Daiiti-Kasima and Katori with special reference to a subduction process of Daiiti-Kasima, *J. Geomag. Geoelectr.*, **37**, 601-625, 1988.

12. Measurement of Geomagnetic Three-component Anomalies in the Southwesternmost Part of the Kuril Trench

A. Kitahara, K. Sayanagi, J. Korenaga and N. Isezaki

1. Introduction

The STCM (Shipboard Three Component Magnetometer ; Isezaki *et al.*,1981) has been used to get the three component geomagnetic fields at sea in the last ten years. The main characteristics of three component anomalies are as follows (*e.g.* Isezaki *et al.*, 1981; Isezaki, 1986; Seama *et al.*, 1992),

1) If the magnetic anomaly source body is two or three dimensional one can be determined from the three component data even a single measurement line.
2) The dip and strike of two dimensional source body can be determined directly (without any assumption) from the three component anomaly data.
3) The three component anomaly is not affected by ambient geomagnetic field and the trend of magnetic anomaly lineation, and can be observed even at the geomagnetic equator, while the total intensity anomaly becomes very small at the equator area if the lineation trends NS.
4) The bottom depth of the two dimensional source body can be estimated directly from the three component anomaly data.

In the KH 92-3 cruise, three component geomagnetic anomalies were measured using two STCMs along the tracks perpendicular to the trench axis with 2.5 mile spacing. In this report we will focus on the following two subjects;

1) detail structure of the magnetic source body beneath the Kuril Trench using the characteristics 1) and 2) mentioned above,
2) comparison of Chiba University's gyrocompass and a vertical gyroscope with those on board the Hakuho-maru.

2. Three-Component Anomalies over the Kuril Trench

To obtain the true X (north) , Y (east) and Z (vertical-down) components of geomagnetic field, we must know 12 constants for anomalies of STCM data (Isezaki, 1986). To fix these constants the ship sailed on the ∞-shape tracks 5 times. Table 12-1 shows the locations where this operation was done and the final 12 constants.

Fig. 12-1. (a), (b), and (c) show the three-component anomalies along the tracks. There are clear magnetic anomaly lineations M5, M6 and M7 from north to south trending not perfectly parallel but slightly oblique to general trend of the trench axis. It must be noted that M5 and M6 lineations are present very clearly on the landward slope of the trench as pointed out previously (*e.g.*, Isezaki, 1973).

The Y component anomalies are generally smaller in amplitude than X and Z component anomalies, implying that the lineation trends nearly EW. Precise direction of lineation can be determined from X and Y component anomalies in detail for each anomaly.

Fig. 12-1. (d) shows the strike angle of two dimensional source body by the bar which calculated from three component magnetic anomaly. These bars are just

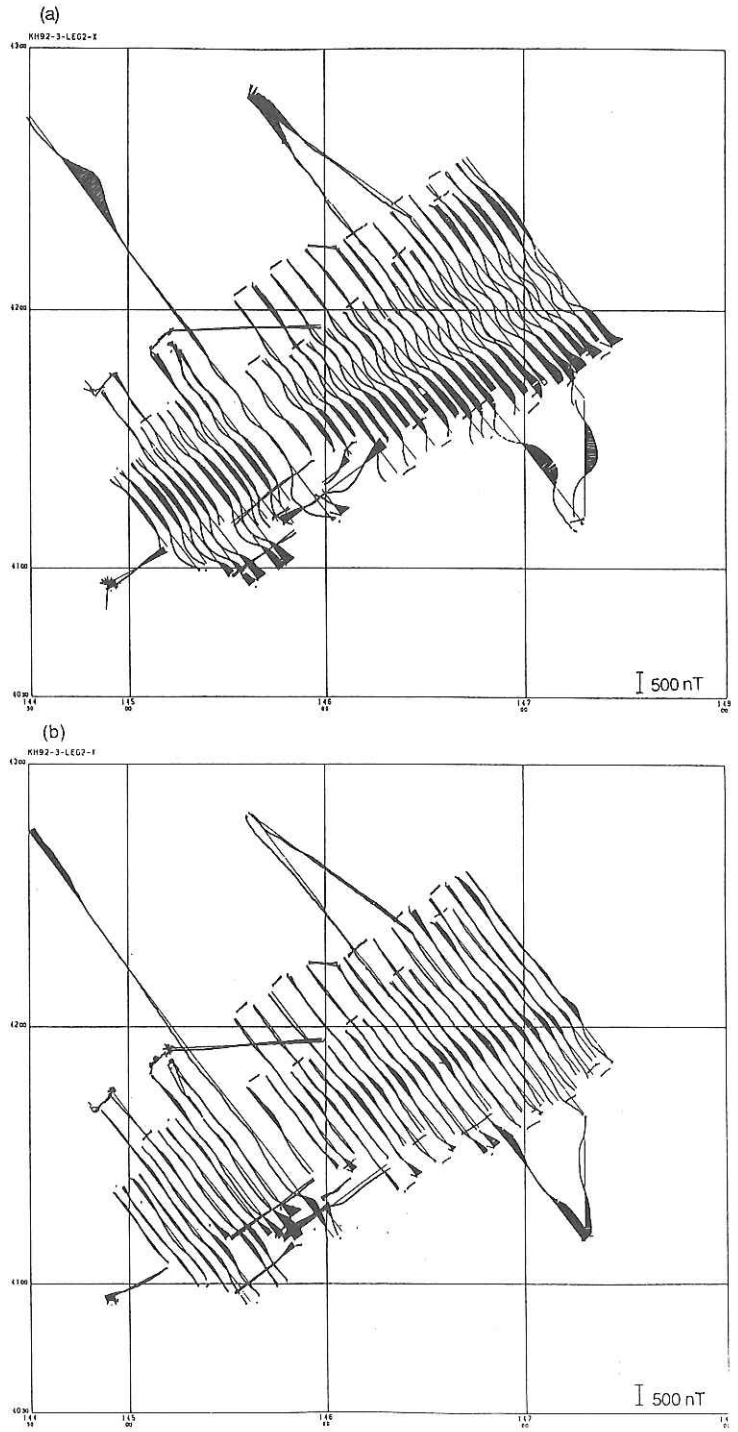

Fig. 12-1. The three component anomaly profiles of geomagnetic field referred to the IGRF90 field along the tracks. Black indicates the positive anomalies.(a) shows X(north) component ,(b) shows Y (east) component and (c) shows Z (vertical) component respectively. (d) shows the strike angle of the two dimensional magnetic source body calculated from (a), (b),and (c) data.

(c)

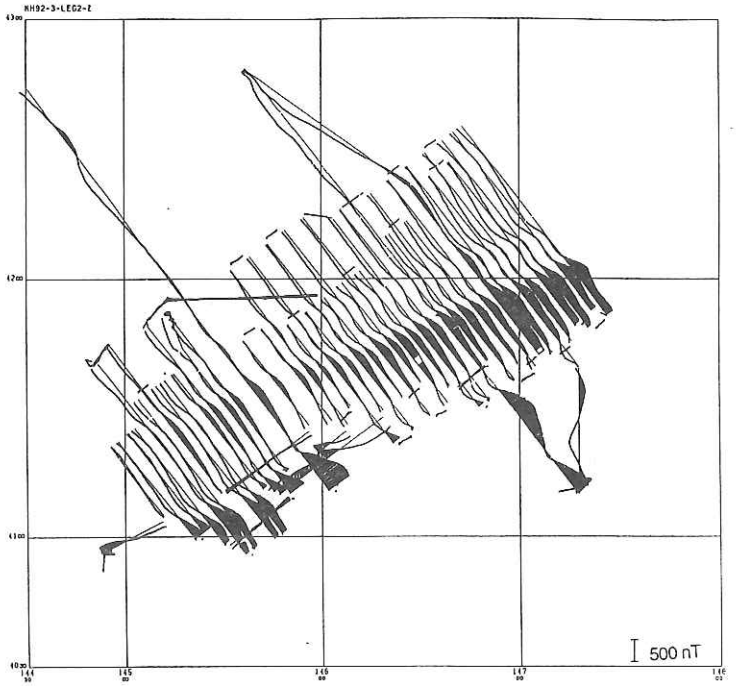

(d)

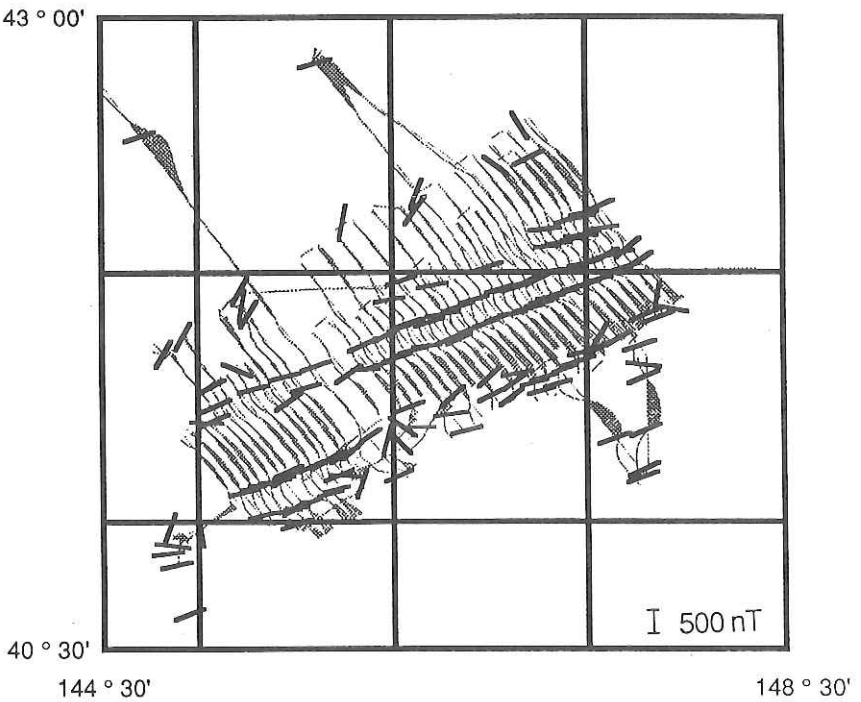

on the boundary of the positive and negative X component magnetic anomalies. The average strike angle is N 108° W (N 76° E) from 147 data. The dip angle of magnetic source body can be also obtained from analysis of three component data. We are trying to determine the subduction angle of the Pacific Plate under the Kuril Trench.

3. Comparison of a Gyrocompass and a Vertical Gyroscope between the Chiba University's STCM and ORI's STCM

The ORI's STCM gets the heading, roll and pitch angles of the ship from the ship's LAN system. These angles are measured by the high-precision gyrocompass (Tokyo Keiki, TG-5000) and the vertical gyroscope (Tokyo Keiki, SGC-1). On the other hand, the Chiba University's STCM uses a regular type gyrocompass (Tokyo Keiki, ES-10) and the vertical gyroscope (Tamagawa Seiki).

The regular type gyrocompass becomes unstable within a few tens of minutes after the large change of ship's heading. Then during this period the STCM becomes unstable and the three component anomalies cannot be obtained. Moreover, the regular type gyrocompass has dependency on the ship's velocity and heading.

We first examined the dependency on the ship's heading measured by the Chiba University's gyrocompass (G1) by comparing it with that measured by the Hakuho-maru's high-precision gyrocompass (G2). Fig. 12-2 shows a result that G1 has the sinuous difference from G2. The data were collected during the ∞-shape sailing mentioned already. Note that G1 presents different heading angles during the clockwise rotation from those during the anticlockwise rotation.

This variation can be expressed by the equation below,

$$\Delta GYRO = a \times \sin(\theta + \phi) + \alpha$$
$$a = 1.5914$$
$$\phi = -91.619$$
$$\alpha = 0.64114$$

The amplitude of change is 1.6 degree which is much significant for STCM. Because G2 is a very precise gyrocompass, we can use this result for correction of the heading angle measured by G1.

Fig. 12-3 shows the effect of heading correction. The top figure shows the change of *Hh* (observed heading component), *Hs* (observed starboard component) and *Hv* (observed vertical component) by thick sinuous curves during the ∞-shape rotation vs the heading angle measured by G1. The small dots represent difference between the observed field and the calculated one using 12 constants. The bottom figure shows the result using the heading angle measured by G2 which is expected after correction on the heading angle measured by G1. The difference between the observed field and the calculated one is very small and distributed randomly around the zero value compared to that in the top figure which means the 12 constants obtained using the heading angle must be much better than those obtained using un-corrected heading angle.

As for a vertical gyroscope, result of comparison of the Chiba University's one (V1) with the Hakuho-maru's (V2) is presented in Figs. 12-4 and -5. Fig. 12-4

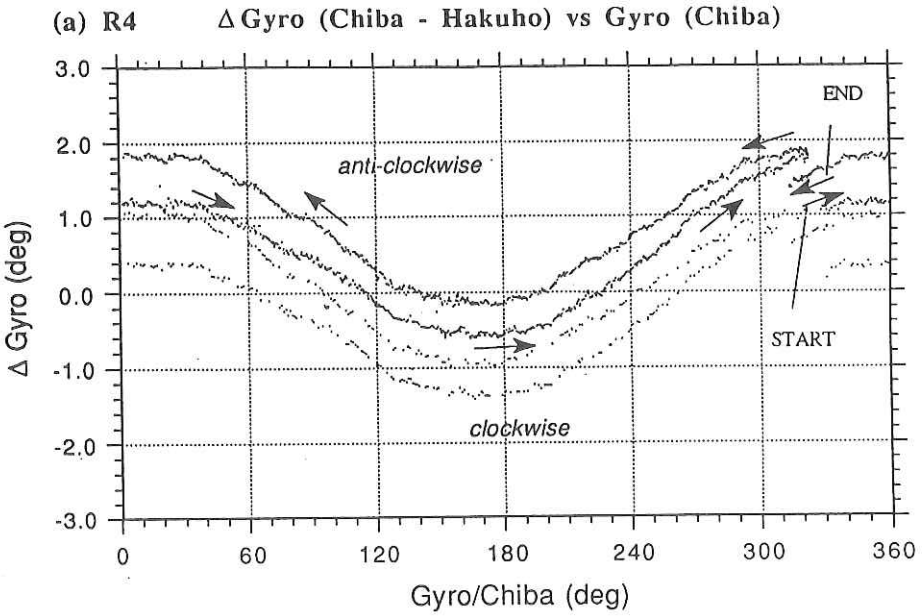

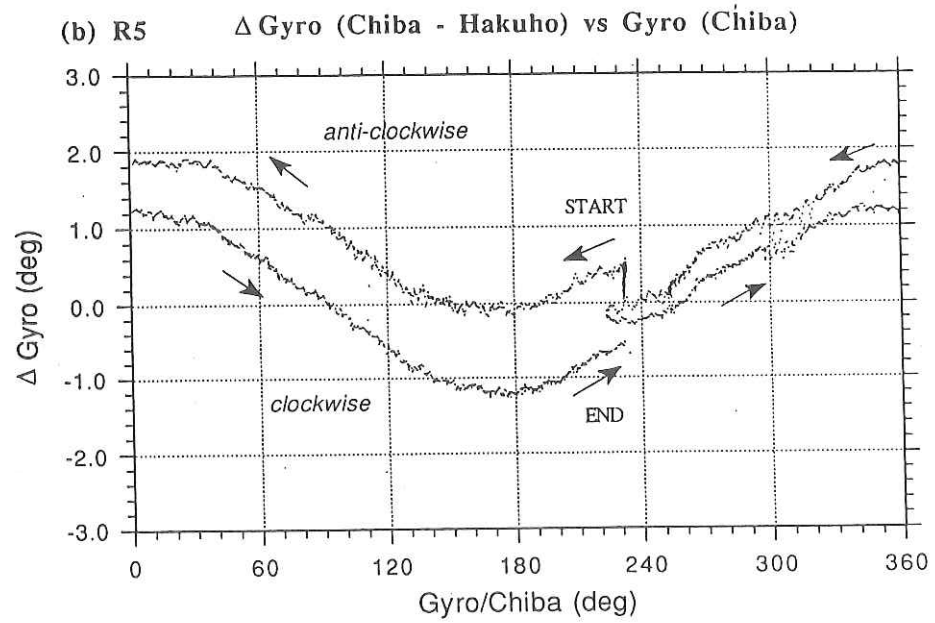

Fig. 12-2. The horizontal axis is the angle of Chiba University's gyrocompass (degree) . Vertical axis is the angle difference between that of the Chiba University' gyrocompass and that of the Hakuho-maru' gyrocompass (degree) .The data were collected during the '8' shape sailing mentioned already. (a) shows the result at the 4th '8' shape sailing station. (b) shows the result at the 5th '8' shape sailing station.

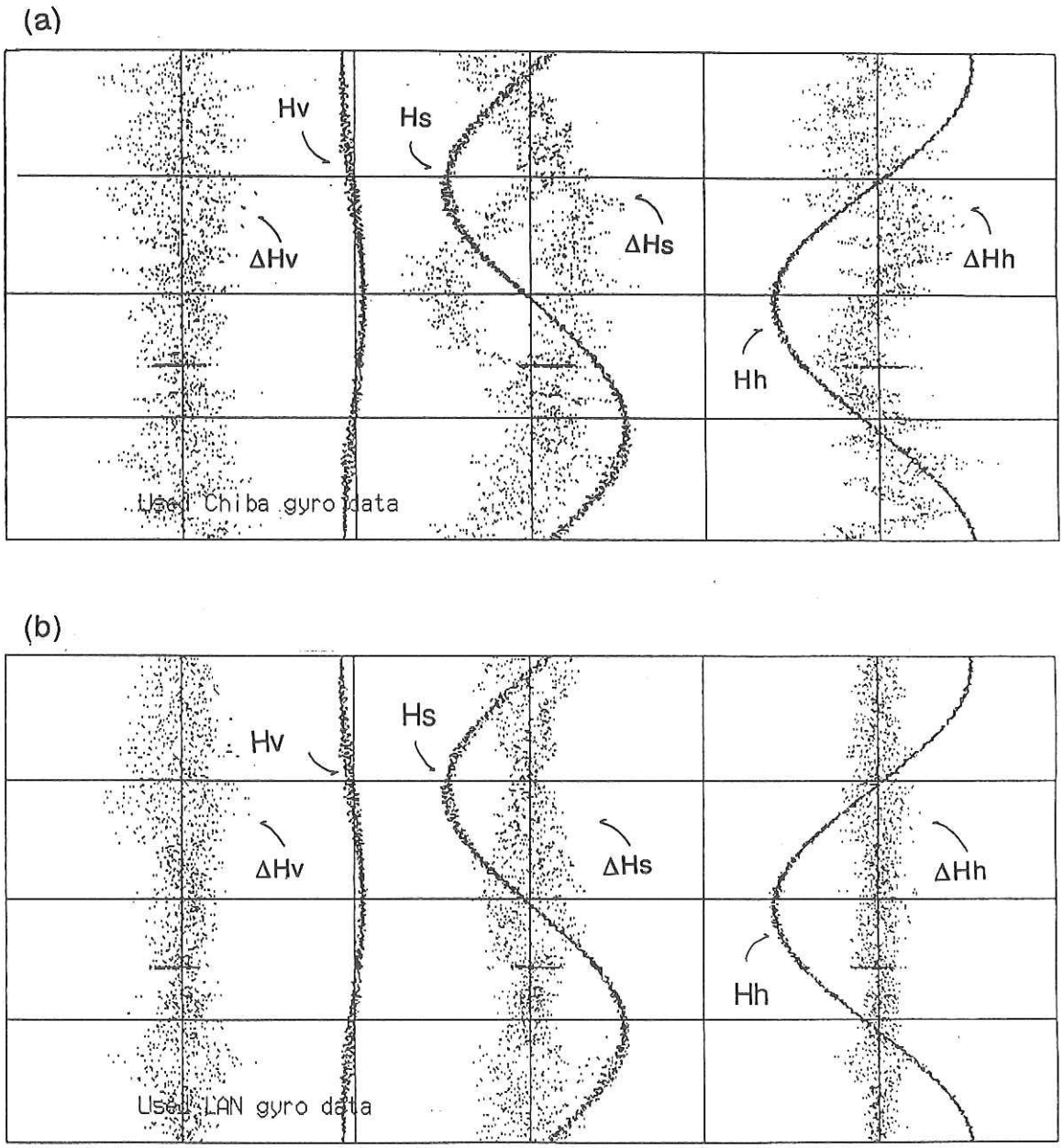

Fig. 12-3. The vertical axis shows the heading angle. The horizontal axis shows the change of Hh (observed heading component), Hs (observed starboard component) and Hv (observed vertical component) and the Hh , Hs , and Hv are the difference between the observed field and the calculated one using 12 constants. (a) shows the result using the heading angle measured by Chiba University's gyrocompass. (b) shows the result using the heading angle measured by Hakuho-maru's one.

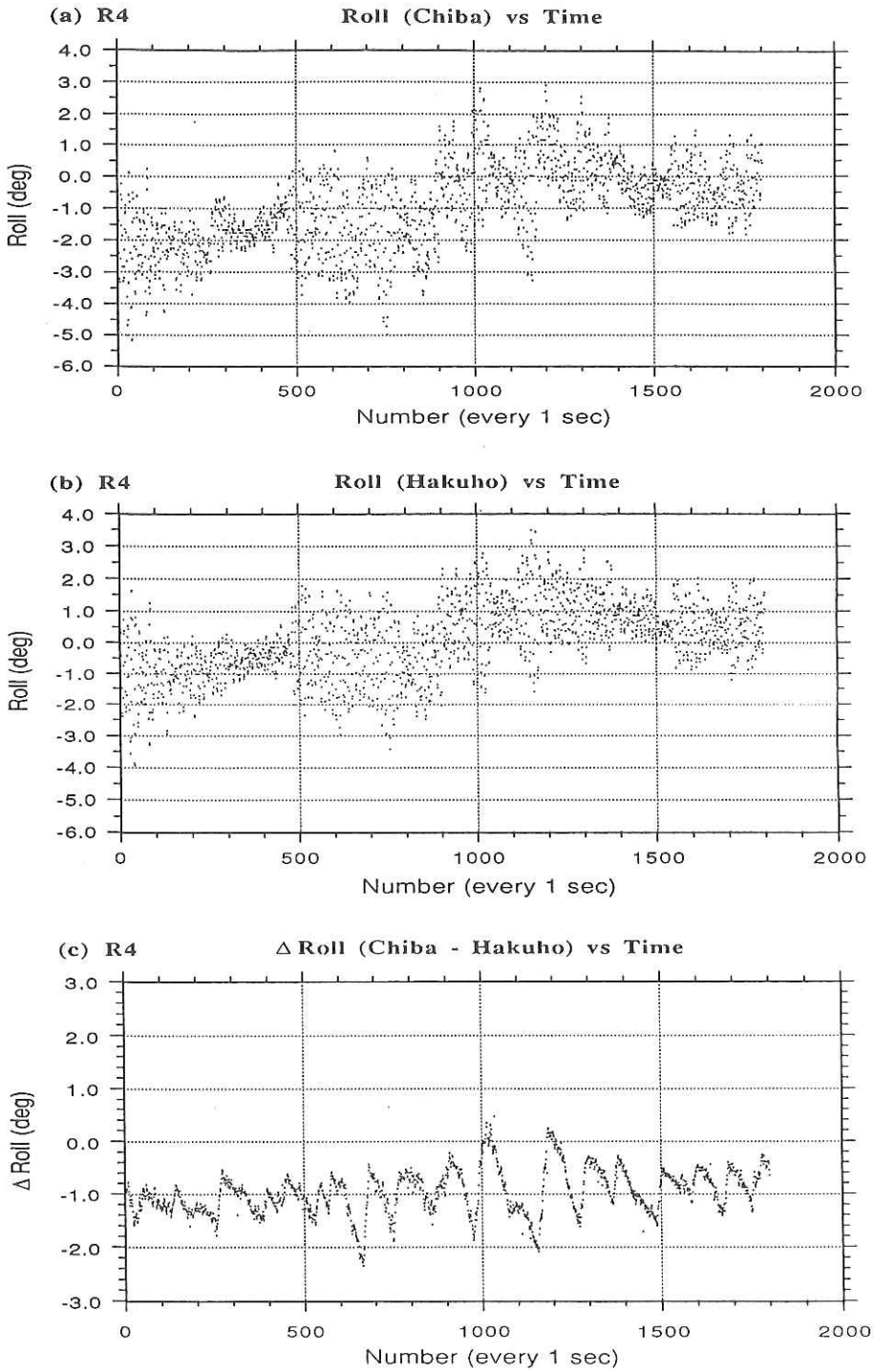

Fig. 12-4. (a) and (b) show the roll angles measured by the Chiba University's vertical gyroscope and the Hakuho Maru's one during about 1800 seconds. (c) shows the difference between the Chiba University's one and the Hakuho Maru's one.

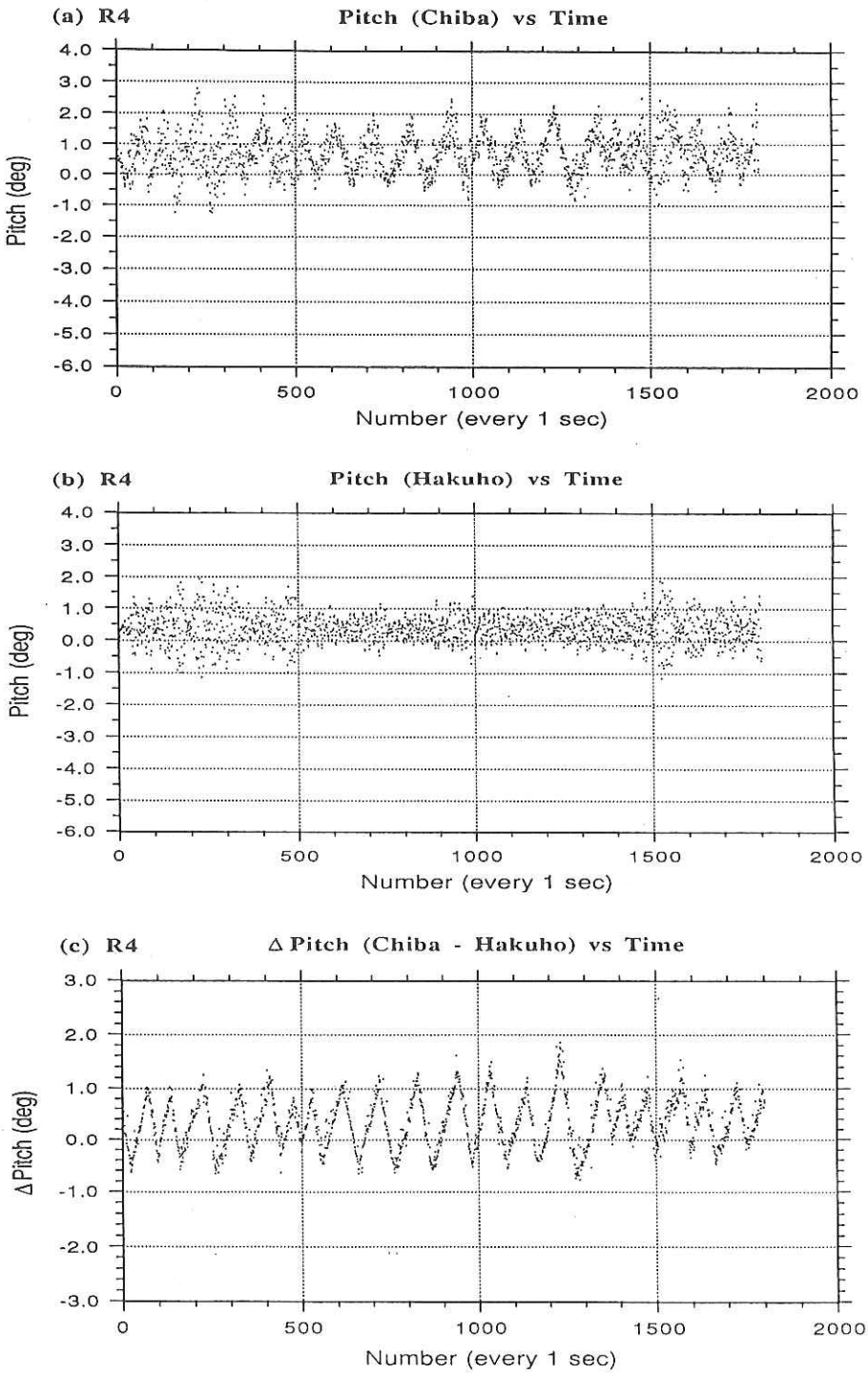

Fig. 12-5. (a) and (b) show the pitch angles measured by the Chiba University's vertical gyroscope(V1) and the Hakuho-maru's one during about 1800 seconds. (c) shows the difference between the Chiba University's one and the Hakuho Maru's one .

shows the roll angles measured by V1 and V2 in about 1800 seconds. General feature of distribution of V1's roll angles is very similar to that of V2's. The difference between them, however, sometimes exceeds 1 degree and includes clearly a periodic change. Fig. 12-4 shows more evident periodic change of pitch angle with time. This periodic change (with a period of 60-100 seconds) may be due to some mechanical defect in the Chiba University's vertical gyroscope.

Because the actual roll and pitch angles are very small and change randomly around the zero degree, as seen in Figs. 12-4 and -5, the effect of rolling and pitching on the STCM can be canceled out by averaging them for a particular time longer than the specific period of rolling and pitching, about 7 seconds for the R.V. Hakuho Maru.

References

Isezaki, N., Geomagnetic anomalies and tectonics around the Japanese Islands, The Oceanographical Magazine , 24 , No.2, 107-158, 1973.

Isezaki, N., J. Matsuda, H. Inokuchi and K. Yaskawa, Shipboard Measurement of Geomagnetic Field, *J. Geomag. Geoelectr.*, 33, 329-334 , 1981.

Isezaki, N., A new shipboard three component magnetometer, *Geophysics*, 51 , 1992-1998 , 1986.

Seama, N., Y. Nogi and N. Isezaki, A new method for precise determination of the position and strike of magnetic boundaries using vector data of the geomagnetic anomaly field , Submitted to *Geophys . J . Int.*, May 13 , 1992.

Table 12-1. (a) Locations of ∞-shape sailing, (b) The final values of 12 constants.

(a)					
Station No.	Date	Latitude(°)	(')	Longitude(°)	(')
KH92-3.R1	92.7.21	N 32	23.59	E 135	0.87
KH92-3.R2	92.7.23	N 38	20.99	E 146	0.00
KH92-3.R3	92. 8. 1	N 41	11.49	E 147	17.91
KH92-3.R4	92. 8. 4	N 41	41.23	E 144	48.21
KH92-3.R5	92. 8. 8	N 36	27.31	E 144	19.77
(b)					
B(1,1)	0.273	B(2,1)	1.003	B(3,1)	0.916
B(1,2)	-1.110	B(2,2)	0.317	B(3,2)	-0.869
B(1,3)	0.551	B(2,3)	0.506	B(3,3)	0.657
Hph	-2410	Hps	-384	Hpv	4852

13. Geomagnetic Measurements over the Kuril Trench by use of an Integrated Data Logger System of Portable GPS/Fluxgate Magnetometer/Proton Magnetometer/Tiltmeter linked with the Onboard LAN Data Network

Y. Nakasa and H. Kinoshita

1. Introduction

It is well established that the onboard three component geomagnetic data are to be analysed by integrating with not only total geomagnetic force data but also other onboard informations, i.e., ships bearing from gyro-compass, instantaneous rolling and pitching angles. A new multi-data logger system has been developed by Earthquake Research Institute with a consultation of Chiba University personnel and tested on KH 92-3 cruise of Hakuho Maru over the Kuril and Japan Trenches from July 17th through August 10th.

The system has four RS-232C serial interface ports linked with shipboard three component magnetometer (fluxgate magnetometer), proton magnetometer, global position-ing system (GPS), inclinometer for rolling and pitching angles, and the onboard local area network (LAN) which offers various ship-borne equipment data including ships bearing, precision depth, gravity, geomagnetic total force, and positioning. This report describes briefly our newly built data logger system, and presents the contents of the dataset obtained by us through the present cruise.

2. Data Acquisition

The following list indicates data available and their format :

No.	Data Item	Leg	Date:time (GMT) month:day:hr:min	Survey*	Dataset
				Lack of data due to business 1-5	
(1)	GPS	Leg. 1 : Leg. 2	no data		
			07:29:04:57~08:02:02:07		Floppy diskette. Latitude, Longitude and GPS time. Every 15 sec, formated as 3 (i3, f5.2).
			---	1	
			08:02:06:50~08:03:04:30		
			---	2	
			08:03:08:00~08:04:04:00		
			---	1	
			08:04:08:00~08:05:00:00		
			---	3	
			08:06:22:30~08:07:15:00		
			---	1, 4	
(2)	Fluxgate	Leg. 1			
			07:17:04:20~07:25:05:30		Floppy diskette. 3 components and 2 tilt angles. Every 15 sec, formatted as 3 (f6.2, 2f5.1).

	Leg.2			
	07:29:04:57~08:02:02:07			Floppy diskette
	----------		1	3 components and
	08:02:06:50~08:03:04:30			2 tilt angles.
	----------		2	Every 15 sec,
	08:03:08:00~08:04:04:00			formatted as
	----------		1	3 (f6.2, 2f5.1).
	08:04:08:00~08:05:00:00			
	----------		3	
	08:06:22:30~08:07:15:00			
	----------		1,4	
	08:04:06:00~08:04:07:00		5	3 components and
	----------		4	Every 5 sec,
				formatted as
				3 (f6.2, 2f5.1).
(3) Proton	Leg. 1 : no data			
	Leg.2			
	07:29:04:57~08:02:02:07			Floppy diskette.
			1	Total force.
	08:02:06:50~08:03:04:30			Every 15sec,
			2	formatted as
	08:03:08:00~08:04:04:00	(f7.1).		
			1	
	08:04:08:00~08:05:00:00			
			3	
	08:06:22:30~08:07:15:00			
			4,5	
	08:08:10:00~08:09:15:00			

* Surveys	1: Proton cable tension test
	2: Beam Trawl
	3: DESMOS
	4: Dredge
	5: Circular tracking

3. Specification of equipment used by ERI measuring system

(1) Sony GPS CORE Model-PIXY

Accuracy	Position 30~100 m with PDOP6
	Velocity 0.3 kt with PDOP6
Receiver	4 Channel (parallel)
	Tracking up to 4 satellites
Frequency	1575.42 MHz C/A Code
Sensitivity	less than -160 dBw/m (-130dBm)
Selectivity	better than -60 dB (at -20~+20MHz)
Update rate	2.3 seconds, typical
Maximum velocity	530 knots (980 km/h)
Maximum acceleration	2G

(2) Fluxgate magnetometer Model-9118

Measurement components	X. Y. Z. three components
	(in reference to ships frame)
Maximum range	65000 nT
Accuracy	1 nT
Data transmission	1200 Baud

(3) Inclinometer

Tilt components	X. Y. components (in reference to geoid surface frame)
Maximum range	29.99 degree
Data transmission	1200 Baud

(4) Proton magnetometer Model-5711ADR

Minim. and Max. Range	30000 and 60000 nT
Accuracy	0.2 nT
Minim. sampling interval	10 sec
Data transmission	1200 Baud

4. Some remarks on the measurements and the data analyses

(1) Three-component fluxgate magnetometer

The fluxgate magnetomater, Model-9118 can measure three components of the geomagnetic field and two components of tilt angles of the inclinometers attached to the bottom of the fluxgate sensor. These data are fed to the data logger system simultaneously through a multi-wire conducting cable. The equipments are set up on the upper deck of the vessel tied to the decks frame with stainless steel wire. In addition to the three components of the geomagnetic field strengh and tilt (pitching and rolling) angles of the magnetic sensor, we need also ship's bearing from onboard gyro-compass and the geomagnetic total force from a proton magnetometer towed astern in order to calculate the three geomagnetic components. For a reduction of the effects from the ships magnetization, remanent as well as induced moments, a rapid measuring sequences were traced along a couple of small circular tracks run by the vessel several times. Dynamic characteristics of the newly built-in tiltometers attached to the fluxgate sensor seem to have worked well but it has to be evaluated statistically by comparing vertical gyro data of the magnetometer system of Chiba University later ashore.

(2) Total force by a proton precession megnetometer

The total force measurement is inevitable as well for reduction of the three components of the geomagnetic field as briefly described in the previous paragraph. Output signal from the new proton magnetometer system was found quite noisy in the initial stage of the measurement trial, and later it completely faded out. It was found that the mechanical coupling between towing cable and the water-tight sensor chamber was not well manifactured and this part was repaired shortly after the first test run. Second test run with a low ship's speed, 2~3 knots, showed that the malfunctioning was well recovered. It is, however, necessary to test this chamber again in much higher ships speed in a later chance. Data analyses including reduction of effect of ships magnetization on three component magnetic field intensity will be made by on shore studies. We show below a diagramatic scheme of the data acquisition system and a part of the data logged during the cruise as an example.

Example of Cruise Data and its Format

Year/Mon/Date Hour:Min:Sec Longitude(deg min sec) Latitude(deg min sec) Heading (deg) Gyro(deg) Roll(deg) Pitch(deg) X-tilt(deg) Y-tilt(deg) X-Y-Z-component(nT) Gyro Roll Pitch Proton(nT) Lan-Latitude(deg min) Lan-Longitude(deg min) Lan-Proton(nT)

92/08/08 19:00:50 E144°35′39.8″ N 36°37°06.6″ -132°233.40 0.75 -1.35 -0.24
2.51 -18656 14034 45822233.43 0.93 -0.52 44557.9 36 37.11 144 35.64 3956
45394
92/08/08 19:01:09 E144°35′34.2″ N 36°37°03.7″ -125°233.78 1.02 0.40 -2.21
-1.06 -19812 14168 45291233.87 0.68 -0.15 44296.3 36 37.10 144 35.61 3956
45394
92/08/08 19:01:28 E144°35′30.6″ N 36°37°00.1″ -124°234.40 -0.27 -0.62 -0.61
1.94 -18647 13726 45941234.68 -0.63 -0.08 44267.7 36 37.01 144 35.46 3988
45390
92/08/08 19:01:46 E144°35′24.1″ N 36°36°57.5″ -127°234.05 0.87 0.20 -0.46
0.15 -19452 14197 45366234.10 0.75 -0.25 44471.5 36 36.99 144 35.44 3991
45391
92/08/08 19:02:05 E144°35′19.7″ N 36°36°54.1″ -124°233.23 1.68 -0.48 -1.46
0.05 -19465 14289 45370233.23 1.97 -0.62 44328.8 36 36.98 144 35.42 3992
45390
92/08/08 19:02:24 E144°35′15.7″ N 36°36°50.1″ -123°233.87 1.45 -1.35 -3.05
0.61 -18582 14573 45389233.62 1.25 -1.42 44388.2 36 36.88 144 35.26 4005
45387
92/08/08 19:02:42 E144°35′09.8″ N 36°36°47.8″ -129°234.07 2.28 0.80 -1.79
-1.55 -19721 14683 45114233.82 2.47 0.10 43876.6 36 36.87 144 35.24 3994
45385
92/08/08 19:03:01 E144°35′04.9″ N 36°36°44.5″ -129°233.30 1.15 0.10 -0.79
1.11 -19547 14061 45452233.52 0.98 0.67 44641.2 36 36.77 144 35.07 3984
45382
92/08/08 19:03:19 E144°35′00.2″ N 36°36°41.8″ -124°233.13 1.38 -0.70 -1.70
2.30 -18938 14245 45704233.47 1.15 0.42 44281.9 36 36.76 144 35.05 3974
45380
92/08/08 19:03:38 E144°34′54.3″ N 36°36°42.9″ -122°233.72 1.78 0.02 -2.06
0.13 -19452 14485 45229233.78 1.45 -0.18 42902.2 36 36.67 144 34.89 3946
45374
92/08/08 19:03:56 E144°34′50.0″ N 36°36°40.2″ -118°233.80 0.95 1.57 0.41
-3.76 -20545 13953 45073233.88 1.25 -0.58 44891.1 36 36.66 144 34.86 3933
45375
92/08/08 19:04:15 E144°34′45.0″ N 36°36°37.4″ -122°233.92 1.68 1.02 -0.13
-2.09 -19765 14154 45544233.58 2.62 0.10 44249.0 36 36.56 144 34.70 3892
45370
92/08/08 19:04:33 E144°34′40.2″ N 36°36°34.9″ -129°234.10 0.07 1.15 0.57
-1.63 -20009 13702 45192233.98 -0.12 -0.38 44171.3 36 36.55 144 34.68 3867
45366
92/08/08 19:04:52 E144°34′35.0″ N 36°36°32.0″ -127°234.17 1.28 0.83 -1.36
-2.23 -19865 14366 45131234.30 1.10 -0.47 44367.2 36 36.54 144 34.65 3871
45366
92/08/08 19:05:11 E144°34′30.1″ N 36°36°28.3″ -132°233.95 2.37 -0.90 -2.09
0.94 -18680 14961 45470233.67 2.83 -0.87 42983.0 36 36.44 144 34.50 3827
45357
92/08/08 19:05:29 E144°34′25.2″ N 36°36°25.3″ -136°231.48 1.78 0.75 -2.51
0.71 -20464 13952 45052231.30 1.45 1.30 44143.7 36 36.43 144 34.48 3827
45357
92/08/08 19:05:48 E144°34′20.9″ N 36°36°21.1″ -139°228.58 2.60 -0.27 -3.48
-0.29 -21284 13632 45149228.40 2.47 -0.30 44517.9 36 36.34 144 34.32 3828
45349
92/08/08 19:06:06 E144°34′16.6″ N 36°36°17.3″ -139°228.30 0.62 0.55 -0.66
-1.00 -22044 12507 45474228.45 0.57 -0.62 42987.8 36 36.32 144 34.30 3827
45348
92/08/08 19:06:25 E144°34′11.8″ N 36°36°13.5″ -137°229.23 2.47 -0.28 -1.64
-0.15 -21109 13531 45653229.08 2.73 -0.52 44459.7 36 36.22 144 34.15 3848
45338
92/08/08 19:06:43 E144°34′08.2″ N 36°36°09.5″ -132°230.00 0.67 -1.02 -1.42

```
 0.95 -20296  13146  45744230.12   0.12  -0.90 43994.3 36 36.21 144 34.13  3851
45336
92/08/08 19:07:02 E144°34'02.9" N 36°36°06.5" -127°229.68   2.65  -0.85  -2.20
 1.61 -20598  14009  45083229.58   2.27  -0.37 42988.2 36 36.10 144 33.98  3843
45327
92/08/08 19:07:20 E144°33'58.6" N 36°36°03.1" -136°230.22   1.58   1.40  -0.07
-3.00 -21651  13353  45354230.22   2.13  -0.08 43906.3 36 36.09 144 33.96  3833
45329
92/08/08 19:07:39 E144°33'53.8" N 36°35°59.6" -124°230.10   2.37   0.38  -3.32
-2.92 -21455  13945  44589229.90   1.95  -1.60 44560.0 36 35.99 144 33.80  3847
45317
92/08/08 19:07:57 E144°33'49.3" N 36°35°56.7" -130°229.87   1.97   0.60  -0.47
 0.23 -21052  13473  45334230.12   2.08   0.83 44144.4 36 35.97 144 33.78  3847
45311
92/08/08 19:08:16 E144°33'43.9" N 36°35°54.7" -128°230.67   1.03   1.28  -0.38
-1.53 -21306  13187  45458230.87   1.23   0.97 42944.2 36 35.96 144 33.76  3842
45311
92/08/08 19:08:35 E144°33'38.0" N 36°35°50.9" -123°230.35   2.78  -0.70  -2.02
 0.46 -20076  14064  45474230.13   3.07  -0.13 44472.0 36 35.86 144 33.61  3793
45304
92/08/08 19:08:53 E144°33'32.9" N 36°35°49.1" -119°229.95   0.88   1.60  -0.01
-1.07 -21865  12877  45174230.17   0.83   1.25 44662.2 36 35.85 144 33.58  3791
45299
92/08/08 19:09:12 E144°33'27.7" N 36°35°46.3" -120°230.72   2.45  -0.88  -2.85
 2.97 -19873  14375  44864230.75   1.83   0.30 44594.1 36 35.75 144 33.44  3788
45289
92/08/08 19:09:30 E144°33'22.5" N 36°35°43.6" -131°231.30   1.10  -0.88  -0.53
 1.81 -20409  13646  45202231.30   1.25  -1.07 44263.2 36 35.74 144 33.41  3788
45285
92/08/08 19:09:49 E144°33'17.1" N 36°35°41.4" -127°232.03   1.40  -0.08  -0.50
 1.24 -19893  13886  45425231.77   1.83   0.07 44640.0 36 35.64 144 33.27  3768
45275
92/08/08 19:10:07 E144°33'12.2" N 36°35°38.5" -125°231.68   1.32  -1.60  -1.49
 1.63 -19704  13939  45267231.82   1.42  -1.62 44182.8 36 35.63 144 33.24  3773
45275
92/08/08 19:10:26 E144°33'06.8" N 36°35°34.5" -129°231.17   1.65  -0.07  -0.34
 1.46 -20217  13769  45401231.45   1.68   0.75 44609.8 36 35.53 144 33.10  3791
45260
92/08/08 19:10:44 E144°33'01.9" N 36°35°32.6" -132°231.13   1.83   0.50  -1.32
-0.35 -20684  13915  44893231.22   1.78   0.22 44266.8 36 35.51 144 33.07  3791
45260
```

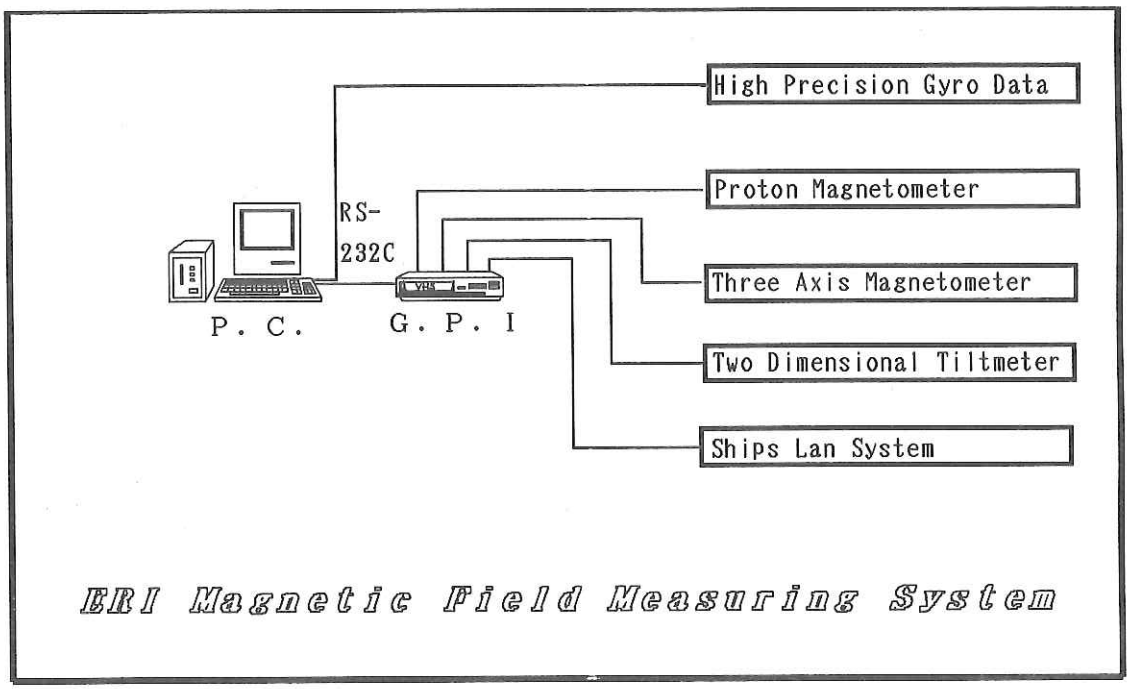

ERI Magnetic Field Measuring System

14. Gravity

K. Koizumi and H. Fujimoto

Gravity was measured throughout the whole survey tracks in the present cruise KH 92-3. A surface ship gravimeter, NIPR-ORI model 2 (1989), was used for the measurement. Gravity values at Tokyo and Kushiro ports were fixed by using La Coste & Romberg portable gravimeter model G-124.

The value at Kushiro port was also connected with a first order gravity station in Kushiro Meteorological Observatory by the G-348 gravimeter. Measured values at Tokyo and Kushiro ports were listed in Table 14-1 and compared with those of the NIPR-ORI model 2 gravimeter.

Preliminary results obtained from real time data processing indicate that an extremely low free air anomaly zone exists along landward toe of the Kuril Trench.

Table 14-1. Gravity values in milligal at Tokyo and Kushiro ports measured by using La Coste & Romberg gravimeter model G (Geodetic use).

Gravimeter	Tokyo	Kushiro		Tokyo
No./ [Date]	17 July '92	25 July '92	29 July '92	10 August '92
G-124	979 774.8	980 602.1		(979 774.8)
G-348	-----	-----	980 600.44	979 772.9
NIPR-ORI 2	979 774.1	980 620.2	980 662.8	979 781.1

15. MCS/OBS Survey by the R.V. Hakuho Maru KH92-3 Cruise, Leg 1

F. Yamamoto, M. Shinohara, N. Takahashi and H. Tokuyama

The multichannel seismic reflection survey was carried out in the KH92-3 cruise, Leg 1, to obtain a high-resolution seismic structure of the eastern Nankai Trough from the 18th to 24th of July, 1992. We also performed a seismic refraction experiment using OBS simultaneously with the seismic reflection survey. The aim of OBS experiment is to determine the velocity structure along the reflection profile.

The locations of the seismic reflection survey profile are shown in Fig. 15-1. Total length of the track lines for seismic reflection survey is ca. 200 miles. The average ship's speed was maintained at 4.9 knots through the reflection survey. Three OBSs were deployed at every 15 miles along the reflection profile prior to the reflection survey (Fig. 15-1) . Table 15-1 shows the observation period and the positions of the deployed OBSs. The profile for OBS experiment is a part of the reflection survey profile, and the profile length is ca. 70 miles. All OBSs were recovered after the reflection survey.

The energy source used mainly during this experiment was 3-airguns with 1000-cubic inches firing chamber towed behind the ship and airguns were fired at a pressure of 10 MPa at every 20 s. Seismic signals were received by the AMG 24-channel hydrophone streamer with channel spacing of 50 m. The hydrophone streamer was towed at a distance of ca. 2,000 m from the stern. The sampling rate of analogue signal was every 1 msec, and the recording length was 8 s par every shot. The signals were recorded on magnetic tapes in SEG-B format after A/D conversion, filtering by means of Texas Instruments DFS-V digital recording system.

The deployed OBSs were pop-up type OBSs, which are equipped with digital data recorders, developed at Ocean Research Institute, the University of Tokyo. Each of them are equipped with 4.5 Hz three-component geophone. The OBSs has a precise quartz clock, and time codes generated by the clock were also recorded with geophone signals.

The ship positions were determined by GPS and Loran-C using Hakuho-maru navigation system. The navigation system recorded system positions which were estimated by hybrid processing of GPS and Loran-C data on magnetic tapes. The system also recorded GPS data, Loran-C data, PDR water depth data, and SeaBeam water depth data.

A profile obtained during this cruise is shown in Fig. 15-2 (a foldout in the back-cover). The depths on the seismic profile are the two-way travel times in second.

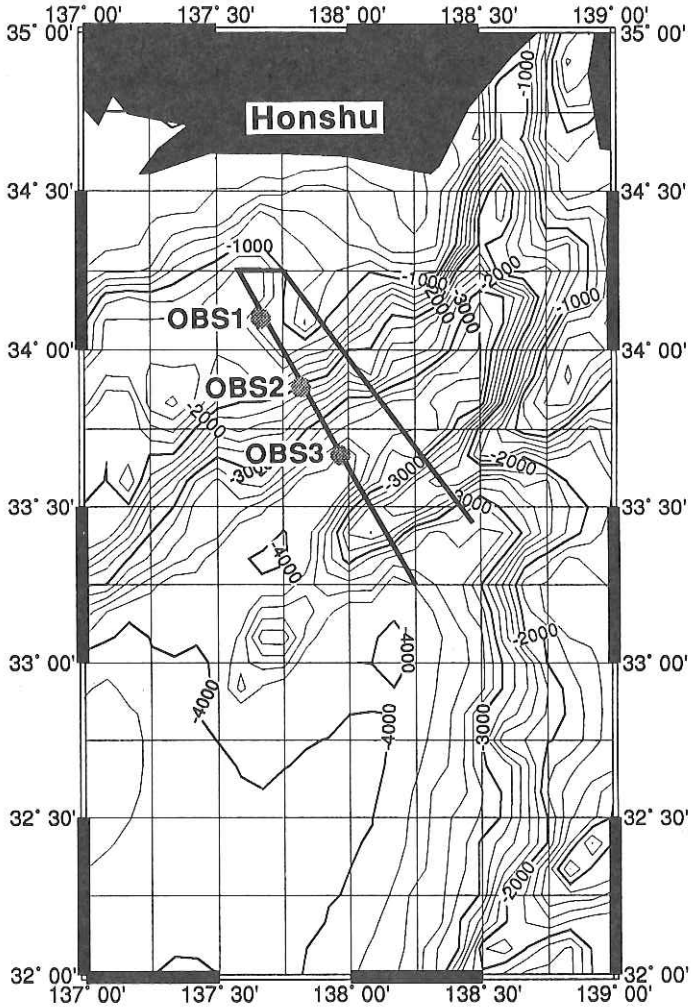

Fig. 15-1. Locations of the reflection/refraction seismic experiment in the eastern Nankai Trough with seafloor topography. Isobaths are in meter. Solid line indicates multichannel reflection survey profile. The deployed OBS positions are shown by solid circles.

Table 15-1. Observation period and positions of the deployed OBS.

OBS	Observational Period		Latitude	Longitude	Depth
	Deploy	Recovery	N	E	(m)
1 ORI6C	92 July 18 06:55	92 July 22 06:13	34° 6.00'	137°40.02'	1179.0
2 ORI8C	92 July 18 05:47	92 July 22 04:10	33°53.27'	137°48.88'	2433.0
3 ORI7C	92 July 18 04:37	92 July 22 01:36	33°39.95'	137°58.04'	3899.0

Table 15-2. Records of data logging on the R.V. Hakuho Maru.

Date	Time	Shot #	delay (s)	MT #	Depth (m)	Latitude	Longitude
92.7.19	21:23:20	1	0	1			
	21:52:00	86	0			33°11.65'	138°18.45'
	22:22:00	113	0			33°12.16'	138°17.83'
	23:17:20	213	4		3997	33°12.84'	138°17.30'
	23:34:20	264	4	2	4002	33°13.10'	138°16.98'
92.7.20	0:00:00	337	4		4002	33°13.46'	138°16.40'
	3:30:00	668	2	3	3589	33°19.86'	138°11.64'
	4:01:00	761				33°21.56'	138°10.60'
	5:00:00	938		4	2963	33°25.23'	138°07.99'
	6:00:00	1118		5	2180	33°29.54'	138°05.23'
	7:00:00	1298			3594	33°33.91'	138°02.22'
	8:00:00	1478		6		33°38.59'	137°59.20'
	8:17:20	1530	3		3927	33°39.79'	137°58.42'
	8:29:40	1567		7	3807	33°40.68'	137°57.81'
	9:00:00	1658			3620	33°42.98'	137°56.42'
	9:33:20	1758			3593	33°45.46'	137°54.75'
	9:45:40	1795	2		3344	33°46.39'	137°54.14'
	9:57:20	1829		8	2937	33°47.26'	137°53.59'
	10:00:00	1838			2808	33°47.41'	137°53.50'
	10:09:00	1865	1		2313	33°48.10'	137°53.08'
	11:00:00	2018			2397	33°51.67'	137°50.60'
	12:00:00	2198			1609	33°55.66'	137°47.91'
	13:00:00	2398		10	1327	33°59.63'	137°45.29'
	13:24:30	2455	0		1020	34°01.58'	137°43.99'
	14:00:00	2558			929	34°01.88'	137°42.29'
	15:00:00	2738		11	1192	34°08.61'	137°39.27'
	16:00:00	2918		12	1636	34°12.87'	137°36.43'
	17:00:00	3098			1551	34°15.04'	137°38.04'
	18:00:00	3278		13	995	34°15.06'	137°43.98'
	19:00:00	3458		14	744	34°11.54'	137°47.91'
	20:00:00	3638			624	34°07.67'	137°51.56'
	21:00:00	3818		15	977	34°03.64'	137°55.20'
	21:35:00	3923	1		1506	34°01.28'	137°57.34'
	22:00:00	3997		16	1745	33°59.65'	137°58.73'
	23:00:00	4182				33°55.82'	138°02.33'
	23:30:00	4268	2	17	3124	33°53.90'	138°03.90'
92.7.20	0:01:00	4361	3				
	1:00:00	4538		18	3707	33°48.77'	138°08.75'
	2:00:00	4718		19	3695	33°45.18'	138°11.92'
	3:00:00	4898			3456	33°41.44'	138°15.32'
	3:23:20	4968	2	20	2701	33°39.80'	138°16.67'
	4:00:00	5078			2092	33°37.44'	138°18.90'
	5:00:00	5258		21	3004	33°33.24'	138°22.65'
	5:30:00	5348	3		3399	33°31.06'	138°24.47'
	6:00:00	5438			3491	33°28.95'	138°26.44'
	6:54:40	5602		22	3496	33°24.88'	138°30.14'

16. Multi-Channel Seismic Reflection Survey across the Kuril Trench

Y. Ariie and K. Suyehiro

Introduction

We carried out a multi-channel seismic reflection profiling across the Kuril Trench on August 1~2, 1992 on Leg 2 of the KH 92-3 cruise. Fig. 16-1 shows the location of this MCS line. The survey line starts at 41°14'N, 147°15'E, about 90km away to the southeast from the trench axis, then extends subparallel to the Kushiro Submarine Canyon (KSC) and perpendicular to the trench axis towards Hokkaido and ends at 42°45'N; 145°41'E on the continent slope at about 2,100 m water depth.

In this subduction zone off the eastern Hokkaido, KSC marks a conspicuous surface feature. It has been pointed out that the morphology changes at KSC such that the continental slope becomes steeper without deep-sea terraces on the east side (Sato, 1962; Sakurai *et al.*, 1975).

A seismicity study from ocean-bottom seismographic and land observations showed that the present seismicity is much higher on the eastern side of KSC, as compared with the western side (Iwasaki *et al.*,1991). They suggested that KSC mechanically divides the area into two blocks.

In 1973, a large inter-plate earthquake of M=7.4 occurred at 43.05°N, 145.76°E, 49 km depth, and the fault plane was estimated to have a dip angle of 27° and dip direction of N40°W. This event fractured about 60 x 100 km^2 area well eastward of KSC (Shimazaki, 1974).

Above studies suggest that KSC may be an important tectonic boundary (*e.g.* Kimura, 1981), but the sparsity of information on the crustal structure covering both areas across KSC has prohibited further confirmation. On the west side of KSC, however, there exists seismic studies on the plate subduction structure using MCS and OBS data (Nishizawa and Suyehiro, 1986; Iwasaki *et al.*, 1989; Amishiki, 1992). The MCS survey across the Kurile Trench was carried out on Tansei-maru Cruise KT-90-9 (Amishiki, 1992; Amishiki and Tokuyama 1991).

The aims of this MCS survey on the east side of KSC were:
1) To obtain a detailed seismic profile across the Kuril Trench as long as possible on the eastern side of KSC;
2) To compare the seismic profiles on the western and eastern sides of KSC;
3) To consider the relationship between the seismic profiles and the earthquake distribution in this area;
4) And finally to interpret the tectonics of this subduction zone, using all the available geophysical data (seismic, magnetic, gravity, bathmetry, etc.).

Experiment

Table-1 is the log record excerpt with operational parameters. The sound sources were two airguns, one with a 17-l chamber and the other with 20-l. They

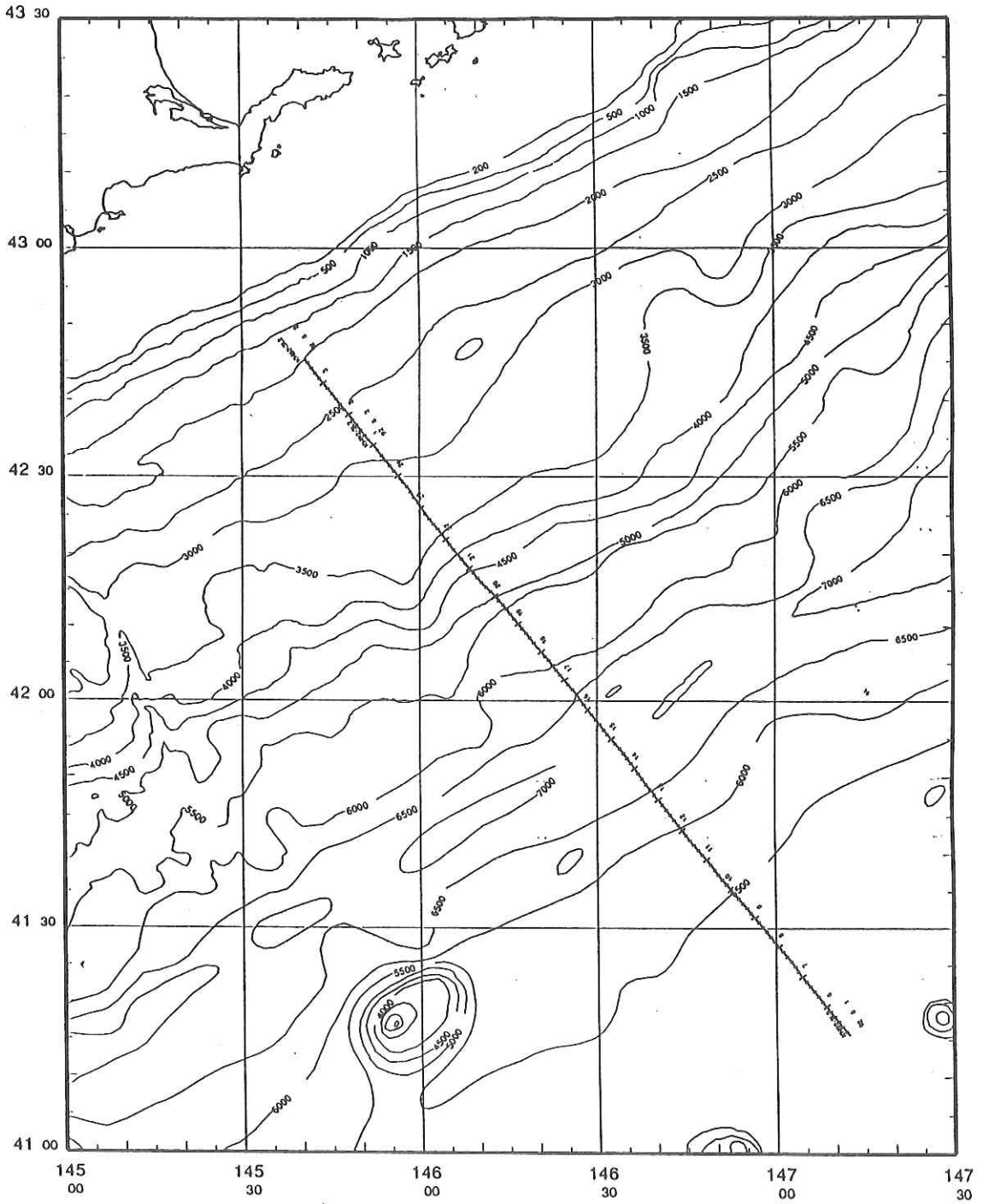

Fig. 16-1. Location map of the seismic profile. It was designed to transect the Kuril Trench east of the Kushiro Submarine Canyon and to shoot over previous OBS survey area (Iwasaki *et al.*, 1991), and the aftershock region of the 1973 Nemuro-Oki Earthquake (Shimazaki, 1974).

Table 1. KH 92-3 LEG 2 Kurile Trench MCS Profile

Date	Time	Latitude	Longitude	Depth (m)	MT	Shot#**	Dly (s)	Remarks
Aug. 1	13:25:40							start shot*
	13:30:00	41°13.54'	147°14.41'	5159				
	13:36:40							gun stop
	13:39:20					33	6	gun resumed
	14:05:00	41°15.86'	147°12.12'	5201	23	110	6	
	15:00:00	41°19.52'	147° 8.41'	5251		275	6	
	15:07:20				24	296	6	
	16:00:00	41°23.52'	147° 4.34'	5277		455	6	
	16:33:40				25	556	6	
	17:00:00	41°27.54'	147° 0.46'	5327		635	6	
	17:30:20					726	7	
	17:40:50					757	6	
	18:00:00	41°31.57'	146°56.45'	5418		815	6	
	18:01:20				26	819	6	
	19:00:00	41°35.39'	146°52.39'	5502		995	6	
	19:28:00				27	1079	6	
	20:00:00	41°39.36'	146°48.45'	5636		1175	6	
	20:47:20					1317	7	
	20:55:40				28	1342	7	
	21:00:00	41°43.26'	146°44.32'	6029		1355	7	
	22:00:00	41°47.18'	146°40.31'	6210		1535	7	
	22:22:40				29	1603	7	
	22:36:20					1644	8	
	23:00:00	41°51.15'	146°36.30'	6767		1715	8	
	23:50:20				30	1866	8	
Aug. 2	0:00:00	41°54.96'	146°32.40'	6913		1895	8	
	0:54:40					2059	7	
	1:00:00	41°58.80'	146°28.39'	6285		2075	7	
	1:26:00					2153	7	MT error-stop
	1:41:20				31	2198	7	
	1:56:20					2244	6	
	2:00:00	42° 2.84'	146°24.49'	5886		2255	6	
	3:00:00	42° 6.59'	146°20.54'	5514		2435	6	
	3:07:00					2456	6	MT End
	3:16:20				32	2484	6	
	4:00:00	42°10.38'	146°16.61'	5564		2615	6	
	4:22:20					2682	5	
	4:42:20					2742	5	MT End
	4:49:40				33	2764	5	
	5:00:00	42°14.29'	146°12.65'	4836		2795	5	
	5:30:20					2886	4	
	6:00:00	42° 18.12'	146° 8.37'	4050		2975	4	

Table 1. continued

Date	Time	Latitude	Longitude	Depth (m)	MT	Shot #	Dly s	Remarks
Aug. 2	6:15:40					3022	4	MT End
	6:22:20				34	3042	4	
	6:45:20					3111	3	
	7:00:00	42° 21.95'	146° 4.39'	3584		3155	3	
	7:48:20					3300	3	MT End
	7:54:20				35	3318	3	
	8:00:00	42° 25.95'	146° 0.27'	3324		3335	3	
	9:00:00	42° 30.13'	145°56.37'	3205		3515	3	
	9:20:20					3576	3	MT End
	9:26:20				36	3594	3	
	9:45:20					3651	2	
	10:00:00	42° 34.19'	145°52.14'	2873		3695	2	
	10:52:20					3852	2	MT End
	11:00:00	42° 38.15'	145°48.03'	2663	37	3875	2	
	12:00:00	42° 42.21'	145°43.79'	2316		4055	2	
	12:26:00					4133	2	MT End
	12:31:40				38	4150	2	
	12:45:00	42°45.18'	145°40.72'	2103		4190	2	EOL

* Two-airgun 20-L Starboard + 17-L Center; 1400-1580 psi; 20 s shot interval
** Shot # (airgun shot sequence) is not the same as FFNO (MT record sequence) of the original MTs, since tape mulfunction occurred.

were shot at 20 s interval, at a pressure of about 1500 p.s.i. The signals were received by the AMG 24-channel hydrophone streamer, with each channel spacing of 50 m. The ship speed over the ground was kept at 4.9kt all through the survey line as correctly as possible to record 12-fold seismic CMP data spaced at 25 m interval. Fig. 16-2 shows the on-board monitor record.

The data were fed into the data acquisition field system, DFS-V (T. I.). DFS-V records onto two MT units, and when one MT tape ends, the other starts recording automatically. The sampling rate was set at 1 ms and 8092 samples per shot were recorded after manually set delay time. Each shot was triggered by a precise time code generator. The trigger signal was fed into the Auto-Sync airgun controller, which automattically syncs the two guns' actual shot time to 462 ms (measured on KH-92-2) after the contact closure exactly at the shot time.

Since the Auto-Sync for airguns that we used on this cruise did not have a time break output, DFS-V ran under ITB, internal time break, which is nominally 128 ms after blast time. But an actual measurement showed that the recording start time of DFS-V was 265 ms after the actual gun shot time (about 0.73 s from time 0). Therefore, care must be taken to correct for the time offset between the shot time and the time of first sample on MT.

During the survey, which lasted about 24 hrs, a tape recorder malfunction occurred in the latter half of this MCS survey line, which corresponds to the landward side of the trench, and we had to rely on a single MT unit, so that about 6 min length data were lost at tape swap time, which appear as gaps on the record section.

Results

Fig. 16-3 (a foldout in the back-cover) is the stacked section of the MCS survey across the Kuril Trench of this cruise. A considerable improvement in signal-to-noise ratio is seen to be achieved by data processing. In the profile, the subducting basement of oceanic crust is clearly observed to about 70 km from the deepest seafloor, till the multiples hide it at more than 4 s below seafloor. A large offset fault exists crossing the basement near the trench. Similar faults show less slips as the distances seaward from the trench become larger.

More than 45 km on the continent side of the trench, we can find two reflectors. One exists at 0.4 sec below the seafloor as a BSR, bottom simulating reflector, perhaps due to gas-hydrates. The other looks perfectly horizontal, which may be the basement of the continental crust. However, it is strange that the reflector should be completely independent of the bathymetry of the seafloor.

Throughout the profile we can find many diffraction signals, scattered from faults or other irregularities. They will be removed after migration processing. The widest record gap near the trench indicates the time when one MT unit started malfunctioning. Despite such losses of some data, we obtained generally a good quality seismic profile for our scientific purposes. With ongoing further processing, we are preparing a paper to present our scientific results.

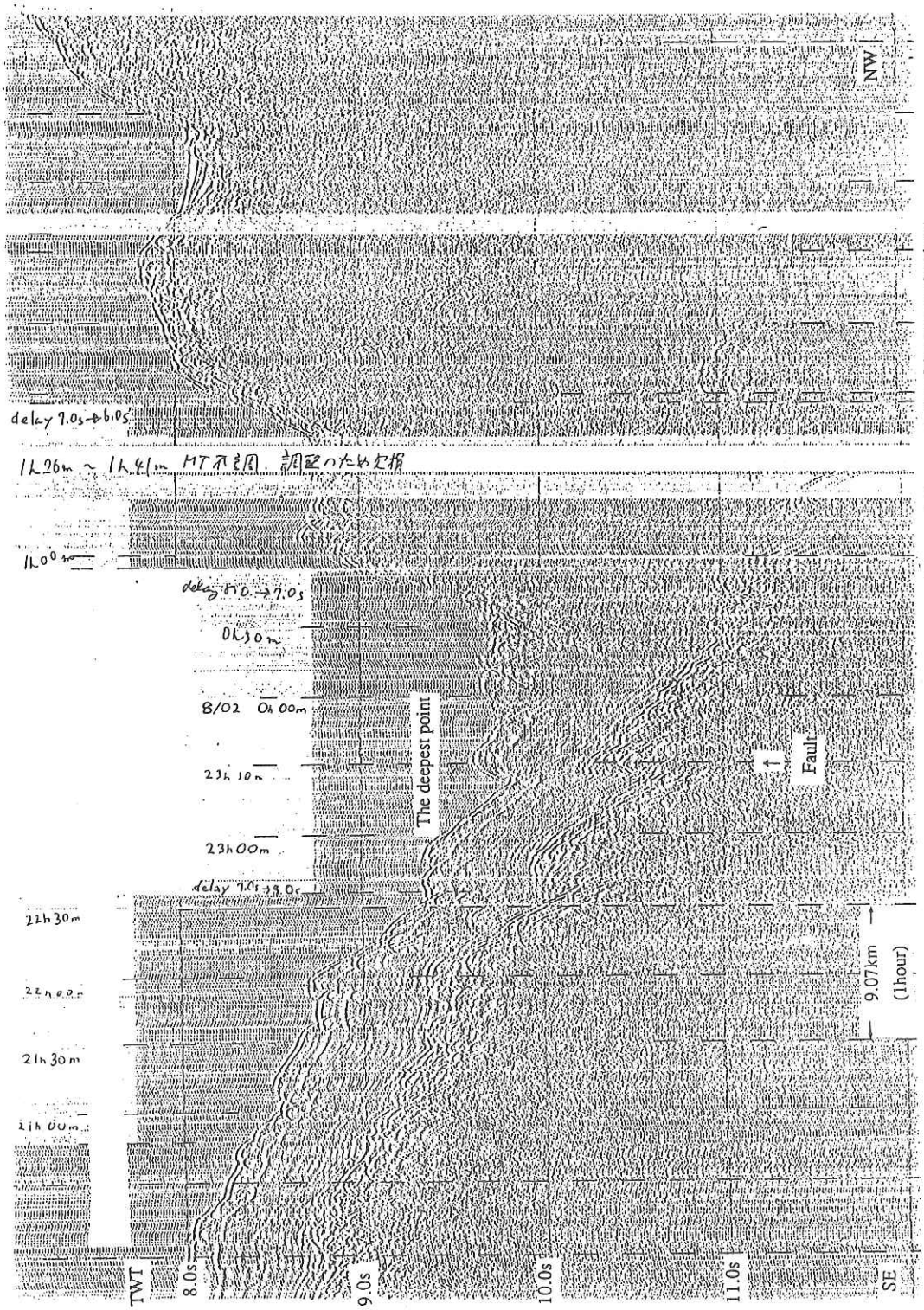

Fig. 16-2. On-board seismic monitor record. Seismic record from ch-1, nearest the ship was output on Line Scan Recorder as recorded on DFS-V system.

References

Amishiki, T., Shallow crustal structure in the southwestern part of Kurile Trench, *M. Sci. Dissertation, Chiba University*, 1992.

Amishiki, T. and H. Tokuyama, Multi-channel seismic reflection survey, in Tsukawaki, S., and N. Nemoto, Preliminary Results on Tansei-maru Cruise KT90-9 in Forearc Areas off Northern Tohoku and Hokkaido, and Sagami Bay, Japan, *Sci. Rep. Hiraosaki Univ.*, **38**, 46-86, 1991.

Iwasaki, T., H. Shiobara, A. Nishizawa, T. Kanazawa, K. Suyehiro, N. Hirata, T. Urabe, and H. Shimamura, A detailed subduction structure in the Kuril Trench deduced from ocean bottom seismographic refraction studies, *Tectonophys.*, **165**, 315-336, 1989.

Iwasaki, T., N. Hirata, T. Kanazawa, T. Urabe, Y. Motoya, and H. Shimamura, Earthquake distribution in the subduction zone off eastern Hokkaido, Japan, deduced from ocean-bottom seismographic and land observations, *Geophys. J. Int.*, **105**, 693-711, 1991.

Kimura, G., Abashiri tectonic line—with special reference to the tectonic significance of the southwestern margin of the Kurile Arc—, *J. Fac. Sci., Hokkaido Univ.*, Ser. IV, **20**, 95-111, 1981.

Nishizawa, A. and K. Suyehiro, Crustal structure across the Kurile trench off southeasten Hokkaido by airgun-OBS profiling, *Geophys. J. R. astr. Soc.*, **86**, 371-397, 1986.

Sakurai, M., T. Nagai, M. Tozawa, and K. Ikeda, Submarine geological structures and crustal movements of the continental margin off Kushiro, Hokkaido, *Rept. Invest. Nemuro-oki Earthq.*, **17**, 10-17, 1975.

Sato, T., Submarine topography in the environs of the Kushiro Submarine Canyon, *J. Geol. Soc. Japan*, **68**, 563-572, 1962 (in Japanese).

Shimazaki, K., Nemuro-Oki earthquake of July 17, 1973: A lithospheric rebound at the upper half of the interface, *Phys. Earth Planet. Inter.*, **8**, 148-157, 1974.

17. Bottom Observations by the Deep-Sea Multi-Monitoring System

S. Ohta, M. Watanabe, D. S. Kim and M. Nakanishi

Outline of Work

Bottom surface features were observed using a deep-tow type bottom surveying system named "DESMOS" (deep-sea multi-monitoring system) during the Hakuho Maru Cruise KH-92-3. In its first leg, two operations were allocated to thc survey on the landward slope of the Nankai subduction zone and one operation to the sites of the ODP drill holes 808D and 808E. In the second leg, one operation was assigned to the observations of the western flank of the Kushiro Submarine Canyon pouring into the Kurile Trench south off Hokkaido and two operations to the exploration of the Erimo Seamount.

Specifications and Operations of the System:

The underwater vehicle of the DESMOS is composed of a pair of stereo-color TVs, a pair of stereo still cameras (up to 1,700 frames using 35mm, 100-foot long strip color negative films), CTD (Sea-Bird Electronics, Inc.: Model SBE 9/11, modified by Tsurumi Seiki Co. Ltd.), 6-bottle rosette water sampler (Niskin-type; 1.5 liter each), a pendulum suspended from the frame of the vehicle and an auto-releasing clamp for auxiliary instruments such as an acoustic altimeter, an inclinometer, an acoustic transponder. Images illuminated by four 300 watt halogen lamps and measured signals are transmitted to the shipboard console via a 6,000m long, 14.4mm ϕ composite armored cable (consisting of 6 optical fibers, 4 signal wires and 6 power cords).

Photographing, water sampling and releasing of any kind of instruments are controlled by the operators based on the real-time information displayed on shipboard monitors. Vertical and horizontal CTD profiles were monitored on CRT, X-Y plotters and printers. Horizontal mode of the CTD profile is specially designed for quick discrimination of thermal anomalies on analog graphics. Video images and basic LAN data are displayed on two monitoring TVs and recorded on S-VHS cassettes together with voice comments of the observers. The vehicle is not equipped with thrusters but simply held by a tethered cable and maneuvered by cable winch operation and surface ship's joy-stick dynamic positioning system.

A pendulum weight suspended by 250cm thread works as a measure of distance for winch operation and dimension of objects. When the tip of the chain touches the bottom, rough estimation of the frame coverage was 2 by 2.5m on the bottom, as, in most cases, cameras were set perpendicular to the bottom and zooming was set as wide as possible. Detailed analysis of dimension and identification of photographed objects are carried out in a laboratory on land.

Note that the depth figures superimposed on video monitor was fed from Seabeam via LAN, and the time in GMT. True vehicle depth was recorded continuously in the CTD graphic and floppy data.

Positions of the underwater vehicle together with surface ship were fixed and guided by means of a SSBL (super-short-baseline) acoustic transponder subnavigation system (OKI Electronic Company Ltd.). LBL (long-base-line) subnavigation was also used in selected sites of DESMOS.

A video channel didn't work after the one trial, and CID and telemetry system 2 went into disorder during the second leg. The system was operated at 6 survey sites (Stations DESMOS-l, DESMOS-2, DESMOS-3, DESMOS-4, DESMOS-S and DESMOS-6). Preliminary results of observations were briefly summarized in the following.

Brief Résumé of the Video Observations

Station **DESMOS–1. 1**

Location; A steep slope south off Tenryu Canyon, Nankai Trough
34°00.87'N: 137°43.19'E (D=1,308m)~34°00.55'N: 137°43.50'E (D=1,348m)
Date and time of operation; July 18, 1992; 09:33~12:31 [JST]
Duration of bottom observations; 01:07~03:33, July 18, 1992 [GMT]
Depth range of bottom observations; 1,308~1,348m [Seabeam]
Still-camera photos; 263 frames [R: Konica Super DD400, L: Konica Super DD400]
Video records; 1 S-VHS cassette for Camera #2 ["14:05~16:09"*=>01:05~03:09 in GMT].
[*Hour figures superimposed on this monitor must be subtracted by 13 to show correct GMT]

Typical Scenery: Bottom water movement appears to be strong, as suggested by the erosive bottom feature and dominance of filter-feeders. Biomass is not high, but not too poor.

Biota: Large organisms observed frequently were sea pens *(Pennatula sp.),* red longlegged shrimps *Nematocarcinus sp., Antedon-type* sea-ferns, ophiuroids *Ophiophthalmus normani* on the stones and *Ophiomusium Iymani* on the sediment, brotulid *Acanthonus armatus* and fishes such as halosaurid *Aldrovandia aJ~inis* and alepocephalid *Rouleina sp.,* holothurians such as deimatid *Peniagone spp.,* synallactid *Paelopatides spp.* in the order of abundance. Other organisms observed were squat lobsters *(Munidopsis sp.),* echinothuriid sea-urchin *(Hygrosoma hoplacantha)* and pycnogonids.

General Remarks: The primary objective of the DESMOS operation at this station was to explore and to locate seeping zones along a cliff on the accretional prism in the Nankai Trough. This operation was interrupted by difficulty in ship's maneuvering and emergency drill.

Station **DESMOS–1. 2**

Location: A steep slope south off Tenryu Canyon, Nankai Trough
34°00.67'N; 137°42.99'E (D=1,321m)~34°01.52'N; 137°43.26'E (D=1,103m)
Date and Time of Operation: July 18,1992;13:13~15:22 [JST]
Duration of Bottom Observations: 04:40~06:01, July 18,1992 [GMT]
Depth Range of Bottom Observations: 1,321~1,103m [Seabeam]
Still-camera Photos: 263~1153 frames [R: Konica Super DD400, L: Konica SuperDD400]
Video Records: 1 S-VHS cassette for #2 ["17:35~19:09"=>04:35~06:09 in GMT]
[* Hour figures superimposed on this monitor must be subtracted by 13 to show correct GMT]

Biota: Larger living organisms frequently observed were basically the same as in thc preceding operation. Organisms to be mentioned were *Euplectella-type* hyaline sponges, galatheid *Munidopsis rostrata,* scarlet shrimp *Acanthephyra eximia,* echinoid *Echinus lucidus,* asteroid *Radiaster sp.,* holothurian *Enypniastes eximia,* and fishes *llyophis brunneus* and *Lepidion sp.*

General Remarks: DESMOS–1. 2 is actually a continuation of DESMOS–l. l. The track followed shallower portion of the slope. However, no remarkable indication of recent seepage as evidenced by dense patches of giant clams was found along the observation track line except for occasional occurrence of few tufts of medium-sized vestimentiferan tube worms and dead shells of *Calyptogena.*

Station **DESMOS–2**

Location: ODP holes 808D and 808E, south off Muroto, Nankai Trough
32°21.06'N: 134°56.55'E (D=4,661m)~32°20.58'N: 134°56.77'E (D=4,747m)
Date and Time of Operation: July 21, 1992; 01:53~12:23 [JST]
Duration of Bottom Observations: 18:27~01:35 July 20~21, 1992 [GMT]
Depth Range of Bottom Observations: 4,660~4,747m [Seabeam]
Still-camera Photos: 1700 frames [R: Konica Super DD400, L: Konica Super DD400]
Video records: 4 S-VHS cassettes for Camera #2 [07:21~09:21, 09:24~25, 11:25~13:27, 13:27~14:53 in JST]
[* Hour figures superimposed on the monitor must be subtracted by 13 to show correct GMT]

Typical Scenery: The "normal" seafloor was blanketed thickly by fine, dart-tint silt. The flat bottom was reworked by bioturbation and studded with the fecal knots of holothurians suggesting very feeble bottom water movement. The area near the bore holes is covered by unusually pale silt, which might be the waste of the drilling. Biomass is apparently depauperated by this anthropogenic disturbance.

Biota: The biomass is relative low, as is usual in the lower bathyal slope. Dominant organisms were, as expected, the holothurians: the tailed holothurian, *Psychropotes longicauda,* swimming holothurians such as *Peniagone leander* and *Paelopatides confundens,* and *Deima validum.* Occurrence of dead shells of *Calyptogena* (3 times) and *Solemya* suggests the near-by presence of biological associations with the cold sceps. Other organisms encountered were galatheids *Munidopsis spp.,* sea pen *Umbellula magniflora.*

General Remarks: The DESMOS–2 operation aimed at locating the re-entry cone of the ODP hole 808E to observe the ONDO system. The artifacts observed were;

18:28'11": slender cables [32°21.07'N: 134°56.54'E, D=4,660m],
18:59'10": long thick pipe (casing of the drill hole 808D),
20:43'31": long thick pipe [32°21.09'N: 134°56.68'E, D=4,663m],
21:06'56": several mooring ropes (transponder?),
22:34'00": slender iron pipe,
23:44'45": large iron weight,
23:45'00": long pile and a wooden block,
23:48'18": two long and thick pipes,
00:51'00": slender cable

Unfortunately the ONDO system was not found.

Station DESMOS-3

Location: Steep landward slope of the Nankai Trough south off Enshunada
34°03.94'N: 138° 06.93'E (D=2,422m)~34°05.78'N: 138°05.67'E (D=1,985m)
Date and Time of Operation: July 22, 1992; 08:05~17:59 [JST]
Duration of Bottom Observations: 23:55~08:00, July 22, 1992 [GMT]
Depth Range of Bottom Observations: 2,422~1,985m [Seabeam]
Still-camera Photos: 1461 frames [R: Konica Super DD400, L: Konica Super DD400]
Video records: 2 S-VHS cassettes of Camera #2 ["12:53~14:55", "14:55~17:00"*]
[* Hour figures superimposed on this monitor must be subtracted by 13 to show correct MT]

Typical Scenery : The bottom at this station primarily consists of relatively thin, coarse silt smoothed by gentle bottom current. Many seemingly free-living sea anemones which must fasten themselves to hard substratum support this view. Sometimes slabs and boulders of sedimentary rocks were scattered on the sea floor. Occasional outcropping of small benches and cliffs from 10cm to 5m in altitude were trending NE-SW.

Biota: Animal frequently observed are listed below in taxonomic order. Coelenterata: *Kophobelemnon stelliferum.* Pycno-gonida: *Colossendeis colossea* Macrura: *Nematocarcinus sp., Glyphocrangon sp.* Anomura: *Paralomis verrilli, Munidopsis rostrata* and other species Holo-thuroidea: *Peniagone monachtinica, Paelopatides confundens, Pseudostichopus unguiculatus, Laetmogone violacea* Ophiuroidea: *Ophiophthalmus normani* Echinoidea: *Hygrosoma hoplacantha, Calveriosoma gracile* Pisces: *Aldrovandia affinis, Halosauropsis macrochir, Acanthonus armatus, Polyacanthonotus challengeri, Histiobranchus bathybius, Nettastoma sp., Ilyophis brunneus.*

General Remarks : Occurrence of small patches of *Calyptogena* [at 15:00'00", D= 2,275m and 15:35'31", D=2,154m] together with scattered dead shells of *Calyptogena* and *Vesicomya spp.* appears to indicate possible existence of cold seepage.

Station DESMOS-4

Location: Mouth of the Kushiro Submarine Canyon toward the Kuril Trench
41°50.32'N: 145°14.92'E (D=5,163m)~41°52.10'N: 145°12.62'E (D=4,610 m)
Date and Time of Operation: August 05, 1992; 09:49~17:25 [JST]
Duration of Bottom Observations: 02:42~07:03, August 5,1992 [GMT]
Depth Range of Bottom Observation: 5,163~4,610m [Seabeam]
Still-camera Photos: 1607 frames [R: Konica Super DD400, L: Konica Super DD400]
Video Records: 2 VHS cassettes for Camera #2 [11:28~13:30, 14:00~16:03 in JST]
[* Hour figures superimposed on this monitor are in JST]

Typical Scenery : Gcneral feature of this station is very flat bottom thickly blanketed with grayish brown silt. Week bottom water current smoothed the canyon floor. Organic detritus feeders are dominating.

Biota : Most of the observation track followed the canyon axis, where ample turbiditic supply of organic nutrients might be expected. Extremely high biomass must be sustained by this mechanism. At the initial stage near the bottom (from

several tens of meters above the bottom down to just above the bottom) the DESMOS went through swarms of small swimming holothurians, probably *Elpidia longicirrata.* The density of the swimming holothurians were very high, about 10 individuals in a frame.

Animals frequently observed are listed below in taxonomic order. Protozoa: Xenophyophores Coelenterata: simple scleractinian corals, *Kophobelemnon stelliferum, Umbellula thomsoni, Liponema multicornis, Branchiocerianthus imperator* Annelida: echiuran worm *Jacobia birsteini* and tubicolous polychaetes. Isopoda: *Storthyngura* sp. Mollusca: *Neptunea sp.* Macrura: *Benthesicymus crenatus* and/or *Hepomadus glacialis* Anomura: *Munidopsis* sp.(abundant) Crinoidea: *Bathycrinus sp.* Asteroidea: *Eremicaster sp.,* 6-armed asteroids *(Freyella oligobrachia)* Ophiuroidea: *Ophiura bathybia, Ophiacantha bathybia* [clinging Echinoidea: *Kamptosoma asteria, Echinocrepis sp.* Holothurioidea: *Elpidia longicirrata, Scotoplanes globosa, Psychropotes longicauda, Psychropotes verrucosa, Peniagone spp., Benthodytes sp., Pseudostichopus sp.,* Pisces: *Coryphaenoidesyaquinae.*

General Remarks : More than half of this observation track followed the western floor of the Kushiro Submarine Canyon.

Station **DESMOS–5**

Location: Northeastern top and flank of the Erimo Seamount
40°53.50'N: 144°51.27'E (D=3,862m)~40°52.00'N: 144°49.58'E (D=4,693m)
Date and Time of Operation: August 06,1992; 08:19~13:23 [JST]
Bottom Observations: 00:40~02:46, August 06,1992 [GMT]
Depth Range of Bottom Observations: 3,832~4,350m [SSBL]
Still-camera Photos: 1461 frames [R: Konica Super DD400, L: Konica Super DD400]
Video Records: 3 S-VHS cassettes for Camera #2 [01:10~03:12, 03:12~05:14, 05:14~06:22
[* Hour figures superimposed on this monitor are in JST]

Typical Scenery : The bottom environment observed during this operation can be divided into two habitats . The anterior half consisted of flat top of the seamount covered with thin sandy sediments. The top of the seamount primarily consisted of the outcrops of rocks covered only slightly with coarse sandy sediments. Most of the bare rock surfaces of angular cobbles and pebbles were darkly encrusted with probably hydro-oxides of Mn and/or Fe. Occasional glimpses of white stuff beneath the black coating on the rocks suggest that they are limestones and/or apatite in nature. The scenery can be interpreted as an ancient coral reef flat. As a whole the bottom environment was errosional from the sedimentological point of view.

Just below the top of the seamount, outcrops of rocks persuadc us the volcanic nature of the basement.

Biota: At the top of the seamount, blocks (boulder to cobble size) of xenophyophores were dispersed everywhere. Biomass was very low. Along the slope, suspension feeding gorgonians such as *Radicipes sp.* and *Bathypathes* spp. are predominated. Stalked tunicates *Culeolus sp.* and crinoid *Bathycrinus* are also

included in this category. *Munidopsis* and 6-armed asteroid *Freyella oligobrachia* are dominated in number.

General Remarks: Main objective of this operation was to relocate an Ocean Bottom Inclinometer set during the 1985 KAIKO Project on a flat outcrop in the northeastern edge of the seamount crest. This was not successful probably because the DESMOS traversed mostly thc northeastern top of the Erimo Seamount only.

Station **DESMOS–6**

Location: Southwestern top and flank of the Erimo Seamount
40°53.50'N: 144°51.27'E (D=3,862m)~40°52.00'N: 144°49.58'E (D=4,693m)
Date and Time of Operation: August 07, 1992; 08:19~13:23 [JST]
Bottom Observations: 00:40~02:46, August 07,1992 [GMT]
Depth Range of Bottom Observations: 3,832~4,350m [SSBL]
Still-camera Photos: 1461 frames [R: Konica Super DD400, L: Konica Super DD400]
Video Records: 1 VHS cassettes for Camera #2 [00:38~02:42]
[* Hour figures superimposed on this monitor are in JST]

Typical Scenery : The southwestern top of the Erimo Seamount was almost flat covered by gray-brown sandy mud sediments, well oxydized and smoothed by rather strong bottom current. Occasional outcrops of white blocks of limestone-nature were observed. The southwestern upper flank of the Erimo Seamount was primarily composed of volcanic rocks.

Data Storage and Inquiries

S. Ohta (ORI) is responsible for storage of original video and film records as well as DESMOS-CTD data on graphic charts and floppy disks, event records and subnavigation records on floppy disks. Chief scientist of the cruise K. Kobayashi is in charge of of distribution and publicity of these data based on the full set of suboriginal copies at his hand.

18. Dredge Hauls

18-1. Dredge Logs

Date 1992.08.06 Ship Hakuho-maru Cruise KH92-3 Station No.D1
Location Erimo Seamount, flank in southeast side
Weather Mist Wind 204°, 9m Sea rough
Bottom Topgraphy slope
Type of Dredge Nalwalk chain-bag with a bucket Add.Wt. 100kg+50kg+chain
Fuse wire 10mm, 1m Life wire 10mm, 7m Pinger position 500m (SSBL)
Time lowered 18h 40m Uncorr.Water Depth 4713m
Initial Time on Bottom 21h 02m Uncorr.Water Depth 4284m
Wire Length 4473m Wire Angle 20°
Ship Position Lat. 40°56.49' N Long. 144°15.19' E
Direction of Haul 245° Ship Speed 0.7kt. (till 22h 45m)
Speed Wire-in 0.25m/min (from 22h 45m) Winch No.1
Final Time on Bottom 23h 16m Uncorr. Water Depth 4275m
Wire Length 4350m Wire Angle 10°
Ship Position Lat. 40°51.27' N Long . 144°59.05' E
Time Surfaced 100h 50 m
Dredged Materials and comments
more than 100 rocks with about 100kg weight in total; lava(about 55%), hyaloclastite(25%), sedimentary rocks(10%), limestone, Mn-nodule, soft sediments(4kg), and ice rafted rocks(5%).

Date 1992.08.07 Ship Hakuho-maru Cruise KH92-3 Station No.D2
Location Erimo Seamount, northwestern slope of lower step.
Weather Mist Wind 221°, 8.6m Sea rough
Bottom Topgraphy slope
Type of Dredge Nalwalk chain-bag with a bucket Add.Wt. 100kg+50kg+chain
Fuse wire 10mm, 1m Life wire 10mm, 7m Pinger position 500m (SSBL)
Time lowered 2h 23m Uncorr.Water Depth 4893m
Initial Time on Bottom 03h 39m Uncorr.Water Depth 4997m
Wire Length 4990m Wire Angle
Ship Position Lat. 40°57.88' N Long. 144°49.14' E
Direction of Haul 125° Ship Speed 0.7kt. (till 5h 10m)
Speed Wire-in 0.2m/min (from 5h 10m) Winch No.1
Final Time on Bottom 6h 8m Uncorr. Water Depth 4555m
Wire Length 4750 m Wire Angle 15°
Ship Position Lat. 40°57.60' N Long . 144°50.33' E
Time Surfaced 07h 31m
Dredged Materials and comments
more than 100 rocks with about 140kg weight in total; lava(70%), sedimentary rocks(10%), soft sediments(5kg), pumice(2%), and ice rafted rocks(20%).

Date 1992.08.08 Ship Hakuho-maru Cruise KH92-3 Station No.D3
Location Mizunagidori Seamount, flank to top in southeast side
Weather Fine Wind 184°, 6.7m Sea carm
Bottom Topgraphy slope to flat
Type of Dredge Nalwalk chain-bag with a bucket Add.Wt. 100kg+50kg+chain
Fuse wire 10mm, 1m Life wire 10mm, 7m Pinger position 500m (SSBL)
Time lowered 10h 30m Uncorr.Water Depth 2531m
Initial Time on Bottom 11h 33m Uncorr.Water Depth 2525m
Wire Length 2900m Wire Angle
Ship Position Lat. 37°08.82' N Long. 145°19.22' E
Direction of Haul Ship Speed 1.0kt. (till13h 15m)
Speed Wire-in 0.2m/min (from 13h 15m) Winch No.1
Final Time on Bottom 14h 02m Uncorr. Water Depth 2529m
Wire Length 2428 m Wire Angle 25°
Ship Position Lat. 37°07.15' N Long . 145°17.25' E
Time Surfaced 14h 41m
Dredged Materials and comments

more than 150 rocks with about 120kg weight in total; Mn-nodule and -crust (75%), hyaloclastite(8%), lava(1%), sedimentary rocks(3%), pumice(6%), scoria(1%), and ice rafted rocks(5%).

18-2. Description of dredged samples from the Erimo and Mizunagidori seamounts during the second leg (Kushiro to Tokyo) of KH92-3 cruise

Teruaki Ishii, Yasuaki Hanamura, Yujiro Ogawa, and Kazuo Kobayashi

More than five hundred rocks (about 450 kg weight in total) were dredged during the second leg (Kushiro to Tokyo) of KH92-3 cruise. Two sites (Stations KH92-3-D1 and D2) and one site (Station KH92-3-D3) were selected to investigate the origin and evolution of the Erimo and Mizunagidori Seamounts, respectively. Precise position, depth of each station and relevant infomation are given at the operation logs of dredge hauls (see, 18-1. Dredge Logs, in this volume), and position of each station is shown in Figs. 18-2-1A and 1B. The dredged materials are listed in Table 18-2-1.

Improved Nalwalk chain-bag dredges with a bucket (Ishii et al., 1985) were usued to collect boulder to granule rock samples as well as psammitic to pelitic soft sediments. The "SSBL-transponder" was installed at about 500 meters above from the dredge at all stations to confirm the position of dredge and its hitting sea bottom. The traces of the "SSBL-transponder" (not ship track) during dredge are shown in Figs.18-2-1A and -1B.

Because most of the dredged rock-samples were more or less covered with soft sediments and/or Mn-coating, these rocks were at first separated from sediments by washing. They were cut by a diamond saw into two or more pieces for observation and description of visual features inside each sample. Washed samples were classified into several groups according to their lithologic characteristics.

After numbering the samples (in the order of size), diameter (L, M and S), roundness, weight and thickness of Mn-coating, lithology and remarks of each sample were observed on board and were described in Table 18-2-1, where roundness is described after the Powers' system (Powers, 1953), that is, 0.10 = very angular, 0.20 = angular, 0.30 = sub-angular, 0.40 = sub-rounded, 0.60 = rounded and 0.85 = well-rounded. Some rock-thin sections were made for microscopic observations.

The Erimo seamount

As shown in Fig. 18-2-1A., the edifice of the Erimo Seamount is geographically divided into two parts (the northwestern and southeastern halves) by the steep fault escarpment with ENE-SSE direction, and about 500m height discrepancy. The Erimo Seamount has been surveyed by several research vessels during the last twenty years. Considering those previous studies, two stations of dredge hauls; Stations KH92-3-1 and -2, were selected at the steepest flank in the upper and lower steps, respectively.

More than 100 kg materials were dredged at Stations KH92-3-1 including vesiculas massive lavas, altered hyaloclastites with brown and/or olive-yellow

color, sedimentary rocks of coarse sandstones & conglomerates, one limestone, one Mn-nodule, soft sediments (4 kg), and ice rafted rocks as shown in Table 18-2-1. Massive lavas are very angular (= 0.1 in Powers' roundness number) to sub-angular (= 0.3) in shape and have relatively thin Mn-coating (= 0-1 mm thick). Recovered one limestone includes shell-like mega-fossils of 'Rudistes' (= Atsuba-nimaigai in Japanese) indicating Cretaceouce age (after Taira, personal communication).

More than one hundred materials with about 140 kg weight in total were dredged at station KH92-3-2. They are massive lavas, sedimentary rocks of coarse sandstones & conglomerates (some are phosphorite), soft sediments (5 kg), pumices, and some ice rafted rocks. Limestone and Mn-nodule were not recovered. Lavas are angular and have very thin filmy Mn-coating. Ice rafted rocks are very fresh and have no Mn-coating.

The Mizunagidori seamount

The Mizunagi-dori seamount is located in the northern end of the Joban seamount chain. Masaru et al. (1993) have investigated magnetic anomaly of the seamount, and he emphasized that the magnetic anomaly of this seamount is very small among these seamounts. Dredge haul of the Station KH92-3-3 (Fig. 18-2-1B) was expected to investigate the magnetic characteristic of the seamount.

Dredged materials are more than one hundred and fity rocks with about 120 kg weight in total. They are Mn-oxides (Mn-nodules and -crusts), hyaloclastites, sedimentary rocks (sandstones and congromerates), pumices, scorias, altered lavas and ice rafted rocks. Mn-coatings are well-developed and are ranging up to about 90 mm thick. Core materials of the Mn-nodules are mainly hyaloclastites, on the other hand altered.lavas and phosphorites are rarely observed in the core. Ice rafted rocks and pumices are almost free from Mn-coating.

Several assumed 'in-situ' rocks composing the volcanic edifice of the Mizunagidori seamount were dredged as cores of Mn-nodules and as lithic fragments in the volcanic conglomerates. A typical example of a lithic fragment in the volcanic conglomerates is shown in Fig. 18-2-2. Magnetic and petrological characteristics will be reported elsewhere.

References

Ishii, T., Kobayashi, K., Shibata, T., Naka, J., Jonson, K., Ikehara, K., Iguchi, M., Konishi, K., Wakita, H., Zang, F., Nakamura, Y. and Kayane, H.: Description of samples from Ogasawara fore-arc, Ogasawara Plateau and Mariana Trough, during KH84-1 Cruise. In Preliminary Report of the Hakuho-Maru Cruise KH84-1 (Ocean Reserch Institute, University of Tokyo), 105-165, 1985.

Msasaru, D. C. P., Tamaki, K. and Kobayashi, K.: Paleomagnetism of the seamounts forming the Joban seamount chain in the northweatern Pacific. J. Geomag. Geoelecter., 45, 1993 (in press).

Powers, M.C.: A new roundness scale for sedimentary particles. J. Sed. Pet., 23, 117-119, 1953.

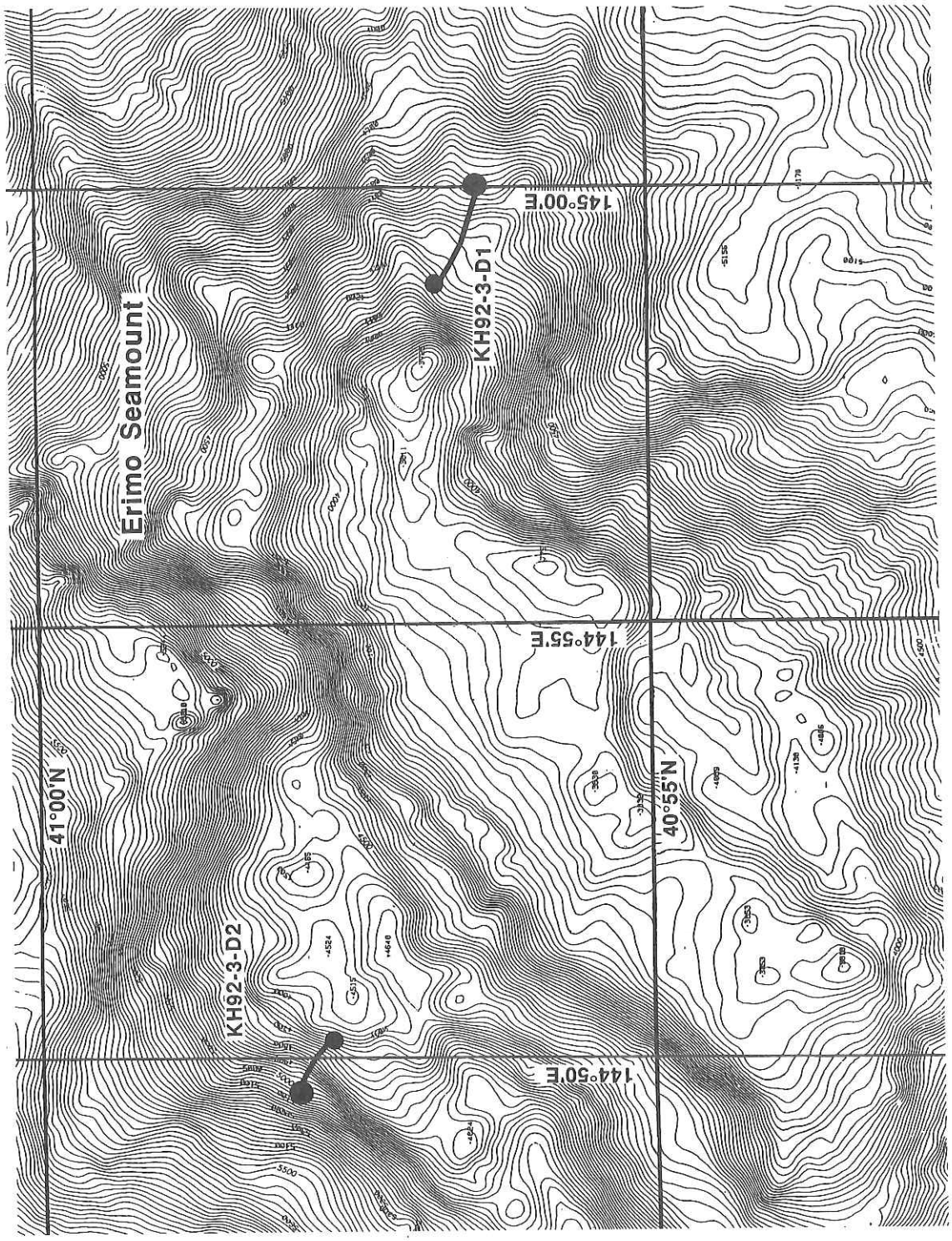

Fig. 18-2-1A. Location map of dredge hauls of the stations KH92-3-D1 and D2 in the Erimo Seamount during the second leg (Kushiro to Tokyo) of KH92-3 cruise. Bathymetry (after R/V "Jean Charcot") in metres. Notes : Large and small circles show initial and final "SSBL-transponder" (not ship) positions, respectively.

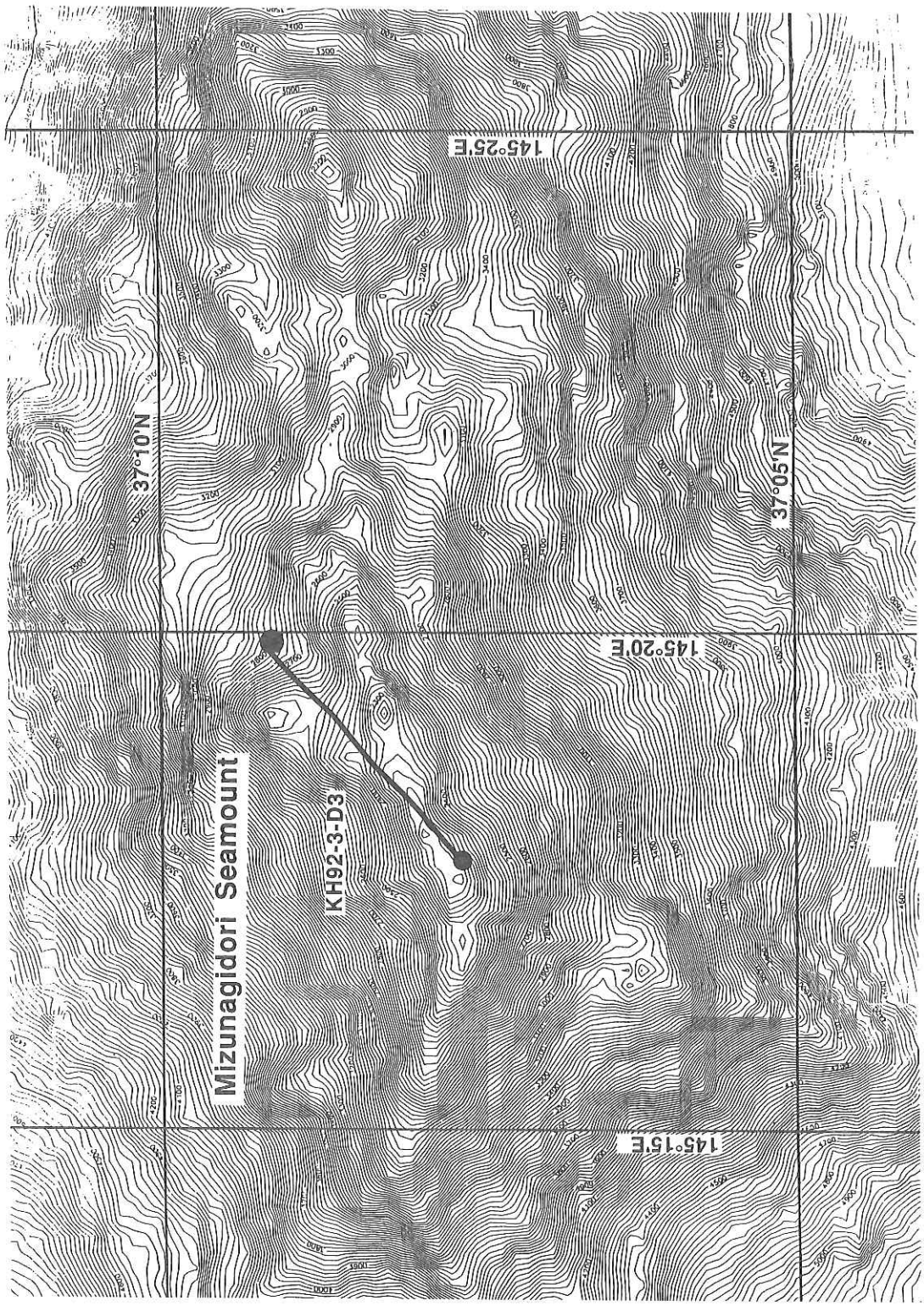

Fig. 18-2-1B. Location map of dredge hauls of the stations KH92-3-D3 in the Mizunagi-dori Seamount during the second leg (Kushiro to Tokyo) of KH92-3 cruise. Bathymetry (after R/V "Hakuho-maru") in metres. Notes : see Fig. 18-2-1A.

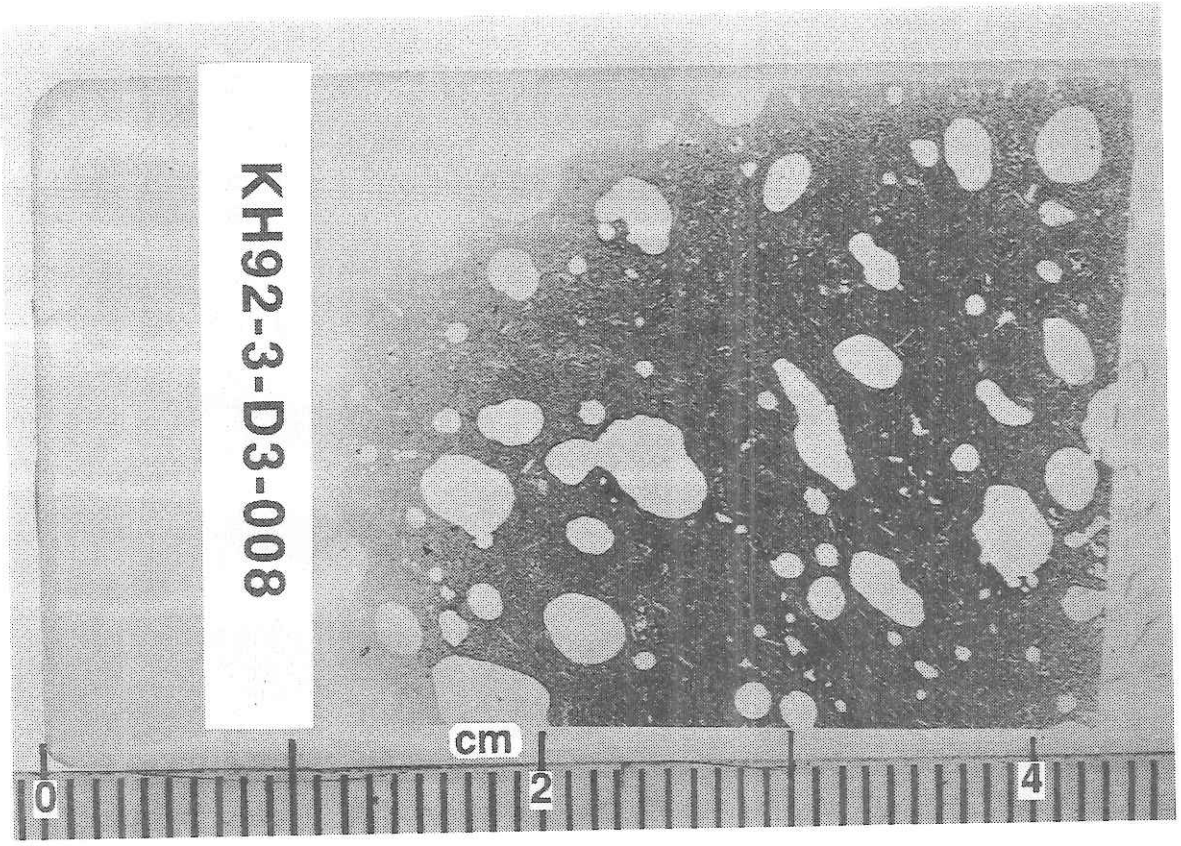

Fig. 18-2-2. Photograph of a rock thin section. A vesiculas altered lava of plagioclase-magnetite-bearing nearly aphyric trachyandesite included in a volcanic conglomerate (sample number : KH92-3-D3-008) from the Mizunagidori Seamount.

Table 18-2-1. List of materials dredged during the second leg (Kushiro-Tokyo) of KH92-3 cruise.

Sample No.	Diameter (mm) L	M	S	Round-ness	Wt(g)	Mn-coating (mm)	Lithology & Remarks
D1-001	450	300	200	0.3	25400	0~2	Hyaloclastite (brown+olive)
002	280	170	160	0.1	3800	0~10	" (olive)
003	200	170	130	0.3	2760	0~3	" "
004	160	140	120	0.2	1850	0~8	Volcanic sandstone
005	130	130	120	0.3	1760	0~1	Hyaloclastite (brown)
006	170	130	80	0.1	1410	0~1	" (olive)
007	140	130	70	0.1	800	0~2	" "
008	110	80	50	0.1	400	0~1	" "
009	150	80	60	0.2	620	0~2	Coarse sandstone
010	90	70	60	0.3	300	0~2	Sandstone
011	110	90	70	0.3	600	0~3	Coarse sandstone
012	120	70	50	0.4	500	0~1	Hyaloclastite (olive)
013	100	60	60	0.1	300	0~4	" "
014	130	80	50	0.1	400	1~10	" "
015	90	70	50	0.2	400	0~2	" "
016	80	70	50	0.3	450	0~1	Sandstone
017	90	80	40	0.2	400	0~10	"
018	90	60	50	0.3	280	0~2	Hyaloclastite (olive)
019	90	70	40	0.2	420	0~2	Sandstone
020	120	70	30	0.2	340	0~1	Hyaloclastite (brown)
021	100	80	30	0.2	340	0~1	" (olive)
022	100	60	40	0.1	300	0~20	Conglomerate
023	80	50	50	0.3	460	0~2	Hyaloclastite (olive)
024	90	70	30	0.2	340	0~1	" "
025	70	40	30	0.1	320	0~1	" "
026	80	50	20	0.2	80	0~1	Volcanic sandstone
027	70	50	40	0.2	120	0~1	Hyaloclastite (olive)
028	80	50	50	0.1	100	0~8	" "
029	60	40	30	0.3	120	0~1	" "
030	90	60	40	0.1	150	0~1	" "
031	70	40	30	0.3	100	0~1	" "
032	60	50	30	0.2	70	0~8	" "
033	70	40	30	0.2	90	0~1	" "
034	70	40	30	0.1	70	0~5	Sandstone
035	80	50	30	0.2	100	1~2	Hyaloclastite (brown)
101	210	200	140	0.3	7150	0~1	Vesiculas massive lava
102	140	130	90	0.3	1500	0~1	Vesiculas massive lava with flow texture
103	200	130	100	0.1	3100	0~1	"
104	180	150	100	0.1	2400	0~10	"
105	150	90	60	0.1	850	0~1	Vesiculas massive lava
106	130	90	50	0.1	650	0~1	Vesiculas massive lava with flow texture
107	130	100	60	0.1	800	0~1	Vesiculas massive lava
108	100	80	60	0.2	500	0~1	"

Sample No.	Diameter (mm) L	M	S	Round-ness	Wt(g)	Mn-coating (mm)	Lithology & Remarks
D1-109	120	110	60	0.1	1000	0～1	Vesiculas massive lava
110	90	70	60	0.2	600	0～1	"
111	100	80	60	0.4	600	0～1	"
112	90	80	40	0.3	500	0～1	"
113	90	80	40	0.2	300	0～1	"
114	110	100	50	0.2	400	0～1	"
115	70	70	60	0.4	400	0～1	"
116	90	70	60	0.4	450	0～1	"
117	90	70	50	0.3	400	0～10	"
118	110	60	50	0.1	280	0～0	"
119	120	80	50	0.3	420	0～1	"
120	100	60	50	0.3	340	0～1	"
121	100	70	50	0.2	340	0～0	"
122	110	40	40	0.4	300	0～0	Compact vesiculas massive lava
123	110	90	50	0.3	460	0～1	Vesiculas massive lava
124	90	70	60	0.2	340	0～10	Hyaloclastite
125	100	70	50	0.3	320	0～1	Vesiculas massive lava
126	120	90	40	0.2	350	0～1	"
127	110	70	40	0.2	250	0～1	"
128	90	80	50	0.3	320	0～1	"
129	100	70	50	0.3	240	0～1	"
130	90	80	50	0.1	300	0～1	"
131	90	70	60	0.1	240	0～5	"
132	90	60	40	0.3	190	0～1	"
133	90	60	50	0.4	260	0～1	"
134	90	60	40	0.2	220	0～1	"
135	90	70	40	0.3	240	0～1	"
136	80	50	40	0.3	150	0～1	"
137	70	60	40	0.3	180	0～1	"
138	80	50	50	0.2	210	0～1	"
139	70	50	40	0.2	110	0～3	Hyaloclastite
140	90	70	50	0.4	340	0～1	Vesiculas massive lava
141	100	50	40	0.3	170	0～1	"
142	120	60	40	0.3	320	0～1	"
143	90	60	30	0.2	170	0～1	"
144	80	70	60	0.3	230	0～3	"
145	90	50	40	0.2	210	0～10	"
146	70	60	40	0.3	190	0～1	"
147	100	60	30	0.2	170	0～1	"
148	100	70	50	0.3	320	0～1	"
149	70	60	50	0.3	160	0～1	"
150	80	50	40	0.2	180	0～1	"
151	70	60	50	0.3	200	0～3	"
152	70	60	40	0.2	160	0～1	"
153	50	50	30	0.4	140	0～1	"
154	80	60	30	0.4	150	0～2	"
155	60	50	40	0.3	130	0～1	"
156	70	50	30	0.3	170	0～1	"

Sample No.	Diameter (mm) L	M	S	Round-ness	Wt(g)	Mn-coating (mm)	Lithology & Remarks
D1-157	60	50	30	0.3	120	0～1	Vesiculas massive lava
158	60	40	40	0.2	150	0～1	"
159	60	60	40	0.3	140	0～1	"
160	-1690				1100		
170	-1790				840		
180	-1890				910		
190	-1940				540		
others					12600		Lava + hyaloclastite
201	200	110	100	0.1	2260	0～1	Limestone with fossile
202	140	120	70	0.4	880	10～20	Mangan nodule (core:Mn-nodule)
203	130	50	80	0.2	400	5～10	Conglomerate
204	80	50	30	0.6	180	none	Ice rafted fine sandstone
205	90	50	40	0.4	180	0～1	Ice rafted acidic lava (dacite)
206	70	60	40	0.4	170	0～1	Ice rafted (?) andesite
207	60	50	20	0.3	100	none	Ice rafted (?) basalt
301					3000		Soft sediments (mud)
302					1300		"

Sample No.	Diameter (mm) L	M	S	Round-ness	Wt(g)	Mn-coating (mm)	Lithology & Remarks
D2-001	330	250	150	0.2	14000	filmy	Massive lava
002	310	170	170	0.1	10300	filmy	"
003	280	160	150	0.2	8800	filmy	" (alterd)
004	300	200	180	0.3	11900	filmy	"
005	170	170	160	0.5	5900	filmy	"
006	190	180	120	0.5	4200	filmy	" (alterd)
007	170	130	130	0.4	4300	filmy	"
008	180	150	130	0.4	5000	filmy	"
009	240	180	130	0.4	7000	filmy	"
010	200	140	130	0.3	4000	filmy	"
011	230	170	110	0.4	4200	filmy	"
012	180	140	100	0.6	2850	filmy	" (coarse grain)
013	160	140	70	0.2	1500	filmy	Conglomerate
014	160	140	80	0.4	2000	filmy	Massive lava
015	220	130	80	0.2	2400	filmy	"
016	180	140	120	0.6	3100	filmy	"
017	220	180	100	0.5	4500	filmy	"
018	140	100	80	0.4	1400	filmy	"
019	200	180	90	0.3	3100	filmy	"
020	180	80	70	0.2	1150	filmy	"
021	120	80	70	0.4	950	filmy	"
022	120	90	60	0.4	700	filmy	" (alterd)
023	140	100	80	0.4	1200	filmy	"
024	140	120	50	0.1	700	filmy	"
025	130	100	80	0.4	880	filmy	" (alterd)
026	100	80	70	0.4	570	filmy	"
027	140	100	60	0.4	800	filmy	"
028	80	70	50	0.4	400	filmy	"
029	140	110	80	0.3	1500	filmy	"
030	90	80	60	0.4	430	filmy	" (alterd)
031	100	60	50	0.4	320	filmy	"
032	130	100	70	0.3	800	filmy	" (alterd)
033	120	100	50	0.3	800	filmy	"
034	120	110	80	0.5	1050	filmy	" (alterd)
035	130	100	70	0.4	1000	filmy	"
036	90	80	60	0.3	550	filmy	"
037	160	80	60	0.3	950	filmy	" (porphyritic)
038	110	80	50	0.3	400	filmy	"
039	140	70	70	0.2	700	filmy	" (basic)
040	100	80	50	0.1	320	filmy	" "
041	140	100	30	0.1	300	filmy	" "
042	100	60	30	0.1	200	filmy	" (aphyric)
043	90	50	30	0.2	180	filmy	"

Sample No.	Diameter (mm) L	M	S	Round-ness	Wt(g)	Mn-coating (mm)	Lithology & Remarks
D2-044	80	70	40	0.2	200	filmy	Massive lava
045	100	60	50	0.2	300	filmy	Conglomerate (phosphorite)
046	80	70	60	0.4	400	filmy	Massive lava (alterd)
047	80	70	40	0.3	200	filmy	" "
048	80	60	60	0.3	300	filmy	" "
049	90	60	30	0.3	200	filmy	" "
050	90	70	40	0.1	240	filmy	"
051	120	60	20	0.1	250	filmy	" (alterd)
052	80	60	50	0.4	300	filmy	"
053	70	70	40	0.4	200	filmy	"
054	120	50	20	0.1	200	filmy	"
055	80	70	30	0.3	200	filmy	"
056	70	60	40	0.4	200	filmy	"
057	70	60	30	0.3	180	filmy	" (alterd)
058	60	50	30	0.4	100	filmy	Conglomerate (phosphorite)
059	70	60	30	0.3	120	filmy	Massive lava (alterd)
060	70	40	30	0.3	100	filmy	"
061	60	50	30	0.3	100	None	" (alterd)
062	70	40	30	0.3	100	None	"
063	70	50	30	0.2	100	filmy	" (basic)
064	50	40	40	0.4	100	filmy	" (alterd)
065	60	40	30	0.3	100	filmy	" "
066	60	50	40	0.2	110	filmy	" "
067	60	50	40	0.4	120	filmy	" "
068	80	50	30	0.2	80	filmy	Conglomerate
069	90	80	20	0.1	70	filmy	Coarse sandstone
070	90	50	30	0.2	120	filmy	Massive lava
071	50	50	30	0.4	100	filmy	" (basic)
072	70	40	40	0.3	100	filmy	Conglomerate
073	80	40	20	0.2	60	filmy	Coarse sandstone
074	60	50	30	0.3	140	filmy	Massive lava (basic)
101	220	120	70	0.4	2000	None	Ice rafted lava(?)
102	100	60	40	0.3	100	filmy	pumice
103	100	70	30	0.2	80	filmy	"
104	80	60	40	0.3	300	filmy	Ice rafted lava (pyrite)
105	80	60	40	0.4	260	filmy	Ice raft
106	70	40	30	0.3	100	filmy	Mangan crust
107	80	60	40	0.2	100	filmy	Lava
108	80	60	50	0.3	180	filmy	Conglomerate
109	80	50	20	0.6	100	None	Ice rafted porohyritic lava
110	80	60	20	0.1	140	filmy	Ice raft
111	60	50	30	0.3	110	filmy	Aphyric lava
112	70	50	30	0.5	120	None	Porohyritic lava

Sample No.	Diameter (mm) L	M	S	Round-ness	Wt(g)	Mn-coating (mm)	Lithology & Remarks
D2-113	60	40	30	0.3	80	filmy	Ice rafted lava
114	60	50	20	0.25	80	None	Ice rafted gabbro
115	60	50	20	0.2	60	filmy	Ice rafted lava
116	40	30	10	0.3	10	filmy	"
117	40	40	20	0.3	10	filmy	"
118	30	20	10	0.4	20	filmy	"
119	40	40	20	0.9	50	filmy	Ice rafted aphyric lava
120	30	20	10	0.3	10	None	Ice rafted granite
121	20	20	10	0.3	10	filmy	Ice rafted lava
122	20	20	10	0.3	10	filmy	"
123	20	20	10	0.3	10	None	Sandstone
124	40	40	20	0.4	50	filmy	Ice rafted aphyric lava
125	40	40	10	0.3	30	None	Ice rafted gabbro
126	40	30	10	0.3	20	None	Ice rafted lava (?)
127	40	30	20	0.3	25	None	Ice rafted sand
128	30	10	10	0.3	10	None	Ice rafted lava (aphyric lava)
129	20	10	10	0.5	10	None	" (coarse grain)
130	20	10	10	0.5	10	None	" (coarse grain)
131	30	30	20	0.3	20	None	" (?)
201					2100		Soft sediments (mud)
202					2700		"
301					6900		Others

Sample No.	Diameter (mm) L	M	S	Round-ness	Wt(g)	Mn-coating (mm)	Lithology & Remarks
D3-001							Skip
002							Skip
003	300	180	110	0.25	5420	0~60	Mangan nodule (core : hyaloclastiye (olive))
004	240	180	100	0.3	4600	0~90	Mangan nodule (core : hyaloclastiye (olive))
005	200	140	120	0.1	3050	0~90	Mangan crust
006	170	170	100	0.35	1750	0~80	"
007	180	180	90	0.2	3100	0~40	"
008	300	230	70	0.1	5360	0~5	Volcanic conglomerate (matrix phosphorite)
009	170	130	100	0.3	1670	9~50	Mangan nodule (core:lava)
010	130	130	80	0.3	1000	80~90	Mangan crust
011	130	120	70	0.3	830	0~50	"
012	140	110	70	0.4	1050	5~20	"
013	150	110	100	0.45	1700	10~25	Mangan nodule (core: phosphorite)
014	200	130	80	0.25	1500	0~70	Hyaloclastite (olive)
015	180	100	60	0.2	1150	0~3	Conglomerate
016	200	140	60	0.1	1300	0~20	Hyaloclastite (olive)
017	210	170	80	0.3	3100	0~5	Hyaloclastite (olive)
018	160	140	90	0.35	1400	0~80	Mangan crust
019	180	120	40	0.2	800	0~20	"
020	160	130	80	0.1	1200	1~80	"
021	150	150	50	0.2	950	0~50	"
022	110	100	50	0.2	500	0~50	"
023	140	80	60	0.3	700	0~15	"
024	140	100	90	0.2	820	1~40	Mangan nodule (core:lava)
025	100	80	70	0.3	550	1~30	Mangan crust
026	150	100	70	0.3	950	5~20	Mangan nodule (core : hyaloclastiye (olive))
027	120	110	60	0.3	600	0~60	Mangan nodule (core : hyaloclastiye (olive))
028	110	90	60	0.35	500	10~20	Mangan crust
029	150	80	50	0.2	600	1~50	Mangan crust (core :hyaloclastite (olive))
030	110	100	80	0.4	800	5~20	Mangan crust (core :hyaloclastite (olive))
031	130	90	80	0.5	800	0~15	Mangan nodule (core:non)
032	130	90	50	0.2	500	0~30	Mangan crust (core :hyaloclastite (olive))
033	100	80	70	0.3	460	0~15	Mangan crust
034	80	70	60	0.4	320	20~30	"
035	120	120	60	0.3	800	30~40	"
036	110	80	70	0.5	500	0~50	"
037	110	90	50	0.3	500	0~50	"
038	140	90	40	0.15	500	0~40	"
039	110	90	40	0.3	400	0~10	"
040	140	110	60	0.2	500	5~80	"
041	110	100	40	0.35	500	0~40	"
042	140	80	60	0.3	450	0~80	"
043	120	70	60	0.2	400	1~20	Mangan crust (core :hyaloclastite (olive))
044	80	80	60	0.2	300	1~30	Mangan crust (core :hyaloclastite (olive))

Sample No.	Diameter (mm) L	M	S	Round-ness	Wt(g)	Mn-coating (mm)	Lithology & Remarks
D3-045	80	60	50	0.4	300	5~50	Mangan crust
046	100	80	70	0.3	450	1~30	Mangan crust (core :hyaloclastite (olive))
047	100	60	40	0.4	300	0~40	Mangan crust
048	70	60	50	0.1	200	0~35	"
049	100	100	30	0.3	250	0~30	"
050	90	80	60	0.2	400	1~40	Mangan crust (core :hyaloclastite (olive))
051	80	80	30	0.3	200	0~30	Mangan crust
052	130	80	50	0.25	400	0~30	"
053	90	60	40	0.3	250	0~40	"
054	90	60	60	0.4	330	0~6	"
055	90	80	40	0.25	300	0~30	"
056	100	90	40	0.3	420	0~40	"
057	80	70	50	0.1	180	10~30	Mangan crust (core :hyaloclastite (olive))
058	120	100	30	0.1	340	0~25	Mangan crust
059	90	70	40	0.5	220	0~25	Mangan nodule
060	90	80	60	0.3	450	0~40	"
061	110	70	50	0.6	380	0~30	"
062	70	60	50	0.3	260	0~25	Mangan crust
063	100	80	60	0.15	460	0~50	"
064	100	90	40	0.2	330	0~40	"
065	80	80	50	0.2	280	0~30	Mangan crust (core :hyaloclastite (olive))
066	80	80	70	0.3	300	0~50	Mangan crust
067	90	80	60	0.25	400	0~30	Mangan crust (core :hyaloclastite (olive))
068	70	70	70	0.35	300	5~20	Mangan nodule (core : hyaloclastiye (olive))
069	80	80	70	0.6	420	0~30	Mangan crust
070	90	80	60	0.2	320	0~50	"
071	120	90	30	0.1	220	0~25	"
072	110	80	60	0.1	200	4~08	"
073	130	80	40	0.3	400	5~40	"
074	120	80	30	0.3	300	0~30	"
075	80	70	60	0.4	320	0~25	"
076	100	80	30	0.25	270	0~30	"
077	100	90	20	0.2	290	0~20	"
078	130	70	20	0.15	300	0~20	"
079	90	70	40	0.25	280	0~40	"
080	60	40	40	0.6	120	0~20	Mangan nodule
081	80	50	40	0.3	180	0~35	Mangan crust (core :hyaloclastite (olive))
082	80	40	40	0.15	140	0~40	"
083	70	60	50	0.3	150	0~55	Mangan crust
084	70	60	40	0.45	140	0~20	Mangan nodule
085	120	60	50	0.15	350	0~50	Mangan crust
086	100	50	40	0.4	180	0~20	Mangan nodule
087	90	60	50	0.35	250	0~25	"
088	80	50	50	0.2	170	0~20	Mangan crust
089	80	70	40	0.2	180	0~30	Mangan crust (core :hyaloclastite (olive))
090	80	40	40	0.2	150	0~10	Mangan crust
091	90	60	50	0.4	300	0~60	"

Sample No.	Diameter (mm) L	M	S	Round-ness	Wt(g)	Mn-coating (mm)	Lithology & Remarks
D3-092	70	60	40	0.2	100	0~30	Mangan crust
093	70	40	30	0.4	100	0~20	Mangan nodule (core : hyaloclastiye (olive))
094	80	70	30	0.2	150	0~30	Mangan crust
095	70	70	40	0.3	170	0~40	"
096	80	70	50	0.25	270	0~50	"
097	80	70	40	0.35	200	0~35	"
098	90	80	30	0.3	250	0~15	"
099	70	70	30	0.3	200	0~30	"
100	70	70	60	0.25	220	0~30	"
101	90	70	40	0.35	250	0~40	Mangan nodule
102	70	60	50	0.45	180	0~25	"
201	200	140	140	0.5	4800	filmy	Ice rafted andesite
202	160	100	70	0.4	360	None	Pumice
203	200	80	60	0.2	1700	filmy	Ice rafted dacite
204	180	130	50	0.3	1080	0~8	Hyaloclastite (olive)
205	180	160	70	0.6	1520	filmy	Ice rafted basalt
206	180	110	40	0.3	940	0~3	Hyaloclastite (olive)
207	140	90	60	0.5	1080	filmy	Ice rafted granite
208	140	80	40	0.2	220	0~0	Sandstone
209	90	80	60	0.4	480	filmy	Ice rafted dacite
210	100	80	40	0.6	160	1~2	Pumice
211	80	80	30	0.3	280	0~1	Hyaloclastite (olive)
212	80	80	50	0.4	210	0~1	Ice rafted andesite
213	100	70	50	0.3	110	0~1	Pumice
214	110	80	50	0.3	400	0~2	Congromerate phosphorite
215	90	70	40	0.5	320	0~0	Ice rafted andesite
216	80	60	30	0.3	190	0~1	Hyaloclastite (olive)
217	70	70	60	0.4	90	1~3	Pumice
218	70	60	40	0.3	160	1~2	Ice rafted andesite
219	60	60	60	0.3	80	filmy	Pumice
220	90	60	40	0.3	240	0~1	Hyaloclastite (olive)
221	90	70	40	0.3	75	filmy	Pumice
222	90	70	50	0.2	250	0~20	Hyaloclastite (olive)
223	90	50	50	0.2	240	0~30	Mn-crust
224	90	60	40	0.25	270	0~15	Mangan nodule (core:phosphorite)
225	80	70	50	0.4	300	0~40	Mangan crust
226	90	80	60	0.3	310	0~25	Mangan nodule (core:lava)
227	70	60	40	0.3	180	0~15	Mangan crust
228	80	70	20	0.2	60	filmy	Sandstone
229	90	90	30	0.3	300	0~2	Hyaloclastite (olive)
230	90	80	30	0.1	50	filmy	Sponge
231	90	80	40	0.1	60	filmy	"
232	80	70	50	0.4	240	2~20	Mangan nodule (core:hyaloclastite)
233	100	80	20	0.2	300	0~20	Mangan crust
234	80	80	40	0.3	250	10~15	"
235	90	80	40	0.35	300	0~20	"
236	110	80	40	0.35	300	0~20	"

Sample No.	Diameter (mm) L	M	S	Round-ness	Wt(g)	Mn-coating (mm)	Lithology & Remarks
D3-237	80	70	40	0.3	60	filmy	Pumice
238	70	40	30	0.6	20	filmy	"
239	70	60	60	0.35	150	0～40	Mangan crust
240	100	50	30	0.2	200	0～10	Hyaloclastite (olive)
241	70	60	30	0.2	50	0～1	Scoria
242	90	70	40	0.3	200	20～40	Mangan crust
243	70	60	50	0.4	100	0～2	Scoria
244	60	60	40	0.4	130	filmy	Lava andecite
245	60	60	50	0.5	240	filmy	"
246	70	60	40	0.3	40	filmy	Pumice
247	80	40	30	0.2	100	0～4	Mangan nodule (core:non)
248	80	70	40	0.2	240	0～4	Hyaloclastite (olive)
249	90	70	50	0.4	230	25～40	Mangan crust
250	60	40	30	0.2	80	0～20	"
251	90	70	30	0.1	200	0～30	"
252	120	90	30	0.1	300	20～30	"
253	80	50	50	0.3	150	20～40	"
254	80	70	50	0.3	240	0～8	Hyaloclastite (olive)
401	470	370	110	0.1	30000	0～10	Conglomerate
501	380	200	150	0.2	10200	0～80	Mangan nodule (core:non)
502	240	180	170	0.3	8700	1～20	Mangan crust (core:hyaloclastite (olive))
503	420	380	140	0.2	18000	1～50	Mangan crust
504	260	180	140	0.4	7000	0～90	Mangan nodule (core:hyaloclastite)
601					2260		Sedimentary fragments
602					1130		"
603					22000		"
604					13500		"

19. Collection of Megabenthos and Macrobenthos with a Beam Trawl

S. Ohta, Dong Sung Kim and T. Ishii

Megabenthos and macrobenthos of abyssal zone were collected at 2 stations using a small Sigsby-Agassiz type beam trawl of 2 m span in the northwestern Pacific (Stations TR-l and TR-2) (see Table 19-1). Both stations were located on the landward trench flank of abyssal zone around 4,500m deep near the mouth of the Kushiro Submarine Canyon pouring into the Kuril Trench. Station TR-l was situated on an anticlinic high expecting errosive environment, whereas Station TR-2 was established at the foot of rather steep slope expecting thick soft sediment.

The main purpose was to collect benthic organisms associated with chemosynthetic symbionts such as pogonophorans and vestimentiferans, and bivalves such as vesicomyids (*Calyptogena, Vesicomya* etc.) and solemyid (*Acharax, Solemya* etc.). However, the main objective was not realized except the catches of dead shells of *Acharax*.

The Sigsby-Agassiz beam trawl was towed with #l wire winch attaching additional thick chains and 150 kg weights in front of the mouth bridle. The net of the trawl was constructed from knotless synthetic webbing of 48 mm stretched mesh, and were furnished with inner liners of 4mm square mesh in the codends to retain smaller organisms. Towing velocity was maintained between 1 and 2 knots. The duration on the bottom was set about one hour, if otherwise permitted. Fixing the mouth span of the net by two beams, well-operated standard towing affords semiquantitative information of the bottom fauna. Comparing the bottom observations with DESMOS within the same habitat, complete faunal composition and catching efficiency of the beam trawl for each life-style can be estimated afterwards.

Catches were washed on 1.0 mm mesh sieve, sorted out on board, identified preliminarily, counted and fixed in 10% seawater formalin buffered with sodium borate. Later the fixed sample were transferred into and preserved in 70% ethanol. A part of the sample were store in a deep freezer and in liquid nitrogen for physiological and analytical purposes, and several bivalve species were fixed in TEM preservative for the observation of symbiotic bacteria.

The samples should be utilized for morphological and taxonomical studies, bathymetrical and zoogeographical distribution analysis, species composition analysis, size and age structure analysis, reproductive ecology, food chain analysis and physiological studies.

Table 19-1. List of operations of 2 m Sigsby-Agassiz beam trawl.

Station TR-1
Location: SSW off Kushiro, NW Pacific
Date and time of operation: 12:30~16:50, August 3,1992 [JST]
On bottom: 13:50 41° 53.95'N; 145°10.92'E D = 4,126m [wireout 4,400m]
Bottom tow: 14:12~15:12 1.0~2.0knots [wireout 5,600m; wire angle 20-35°]
Off bottom: 15:31 41° 52.31'N; 145°08.83'E D = 4,159m [wireout 5,040m]
Overall depth range: 4,084~4,409m

Station TR-2
Location: SSW off Kushiro, NW Pacific
Date and time of operation: 10:17~14:30, August 4,1992 [JST]
On bottom ~ 11:57 41° 43.46'N; 144°53.63'E D = 4,704m [wireout 5,100m]
Bottom tow: 12:10~13:10 1.0~2.0 knots [wireout 5,800m; wire angle 20~35°
Off bottom: 13:10 41°43.46'N; 144°53.63'E D = 4,744m [wireout 5,800m]
Overall depth range: 4,671~4,775m

20. Test of a Personal GPS Receiver for Navigation

T. Tanaka, Y. Kono, and T. Kudo

Introduction

GPS (Global Positioning System) observations were carried out using a point positioning receiver named "GPS RECEIVER" made by HAL Corp. (hardware is made by SONY Corp.) during leg 2 of Hakuho Maru cruise KH 92-3. Aim of the observations is to evaluate the basic performance of personal GPS receivers.

Observation system

The GPS antenna was set up on the top deck of port side. The distance from the antenna owned by ERI("GPS CORE") is about 1 m, but almost the same height. The "GPS CORE" is manufactured by SONY Corp. too but with different software. Received data were recorded in floppy disk through RS-232C cable and processed using personal computer and software offered from the manufacture.

Results

Data analysis was carried out comparing positioning data acquired by the "GPS RECEIVER" and the "GPS CORE". Fig. 20-1 shows plots of data from about 01:30 to 11:10 in August 2, 1992. Ordinate and abscissa indicate latitude and longitude, respectively. Time in Fig. 20-1 is JST. Sampling interval is about 1 min for "GPS RECEIVER" and about 15sec for "GPS CORE". Total numbers are 611 and 2293, respectively. As shown in Fig. 20-1, data of "GPS RECEIVER" have swing broadly in the direction of longitude. The deflection reached about 1km. On the other hand, "GPS CORE"'s were displayed smoothly.

Fig. 20-2 is magnified plot of a small rectangular part of Fig. 20-1. This shows datum of "GPS RECEIVER" jumped significantly in the vicinity of Lat. 42.635.

Summary

It was proved that "GPS RECEIVER" did not offer sufficient accuracy compared with "GPS CORE". There are, however, no significant differences between two receivers in their specifications. We inquired these results to HAL Corp. after the cruise. They replied that some bugs were found in a coordinates transformation subroutine program.

From our experiments mentioned above, it may be necessary to point out importance of tests before to employ personal GPS receiver systems for navigation positioning.

Acknowledgment

We wish to thank Yukari Nakasa for offering comparative data and Jun Korenaga for assisting to construct Figs. 20-1, and 20-2.

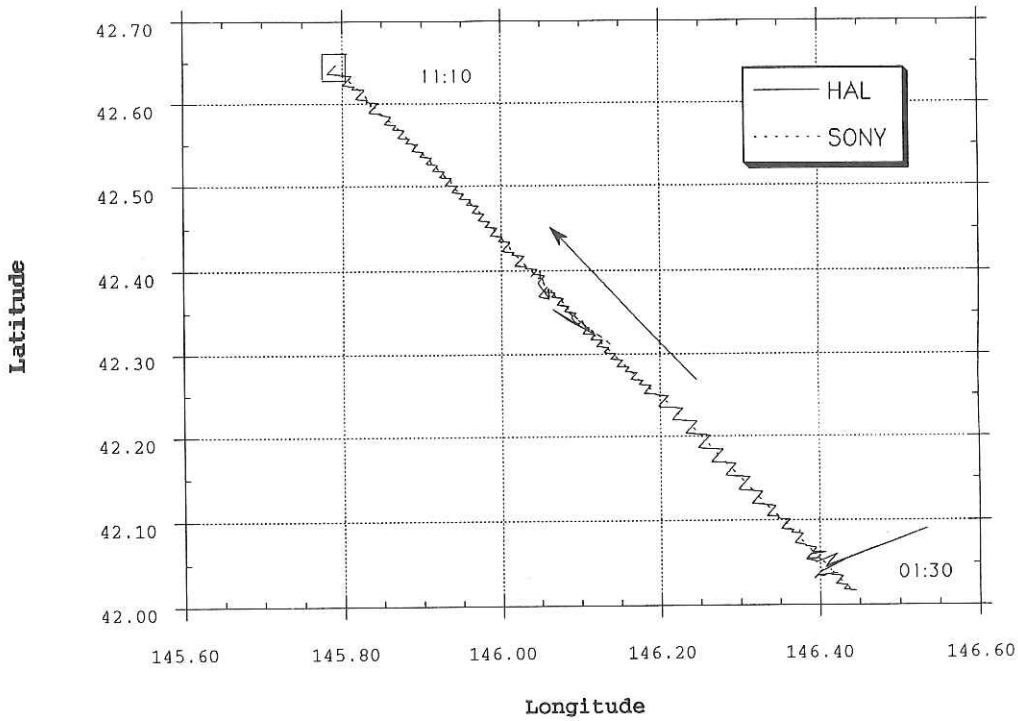

Fig. 20-1. Plots of data from two receivers.

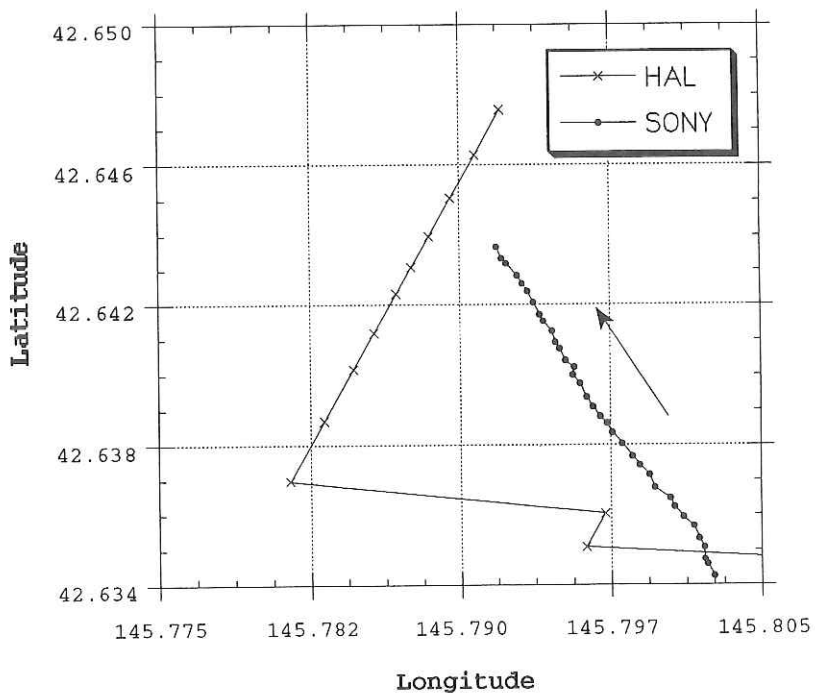

Fig. 20-2. Magnified plots of data for a small rectangular in the upper left corner of Fig. 20-1.

21. Collection of Acoustic Backscattering Wave Level Data from the Sea Bottom in Sea Beam Survey in the Kuril Trench

T. Takeuchi and K. Ogura

In order to develop a software for making the sea bed characteristics map based upon the developed algorithm (Takeuchi et *al.*, 1992) for the classification of sea bed characteristics, acoustic backscattering wave levels from the sea bottom were recorded in 19 cassette tapes by using digital recording system in Sea Beam survey in the Kuril Trench during KH 92-3 research cruise. Fig. 21-1 shows the schematic diagram of the recording system. DAT has 8 recording channels of frequency bandwidth between 0 and 5 kHz, and it can record 8 backscattering wave levels from sea bottom corresponding to each of 8 narrow beams of port or starboard of which each grazing angle is from 68.34° to 90° at the interval of 2.66°.

An example of recorded backscattering wave levels is shown in Fig. 21-2. The lines of Sea Beam survey including acoustic backscattering level records are shown in Fig. 21-3. We can obtain the backscattering intensities from these levels and can also obtain backscattering intensities from the sea bottom in all area where Sea Beam survey was conducted in the Kuril Trench as a reference of them from relative backscattering levels which are memorized corresponding to 16 beams of port-side and starboard in Sea Beam system.

Sound velocity and acoustic ray path are determined due to computation based upon the water temperature profile measured with XBT. The measured water temperature profile and the corresponding computed sound velocity profile are shown in Fig. 21-4. Table 21-1 shows D-T and T-D diagram. Surface water temperature is 19.49°C, and water temperature decreases rapidly as water depth increases and reaches smaller than 5°C within the depth of 100 m. Only thin mixed layer is observed in surface several meters although in summer. Fig. 21-5 shows acoustic ray path when source emitted at water surface. It is a straight line and there is no bending.

Reference

Takeuchi, T., Hirari Mehrez, S. Tsukioka and Y. Nagai, Seafloor characteristics and roughness using Sea Beam (in Japanese with English abstr.), *J. Jpn. Soc. Mar. Surv. Tech..*, **4**, 19-28, 1992.

Table 21-1. D-T and T-D table based on a water temperature profile measured with XBT.

D - T TABLE		T - D TABLE		STATION : KH92-S2			
D(m)	T(°C)	T(°C)	D(m)				
1.0	19.49	17.0	5.4				
10.0	16.89	16.0	17.4				
20.0	12.07	15.0	18.1				
40.0	8.17	14.0	18.5				
60.0	4.99	13.0	19.1				
80.0	2.19	12.0	20.5				
100.0	1.85	11.0	23.5				
120.0	2.25	10.0	26.5				
140.0	1.67	9.0	29.2				
160.0	1.71	8.0	35.2	42.2			
180.0	2.36	7.0	50.2				
200.0	1.89	6.0	53.9				
250.0	2.17	5.0	60.2				
300.0	2.59	4.0	68.9				
350.0	2.63	3.0	72.9	424.2	824.3		
400.0	2.75	2.0	82.2	102.2	122.7	171.0	206.1
450.0	3.25						
500.0	3.08						
550.0	3.06						
600.0	3.18						
650.0	3.22						
700.0	3.13						
750.0	3.08						
800.0	3.03						
850.0	2.96						
900.0	2.94						
950.0	2.86						
1000.0	2.80						
1050.0	2.71						
1100.0	2.63						
1150.0	2.59						
1200.0	2.52						
1250.0	2.49						
1300.0	2.43						
1350.0	2.40						
1400.0	2.37						
1450.0	2.35						
1500.0	2.32						
1550.0	2.26						
1600.0	2.22						
1650.0	2.20						

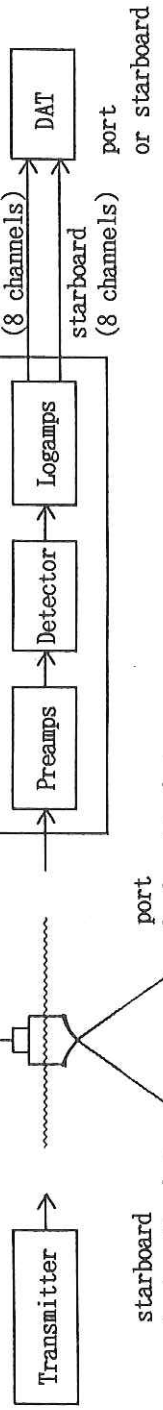

Fig. 21-1. Schematic diagram for recording acoustic backscattering waveforms.

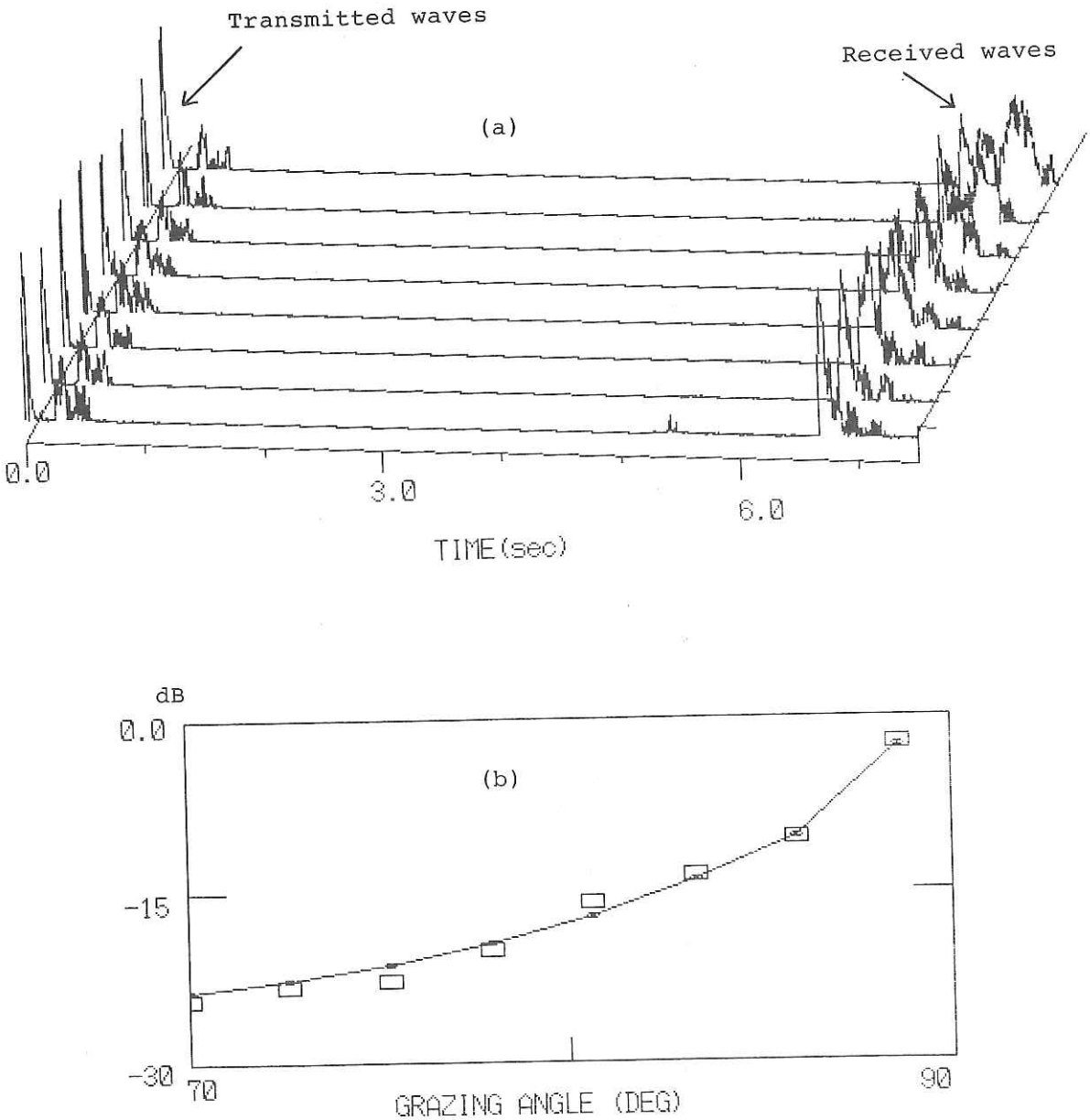

Fig. 21-2. An example of recorded backscattering wave levels.
(a) Example of transmitted and received waves of SEA BEAM.
(b) Estimated backscattering strength of a site (42°13.0'N; 146°4.3'E). Parameters are ρ = 1.48, μ = 1.01, and slope = 3.14, where sea bottom material is sandy silt and roughness is 3.3 cm.

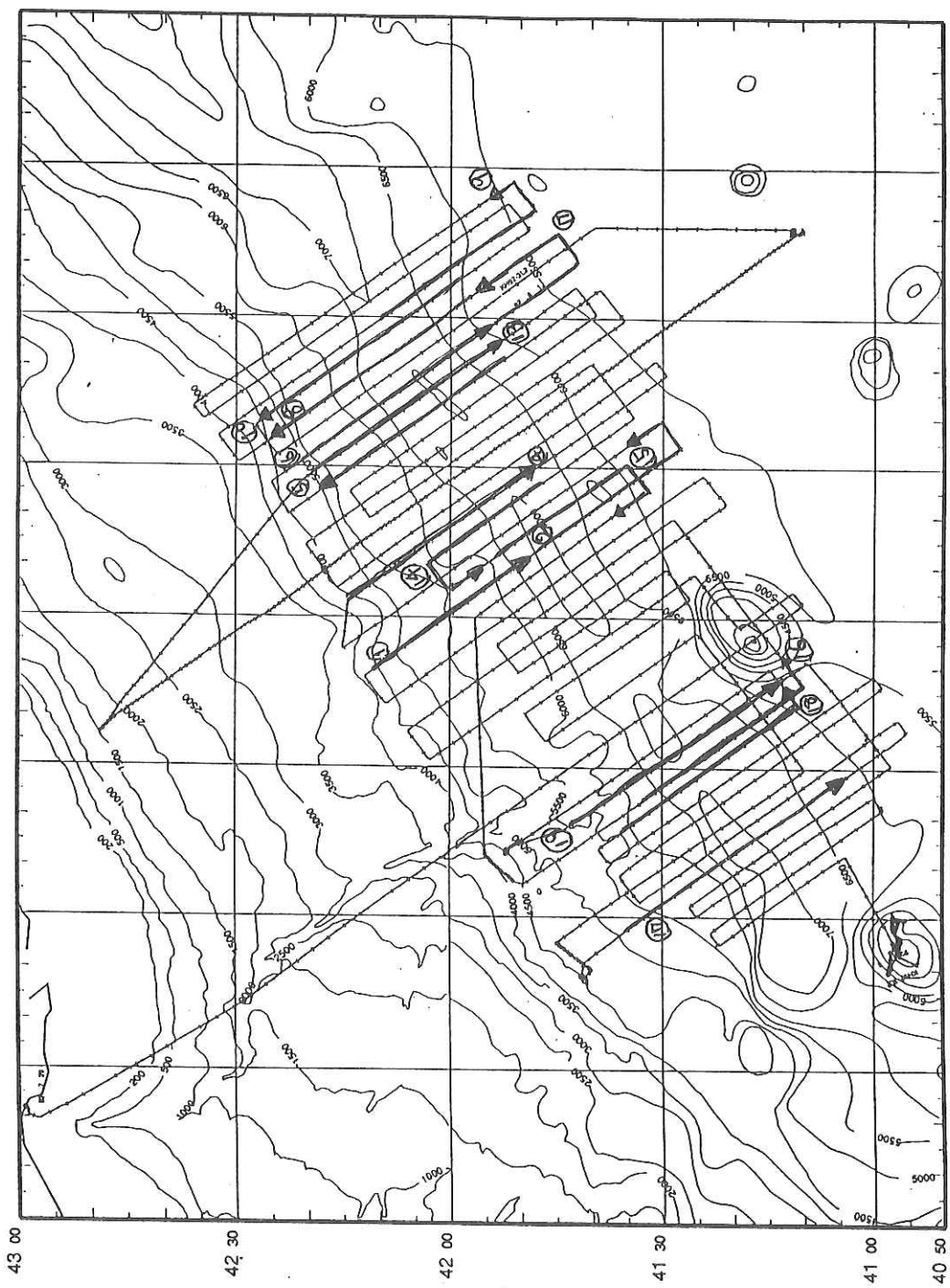

Fig. 21-3. Location of acoustic backscattering wave level record (thick arrow lines).

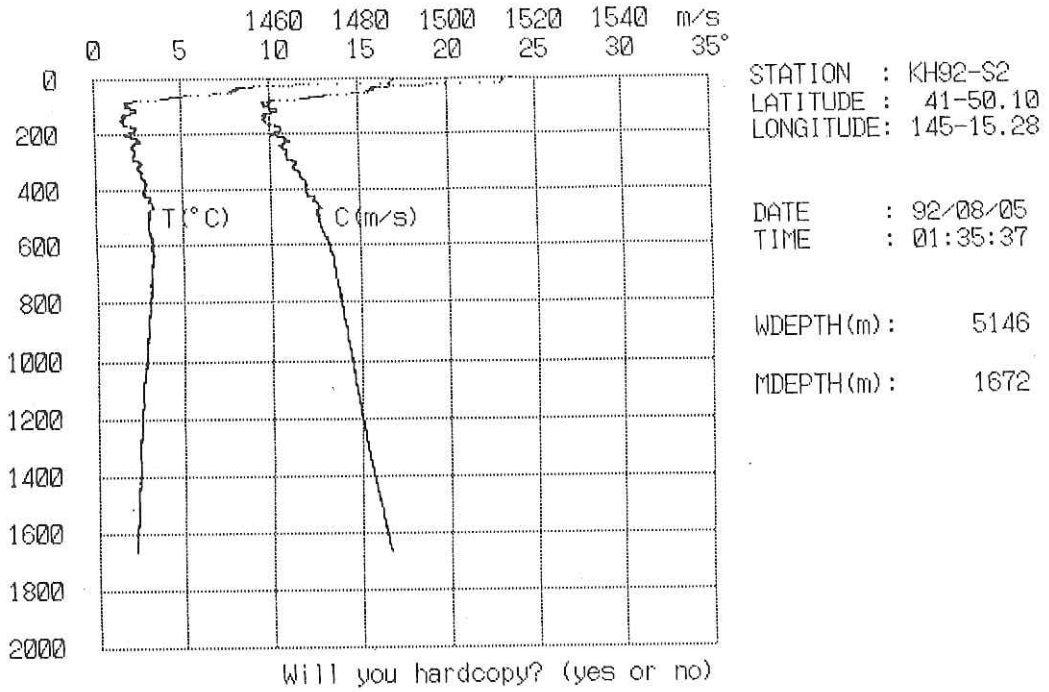

Fig. 21-4. Profiles of water temperature measured with XBT and computed sound velocity.

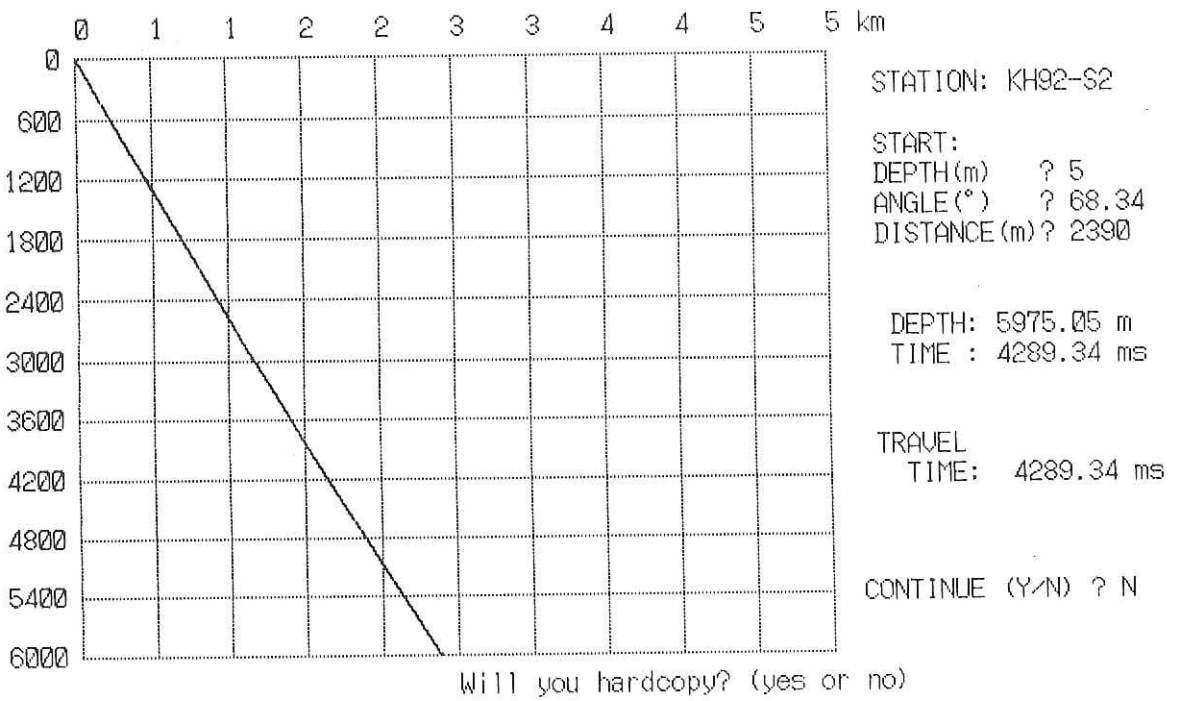

Fig. 21-5. Acoustic ray path computed based upon water temperature profile meausured with XBT.

22. SSBL Navigation in KH 92-3 Cruise Leg 2

T. Furuta, M. Nakanishi and M. Watanabe

An acoustic transponder navigation system is very useful for precise position fixing of a ship and underwater equipments and/or vehicles. Two different acoustic navigation systems have been accommodated on the Hakuho Maru: super short baseline (SSBL) and long baseline (LBL). The SSBL system is utilized in the following two modes; one is to carry out precise ship's navigation when more than one acoustic source is deployed on the seafloor, and the other is to determine position of the underwater target when one acoustic transponder is installed on a deep-towed system. These two modes can be, of course, operated simultaneously. During Leg 2 of KH 92-3 cruise, navigation of DESMOS and dredge was carried out by the SSBL system, since SSBL is very convenient for three-dimensinally determining positions of underwater equipments with no acoustic source moored on the seafloor.

On practical operation during this cruise, the scale of the Sea Beam map which was produced by the previous site survey was adapted to that of A3-size X-Y graphic recorder which is interfaced with SSBL shipboard unit. Every target positions obtained by the SSBL were plotted on this map. The position acquisitions for DESMOS were performed successfully with very fantastic results through the SSBL aid operation.

During the DESMOS surveys, an acoustic transponder installed on the DESMOS frame was set on 13.5 kHz or 14 kHz of transmition frequency. When it received interrogating command fed from the shipboard unit, it returned a response signal on every interrogation. The interrogating interval was selected on the shipboard unit, usually 4 to 16 seconds (3,000 m to 12,000 m of slant range). When the shipboard unit received a response signal from the DESMOS, it showed the direction (either absolute or relative), horizontal distance and slant range on CRT, and positions on graphic displays (color CRT and A3-size X-Y graphic recorder).

Finally we estimate that the accuracy of position of deep-towed equipments is better than one percent of the slant range. The accuracy is satisfied for navigation and operation of deep-towed equipments for specific submarine exploration.

23. STATION AND WORK LOG
IN THE R. V. HAKUHO MARU CRUISE KH 92-3

Leg 1: Tokyo (July 17) to Kushiro (July 25) [JST = GMT + 8]

Day (GMT) M D	Time HrMin	Position Latitude	Longitude	Water Depth (m)	Head-ing (deg)	Log Speed (kt)	System Dir. (deg)	Vel. (kt)	Works
0717	0434	35°38.60N	139°46.50E	n.d.	140	0.1	270	0.0	Pilot On Board
0717	0455	35°38.58N	139°46.49E	n.d.	56	0.1	250	0.1	Slow Ahead ENG
0717	0455	35°38.58N	139°46.49E	n.d.	157	0.1	250	0.1	Retr.Anchor **Lv. Harumi**
0717	0457	35°38.53N	139°46.48E	n.d.	212	3.9	187	0.2	Half Ahead ENG
0717	0458	35°38.45N	139°46.45E	n.d.	217	7.7	192	0.6	Full Ahead ENG
0717	0517	35°35.25N	139°47.31E	n.d.	130	11.8	158	9.8	Slow Ahead ENG
0717	0520	35°35.01N	139°47.67E	n.d.	127	4.1	150	9.8	Pilot Left Ship
0717	0523	35°34.91N	139°47.83E	n.d.	130	3.8	147	7.9	Tandem Motion
0717	0525	35°34.82N	139°47.96E	n.d.	130	6.0	145	6.9	Half Ahead ENG
0717	0529	35°34.51N	139°48.41E	n.d.	134	10.9	139	6.9	Full Ahead ENG
0717	0622	35°24.46N	139°43.58E	n.d.	225	17.1	232	15.6	a/co to 208°
0717	0629	35°22.87N	139°42.53E	n.d.	185	16.4	219	15.4	a/co to 177°
0717	0641	35°19.84N	139°42.75E	n.d.	159	15.1	186	15.0	Full Ahead ENG
0717	0642	35°19.61N	139°42.85E	n.d.	154	13.2	184	14.8	in Uraga Suido Traffic Rt
0717	0722	35°12.80N	139°46.27E	n.d.	180	14.8	174	11.9	out of Uraga Suido Traffic
0717	0724	35°12.32N	139°46.13E	n.d.	202	16.2	178	12.3	Run-up ENG
0717	0724	35°12.27N	139°46.11E	n.d.	202	16.4	178	12.3	set/co on 202°
0717	0931	34°39.70N	139°30.10E	857	218	14.8	204	17.0	a/co to 245°
0717	1014	34°34.91N	139°16.39E	121	241	16.1	249	17.0	Half Ahead ENG
0717	1019	34°34.64N	139°15.65E	332	241	4.0	248	13.8	**Start Proton Mag Survey**
0717	1032	34°33.70N	139°13.13E	448	241	15.4	245	12.2	Run-up ENG
0717	1116	34°28.22N	138°59.98E	677	243	16.7	245	16.4	a/co to 242°Nankai Trough
0717	1333	34°10.39N	138°19.93E	2243	241	16.2	238	16.5	a/co to 247° Upper Slope
0717	1344	34°09.22N	138°16.76E	1195	247	16.5	244	16.4	a/co to 243° Survey
0717	1420	34°04.82N	138°06.35E	2437	260	16.1	243	16.2	a/co to 259°
0717	1548	34°00.10N	137°37.41E	1997	258	16.5	259	16.2	a/co to 169°
0717	1556	33°58.32N	137°37.60E	1842	166	15.5	209	11.4	a/co to 79°
0717	1632	33°59.93N	137°49.08E	1359	077	15.7	079	15.7	a/co to 349°
0717	1647	34°03.63N	137°48.46E	821	350	16.1	001	13.3	a/co to 259°
0717	1725	34°02.00N	137°36.55E	1945	247	15.8	260	15.7	a/co to 140°
0717	1906	33°41.03N	137°57.07E	3708	141	15.3	138	16.5	Half Ahead ENG
0717	1911	33°40.51N	137°57.67E	3820	148	3.7	137	12.0	**End Proton Mag Survey**
0717	1937	33°39.95N	137°58.05E	3903	185	0.7	178	1.7	**End Launch OBS-3**
0717	1954	33°41.33N	137°57.34E	3700	320	15.9	327	7.1	Run-up ENG
0717	2042	33°52.75N	137°49.10E	2498	331	16.4	331	16.6	Half Ahead ENG
0717	2047	33°53.27N	137°48.88E	2433	337	0.7	333	12.5	**End Launch OBS-2**
0717	2104	33°54.92N	137°47.63E	2454	330	15.3	328	9.8	Run-up ENG
0717	2150	34°05.59N	137°40.19E	1155	332	16.5	328	15.8	Half Ahead ENG
0717	2155	34°06.00N	137°40.02E	1178	300	0.6	331	11.2	**End Launch OBS -1**
0717	2259	33°57.41N	137°46.85E	1676	182	0.8	150	11.7	Stop ENG
0717	2302	33°57.38N	137°46.93E	1679	138	0.4	149	8.3	Prop to Electric Motors
0718	0011	34°00.80N	137°42.57E	1302	229	0.2	265	2.8	**Start DESMOS-1. 1**
0718	0012	34°00.80N	137°42.59E	1305	230	0.2	263	2.4	Lowering DESMOS
0718	0035	34°01.06N	137°43.24E	1222	229	0.0	059	1.4	Lowering DESMOS
0718	0107	34°00.87N	137°43.19E	1308	236	1.0	214	1.1	**DESMOS Near Bottom**
0718	0331	34°00.44N	137°44.01E	1348	212	0.6	135	0.9	End DESMOS-1.1
0718	0350	34°00.40N	137°43.21E	1388	268	6.5	273	3.4	Start Boat Drill
0718	0408	34°00.26N	137°42.49E	1406	221	0.2	253	0.8	**Start DESMOS-1. 2**
0718	0420	34°00.39N	137°42.73E	1385	147	0.0	045	0.7	End Boat Drill
0718	0440	34°00.67N	137°42.99E	1322	115	0.0	041	1.0	**DESMOS Near Bottom**

Day (GMT) M D	Time HrMin	Position Latitude	Longitude	Water Depth (m)	Head-ing (deg)	Log Speed (kt)	System Dir. (deg)	Vel. (kt)	Works
0718	0522	34°01.13N:	137°43.20E	1202	122	0.0	022	0.7	Adjust DESMOS Position
0718	0601	34°01.52N:	137°43.26E	1107	118	0.0	012	0.6	DESMOS Lv Bottom
0718	0624	34°01.37N:	137°43.49E	1108	228	0.0	146	0.8	DESMOS-1. 2 On Deck
0718	0637	34°01.28N:	137°43.74E	1152	136	0.1	114	0.9	Start Electric Prop.
0718	0640	34°01.18N:	137°43.91E	1204	159	5.1	119	1.6	s/co on 150°
0718	0657	33°58.40N:	137°45.91E	1458	149	14.8	149	11.2	Run-up ENG
0718	1019	33°09.55N:	138°18.69E	3935	311	1.1	152	15.1	Stop ENG
0718	1023	33°09.56N:	138°18.99E	3918	338	0.7	145	9.9	Prop to Electric Motors
0718	1050	33°09.79N:	138°19.27E	3907	287	1.6	330	0.4	Launch Streamer Cable
0718	1202	33°10.87N:	138°19.16E	3931	275	4.0	336	0.6	Start Water-Gun
0718	1638	33°15.14N:	138°14.96E	4018	294	5.4	335	2.2	Hove up Water-Gun
0718	1806	33°18.76N:	138°12.44E	4040	295	5.2	328	2.8	Start Air-Gun
0718	1810	33°18.89N:	138°12.31E	4039	298	5.0	324	3.0	**Start Seismic Profiling**
0719	0400	33°59.64N:	137°45.29E	1327	327	5.5	330	4.7	Com'ced Fire Drill
0719	0430	34°01.84N:	137°43.83E	1037	324	5.4	330	5.0	Finish Fire DrillL
0719	0742	34°15.18N:	137°36.28E	1532	101	4.8	076	3.6	a/co to 090° at 16:26JST
0719	0904	34°15.06N:	137°44.38E	976	097	5.2	091	5.2	a/co to 143°
0719	1439	33°53.38N:	138°04.38E	3411	128	4.8	144	4.5	Change Air Gun, ENG var.
0719	1448	33°52.95N:	138°04.79E	3576	126	4.9	143	3.8	Set Speed 5kt
0719	1455	33°52.53N:	138°05.20E	3583	126	5.3	143	4.2	Set Air Gun Again
0719	2153	33°25.00N:	138°30.01E	3516	159	5.1	147	5.8	**End Seismic Profiling**
0719	2211	33°23.41N:	138°31.07E	3455	161	4.0	150	5.8	End AIR-GUN
0719	2307	33°22.14N:	138°31.60E	3348	216	0.5	146	1.3	Retrieve Streamer Cable
0719	2309	33°22.09N:	138°31.61E	3360	213	0.4	151	1.3	Prop to Diesel ENG
0719	2309	33°22.09N:	138°31.61E	3351	212	0.4	151	1.3	Slow Ahead ENG
0719	2313	33°21.95N:	138°31.45E	3431	250	6.1	191	1.5	s/co on 251°
0719	2317	33°21.81N:	138°31.12E	3559	253	5.9	227	2.5	Start Proton Mag Survey
0719	2327	33°21.18N:	138°28.92E	3725	254	16.4	250	9.1	Run-up ENG.
0720	0400	33°01.34N:	137°18.25E	4158	254	16.4	252	14.5	Com'ced Leak Drill
0720	0430	32°58.99N:	137°09.97E	4228	254	16.5	251	14.9	Finish Leak Drill
0720	1152	32°21.11N:	134°56.67E	4673	264	15.5	251	17.0	a/co to 270°
0720	1156	32°21.07N:	134°55.58E	4578	270	16.7	256	16.8	Slow Ahead ENG
0720	1204	32°21.06N:	134°54.40E	4549	278	2.8	261	10.1	End Proton Survey
0720	1216	32°21.17N:	134°53.29E	4482	283	0.7	271	5.9	Stop ENG
0720	1221	32°21.16N:	134°53.27E	4477	298	0.3	270	3.3	Start Transponder Test
0720	1222	32°21.16N:	134°53.27E	4477	298	0.3	270	2.9	Prop to Electric Motors
0720	1251	32°21.02N:	134°54.76E	3838	125	1.7	104	3.9	End Launch Transponders
0720	1418	32°23.20N:	134°55.27E	4522	326	0.3	049	0.7	Transponders on Bottom
0720	1425	32°23.21N:	134°55.34E	4520	329	0.3	068	0.6	Fix Transponder positions
0720	1524	32°19.97N:	134°52.92E	4528	175	0.0	179	0.3	Fix Transponder positions
0720	1611	32°19.97N:	134°56.81E	4747	135	0.2	087	1.3	Fix Transponder positions
0720	1642	32°21.12N:	134°56.65E	4664	024	0.3	002	1.4	**Start DESMOS-2**
0720	1827	32°21.06N:	134°56.55E	4660	039	0.0	181	0.3	**DESMOS Near Bottom**
0721	0153	32°20.51N:	134°56.82E	4739	359	0.1	180	1.7	DESMOS Leave Bottom
0721	0313	32°20.53N:	134°57.90E	4754	214	0.0	049	1.4	Release Transponder
0721	0322	32°20.52N:	134°58.04E	4769	214	0.0	074	0.9	DESMOS on Deck
0721	0328	32°20.51N:	134°58.16E	4772	208	0.0	085	0.9	Prop to Diesel ENG
0721	0331	32°20.50N:	134°58.19E	4778	216	2.3	092	0.9	Course Variable
0721	0347	32°20.84N:	134°55.61E	4617	282	9.9	281	7.2	Transponder coming-up
0721	0358	32°21.09N:	134°55.12E	4543	008	0.7	296	3.3	End Retrieve Transponders

Day (GMT) M D	Time HrMin	Position Latitude	Longitude	Water Depth (m)	Head-ing (deg)	Log Speed (kt)	System Dir. (deg)	Vel. (kt)	Works
0721	0415	32°21.15N:	134°55.41E	4541	343	0.9	045	0.5	Slow Ahead ENG
0721	0420	32°21.34N:	134°55.71E	4555	062	5.8	052	1.9	Start Proton Mag Survey
0721	0421	32°21.39N:	134°55.84E	4575	062	6.8	056	2.4	s/co on 63°
0721	0445	32°23.58N:	135°00.85E	4781	061	9.8	063	12.0	∞-Shape Rotation R-Turn
0721	0500	32°23.60N:	135°01.25E	4793	061	9.0	030	3.6	∞-Shape Rotation L-Turn
0721	0517	32°23.70N:	135°01.99E	4790	062	12.5	089	4.6	s/co on 63°
0721	0525	32°24.59N:	135°04.09E	4784	061	16.4	067	11.3	Run-up ENG
0721	1430	33°39.41N:	137°56.67E	3849	062	16.8	063	15.1	Slow Ahead ENG
0721	1437	33°39.68N:	137°57.36E	3904	064	2.4	063	9.8	End Proton Mag Survey
0721	1443	33°39.91N:	137°57.91E	3905	161	0.7	064	7.5	Stop ENG
0721	1448	33°39.92N:	137°57.91E	3906	140	0.3	063	4.0	Release OBS-3
0721	1608	33°40.04N:	137°57.43E	3896	115	1.7	320	0.3	Com'ced Shifting
0721	1614	33°39.98N:	137°57.88E	3914	124	0.8	094	1.9	OBS-3 coming up
0721	1634	33°40.02N:	137°57.78E	3930	305	0.5	326	0.5	End Retrieve OBS-3
0721	1638	33°40.04N:	137°57.77E	3931	316	1.0	349	0.3	Slow Ahead ENG
0721	1656	33°42.64N:	137°55.82E	3518	331	16.7	327	11.0	Run-up ENG
0721	1738	33°52.74N:	137°49.19E	2486	336	16.7	330	16.1	Slow Ahead ENG
0721	1745	33°53.17N:	137°48.68E	2458	167	0.6	326	10.2	Stop ENG
0721	1755	33°53.10N:	137°48.82E	2450	126	0.3	334	2.4	Release OBS-2
0721	1850	33°52.95N:	137°49.26E	2420	123	0.2	133	0.4	Com'ced Shifting
0721	1853	33°52.94N:	137°49.40E	2440	022	2.8	111	0.9	OBS-2 coming up
0721	1909	33°53.12N:	137°48.73E	2466	258	0.5	281	1.5	End Retrieve OBS-2
0721	1914	33°53.10N:	137°48.69E	2469	290	0.3	273	1.0	Prop to Diesel ENG
0721	1914	33°53.10N:	137°48.68E	2469	291	0.3	273	1.0	Slow Ahead ENG
0721	1916	33°53.17N:	137°48.58E	2490	332	5.0	282	1.3	s/co on 331°
0721	1927	33°54.82N:	137°47.44E	2458	332	16.1	329	8.9	Run-up ENG
0721	2013	34°05.63N:	137°40.25E	1151	329	16.4	330	15.9	Half Ahead ENG
0721	2017	34°06.05N:	137°39.94E	1176	290	1.2	330	12.1	Stop ENG
0721	2037	34°06.00N:	137°40.25E	1159	337	0.3	015	0.8	Release OBS-1
0721	2100	34°05.98N:	137°39.99E	1174	158	0.4	269	1.4	OBS-1 coming up
0721	2112	34°05.77N:	137°40.15E	1166	210	0.2	170	0.9	End Retrieve OBS -1
0721	2137	34°06.20N:	137°45.03E	664	075	16.2	080	12.6	Run-up ENG
0721	2159	34°06.15N:	137°52.52E	821	099	16.4	092	16.1	co variable
0721	2242	34°04.09N:	138°06.07E	2429	100	15.9	099	16.1	Half Ahead ENG
0721	2248	34°03.96N:	138°06.97E	2422	106	1.1	099	11.9	Stop ENG
0721	2303	34°03.98N:	138°06.95E	2423	316	0.3	095	1.6	**Start DESMOS -3**
0721	2355	34°03.91N:	138°06.96E	2422	338	0.9	300	0.2	**DESMOS Near Bottom**
0722	0400	34°05.78N:	138°05.67E	1987	339	0.6	310	0.4	DESMOS Lv Bottom
0722	0500	34°06.03N:	138°05.59E	1979	030	0.5	005	0.4	DESMOS On Deck
0722	0507	34°06.10N:	138°05.63E	1960	344	0.8	014	0.5	Prop to Diesel ENG
0722	0508	34°06.10N:	138°05.63E	1960	341	0.7	018	0.5	Slow Ahead ENG
0722	0511	34°06.23N:	138°05.67E	1946	062	4.2	014	1.1	s/co on 65°
0722	0514	34°06.39N:	138°06.04E	1922	064	6.6	046	2.5	Start Proton Mag Survey
0722	0528	34°07.57N:	138°09.08E	2324	064	16.2	064	11.1	Run-up ENG
0722	0644	34°17.04N:	138°32.37E	1730	062	13.7	064	17.2	Full Ahead ENG
0722	0649	34°17.67N:	138°33.91E	1580	062	16.5	064	16.2	Run-up ENG
0722	0813	34°28.37N:	139°00.20E	684	061	16.4	064	17.5	a/co to 066°
0722	0903	34°34.21N:	139°15.84E	388	075	16.5	066	16.6	a/co to 075°
0722	0946	34°38.15N:	139°29.62E	658	065	16.7	066	16.7	a/co to 067°
0722	1124	34°48.70N:	139°59.62E	1386	071	16.2	066	16.7	a/co to 072°

Day (GMT) M D	Time HrMin	Position Latitude	Longitude	Water Depth (m)	Head-ing (deg)	Log Speed (kt)	System Dir. (deg)	Vel. (kt)	Works
0722	1135	34°49.69N:	140°03.21E	2104	067	16.7	070	16.6	a/co to 67°
0722	1329	35°02.48N:	140°38.83E	634	082	15.8	067	17.4	a/co to 90°
0722	2039	35°02.53N:	143°15.08E	5466	079	17.1	090	17.0	a/co to 053°
0723	0634	36°43.89N:	145°59.77E	5466	052	17.0	053	16.1	a/co to 360°Survey Seamt
0723	1033	37°47.09N:	145°59.42E	4761	215	14.6	346	11.2	a/co to 217°
0723	1124	37°35.16N:	145°48.02E	5493	204	16.7	218	17.1	a/co to 90°
0723	1231	37°35.05N:	146°09.72E	5528	083	17.0	089	15.6	a/co to 360°
0723	1242	37°37.81N:	146°10.06E	5543	349	16.8	024	12.7	a/co to 270°
0723	1350	37°37.97N:	145°45.33E	5396	270	16.8	270	17.3	a/co to 360°
0723	1358	37°39.82N:	145°44.95E	5441	004	17.1	318	12.1	a/co to 90°
0723	1513	37°40.03N:	146°10.04E	5526	091	16.8	090	16.0	a/co to 360°
0723	1523	37°42.65N:	146°10.32E	5531	339	15.8	024	12.6	a/co to 270°
0723	1626	37°42.48N:	145°47.94E	5389	271	16.7	270	17.2	a/co to 360°
0723	1633	37°44.28N:	145°47.41E	5457	360	16.8	315	12.7	a/co to 90°
0723	1732	37°44.52N:	146°07.01E	5519	090	16.4	090	16.1	a/co to 302°
0723	1757	37°47.92N:	146°00.23E	5156	301	17.0	304	15.4	a/co to 360°Ryofu Seamt
0723	1955	38°20.17N:	146°00.00E	5256	359	15.9	000	15.9	Half Ahead ENG
0723	2000	38°21.02N:	146°00.00E	5250	010	9.6	000	13.3	∞-Shape Rotation R-Turn
0723	2015	38°20.71N:	145°59.98E	5255	002	9.0	300	2.9	∞-Shape Rotation L-Turn
0723	2036	38°21.65N:	145°59.93E	5229	003	15.9	008	6.2	Run-up ENG
0724	0813	41°27.88N:	145°59.97E	6217	326	15.4	001	17.5	a/co to 270°Takuyo Daiichi
0724	0821	41°28.08N:	145°57.26E	6293	260	16.8	308	12.5	a/co to 18° Seamt Survey
0724	0936	41°08.24N:	145°57.02E	5344	182	16.4	179	16.2	a/co to 270°
0724	0944	41°08.08N:	145°54.16E	5432	293	14.9	237	11.9	a/co to 360°
0724	1033	41°22.05N:	145°54.02E	3193	098	16.5	087	15.6	a/co to 90° Kuril Trench
0724	1057	41°21.99N:	146°02.67E	3193	098	16.5	087	15.6	a/co to 180° Survey -1
0724	1157	41°06.13N:	146°02.95E	5545	191	15.5	180	16.0	a/co to 323° [14]
0724	1558	41°59.77N:	145°09.37E	3549	324	16.8	323	16.4	a/co to 53°
0724	1635	42°05.96N:	145°19.72E	3462	056	15.8	051	16.2	a/co to 143° [18]
0724	1938	41°26.23N:	145°59.98E	5777	154	15.9	143	16.2	a/co to 233°
0724	1957	41°23.19N:	145°55.00E	5388	233	16.1	226	14.5	a/co to 323° [16]
0724	2256	42°03.12N:	145°14.40E	3639	323	16.8	323	16.8	a/co to 322°Kushiro Canyn
0725	0146	42°40.47N:	144°36.49E	234	312	17.1	323	16.8	co variable
0725	0200	42°42.48N:	144°31.88E	156	299	17.0	304	16.8	Slow Ahead ENG
0725	0203	42°42.79N:	144°31.24E	147	305	4.4	304	14.7	End Proton Mag Survey
0725	0214	42°43.99N:	144°30.13E	136	329	16.1	320	10.6	Run-up, a/c to 330°
0725	0234	42°48.99N:	144°26.23E	107	324	17.1	330	16.5	co variable
0725	0300	42°54.87N:	144°20.70E	53	332	16.4	330	17.0	Slow Ahead ENG
0725	0344	42°58.74N:	144°20.58E	62	069	2.2	032	4.9	Pilot on Board
0725	0433	42°59.10N:	144°22.03E	62	196	0.2	077	0.1	arr. Kushiro pier

Numerical figures in [ ] denote track numbers for Kuril Trench survey shown in Fig. 5-2.

Leg 2: Kushiro (July 29) to Tokyo (August 10) -1-

[JST = GMT + 8]

(Numerical figures in [ ] denote track numbers for Kuril Trench survey shown in Fig. 5-2)

Day (GMT) M D	Time HrMin	Position Latitude	Longitude	Water Depth (m)	Head-ing (deg)	Log Speed (kt)	System Dir. (deg)	Vel. (kt)	Works
0729	0441	42°59.13N:	144°22.02E	0	197	0.0	344	0.0	Lv Kushiro Pier
0729	0451	42°59.13N:	144°22.03E	0	199	0.1	354	0.1	Lv Kushiro Hbr
0729	0451	42°58.65N:	144°21.38E	0	280	3.5	245	2.1	Pilot Left Ship
0729	0511	42°58.68N:	144°21.17E	n.d.	270	3.1	258	2.4	TANDEM MOTION
0729	0525	42°56.66N:	144°20.00E	n.d.	148	15.7	200	9.0	Run-up ENG s/co on 248°
0729	0538	42°53.66N:	144°22.23E	n.d.	155	15.5	157	14.1	co variable
0729	0539	42°53.39N:	144°22.40E	n.d.	148	16.1	157	14.3	s/co on 148°
0729	0616	42°45.12N:	144°29.40E	n.d.	145	15.7	148	16.0	Slow Ahead ENG
0729	0620	42°44.49N:	144°29.93E	n.d.	149	4.3	148	14.2	Start Proton Mag Survey
0729	0637	42°42.33N:	144°31.84E	n.d.	147	15.5	148	11.3	Run-up ENG
0729	0731	42°29.97N:	144°42.40E	2105	148	15.4	147	16.5	a/co to 143° Kushiro Cyn
0729	1327	41°10.15N:	146°02.79E	5402	138	16.4	143	16.1	a/co to 53° Kuril Trench
0729	1336	41°11.33N:	146°05.23E	5477	048	16.7	084	11.6	a/co to 323° [15] Survey-2
0729	1409	41°18.81N:	145°58.19E	2961	325	17.0	324	16.5	a/co to 53°
0729	1446	41°25.32N:	146°08.44E	5757	044	16.4	051	16.5	a/co to 323° [20]
0729	1734	42°02.60N:	145°31.55E	4435	322	16.5	324	16.6	a/co to 53°
0729	1752	42°05.79N:	145°36.69E	4552	051	16.8	045	14.9	a/co to 143° [22]
0729	2123	41°21.09N:	146°22.50E	5585	115	16.5	144	15.6	a/co to 053°
0729	2143	41°24.20N:	146°28.24E	5599	049	16.7	059	14.7	a/co to 323° [24]
0730	0105	42°08.77N:	145°42.60E	4417	322	16.7	322	16.0	a/co to 53°
0730	0123	42°11.86N:	145°47.56E	4229	054	16.5	046	15.0	a/co to 143° Kuril Trench
0730	0205	42°02.89N:	145°57.37E	5215	145	16.1	142	16.8	s/co on 143°[36] Survey
0730	0400	41°38.31N:	146°22.81E	6380	144	15.9	142	15.8	Com`ced Boat Drill
0730	0430	41°32.18N:	146°29.16E	5668	144	15.7	143	15.4	Dismissed Boat Drill
0730	0452	41°27.69N:	146°33.79E	5568	144	15.9	142	15.4	a/co to 53°
0730	0509	41°29.92N:	146°39.11E	5572	065	16.4	067	14.7	a/co to 323° [28]
0730	0829	42°14.78N:	145°53.62E	3950	320	16.8	323	16.8	a/co to 96°
0730	0856	42°14.31N:	146°02.85E	4388	122	15.1	094	15.6	a/co to 143° [30]
0730	1222	41°29.58N:	146°48.59E	5437	141	15.9	143	16.2	a/co to 53°
0730	1232	41°30.83N:	146°51.42E	5452	051	15.9	081	12.4	a/co to 323° [31]
0730	1557	42°15.58N:	146°05.84E	4532	320	16.7	323	16.2	a/co to 53° Kuril Trench
0730	1624	42°20.20N:	146°13.84E	4172	063	15.9	052	16.7	a/co to 143° [34] Survey
0730	1946	41°35.52N:	146°59.63E	5445	105	15.7	143	16.3	a/co to 053°
0730	2006	41°38.79N:	147°05.48E	5345	037	16.8	059	14.9	a/co to 323° [36]
0730	2335	42°23.29N:	146°19.68E	4301	325	17.0	323	16.2	a/co to 53°
0730	2353	42°26.45N:	146°24.82E	4162	051	16.1	045	15.1	a/co to 143° [38]
0731	0310	41°42.12N:	147°10.84E	5422	144	15.5	142	17.0	a/co to 53°
0731	0328	41°44.73N:	147°16.30E	5479	045	16.8	062	15.2	a/co to 323° [40]
0731	0705	42°29.41N:	146°30.94E	4136	322	16.2	323	15.8	a/co to 53°
0731	0723	42°32.43N:	146°35.99E	3864	068	15.3	046	15.0	a/co to 143° [42]
0731	1036	41°48.12N:	147°21.54E	5516	125	15.7	143	17.4	a/co to 53°
0731	1054	41°50.84N:	147°26.82E	5486	048	16.4	062	14.8	a/co to 323° [44]
0731	1437	42°35.82N:	146°42.22E	3942	321	15.3	323	16.2	a/co to 233°
0731	1445	42°34.64N:	146°39.63E	3821	227	16.4	267	11.9	a/co to 143° [43]
0731	1752	41°51.94N:	147°22.55E	5642	146	15.4	143	17.5	a/co to 233°
0731	1810	41°48.85N:	147°17.61E	5545	244	15.3	225	14.9	a/co to 323° [41]
0731	2117	42°27.21N:	146°38.39E	5164	320	15.1	324	15.8	a/co to 233°
0731	2138	42°24.36N:	146°32.40E	5029	229	15.8	240	14.4	a/co to 143° [39]
0801	0058	41°39.71N:	147°17.83E	5282	144	15.9	143	16.9	a/co to 180°
0801	0235	41°12.38N:	147°18.01E	5112	176	16.1	180	16.8	ENG variable

Day (GMT) M D	Time HrMin	Position Latitude	Longitude	Water Depth (m)	Head-ing (deg)	Log Speed (kt)	System Dir. (deg)	Vel. (kt)	Works
0801	0238	41°11.83N:	147°17.92E	5110	174	9.8	182	15.6	Set Speed 10kt
0801	0240	41°11.46N:	147°17.91E	5109	179	9.6	182	14.5	∞-Shape Rotation R-Turn
0801	0255	41°11.37N:	147°17.62E	5110	181	9.5	152	3.4	∞-Shape Rotation L-Turn
0801	0317	41°10.57N:	147°17.02E	5100	169	3.5	204	4.5	End Proton Mag Survey
0801	0319	41°10.46N:	147°16.96E	5100	171	1.4	202	4.2	Stop ENG
0801	0322	41°10.41N:	147°16.94E	5100	174	1.3	203	3.4	Prop to Electric Motors
0801	0333	41°09.84N:	147°17.54E	5090	093	5.6	153	3.6	Start Proton Mag Survey
0801	0350	41°10.72N:	147°17.08E	5103	333	4.6	323	3.6	Start Air-Gun [32]
0801	0420	41°12.95N:	147°14.95E	5144	335	4.3	323	5.2	Launch Streamer Cable
0801	0448	41°14.78N:	147°13.18E	5178	337	4.2	323	4.8	**Start Seismic Survey**
0802	0345	42°45.25N:	145°40.64E	2098	340	4.7	322	5.1	**End Seismic Survey**
0802	0356	42°45.96N:	145°39.98E	2018	339	4.8	325	5.2	End Proton Mag Survey
0802	0400	42°46.29N:	145°39.67E	1964	339	4.6	326	5.2	End Air-Gun
0802	0450	42°48.59N:	145°36.61E	1629	356	1.3	313	3.3	Retrieve Streamer Cable
0802	0456	42°48.64N:	145°36.45E	1608	358	0.5	308	2.4	Prop to Diesel ENG
0802	0457	42°48.63N:	145°36.43E	1607	356	0.4	305	2.1	Slow Ahead ENG
0802	0502	42°48.67N:	145°36.48E	1606	128	4.5	320	1.1	s/co on 127°
0802	0509	42°48.30N:	145°36.91E	1665	121	5.0	140	1.9	Start Proton Mag Survey
0802	0656	42°42.02N:	145°48.70E	2464	124	6.7	129	5.6	End Proton Mag Test
0802	0656	42°42.00N:	145°48.74E	2467	125	7.3	129	5.6	Half Ahead ENG
0802	0706	42°40.91N:	145°50.75E	2579	126	15.8	127	9.9	Run-up ENG
0802	0905	42°21.05N:	146°26.71E	4847	134	16.7	127	17.1	a/co to 143° [37]
0802	1159	41°42.46N:	147°05.96E	5540	152	16.1	142	16.8	a/co to 233°
0802	1216	41°39.50N:	147°00.98E	5515	241	15.8	225	14.7	a/co to 323° [35]
0802	1455	42°13.96N:	146°25.06E	5596	319	16.1	322	16.5	a/co to 233°
0802	1514	42°11.32N:	146°19.62E	5655	230	16.4	242	14.0	a/co to 143° [33]
0802	1738	41°40.29N:	146°50.83E	5615	142	16.5	143	15.9	a/co to 233°
0802	1813	41°34.25N:	146°40.48E	5595	231	16.2	232	16.7	a/co to 323° [29]
0802	2019	42°02.75N:	146°10.59E	5330	304	16.7	322	16.8	a/co to 233°
0802	2037	42°00.08N:	146°05.51E	5774	228	16.8	241	14.5	a/co to 143° [27]
0802	2236	41°35.12N:	146°30.86E	5750	158	15.4	142	15.5	a/co to 233°
0802	2256	41°31.92N:	146°25.49E	5675	240	15.5	226	15.0	a/co to 323° [25]
0803	0042	41°56.34N:	146°00.14E	5729	317	16.5	323	17.3	a/co to 268°
0803	0250	41°55.05N:	145°14.12E	4567	269	17.0	268	15.7	Slow Ahead ENG
0803	0257	41°54.99N:	145°13.06E	4173	270	2.3	267	10.1	End Proton Mag Survey
0803	0258	41°54.99N:	145°13.04E	4170	267	2.3	267	9.1	Stop ENG
0803	0303	41°54.99N:	145°12.97E	4163	290	1.1	267	5.2	Prop TO Electric Motors
0803	0331	41°54.80N:	145°12.30E	4088	229	1.1	218	0.6	Start Beam Trawl
0803	0449	41°53.95N:	145°10.93E	4123	248	1.6	226	0.8	Beam Trawl on Bottom
0803	0513	41°53.63N:	145°10.45E	4167	243	2.0	228	1.1	Confirm Position
0803	0614	41°52.66N:	145°09.17E	4159	239	2.3	226	1.5	Confirm Position
0803	0631	41°52.32N:	145°08.83E	4159	232	1.3	214	1.4	Beam Trawl Lv Bottom
0803	0752	41°50.92N:	145°07.11E	4343	270	1.0	214	1.4	Beam Trawl on Deck
0803	0756	41°50.90N:	145°07.15E	4336	298	0.8	199	0.8	Prop to Diesel ENG
0803	0756	41°50.89N:	145°07.14E	4337	299	0.8	199	0.8	Slow Ahead ENG
0803	0800	41°50.70N:	145°06.90E	4380	197	4.7	220	1.9	Start Proton Mag Survey
0803	0806	41°49.69N:	145°06.53E	4598	191	12.6	199	5.9	a/co to 143° [11]
0803	0810	41°49.00N:	145°07.05E	4767	143	15.8	175	8.2	Run-up ENG
0803	1104	41°09.90N:	145°46.12E	5938	127	16.7	143	16.5	a/co to 53° [23]
0803	1302	41°28.35N:	146°19.51E	5720	034	16.1	053	15.7	a/co to 323°

Day (GMT) M D	Time HrMin	Position Latitude Longitude	Water Depth (m)	Head-ing (deg)	Log Speed (kt)	System Dir. (deg)	Vel. (kt)	Works
0803	1450	41°53.21N:145°54.55E	5716	317	15.8	323	17.4	a/co to 233°
0803	1509	41°50.35N:145°49.00E	5841	230	16.1	239	14.8	a/co to 143° [21]
0803	1646	41°29.57N:146°09.50E	6192	146	16.5	143	15.8	a/co to 233°
0803	1705	41°26.21N:146°04.30E	5609	227	17.1	224	15.1	a/co to 323° [19]
0803	1849	41°49.29N:145°40.83E	5785	319	15.8	323	17.2	a/co to 233°
0803	1908	41°46.51N:145°35.25E	5906	212	16.1	240	14.9	a/co to 143° [17]
0803	2047	41°25.09N:145°56.89E	5648	206	14.2	142	16.0	a/co to 232°
0803	2216	41°09.84N:145°29.95E	6311	252	15.3	234	17.2	a/co to 323° [7]
0804	0051	41°44.10N:144°55.88E	4783	323	15.8	323	16.5	Slow Ahead ENG
0804	0058	41°44.78N:144°55.24E	4794	327	2.1	324	10.7	End Proton Mag Survey
0804	0059	41°44.83N:144°55.20E	4786	312	2.3	324	9.8	Stop ENG
0804	0103	41°44.90N:144°55.12E	4777	317	1.1	324	6.5	Prop to Electric Motor
0804	0112	41°44.94N:144°55.03E	4772	216	0.5	321	2.4	**Start BeamTrawl**
0804	0256	41°43.64N:144°53.63E	4708	224	1.4	225	1.3	**Beam Trawl on Bottom**
0804	0416	41°42.08N:144°51.93E	4730	219	1.8	219	1.9	Beam Trawl Lv Bottom
0804	0530	41°40.12N:144°50.03E	4725	259	1.6	226	1.4	Beam Trawl on Deck
0804	0541	41°40.02N:144°49.78E	4720	246	0.8	236	1.2	Prop to Diesel ENG
0804	0541	41°40.02N:144°49.77E	4718	245	0.9	236	1.2	Slow Ahead ENG
0804	0546	41°40.09N:144°49.51E	4703	320	5.1	268	1.6	Start Proton Mag Survey
0804	0557	41°41.18N:144°48.29E	4546	320	9.9	318	6.3	∞-Shape Rotation R-Turn
0804	0612	41°41.14N:144°48.21E	4545	319	9.5	249	2.8	∞-Shape Rotation L-Turn
0804	0627	41°41.07N:144°48.23E	4554	316	10.2	055	1.8	End ∞-Shape Rotation
0804	0632	41°41.46N:144°48.31E	4536	101	8.5	012	3.4	s/co on 100°
0804	0640	41°41.09N:144°50.72E	4714	107	15.9	093	8.8	Run-up ENG
0804	0641	41°40.97N:144°51.20E	4717	107	16.2	098	10.3	a/co to 143° [5]
0804	1008	40°55.37N:145°37.15E	5640	144	16.7	141	16.9	a/co to 53°
0804	1016	40°56.35N:145°39.62E	5606	055	16.2	092	12.4	a/co to 324° [6]
0804	1304	41°32.97N:145°03.04E	5674	328	16.5	322	16.8	a/co to 53°
0804	1322	41°35.95N:145°08.03E	5725	059	16.7	046	14.6	a/co to 143° [8]
0804	1611	40°58.89N:145°46.16E	5538	133	16.8	142	16.6	a/co to 53°
0804	1618	40°59.84N:145°48.25E	5500	048	17.0	092	11.9	a/co to 323° [9]
0804	1908	41°37.42N:145°10.94E	5488	354	14.8	324	16.4	a/co to 53°
0804	1917	41°38.96N:145°13.45E	5396	069	15.1	026	12.6	a/co to 143° [10]
0804	2126	41°10.71N:145°43.12E	6020	051	15.7	136	15.7	a/co to 53°
0804	2148	41°14.56N :145°49.60E	5243	039	17.1	056	16.0	a/co to 323° [13]
0805	0023	41°49.13N:145°15.83E	5124	323	17.0	324	16.3	Slow Ahead ENG
0805	0030	41°49.75N:145°15.21E	5119	306	2.4	323	11.3	End Proton Mag Survey
0805	0032	41°49.78N:145°15.17E	5119	005	1.9	323	8.9	Stop ENG
0805	0038	41°49.80N:145°15.24E	5124	076	0.5	327	4.1	Prop to Electric Motors
0805	0047	41°49.89N:145°15.27E	5133	340	0.9	337	1.8	**Start DESMOS-4**
0805	0242	41°50.33N:145°14.91E	5160	059	0.0	340	0.3	**DESMOS Near Bottom**
0805	0705	41°52.09N:145°12.60E	4510	042	0.0	254	0.5	DESMOS Lv Bottom
0805	0826	41°51.72N:145°13.09E	4581	030	0.0	109	0.5	DESMOS on Deck
0805	0836	41°51.91N:145°13.21E	4587	077	0.5	034	0.8	Prop to Diesel ENG
0805	0837	41°51.92N:145°13.22E	4588	078	0.5	030	1.0	Slow Ahead ENG
0805	0839	41°51.90N:145°13.39E	4601	161	3.9	054	1.4	s/co on 160°
0805	0840	41°51.77N:145°13.49E	4622	160	5.4	081	1.3	Start Proton Mag Survey
0805	0850	41°50.09N:145°14.47E	5156	162	15.4	154	8.5	Run-up ENG
0805	0913	41°44.16N:145°17.15E	5638	158	16.4	162	15.8	a/co to 143° [12]
0805	1150	41°09.33N:145°51.24E	5573	207	13.5	141	16.5	a/co to 233°

Day (GMT) M D	Time HrMin	Position Latitude	Longitude	Water Depth (m)	Head-ing (deg)	Log Speed (kt)	System Dir. (deg)	Vel. (kt)	Works
0805	1302	40°57.56N:	145°30.72E	5828	298	14.1	234	16.2	a/co to 323° Kuril Trench
0805	1511	41°26.07N:	145°02.27E	5722	317	17.0	324	16.3	a/co to 233° [4] Survey
0805	1518	41°25.28N:	145°00.35E	5751	233	16.5	278	11.5	a/co to 143°
0805	1712	41°00.29N:	145°24.21E	6096	146	15.8	144	16.5	a/co to 233° [3]
0805	1721	40°58.71N:	145°22.17E	6094	232	16.5	200	12.0	a/co to 323°
0805	1912	41°23.12N:	144°57.01E	5662	296	15.7	323	16.7	a/co to 233° [2]
0805	1920	41°22.00N:	144°54.82E	5891	220	15.9	269	11.9	a/co to 143°
0805	2043	41°04.05N:	145°12.41E	6590	201	13.5	143	16.0	a/co to 243° [1]
0805	2146	40°56.53N:	144°53.54E	3969	243	15.7	243	15.5	Slow Ahead ENG
0805	2149	40°56.31N:	144°53.01E	3992	243	5.9	243	13.7	End Proton Mag Survey
0805	2208	40°56.21N:	144°55.03E	3847	115	0.9	094	5.3	Stop ENG
0805	2212	40°56.26N:	144°55.09E	3842	090	0.6	091	3.4	Prop to Electric Motors
0805	2215	40°56.32N:	144°55.20E	3837	088	1.1	081	2.8	Com'ce Set Transponders
0805	2217	40°56.30N:	144°55.31E	3832	080	1.3	083	2.7	Release Down Transponder
0805	2303	40°56.10N:	144°55.44E	3812	274	3.6	283	1.9	Release Down Transponder
0805	2313	40°56.23N:	144°54.90E	3873	274	5.0	286	2.4	Transponders on Bottom
0805	2348	40°56.32N:	144°53.22E	3986	067	0.1	320	0.4	**Start DESMOS-5**
0805	2350	40°56.30N:	144°53.21E	3983	067	0.1	290	0.3	Lower DESMOS
0806	0116	40°56.80N:	144°54.16E	3959	118	0.0	052	0.8	**DESMOS Near Bottom**
0806	0558	40°56.92N:	144°54.83E	3938	080	0.0	245	0.2	DESMOS Lv Bottom
0806	0716	40°56.83N:	144°55.14E	3912	017	0.6	104	0.3	DESMOS on Deck
0806	0830	40°56.15N:	144°55.64E	3796	297	1.9	048	0.3	Release Transponder
0806	0857	40°56.17N:	144°56.24E	4084	095	1.0	074	1.4	Retrieve Transponder
0806	0939	40°55.31N:	144°59.48E	4667	187	0.6	163	4.4	**Start Dredge Haul-1**
0806	1103	40°56.30N:	144°59.78E	4371	302	0.1	027	1.2	Lower Dredge
0806	1202	40°56.49N:	144°59.24E	4286	243	1.9	254	0.9	**Dredge on Bottom** Erimo
0806	1448	40°57.27N:	144°59.05E	4325	010	0.7	104	1.4	Dredge Lv Bottom
0806	1550	40°57.18N:	145°00.59E	4659	050	0.2	101	0.9	Dredge on Deck
0806	1649	40°56.51N:	144°53.13E	4025	295	9.8	270	8.3	a/co to 298°
0806	1708	40°57.91N:	144°49.66E	4938	290	10.1	296	8.9	co variable
0806	1721	40°57.87N:	144°49.33E	5195	003	1.3	298	2.4	**Start Dredge Haul-2**
0806	1739	40°57.84N:	144°49.69E	4956	058	0.1	119	0.4	Set SubNav at 500M
0806	1839	40°57.86N:	144°49.78E	4979	078	0.0	092	0.2	**Dredge on Bottom** Erimo
0806	2108	40°57.59N:	144°50.31E	4560	101	0.0	020	0.2	Dredge Lv Bottom
0806	2124	40°57.75N:	144°50.53E	4550	104	1.8	047	0.8	Com'ce Proton Mag Test
0806	2211	40°57.51N:	144°53.51E	4325	098	0.7	094	2.8	End Proton Mag Test
0806	2231	40°57.76N:	144°53.83E	4591	003	1.1	053	1.4	Dredge on Deck
0806	2231	40°57.76N:	144°53.84E	4582	356	1.2	053	1.4	Com'ce Shift Position
0806	2302	40°54.56N:	144°51.78E	3910	210	8.3	204	7.9	Move to DESMOS Point
0806	2325	40°53.79N:	144°51.52E	3854	095	0.2	184	0.9	**Start DESMOS-6**
0807	0041	40°53.54N:	144°51.29E	3861	059	0.3	168	0.3	**DESMOS Near Bottom**
0807	0245	40°52.07N:	144°49.58E	4693	049	0.0	201	0.7	DESMOS Lv Bottom
0807	0424	40°52.43N:	144°50.49E	4301	044	0.3	090	0.4	DESMOS on Deck
0807	0434	40°52.50N:	144°50.77E	4220	093	1.0	075	1.1	Prop to Diesel ENG
0807	0435	40°52.53N:	144°50.80E	4216	103	1.1	075	1.2	Slow Ahead ENG
0807	0446	40°52.34N:	144°50.74E	4279	230	5.1	200	1.3	Start Proton Mag Survey
0807	0500	40°49.94N:	144°51.67E	5024	165	15.1	163	10.2	Run-up ENG
0807	1535	38°00.00N:	145°57°99E	2985	161	16.2	164	16.4	a/co to 153°Survey Joban
0807	1554	37°55.36N:	146°00.97E	5186	154	15.5	154	16.4	a/co to 270° Seamounts

Day (GMT) M D	Time HrMin	Position Latitude	Longitude	Water Depth (m)	Head-ing (deg)	Log Speed (kt)	System Dir. (deg)	Vel. (kt)	Works
0807	1608	37°54.90N:	145°56.34E	5248	269	16.4	251	12.2	a/co to 360° Survey Joban
0807	1637	38°02.71N:	145°55.96E	4695	359	16.8	358	16.1	a/co to 270° Seamt cont'd
0807	1646	38°02.95N:	145°53.35E	5046	270	16.2	303	12.1	a/co to 180°
0807	1709	37°56.74N:	145°53.02E	5186	181	15.7	183	15.0	a/co to 52°
0807	1745	38°02.27N:	146°02.64E	5062	050	17.1	052	16.3	a/co to 180°
0807	1845	37°46.18N:	146°02.92E	4881	177	15.5	181	16.4	a/co to 233°
0807	1917	37°40.84N:	145°54.22E	3868	288	14.3	232	16.5	a/co to 360°
0807	1936	37°46.06N:	145°54.03E	4875	007	16.1	355	14.3	a/co to 90°
0807	1945	37°46.32N:	145°56.75E	4687	114	15.0	059	11.2	a/co to 180°
0807	2059	37°26.34N:	145°57.01E	5497	166	16.5	180	16.3	a/co to 47°
0807	2118	37°29.60N:	146°01.58E	5487	037	17.3	049	13.7	a/co to 270°
0807	2248	37°29.94N:	145°30.23E	5504	232	14.9	269	17.1	a/co to 180°
0807	2256	37°27.87N:	145°30.09E	5497	171	16.2	215	12.0	a/co to 90°
0807	2334	37°27.48N:	145°42.96E	5569	099	16.4	091	15.9	a/co to 225°
0808	0109	37°09.61N:	145°20.21E	3029	226	16.4	225	16.3	Slow Ahead ENG
0808	0119	37°08.93N:	145°19.36E	2525	237	2.1	224	8.1	End Mag Svy., Stop ENG
0808	0123	37°08.98N:	145°19.22E	2514	236	0.6	230	5.2	Prop to Electric Motors
0808	0127	37°08.98N:	145°19.26E	2531	133	0.5	230	3.0	**Start Dredge Haul-3**
0808	0233	37°08.88N:	145°19.23E	2520	210	1.3	229	0.7	**Dredge on Bottom (Bosei)**
0808	0502	37°07.15N:	145°17.25E	2512	216	0.9	196	1.1	**Dredge Lv Bottom**
0808	0541	37°07.00N:	145°17.00E	2723	189	0.4	199	0.3	Dredge on Deck
0808	0548	37°07.03N:	145°17.07E	2718	215	0.2	103	0.1	Prop to Diesel ENG
0808	0549	37°07.04N:	145°17.07E	2688	223	0.2	057	0.3	Slow Ahead ENG
0808	0551	37°07.03N:	145°16.96E	2711	274	2.7	358	0.1	s/co on 276°
0808	0553	37°07.05N:	145°16.82E	2718	275	4.9	281	1.0	Start Proton Mag Survey
0808	0609	37°07.32N:	145°13.46E	3993	275	16.1	276	9.9	Run-up ENG
0808	0747	37°09.98N:	144°39.99E	4230	274	17.0	276	16.5	a/co to 275°
0808	0755	37°10.16N:	144°37.34E	4765	272	17.0	276	16.5	a/co to 180°
0808	0955	36°37.97N:	144°36.99E	4243	208	15.1	180	16.2	a/co to 233°
0808	1103	36°27.30N:	144°19.75E	5539	230	9.9	233	14.4	∞-Shape Rotation R-Turn
0808	1118	36°27.41N:	144°19.87E	5545	224	9.3	281	3.4	∞-Shape Rotation L-Turn
0808	1155	36°26.35N:	144°18.25E	5555	232	4.2	235	3.8	Start Proton Mag Survey
0808	1156	36°26.25N:	144°18.05E	5557	233	9.2	235	3.9	s/co on 232°
0808	1202	36°25.54N:	144°16.89E	5574	232	16.2	234	8.6	Run-up ENG
0808	1326	36°12.03N:	143°55.18E	5388	248	15.3	232	15.8	a/co to 360°
0808	1404	36°22.35N:	143°54.96E	5417	005	16.5	359	16.8	a/co to 141°
0808	1429	36°17.41N:	144°00.16E	3361	145	8.8	139	14.8	Half Ahead ENG
0808	1453	36°14.48N:	144°03.06E	4696	145	15.5	142	10.4	Run-up ENG
0808	1600	36°00.12N:	144°17.41E	5741	144	15.5	141	16.5	a/co to 166°
0808	1719	35°38.10N:	144°24.56E	5309	182	15.7	166	17.9	a/co to 14°
0808	1802	35°47.66N:	144°27.24E	4218	008	16.1	012	15.7	a/co to 255°
0808	1850	35°44.95N:	144°13.64E	4015	261	15.4	254	13.6	Wind high up to 14m/s
0809	0029	35°25.99N:	142°44.91E	6312	253	15.8	255	14.2	Slow Ahead ENG
0809	0100	35°25.00N:	142°40.04E	6341	250	14.5	254	9.2	Run-up ENG
0809	0303	35°18.01N:	142°07.70E	7413	249	13.7	255	12.7	Full Ahead ENG
0809	0310	35°18.50N:	142°07.22E	7227	325	6.3	281	7.2	co variable
0809	0321	35°19.93N:	142°07.08E	6774	337	6.5	340	6.6	Slow Ahead ENG
0809	0330	35°21.17N:	142°07.00E	6549	335	6.9	351	7.4	Half Ahead ENG
0809	0346	35°20.86N:	142°04.56E	6508	243	13.4	262	7.9	Run-up ENG
0809	0400	35°20.03N:	142°01.41E	5701	248	14.6	254	11.2	Com'nce Fire Drill

Day	Time (GMT)	Position	Water Depth	Head-ing	Log Speed	System Dir.	System Vel.	Works
M D	HrMin	Latitude Longitude	(m)	(deg)	(kt)	(deg)	(kt)	
0809	0430	35°18.41N:141°54.32E	5379	245	14.2	254	12.2	End Fire Drill
0809	0430	35°18.38N:141°54.19E	5373	246	14.1	254	12.2	Com'nce Leak Drill
0809	0440	35°17.80N:141°51.80E	5104	246	14.0	254	12.2	Full Ahead ENG
0809	0500	35°16.91N:141°47.59E	4485	242	12.6	256	10.9	End Leak Drill
0809	0942	35°03.60N:140°54.74E	1488	226	5.8	242	5.3	**End Proton Mag Survey**
0809	0942	35°03.59N:140°54.73E	1485	226	6.5	242	5.3	Half Ahead ENG
0809	1030	35°00.54N:140°42.25E	1641	254	16.4	254	14.9	Run-up ENG
0809	1238	34°51.60N:140°05.31E	222	254	15.7	251	14.5	a/co to 255°
0809	1318	34°49.07N:139°53.87E	97	258	16.2	254	14.5	a/co to 257°
0809	1432	34°44.61N:139°30.57E	199	256	16.5	256	16.7	Slow Ahead ENG
0809	1437	34°44.34N:139°29.93E	85	120	0.9	253	12.6	Stop ENG
0809	1440	34°44.37N:139°30.02E	173	095	0.7	254	7.9	Prop to Electric Motors
0809	1916	34°46.07N:139°29.64E	243	063	1.9	355	0.7	Prop to Diesel ENG
0809	1916	34°46.07N:139°29.64E	250	061	2.5	355	0.7	Slow Ahead ENG
0809	1930	34°47.76N:139°31.46E	208	042	15.9	041	9.4	Run-up ENG
0809	2018	34°57.90N:139°42.23E	168	025	17.0	041	16.6	a/co to 15°
0809	2112	35°12.20N:139°47.05E	150	013	15.1	014	16.6	Half Ahead ENG
0809	2150	35°18.95N:139°44.05E	210	013	13.0	334	11.2	Pass Uraga, in Nakanose
0809	2217	35°24.20N:139°46.57E	n.d.	022	12.9	020	12.0	Out Nakanose Traffic Rt
0809	2245	35°28.00N:139°50.97E	n.d.	040	11.6	043	11.3	a/co to 40°in East Passage
0809	2255	35°29.63N:139°52.53E	n.d.	029	13.0	039	11.9	out East Pass, a/co to 328°
0809	2313	35°32.54N:139°50.48E	n.d.	331	2.8	328	9.9	ENG to S/M
0809	2324	35°32.73N:139°50.17E	n.d.	331	1.7	322	4.0	Pilot on Board
0809	2336	35°34.15N:139°48.88E	n.d.	324	9.9	322	7.9	into Tokyo Nishi Passage
0810	0017	35°38.53N:139°46.44E	n.d.	057	0.7	008	3.9	Anchor on
0810	0031	35°38.60N:139°46.50E	n.d.	140	0.0	018	0.9	Stop ENG
0810	0047	35°38.60N:139°46.50E	n.d.	140	0.0	040	0.2	**Arr. Harumi Pier**

Map attached to Preliminary Report of Hakuho Maru Cruise KH-92-3
Ocean Research Institute, University of Tokyo. March 1993

Bathymetric Map of the Western Kuril Trench

(1 of 2: Eastern Part)

1/300,000 at 35°

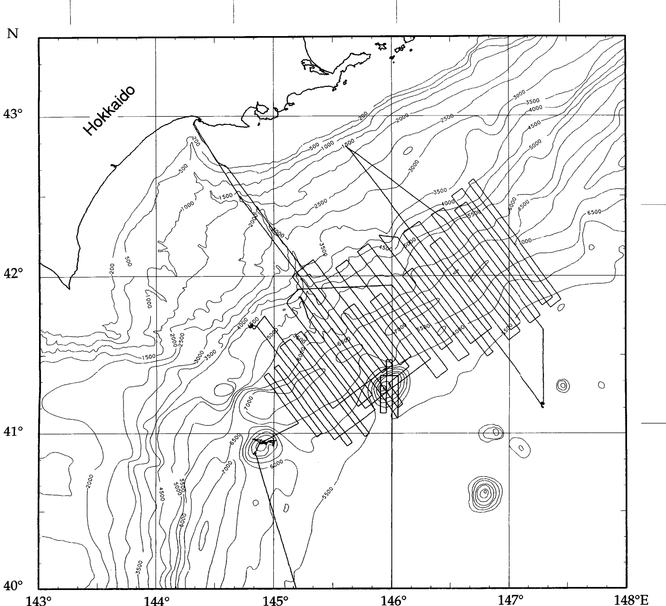

42°40'N
42°30'
42°20'
42°10'
42°00'
41°50'
41°40'
41°30'
41°20'
41°10'
41°00'
40°50'
146°05'
146°10'
146°20'
146°30'
146°40'
146°50'
147°00'
147°10'
147°20'
147°30'E

Map attached to Preliminary Report of Hakuho Maru Cruise KH-92-3
Ocean Research Institute, University of Tokyo. March 1993

Bathymetric Map of the Western Kuril Trench

(1 of 2: Western Part)

1/300,000 at 35°

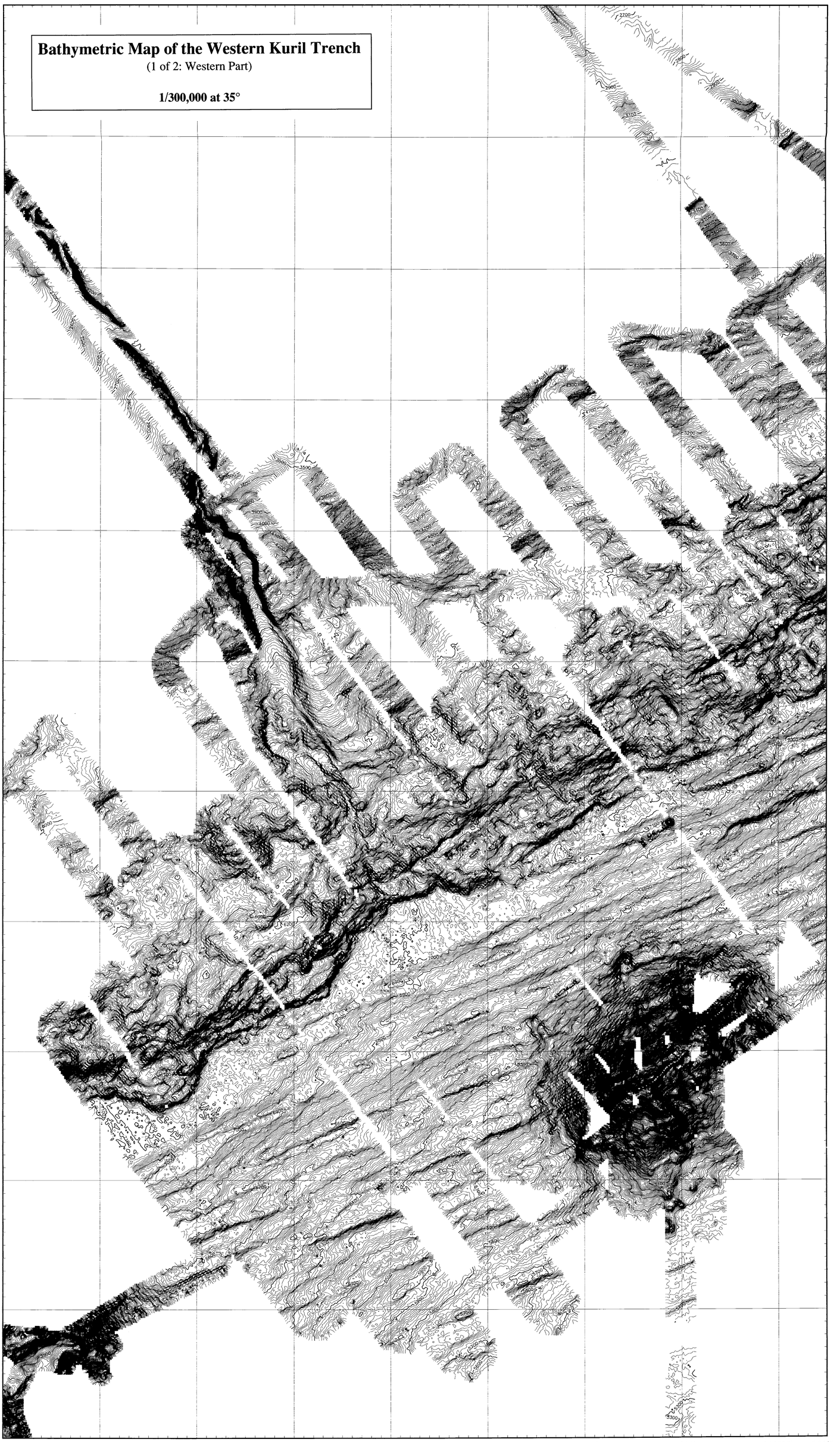

Fig. 5-5. 3.5 KHz profile along line #32 measured during the multichannel seismic profiling across the Kuril Trench off east Hokkaido. Vertical exaggeration is 1 : 21.

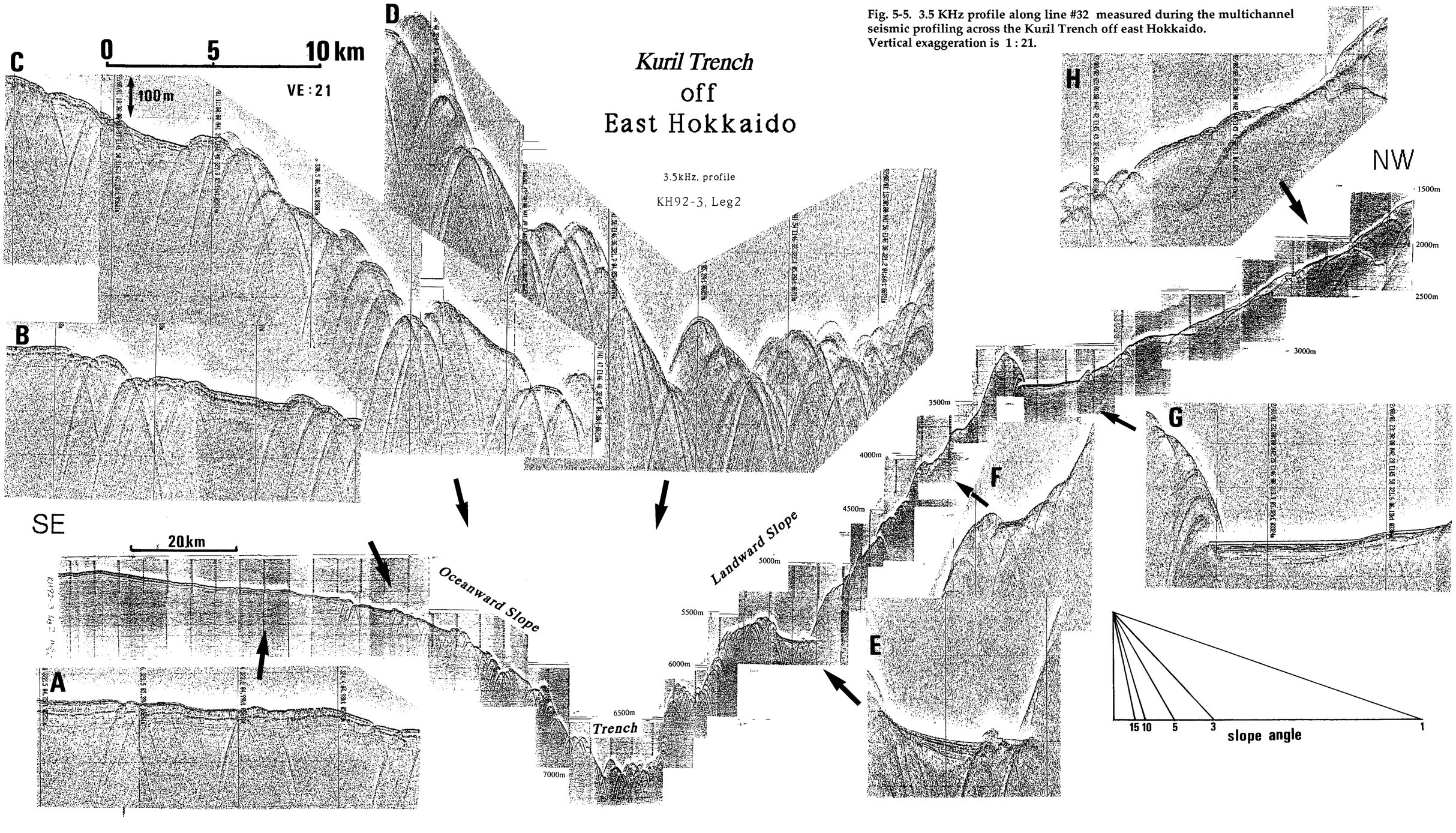

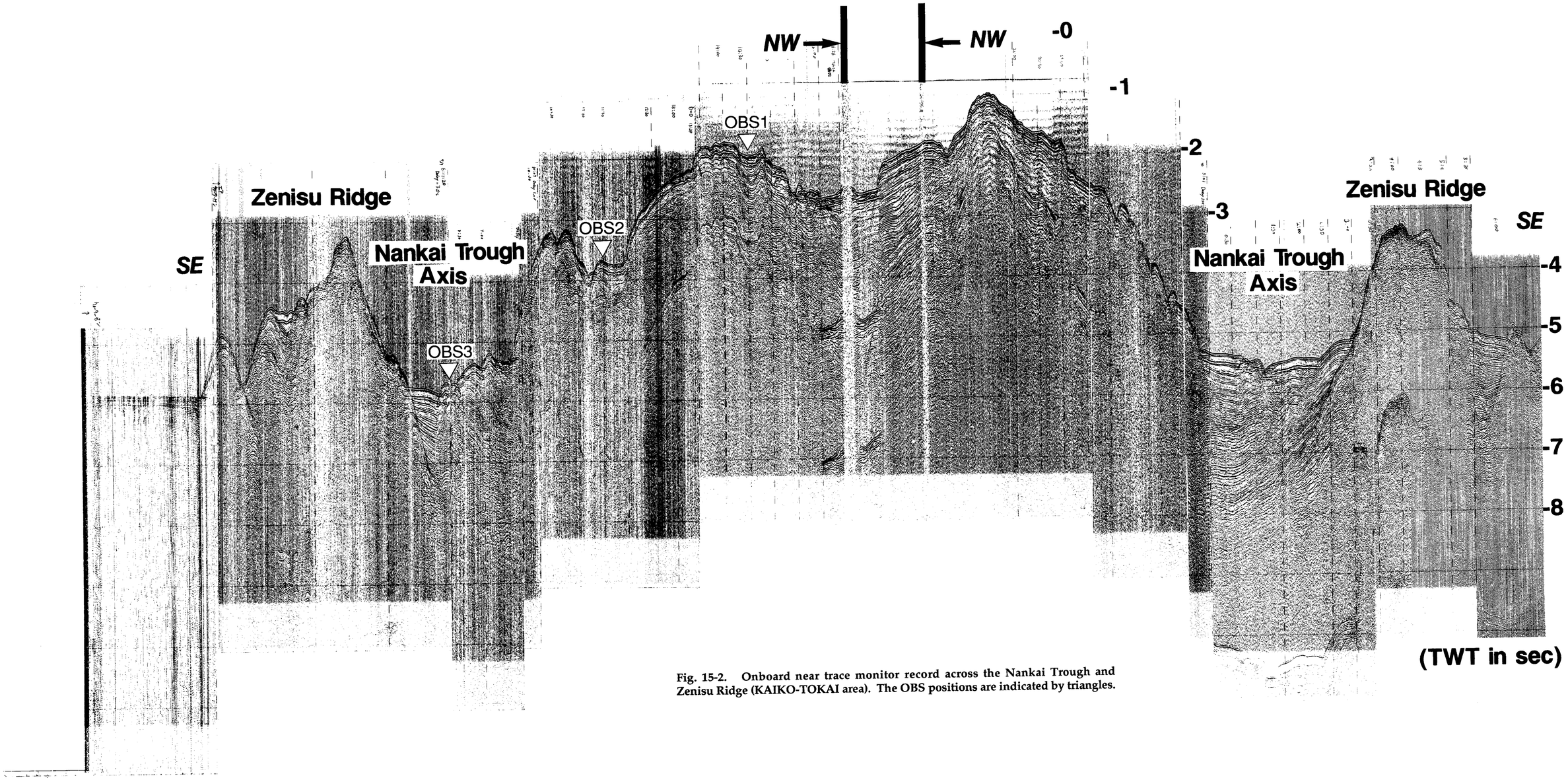

Fig. 15-2. Onboard near trace monitor record across the Nankai Trough and Zenisu Ridge (KAIKO-TOKAI area). The OBS positions are indicated by triangles.

KH923LEG2;KURILE-1
STACKED,UNMIGRATED

Western Kuril Trench–Lower Slope

Fig. 16-3. Stacked section of the 24-ch data. Raw data records of 8192 samples of 1-ms interval were resampled to 4-ms interval records. After velocity analysis, records were deconvolved, filtered, applied NMO and stacked. The subducting oceanic crust is much better imaged than the near-trace record (Fig.16-2). Lower slope.

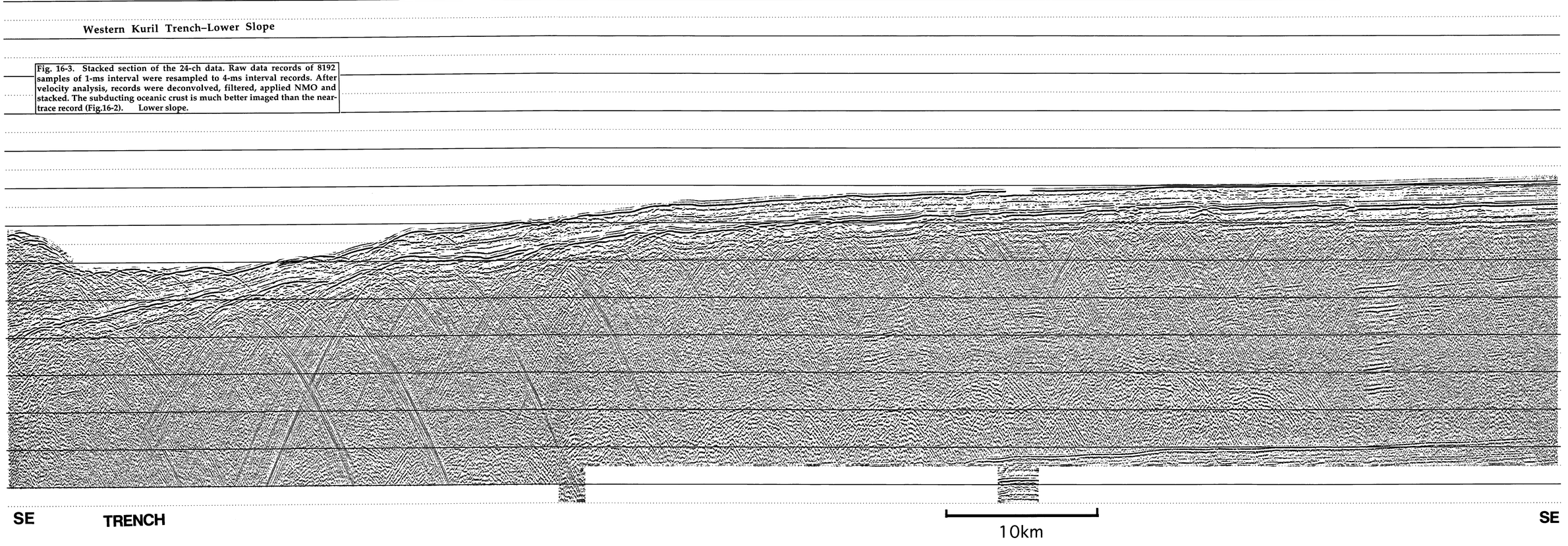

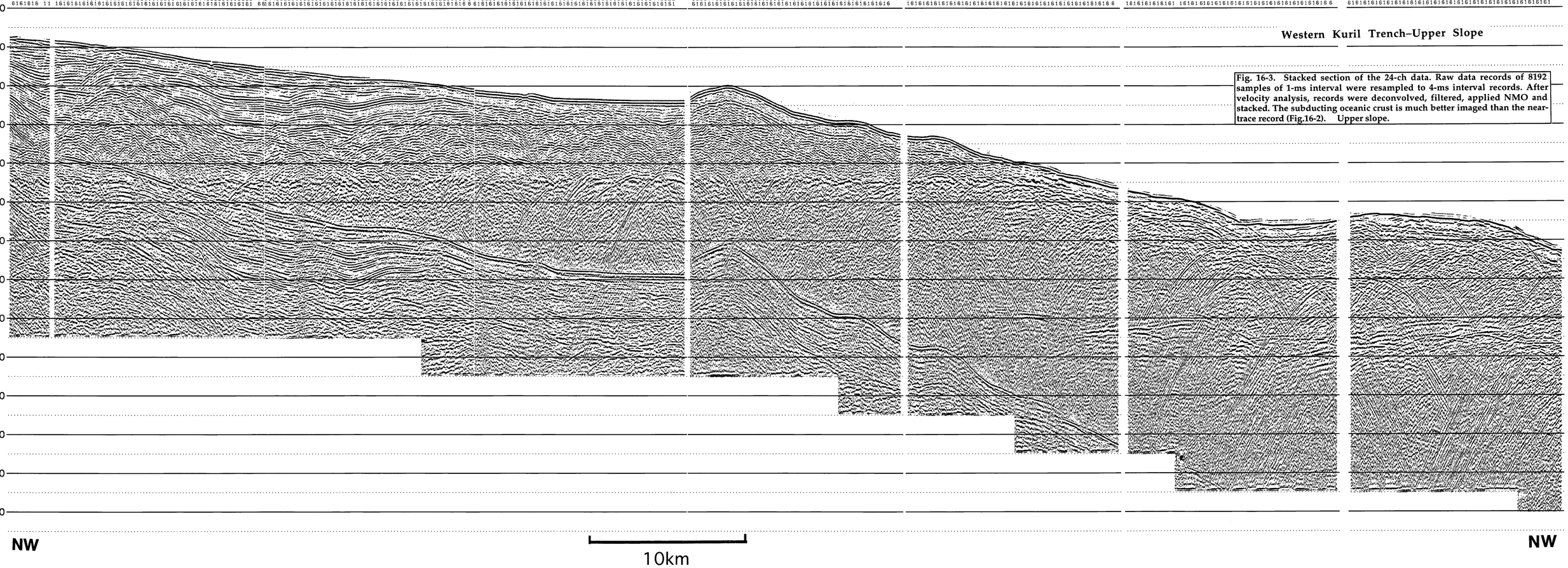

Fig. 16-3. Stacked section of the 24-ch data. Raw data records of 8192 samples of 1-ms interval were resampled to 4-ms interval records. After velocity analysis, records were deconvolved, filtered, applied NMO and stacked. The subducting oceanic crust is much better imaged than the near-trace record (Fig.16-2). Upper slope.